



January 2017

# Chromatographic Analysis Of Low Molecular Weight Polar Compounds In Complex Environmental Matrices And Renewable Materials

Jana Rousova

Follow this and additional works at: <https://commons.und.edu/theses>

---

## Recommended Citation

Rousova, Jana, "Chromatographic Analysis Of Low Molecular Weight Polar Compounds In Complex Environmental Matrices And Renewable Materials" (2017). *Theses and Dissertations*. 2329.  
<https://commons.und.edu/theses/2329>

This Dissertation is brought to you for free and open access by the Theses, Dissertations, and Senior Projects at UND Scholarly Commons. It has been accepted for inclusion in Theses and Dissertations by an authorized administrator of UND Scholarly Commons. For more information, please contact [zeinebyousif@library.und.edu](mailto:zeinebyousif@library.und.edu).

CHROMATOGRAPHIC ANALYSIS OF LOW MOLECULAR WEIGHT POLAR COMPOUNDS  
IN COMPLEX ENVIRONMENTAL MATRICES AND RENEWABLE MATERIALS

by

Jana Rousová

Bachelor of Science, University of Chemical Technology, 2008

Master of Science, University of Chemical Technology, 2011

A Dissertation

Submitted to the Graduate Faculty

of the

University of North Dakota

in partial fulfillment of the requirements

for the degree of

Doctor of Philosophy

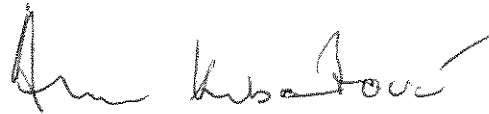
Grand Forks, North Dakota

August

2017

Copyright 2017 Jana Rousová

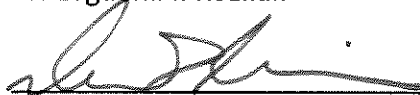
This dissertation, submitted by Jana Rousová in partial fulfillment of the requirements of the Degree of Doctor of Philosophy from the University of North Dakota, has been read by the Faculty Advisory Committee under whom the work has been done and is hereby approved.



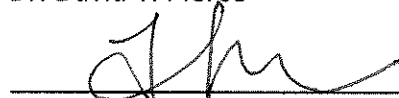
Dr. Alena Kubatova (Chairperson)



Dr. Evguenii I. Kozliak



Dr. David T. Pierce

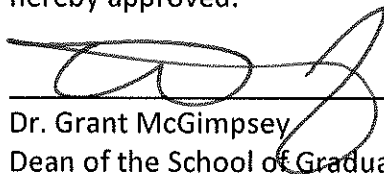


Dr. Julia Zhao



Dr. David Delene

This dissertation is being submitted by the appointed advisory committee as having met all the requirements of the School of Graduate Studies at the University of North Dakota, and is hereby approved.



Dr. Grant McGimpsey  
Dean of the School of Graduate Studies

July 28, 2017

Date

## PERMISSION

Title	Chromatographic Analysis of Low Molecular Weight Polar Compounds in Complex Environmental Matrices and Renewable Materials.
Department	Chemistry
Degree	Doctor of Philosophy

In presenting this dissertation in partial fulfillment of the requirement for a graduate degree from the University of North Dakota, I agree that the library of this University shall make it freely available for inspection. I further agree that permission for extensive copying for scholarly purposes may be granted by the professor who supervised my dissertation work or, in her absence, by the chairperson of the department or the dean of the graduate school. It is understood that any copying or publication or other use of this dissertation or part thereof for financial gain shall not be allowed without my written permission. It is also understood that due recognition shall be given to me and the University of North Dakota in any scholarly use which may be made of any material in my dissertation.

Jana Rousová  
07/21/2017

## TABLE OF CONTENT

<b>LIST OF TABLES .....</b>	<b>ix</b>
<b>LIST OF FIGURES .....</b>	<b>xii</b>
<b>LIST OF ABBREVIATIONS .....</b>	<b>xvi</b>
<b>ACKNOWLEDGMENTS.....</b>	<b>xviii</b>
<b>ABSTRACT .....</b>	<b>xviii</b>
<b>I. CHAPTER CHALLENGES IN ANALYSIS OF LOW MOLECULAR WEIGHT POLAR COMPOUNDS &amp; STATEMENT OF PURPOSE.....</b>	<b>1</b>
<b>II. CHAPTER DETERMINATION OF IMPURITIES IN BIOPRODUCED SUCCINIC ACID .....</b>	<b>6</b>
<b>II.1. BACKGROUND .....</b>	<b>6</b>
<b>II.2. MATERIALS AND METHODS.....</b>	<b>8</b>
II.2.1 Studied samples .....	8
II.2.2 Chemicals .....	9
II.2.3 Sample preparation .....	10
II.2.4 Instrumentation .....	12
II.2.5 Data processing.....	12
<b>II.3. RESULTS AND DISCUSSION .....</b>	<b>14</b>
II.3.1 Extraction vs direct analysis.....	14
II.3.2 Initial identification of impurities .....	15
II.3.3 Development of quantification method for analysis of acids and saccharides as the most abundant impurities .....	17
II.3.4 Limits of detection and repeatability.....	22
II.3.5 Characterization of succinic acid samples .....	22

	II.3.5.1 Abundance of acids, saccharides, and polyalcohols .....	23
	II.3.5.2 Final Bacterial Process Samples .....	25
	<b>II.4 CONCLUSIONS.....</b>	<b>25</b>
<b>III.</b>	<b>CHAPTER CHARACTERIZATION OF BIOLOGICALLY ACTIVE MOLECULES IN PULICARIA JAUBERTII EXTRACTS USING GAS AND LIQUID CHROMATOGRAPHY AND MASS SPECTROMETRY .....</b>	<b>27</b>
	<b>III.1. BACKGROUND .....</b>	<b>27</b>
	<b>III.2. MATERIALS AND METHODS.....</b>	<b>28</b>
	III.2.1 Plant collection.....	28
	III.2.2 Chemicals .....	28
	III.2.3 Preparation of the PJ extract and its fractionation.....	28
	III.2.4 Chemical characterization of PJ fractions.....	29
	<b>III.3. RESULTS AND DISCUSSION .....</b>	<b>31</b>
	III.3.1 Determination of bioactive fractions.....	31
	III.3.2 Chemical characterization of PJ fractions.....	31
	<b>III.4 CONCLUSIONS.....</b>	<b>38</b>
<b>IV.</b>	<b>CHAPTER DETERMINATION OF <i>TRANS</i>-RESVERATROL AND ITS METABOLITES IN RAT SERUM USING LIQUID CHROMATOGRAPHY WITH HIGH-RESOLUTION TIME OF FLIGHT MASS SPECTROMETRY.....</b>	<b>39</b>
	<b>IV.1. BACKGROUND .....</b>	<b>39</b>
	<b>IV.2. MATERIALS AND METHODS .....</b>	<b>41</b>
	IV.2.1 Materials.....	41
	IV.2.2 Synthesis and purification of RES analogs and deuterated RSs .....	42
	IV.2.3 Sample preparation .....	43
	IV.2.4 Instrumentation.....	44
	IV.2.5 ESI optimization .....	44
	IV.2.6 LC-ESI-HRMS conditions for serum analysis .....	47

IV.2.7 Data processing .....	47
<b>IV.3. RESULTS AND DISCUSSION .....</b>	<b>48</b>
IV.3.1 Evaluation of ESI conditions .....	48
IV.3.2 Calibration parameters and limits of detection .....	50
IV.3.3 Concentration of RES and its metabolites in rat serum and their impact on tumor growth.....	52
<b>IV.4. CONCLUSIONS .....</b>	<b>57</b>
<b>V. CHAPTER METHOD DEVELOPMENT FOR DETERMINATION OF TRACE CONCENTRATIONS OF ALDEHYDES AND CARBOXYLIC ACIDS IN PARTICULATE MATTER.....</b>	<b>58</b>
<b>V.1. BACKGROUND .....</b>	<b>58</b>
<b>V.2. MATERIALS AND METHODS .....</b>	<b>66</b>
V.2.1 Materials .....	66
V.2.2 Sample preparation .....	67
V.2.2.1 Evaluation of derivatization conditions .....	67
V.2.2.2 Extraction and derivation of PM samples .....	69
V.2.3 Instrumentation.....	69
V.2.4 Data processing .....	70
<b>V.3. RESULTS AND DISCUSSION.....</b>	<b>75</b>
V.3.1 Evaluation of derivatization and extraction .....	75
V.3.1.1 Efficiency of esterification of aromatic acids .....	77
V.3.1.2. Trimethylsilylation of aromatic acids.....	79
V.3.1.3. Quantification of aldehydes and acids and calibration parameters .....	81
V.3.2 Determination of acids and aldehydes in PM samples .....	83
<b>V.4. CONCLUSIONS .....</b>	<b>87</b>
<b>APPENDICES .....</b>	<b>88</b>
<b>APPENDIX A.....</b>	<b>89</b>
<b>APPENDIX B.....</b>	<b>107</b>



<b>APPENDIX C</b> .....	<b>110</b>
<b>APPENDIX D</b> .....	<b>150</b>
<b>REFERENCES</b> .....	<b>158</b>

## LIST OF TABLES

Table II.1 List of acids, saccharides and polyalcohols studied, their suppliers, the GC–MS retention times, target and confirmation ions (used for quantification) of their trimethylsilyl derivatives used for data processing, and limits of detection (LODs).....	10
Table II.2 Contaminants and their percent responses, with respect to an internal standard, observed upon BSTFA derivatization of an ACN extract of petroleum produced succinic acid and initial process bio-based succinic acid samples.....	16
Table II.3 GC intra, interday, and extraction method repeatability for a bioprocessed sample of succinic acid (sample C) reported as a mean value (in $\mu\text{g/g}$ ) $\pm$ one standard deviation (n=3). ...	22
Table II.4 Concentrations of acids and saccharides in bioprocessed succinic acid samples reported as a mean value (in $\mu\text{g/g}$ ) $\pm$ one standard deviation (n=3).....	23
Table IV.1 Target analytes, their structures, the mass of the ions used for quantification, and determination of LODs.....	41
Table IV.2 Summary of experimental conditions used for flow injection analysis of individual target analytes with ESI in negative mode with 50% MeOH or 50% ACN as the mobile phase. All experiments were run in two blocks. ....	46
Table IV.3 Concentration (ng/mL) of RES and its metabolites in serum samples of rats exposed to RES. The data are presented as mean with one standard deviation (n=3). ....	53
Table V.1 Comprehensive summary of derivatization protocols using sequential derivatization with PFBHA and BSTFA for determination of carboxylic and carbonyl compounds in atmospheric samples. ....	60
Table V.2 List of aldehydes studied with their supplier, the corresponding GC-MS relative retention, target and confirmation ions and theirs relative abundance (listed in parenthesis) used for data acquisition and processing.....	71
Table V.3 List of carboxylic acids studied with their supplier, the corresponding GC-MS relative retention, target and confirmation ions and theirs relative abundance (listed in parenthesis) used for data acquisition and processing.....	73
Table A.1 Summary of previous studies focusing on simultaneous GC-MS determination of acids, saccharides and polyalcohols in various sample matrices. ....	94

Table A.2 Optical microscope images of succinic acid samples .....	97
Table A.3 Contaminants observed upon BSTFA derivatization of ACN extract of petroleum based and initial processed succinic acid samples.....	102
Table B.1 Determination of bioactive fractions of <i>Pulicaria jaubertii</i> .....	107
Table B.2 Compounds observed in <i>Pulicaria</i> extract and its fractions using GC-MS. Amount is reported as percentage of TIC together with amount normalized by internal standard amount. Only compounds with amount higher than 0.5% were reported. ....	108
Table B.3 Compounds observed in <i>Pulicaria</i> extract and it's fractions using GC-MS after derivatization with BSTFA. Amount is reported as percentage of TIC together with amount normalized by internal standard amount. Only compounds with amount higher than 0.5% were reported .....	109
Table C.1: Summary of LC-MS methods previously used for detection of RES and its metabolites in blood and tissue matrices .....	116
Table C.2 ESI conditions for RES samples introduced to TOF-MS via LC for DOE optimization in negative mode (FIA, 50% MeOH/H <sub>2</sub> O solvent, drying gas at 350 °C and 10 L/min; nebulization pressure at 25 psig).....	125
Table C.3 ESI conditions for R3G samples introduced to TOF-MS via LC for DOE optimization in negative mode (FIA, 50% MeOH/H <sub>2</sub> O solvent, drying gas at 350 °C and 10 L/min; nebulization pressure at 25 psig).....	130
Table C.4 ESI conditions for R3S samples introduced to TOF-MS via LC for DOE optimization in negative mode (FIA, 50% MeOH/H <sub>2</sub> O solvent, drying gas at 350 °C and 10 L/min; nebulization pressure at 25 psig).....	137
Table C.5 Nebulization ESI conditions in negative mode for samples introduced to TOF-MS via LC for DOE optimization of nebulization conditions for RES (FIA, 50% MeOH/H <sub>2</sub> O solvent, fragmentor at 175 V; capillary at 4500 V, electrolyte: 0.1 mM acetic acid in mobile phase)....	144
Table C.6 Solvents and electrolytes employed for solvent optimization (FIA, negative mode, drying gas at 350 °C and 12 L/min; nebulization pressure at 25 psig, capillary at 4000 V, fragmentor at 175 V) .....	146
Table C.7 Effect of electrolyte concentrations of 0–400 mM acetic acid and 0–40 mM ammonium acetate in injected sample (FIA, ACN/H <sub>2</sub> O solvent, negative mode, drying gas at 350 °C and 12 L/min; nebulization pressure at 25 psig, capillary at 4000 V, fragmentor at 175 V).....	147

Table C.8 Recoveries of spiked RES and R3S from control serum samples following the SPE purification method and LC-ESI-HRMS analysis using different electrolytes as the mobile phase..... 149

Table C.9 Calibration parameters and LODs of RES, R3G, and R3S obtained using a linear least square regression. The internal standard was pinosylvin with a final concentration of 11.35 µg/mL ..... 149

Table C.10 Interday and intraday repeatability of RES, R3G, and R3S concentrations (ng/mL) in a representative serum sample. The data are presented as mean with one standard deviation (n=3) ..... 149

Table D.1 Calibration parameters of aldehydes as PFBHA oximes and acids as methyl esters or trimethylsilyl esters (denoted TMS). All areas were normalized to area of internal standard (aldehydes – octafluoronaphthalene, acids – o-terphenyl) ..... 150

Table D.2 Aldehydes and acids observed in WS and UA PM ..... 152

## LIST OF FIGURES

- Figure II.1 GC-MS analyses following a) direct BSTFA derivatization and b) derivatization of ACN extracted bacterial sample F. Stars mark the peaks of impurities in observed in bacterial samples. Chromatograms are scaled to the internal standard height. .... 14
- Figure II.2 Comparison of GC-MS chromatograms of analysis BSTFA derivatization of ACN extracted bioproduced succinic acid samples, normalized to the same percent response of internal standard. Samples F(a) and K(b) were initial process samples. .... 17
- Figure II.3 GC-MS extracted ion chromatograms ( $m/z = 217$ ) of a mixture of standard saccharides and polyalcohols upon derivatization (18 h at 70 °C) with a) MSFTA with ACN, b) BSTFA (1%TMCS), c) BSTFA 1% TMCS with ACN, d) BSTFA (1% TMCS) with pyridine. The stars mark peaks of the completely derivatized sucrose and glucose. .... 19
- Figure II.4 GC-MS extracted ion 204 chromatograms of bio-produced succinic acid (sample F) upon derivatization with various derivatization agents for 18 hours at 70 °C. Derivatization with pyridine (solid line) provided higher response than derivatization with ACN (dashed line). IS denotes internal standard. The IS co-elutes with other derivatized hexose which is believed to be an impurity in the glucose standard. .... 20
- Figure II.5 GC-MS extracted ion chromatograms ( $m/z = 117$ ) of an acetic acid standard upon derivatization (18 h at 70 °C) with a) MSFTA with ACN, b) BSTFA (1%TMCS), c) BSTFA 1% TMCS with ACN, d) BSTFA 1% TMCS with pyridine. .... 21
- Figure III.1 GC-MS total ion current chromatograms of methanol extract and its fractions without TMS derivatization. (A) methanol extract (PJM), (B) DCM fraction (PJD), (C) n-hexane fraction (PJH), (D) water/methanol fraction (PJA). All chromatograms are normalized to the response of internal standard, thus providing proportional response based on quantities extracted. .... 32
- Figure III.2 GC-MS total ion current chromatograms of methanol extract and its fractions with TMS derivatization. (A) methanol extract (PJM), (B) DCM fraction (PJD), (C) n-hexane fraction (PJH), (D) water/methanol fraction (PJA). Note that analysis of TMS derivatives allowed for enhanced characterization of the fractions and allowed for identification of catechin-like compounds in the methanol extract and the DCM fraction. All chromatograms are normalized to the response of internal standard, thus providing proportional response based on quantities extracted. Dichloromethane (DCM). .... 33
- Figure III.3 GC-MS characterization of DCM fraction (PJD) and EI-MS spectrum of most abundant catechin-like compounds. (A) Total ion current chromatogram (B-G) EI-MS spectra of peaks D1-

D6. Compounds D2, D3, D4 showed high identity (> 80%) with the EI/MS NIST library for catechin. Compounds were analyzed as TMS derivatives. .... 34

Figure III.4 GC-MS characterization of catechin and epicatechin standards. (A) TMS-derivatives of catechin and epicatechin standards were analyzed by GC-MS in comparison to the TMS-derivatized DCM fraction, PJD. Note that the retention times for the standards do not match that of the compounds observed in the PJD. The EI-MS spectra of catechin and epicatechin are provided in (B) and (C). Note that of the 368.2 ions present in the standards is also enriched in the TMS-derivatized compounds observed in the DCM fraction detailed in Figure III.3. .... 36

Figure III.5 Extracted ion chromatograms and mass spectra of LC-HR-MS analysis of the DCM fraction PJD. (A) Extracted ion chromatogram (EIC) of ions 289.07, 317.05 and 359.19. (B) Time of flight (TOF) mass spectrum of L1 peak, C) TOF mass spectra of L2 peak and mass accuracy confirming the catechin-like structure. The structure of catechin ( $m/z$  289.0718) is provided for comparison. .... 37

Figure IV.1 Synthesis of RES-d5..... 42

Figure IV.2 ESI-MS normalized response for RES (A), R3G (B), and R3S (C), comparing the solvents 50% MeOH/H<sub>2</sub>O and 50% ACN/H<sub>2</sub>O, with no electrolyte, 0.1 mM acetic acid, and 0.1 mM ammonium acetate, determined using FIA in the negative mode (for RES: solvent  $p=0.288$ , for R3G: solvent  $p=0.065$ , for R3S: solvent  $p=0.045$ ). ESI-MS normalized response of RES (D), R3G (E), and R3S (F) in 50% ACN/H<sub>2</sub>O solutions with acetic acid (AcOH) and ammonium acetate (NH<sub>4</sub>OAc) (0–10 mM in sample) determined in the negative mode using FIA (for RES: concentration  $p<0.0005$ , electrolyte and concentration interaction  $p=0.012$ ; for R3G: electrolyte  $p=0.002$ , concentration  $p<0.0005$ , electrolyte and concentration interaction  $p=0.002$ ; for R3S: concentration  $p<0.0005$ ) ..... 50

Figure IV.3 Representative LC-ESI-HRMS extracted ion chromatograms (EIC) of control serum spiked with RES, R3G, R3S (0.32, 3.9, 0.48  $\mu\text{g/mL}$ , respectively; scaled to same peak height) ... 51

Figure IV.4 Representative LC-ESI-HRMS analysis of in vivo rat serum sample; extracted ion chromatogram (EIC) for R3G (A), EIC for R3G-d5 (B), EIC for resveratrol sulfates (C), EIC for R3G-d5 (D), EIC for internal standard (IS, E). Peaks X1 and X2 represent suspected derivatives of resveratrol sulfate..... 54

Figure IV.5 Boxplots representing measured concentrations (ng/mL) of RES, R3G and R3S in rat serum and tumor after exposure to RES after 21 weeks ..... 56

Figure V.1 The proposed derivatization scheme using PFBHA·HCl with BSTFA for derivatization of aldehydic, carboxylic and hydroxylic groups on air PM..... 65

Figure V.2 The effect of time on methylation of dicarboxylic acids with PFBHA·HCl in MeOH. A) 1 h, B) 3 h, C) 18 h. The acids labels are provided in Table V.2. .... 76

Figure V.3 Demonstration of derivatization efficiency of monocarboxylic acid with 18 h sonication in two solvent systems A) PFBHA in ACN/DCM/MeOH and B) PFBHA in MeOH. The acids labels are provided in Table V.2. Denotation “a” stands for methyl ester, “b” stands for trimethylsilyl ester. The acids labels are provided in Table V.2. .... 77

Figure V.4 Comparison of BF<sub>3</sub>/MeOH with PFBHA methylation protocols each followed by BSTFA trimethylsilylation shown for representative model acid mixture: A) BF<sub>3</sub>/MeOH, B) BF<sub>3</sub>/MeOH with subsequent BSTFA, C) PFBHA·HCl in MeOH, and D) PFBHA·HCl in MeOH with subsequent BSTFA The acids labels are provided in Table V.2. Denotation “a” stands for methyl ester, “b” stands for trimethylsilyl ester. .... 78

Figure V.5 The efficiency of trimethylsilylation of aromatics acids: A) GC-MS TIC chromatogram with TMS derivatives following using PFBHA·HCl/BSTFA protocol; B) Efficiency of derivatization of aromatic acids with different catalyst system of subsequent BSTFA; C) Calibration curves obtained for trimethylsilyl esters of aromatic acids prepared with PFBHA/BSTFA protocol. The acids labels are provided in Table V.2. .... 80

Figure V.6 GC-MS TIC analysis of A) Aldehyde standards after derivatization with PFBHA·HCl, B) Acid standards (dicarboxylic acids, ketoacids and long monocarboxylic acids) after derivatization with PFBHA·HCl, and C) (hydroxy and aromatic acids) after esterification with MeOH in presence of PFBHA·HCl and subsequent BSTFA trimethylsilylation. The acids labels are provided in Table V.2. “HA3a” stands for vanillic acid methyl ester, “HA3b” stands for vanillic acid trimethylsilyl ester. .... 82

Figure V.7 Occurrence of aldehydes (A) and acids (B) determined in different amounts of WS PM using the developed PFBHA·HCl /BSTFA protocol. Aldehydes analysis performed by Mr. Chintapalli [118]..... 84

Figure V.8 Occurrence of aldehydes (A) and acids (B) determined in WS PM and UA PM using the developed PFBHA·HCl /BSTFA protocol..... 86

Figure A.1 Comparison of elution of succinic acid and its isomer methylsuccinic acid using developed GC-MS program ..... 106

Figure C.1 ESI-TOF-MS spectrum acquired using FIA in negative mode for RES, showing deprotonated molecular ion 227.07137 and confirmation ion 228.07765 (electrolyte: 0.1 mM acetic acid; fragmentor: 225 V; capillary: 3500 V) (A), R3G, showing deprotonated molecular ion 403.103456 and confirmation ion 227.07137 (no electrolyte; fragmentor: 200 V; capillary: 4500 V) (B), and R3S, showing deprotonated molecular ion 307.028182 and confirmation ion 227.07137 (electrolyte: 1 mM ammonium acetate; fragmentor: 175 V; capillary: 4500 V) (C), with proposed fragmentation pathways inset, with all but the sodium adducts confirming previous interpretations [64,68,76,77]. .... 112

Figure C.2 Response (based on MS peak area) of RES, R3G, and R3S deprotonated ions at three capillary voltages (A) and four fragmentor voltages (B), determined in the negative mode using

FIA with 50% MeOH/H <sub>2</sub> O solvent. (For RES, R3G, and R3S, fragmentor and capillary p<0.0005.).....	113
Figure C.3 Response (based on MS peak area) of deprotonated RES ions, from DOE optimization of nebulization conditions, determined in the negative mode using FIA with 50% MeOH/H <sub>2</sub> O solvent. (For gas temperature, nebulization pressure, and flow rate: p<0.0005; gas temperature and nebulizer pressure p=0.001, gas temperature and flow rate p=0.001, nebulizer pressure and flow rate p=0.033.).....	114
Figure C.4 ESI-TOF-MS spectrum of suspected resveratrol sulfate derivatives X1 (A) and X2(B) acquired using in negative mode.....	115
Figure D.1 Effect of sonication on derivatization of aldehydes with ACN/DCM/MeOH (1:8.5:0.5 v/v/v). The arrow denotes statistically significant difference between no sonication and overnight sonication (t-test at 95 % confidence level). Analysis performed by Mr. Chintapalli [118].....	155
Figure D.2 The effect of heat and mixing compared to sonication. A) mixing and heating, b) sonication. Peaks 1-7 correspond to dimethyl esters of dicarboxylic acids in following order: suberic, azelaic, sebacic, undecanedioic, dodecanedioic, tridecanedioic, tetradecanedioic, respectively. Peaks 8-14 correspond to monomethyl esters of dicarboxylic acids in following order: suberic, azelaic, sebacic, undecanedioic, dodecanedioic, tridecanedioic, tetradecanedioic, respectively.....	156
Figure D.3 The comparison of normalized peak area of TMS derivatives of aromatic acids in system with initial and increased content of PFBHA.HCl and methanol.....	157
Figure D.4 GC-EI-MS chromatograms showing composition of extracts obtained by sequential extraction of aldehydes from WS PM (2 mg) a) Sonication with MeOH in the presence of 2 mg WS PM under sonication b) Extraction from ACN/DCM/MeOH under sonication c) Soxhlet extraction with MeOH for 18h. Analysis performed by Mr. Chintapalli [118]. .....	157



## LIST OF ABBREVIATIONS

AA	Aromatic Acids
ACN	Acetonitrile
AL	Aldehydes
AMDIS	Automated Mass Spectral Deconvolution and Identification System
BSA	<i>N,O</i> -bis(trimethylsilyl)acetamide
BSTFA	<i>N,O</i> -bis(trimethylsilyl)trifluoroacetamide
DA	Dicarboxylic Acids
DCM	Dichloromethane
DOE	Design of Experiments
E2	Estradiol
EI	Electron Ionization
ESI	Electrospray Ionization
FIA	Flow Injection Analysis
GC	Gas Chromatography
GSH	Glutathione
HA	Hydroxyacids
HMDS	Hexamethyldisilazane
HRMS	High Resolution Mass Spectrometry
IS	Internal Standard
KA	Ketoacids
LC	Liquid Chromatography
LOD	Limit of Detection
LOQ	Limit of Quantification
MA	Monocarboxylic acids
MeOH	Methanol
MS	Mass Spectrometry
MSTFA	<i>N</i> -methyl- <i>N</i> -(trimethylsilyl) trifluoroacetamide
MW	Molecular Weight
NCI	Negative Chemical Ionization
OFN	Octafluoronaphthalene
PFBHA·HCl	<i>O</i> -(2,3,4,5,6-pentafluorobenzyl)hydroxylamine hydrochloride
PJ	<i>Pulicaria jaubertii</i>
PM	Particulate Matter
PT	Purge & Trap

R3G	<i>trans</i> -Resveratrol-3- <i>O</i> - $\beta$ -D-glucuronide
R3S	<i>trans</i> -Resveratrol-3- <i>O</i> -sulfate
RES	<i>trans</i> -Resveratrol
RS	Recovery Standard
RSD	Relative Standard Deviation
RtS	Resveratrol trisulfate
SRM	Standard Reference Material
TG	Triacylglyceride
TIC	Total Ion Current
TMCS	Trimethylchlorosilane
TMS	Trimethylsilyl
TMSI	Trimethylsilylimidazole
TOF	Time-of-Flight
UA	Urban Air
WS	Wood Smoke
$r_{12}$	Relative retention time to internal standard
$t_R$	Retention time
AcOH	Acetic acid
NH <sub>4</sub> OAc	Ammonium acetate
NA	Not Applicable
ND	Not Detected
NR	Not Reported
$m/z$	Mass-to-charge ratio
CI	Chemical Ionization
NCI	Negative Chemical Ionization
PCI	Positive Chemical Ionization
SITI	Single Ion – Total Ion
SIM	Single Ion Monitoring

## ACKNOWLEDGMENTS

I would like to express my sincere appreciation my advisor, Dr. Alena Kubátová for her unwavering support, guidance, motivation and mentoring throughout my Doctoral Studies. I would like to thank to Dr. Evguenii Kozliak for his thorough help with revising my manuscripts as well as guidance, advice and support. I also appreciate the support of my other committee members Dr. David Pierce, Dr. Julia Zhao, and Dr. David Delene.

Big thanks go to Klára Kukowski for her work on the succinic acid project (Chapter II), to Dr. Matthew Picklo and Dr. Ghanya Al-Naqeeb for allowing me to collaborate with them on the *Pulicaria* project (Chapter III), to Kari Kusler, Dr. Edward Sauter, Dr. Ke Zhang and Dr. Novikov for collaboration on the resveratrol project (Chapter IV), to Manik Chintapalli for his work on aldehydes in the acids and aldehydes project (Chapter V). I would also like to thank everyone in my research group (Klára, Honza, Nastya, Keith, Rich, Josh S., Josh H., Brett and Audrey) and collaborators from outside UND Chemistry Department, particularly Pavlína (Karlička) Karlová (University of Chemical Technology in Prague), Jeff Warwick and Jennifer Zabel (BioAmber Inc.).

I would like to thank to the University of North Dakota, UND Chemistry Department, and UND Graduate School for accepting me to the program and supporting me financially.

I appreciate the financial support from the following funding agencies: The North Dakota EPSCoR Programs (Sunrise, Advanced Undergraduate Research Award, Doctoral Dissertation Award, Dakota BioCon), UND Graduate School, UND Faculty Research Seed award, USDA-ARS Projects 5450-51000-048-00D, and BioAmber Inc.

Finally, I would like to thank my family and friends (particularly Jeff Zimney, Ivana Brzoňová, Matthew Leiphon, Rachel Leiphon, Marie Koubková, Shawn Spence, Megan Fruen, Kridhita Rana Magar, and Asina) for their consistent support, understanding and encouragement to pursue my Doctoral degree.

To my parents Dana and Mirek Rousovi,  
Because without you this could not (literally!) have happened.

You are the best!

## ABSTRACT

One of the challenges in characterization of complex environmental matrices and renewable materials is the determination low molecular weight polar compounds (LMWPCs). Depending on the matrix, the targeted LMWPCs include acids, aldehydes, sugars, sugar alcohols or aminoacids. To investigate the role and impact of these species, a development of accurate and precise analytical protocols is essential. One of the challenges in analysis of LMWPCs is their volatility and thus potential losses during sample preparation. The various matrices including renewable materials may contain >100 compounds that are either non-targeted (i.e., their identity is not known prior to the analysis) or targeted (specific compounds within the matrix). Gas or liquid chromatography coupled with mass spectrometry (GC-MS or LC-MS, respectively) are the preferred methods of analysis because they adequately address the simultaneous identification of numerous non-targeted compounds and quantification of targeted compounds. Analysis of low molecular weight polar compounds in four different matrices and materials, each representing a unique challenge, are presented in this dissertation including characterization of biologically produced succinic acid (Chapter II), investigation of the composition of a methanolic extract of *Pulicaria jaubertii* and its fractions (Chapter III), serum of rats after exposure to resveratrol (Chapter IV) and atmospheric particulate matter (PM, Chapter V).

Biologically produced succinic acid needs to be free of undesirable compounds, such as short-chain carboxylic acids, which cause odor, and sugars and sugar alcohols, which can partake

in a Maillard reaction in the presence of nitrogen containing compounds. We have adapted derivatization followed by GC-MS to identify and quantify more than 120 impurities in several succinic acid samples. This study focused on petroleum based succinic acid as well as bio-based samples that use a modified *E. coli* strain for fermentation. To enable an accurate quantification of both the target product and common impurities, we evaluated the acetonitrile extraction efficiency as an alternative to direct derivatization, and then compared several derivatization agents for trimethylsilylation. A prior ACN extraction was shown to be essential to detect impurities in trace concentrations. *N,O*-bis(trimethylsilyl)trifluoroacetamide (BSTFA) was most efficient for derivatization of saccharides and low molecular weight monocarboxylic acids. However, the presence of pyridine was shown to be necessary for derivatization of saccharides and polyalcohols with BSTFA, whereas low molecular weight acids had to be quantified without pyridine. Fourteen representative bioproduced succinic acid samples differing in production stage and cultivation method were characterized. The screening of initial-process (1<sup>st</sup> stage of synthesis) samples showed that monocarboxylic acids were the most abundant and suggested the occurrence of saccharides. Thus, we have developed a method allowing for quantification of carboxylic acids and saccharides with limits of detection between 0.02–0.3 ng. In the initial-process bacterial samples and petrochemical sample, formic, acetic, lactic, oxalic, benzoic, citric and malic acids as well as glycerol, butanediol and glucose were found in a range of 0.02–1160 µg/g. In final-process samples, formic and acetic acid, and glucose were found in concentrations lower than 0.001%, thereby demonstrating the effectiveness of the process as well as the applicability of the method for quality control measure of the process.

*Pulicaria jaubertii* is a Middle Eastern medicinal plant with anti-obesity potential. To characterize its biologically active compounds, extraction with methanol was performed. This extract was further fractionated to hexane, dichloromethane and water/methanol. Analysis by GC-MS and LC coupled with high resolution mass spectrometry (HRMS) demonstrated the presence of catechin-like moieties in the dichloromethane and methanolic fractions and suggested that these components were partially responsible for the bioactivity of these fractions. Our data indicate that fractions derived from PJ exhibit anti-adipogenic properties in part owing to the presence of catechin-like compounds.

*Trans-resveratrol* (3,5,4'-trihydroxy-*trans*-stilbene) (RES) is a polyphenol found in many foods, such as peanuts, berries and red wine. In this study we developed a sensitive method using LC coupled to electrospray ionization (ESI) with high resolution time of flight (TOF) MS for the determination of RES. This method enabled an investigation of a relationship between tumor growth in rats and concentration of RES and its primary metabolites, *trans-resveratrol*-3-*O*-sulfate (R3S) and *trans-resveratrol*-3-*O*- $\beta$ -D-glucuronide (R3G), in rat serum after RES exposure (5 or 25 mg/kg/day). RES levels in rat serum were near the limit of detection, showing concentrations of  $4\pm 1$  and  $12\pm 4$  ng/mL for low and high-dose exposure, respectively. Compared to RES, higher concentrations were found for its metabolites (R3G:  $4.8\pm 0.3$  and  $6.8\pm 0.3$   $\mu$ g/mL; R3S:  $0.27\pm 0.09$  and  $0.34\pm 0.04$   $\mu$ g/mL, respectively). Using LC-ESI-HRMS, for the first time, we measured the matrix-affected limits of detection (LODs) in plasma (3.7, 82.4, and 4.7 ng/mL for RES, R3G, and R3S, respectively), which were comparable to those reported in previous work using LC tandem mass spectrometry, but with a benefit of obtaining a full mass spectral profile. The additional novelty of our study is in synthesis and application of deuterated recovery



standards enabling accurate and precise quantification. In order to develop a robust method, the ESI conditions were optimized using a multilevel full factorial design of experiments.

Understanding the occurrence of polar organic species in PM is essential because they are significant constituents of atmospheric carbonaceous PM and are also suggested to serve as cloud condensation nuclei. In this study, we propose a new analytical method allowing for the simultaneous methylation of the majority of carboxylic acids and derivatization of aldehydes (in contrast to sequential trimethylsilylation) enabling an easier interpretation of acids' mass spectra without any interference from hydroxy groups. The sequential trimethylsilylation is still employed though targeting only the remaining aromatic acids and compounds with hydroxy groups. The developed quantitative method for simultaneous determination of aldehydes and acids using PFBHA·HCl in methanol results in oximes and methyl esters, respectively; with the limits of detection between 0.04–1 µg/mL. The method has been successfully applied to a broad range of species with various functionalities (ca. 95 compounds), including long chain monocarboxylic acids, dicarboxylic acids, aromatic acids, ketoacids, hydroxyacids and aldehydes. The developed protocol was applied to wood smoke and urban air standard reference material 1648b PM. The aldehydes were observed in concentrations 10–3000 µg/g in wood smoke PM and 10–900 µg/g in urban air PM, while the observed acids were in concentrations 20–1800 µg/g in wood smoke PM and 15–1200 µg/g in urban air PM. The most prominent aldehydes were syringaldehyde and vanillin in wood smoke PM and glyoxal in urban air PM. The most abundant acids in both PM samples were short-chain dicarboxylic acids ( $\leq C_{10}$ ), while wood smoke PM had a high abundance of hydroxyacids (vanillic and malic acids), as well as ketoacids (glutaric and

oxalacetic), urban air PM also featured a high abundance of long-chain monocarboxylic acids ( $\geq C_{16}$ ).

# I. CHAPTER

## CHALLENGES IN ANALYSIS OF LOW MOLECULAR WEIGHT POLAR COMPOUNDS & STATEMENT OF PURPOSE

One of the challenges in characterization of complex environmental matrices and renewable materials is the determination of low molecular weight polar compounds (LMWPC). For the purpose of this dissertation, LMWPCs are defined as compounds with the molecular weight less than 500 amu and with at least one or more polar functional group, such as carbonyl, carboxyl or hydroxyl group. Depending on the matrix, the targeted LMWPCs may be acids, aldehydes, sugars, sugar alcohols or aminoacids. These compounds can either be desirable, such as polyphenols with antioxidant properties in plants or plant products [1], or undesirable in the case of impurities in renewable chemicals [2]. The adverse effect of the impurities may be odors or coloration of downstream products [2]. In the case of atmospheric chemistry, LMWPCs are significant constituents of atmospheric carbonaceous particulate matter (PM) formed as a result of both primary emissions and secondary atmospheric reactions as well as a potential source of cloud condensation nuclei [3–5].

To investigate the role and impact of the LMPWC species, development of accurate and precise analytical protocols is essential. For analysis of these compounds, one must optimize a sample preparation, e.g., derivatization, together with an appropriate choice of a chromatographic method, i.e., liquid or gas chromatography coupled with mass spectrometry (LC-MS and GC-MS, respectively). One of the challenges in the LMWPC analysis is their volatility

and thus potential losses during sample preparation. Another obstacle may be their high polarity leading to a possible adhesion to a surface and possibly inefficient extraction from a broad range of matrices. The matrices and renewable materials may contain >100 compounds that are either non-targeted (i.e., their identity is not known prior to the analysis) or targeted (specific compounds monitored within the matrix). Analyses of both types of compounds can take advantage of the chromatographic separation methods and mass spectra identification. For instance, when using GC-MS for non-targeted analysis, spectra generated with electron ionization (EI) can be matched to an extensive NIST mass spectra library. Complementary to using GC-MS with EI is LC coupled to high resolution mass spectrometry (HRMS), which provides exact molecular mass values, thus benefiting both targeted and non-targeted analysis.

In this dissertation, the development of analytical methods for LMWPC in four different matrices and materials are presented:

- Characterization of biologically produced succinic acid (Chapter II)
- Investigation of the composition of a methanolic extract of *Pulicaria jaubertii* and its fractions (Chapter III)
- Determination of *trans*-resveratrol (RES) and its metabolites in serum of rats after their exposure to resveratrol (Chapter IV)
- Determination of occurrence of aldehydes and acids in atmospheric PM (Chapter V).

General purposes of the specific projects are described below:

**Biologically produced succinic acid** has to be free of undesirable compounds, such as short-chain carboxylic acids, causing odor, and sugars and sugar alcohols, which can partake in a

Maillard reaction in presence of nitrogen containing compounds. The succinic acid itself can affect the analysis simply because of its overwhelming concentration. Thus, we developed a method for simultaneous saccharide and carboxylic acid determination using a GC-MS analysis ensuring efficient derivatization. The efficiency of a prior ACN extraction compared to a direct derivatization, and effectiveness of several derivatization agents/conditions for trimethylsilylation were evaluated. Finally, the effectiveness of the manufacturing processing and purification were assessed based on the concentrations of target species found in the samples.

***Pulicaria jaubertii*** is a Middle Eastern medicinal plant with potential for anti-obesity treatment. In order to characterize its biologically active constituents, the composition of the active fraction of methanol (MeOH) extracts was evaluated. For this project, the MeOH extract was dried and subsequently fractionated using liquid-liquid extraction from MeOH/water system first into hexane, then dichloromethane (DCM) and remaining MeOH/water was collected as the last fraction. A two-fold analysis was performed; first to identify which fraction has the greatest potential as medical treatment, and second to characterize all the fractions and identify the possible active compounds. In this case, combining both GC-MS and LC-HRMS takes advantage of both the EI spectral library (GC-MS) and accurate molecular mass determination (LC-HRMS).

**RES (3,5,4'-trihydroxy-*trans*-stilbene)** is a polyphenol found in many foods, such as peanuts, berries, and red wine. RES and its metabolites have been reported to exhibit anticancer, analgesic, cardioprotective, and neuroprotective effects. The goal of this study was to develop a method enabling an investigation of a relationship between the tumor growth in rats and concentration of RES and its primary metabolites, *trans*-resveratrol-3-*O*-sulfate (R3S) and *trans*-resveratrol-3-*O*- $\beta$ -D-glucuronide (R3G), in rat serum after a RES exposure (5 or 25 mg/kg/day) by

using LC coupled to electrospray ionization (ESI) with HRMS. To increase the method precision, deuterated standards of RES, R3G, and R3S were synthesized and used as recovery standards (RSs) added prior to the sample preparation in combination with an IS (pinosylvin), which was added before injection. This combination of RSs and IS (used frequently in environmental studies) allowed for an improved assessment of repeatability issues (i.e., whether the issues arise from sample preparation or analysis). The developed method was applied to rat serum samples following their exposure to RES.

**Understanding the occurrence of polar organic species in PM** is essential because they are significant constituents of atmospheric carbonaceous particulate matter (PM) and are also suggested to serve as cloud condensation nuclei [3–5]. The observed variety of carboxylic and carbonyl compounds in PM includes linear monocarboxylic acids, dicarboxylic acids, aromatic polycarboxylic acids, polycyclic quinones, hydroxyacids, oxoacids, aldehydes, dialdehydes, ketones and multifunctional aliphatic and aromatic compounds. To investigate the occurrence of compounds with various polar functional groups, such as hydroxyl, carbonyl or carboxyl groups present in PM, a multi-step derivatization is often employed prior to their GC analysis. The most common approach is the derivatization of carbonyl groups with *O*-(2,3,4,5,6-pentafluorobenzyl)hydroxylamine hydrochloride (PFBHA·HCl) and then a separate derivatization of carboxyl and hydroxy groups via either their trimethylsilylation with *N,O*-bis(trimethylsilyl)trifluoroacetamide (BSTFA).

Our goal was to first extract and derivatize aldehydes to stabilize them prior to further derivatization. We have evaluated two solvent systems used previously for extraction, ACN/DCM/MeOH and MeOH alone. An advantage of the use of MeOH in the presence of a HCl

salt was the concomitant methylation of carboxylic acids, allowing for simultaneous derivatization of both aldehydes and acids. Thus, in addition, we evaluated the influence of the methylation reaction conditions on the process efficiency and compared that to the methylation with  $\text{BF}_3$  and silylation with BSTFA. The efficiency of the proposed extraction method was studied using wood smoke (WS) PM, which has a higher abundance of organic compounds. The concentrations of acids and aldehydes were compared for two common PM matrices: WS and urban air (UA) standard reference material (SRM) PM.

## II. CHAPTER DETERMINATION OF IMPURITIES IN BIOPRODUCED SUCCINIC ACID

### II.1. BACKGROUND

At present, significant research resources are directed towards development of renewable products for replacing petrochemicals [2,6,7]. Among them, succinic acid, a precursor of a wide range of polyesters, has a market of 270,000 ton per year [6]. Consequently, bio-based succinate is receiving increasing attention, and with rising oil prices it has become a worthy competitor of petrochemical-based succinate [2,6]. The challenge of being cost competitive with petrochemical-based alternatives is being able to obtain high rates of production with little or no by-products, to efficiently use substrates, and to simplify the purification process [2]. The expected by-product of bioproduced succinic acid is acetic acid; however, other impurities, such as other carboxylic acids, amino acids, saccharides and polyalcohols might be present in trace amounts [2].

Chromatography is the preferred method of analysis because it adequately addresses a simultaneous identification and quantification of the targeted compounds (i.e., carboxylic acids, saccharides, and polyalcohols) [8]. However, not all chromatographic protocols are suitable for the given task. For example, the LC of short-chain carboxylic acids (e.g., acetic or formic) is usually performed in the presence of a strong acid, such as diluted sulfuric acid [8], which is not compatible with mass spectrometry thus preventing the identification of numerous species potentially present in samples. The determination of acetic acid is crucial, because it is considered



as the main impurity [2]. The alternative to LC is GC-MS. Although the separation using this method generally targets volatile, non-polar species, the use of derivatization for polar low molecular weight species (i.e., the expected impurities) enables detection with a good resolution and sensitivity [8].

Numerous studies addressing acids, saccharides and polyalcohols were performed using GC-MS with trimethylsilylation [9–23] (see Appendix A Table A.1 for their overview). Most of these studies characterize food products, focusing on relevant species occurring in fairly high concentration [8–13,20,22,24]. To our knowledge, no short-chain (i.e., highly volatile) monocarboxylic acids were reported. The shortest-chain acid reported was oxalic acid [15,16,20], which has two carboxylic groups available for derivatization and thus is less volatile than the derivatives of C<sub>1</sub> and C<sub>2</sub> monocarboxylic acids. Similarly, we did not find any study simultaneously addressing both saccharides and short-chain monocarboxylic acids. Finally, to our best knowledge, no study has yet addressed the most practical case characteristic for industrial production of pure chemicals when the trace amounts of impurities, such as acids, sugars and polyalcohols, were analyzed in the presence of a high concentration of one major mixture component, e.g., succinic acid.

Several options are available for selecting the derivatization agents for GC-MS analysis of both acids and saccharides. The most common approach is derivatization with hydroxylamine in pyridine in combination with hexamethyldisilazane (HMDS) with trifluoroacetic acid [9,10,12–14], where hydroxylamine reacts with the saccharide carbonyl group while HMDS functionalizes the moiety containing a reactive hydrogen atom, i.e., carboxyl, hydroxyl and phenyl groups. However, the use of two derivatization agents may lead to uncertainties as the optimal

conditions for two different derivatization methods may not match. Also, HMDS is not the most efficient derivatization agent, leaving less reactive sources of active hydrogen, e.g., amino groups, unaltered [23]. For a more efficient derivatization of active hydrogen groups, including amino groups, either N-methyl-N-(trimethylsilyl) trifluoroacetamide [17,20] (MSTFA) or BSTFA [15,16,18,19] is typically employed. The derivatization with BSTFA is often catalyzed with trimethylchlorosilane [15] (TMCS) or, in specific cases, trimethylsilylimidazole [11]. Because trimethylsilylation is water-sensitive, the most common pretreatment of samples is either evaporation [9–11,13,19,20,25] or lyophilization [17]. However, the short-chain monocarboxylic acids are volatile and thus may be lost together with the solvent, which might lead to underestimation of their content.

Thus, in order to provide a comprehensive characterization of impurities in bioproduced succinic acid samples, we developed a method for simultaneous saccharide and carboxylic acid determination using a GC-MS analysis and ensuring efficient derivatization. The efficiency of prior ACN extraction compared to direct derivatization, and effectiveness of several derivatization agents/conditions for trimethylsilylation was evaluated. Finally, the effectiveness of the manufacturing processing and purification were assessed based on the concentrations of target species found in the samples.

## II.2. MATERIALS AND METHODS

### II.2.1 Studied samples

Fifteen samples of succinic acid were used (labeled A–P; the complete list including detailed sample descriptions is provided in Appendix A Table A.2). Samples C–P were produced

on a large scale with *E. coli* bacteria using adapted protocol [26]. Briefly, the fermentation took place for 36 hours at 35 °C using glucose based media enriched with ammonia as nitrogen source. The purification was accomplished via anion and cation exchange followed by electro dialysis to remove ammonium. Crystallization was used to further improve quality (samples G and L). Samples M–O were produced using a corn steep liquor, which is a by-product of corn wet milling. An analytical standard of succinic acid (99% purity; Sigma-Aldrich, St. Louis, MO, USA) and sample A were used as references, where sample A was petroleum based succinic acid.

## II.2.2 Chemicals

ACN, MeOH (both LCMS Optima grade), and DCM (GC quality) were purchased from Fisher Scientific (Waltham, MA, USA). Water was purified using a Direct-Q3 water purification system with incorporated dual wavelength UV lamp (Millipore, Billerica, MA, USA) for low total carbon content (the manufacturers claimed impurity is less than 5 ng/g). Derivatization agents BSTFA (99%) with 1% of TMCS, BSTFA with 10% of TMCS, and MSTFA were obtained from Sigma-Aldrich. Pyridine (99%) was obtained from Alfa Aesar (Ward Hill, MA, USA). The compounds quantified are listed in Table II.1 along with their suppliers.

**Table II.1** List of acids, saccharides and polyalcohols studied, their suppliers, the GC–MS retention times, target and confirmation ions (used for quantification) of their trimethylsilyl derivatives used for data processing, and LODs. All acronyms are defined in the list of abbreviations.

	Supplier	t <sub>r</sub> [min]	r <sub>12</sub>	MW ion	Target ion	Confirmation ions	LOD [ng]
formic acid	Fluka <sup>a</sup>	2.8	0.1	118	103	73, 45	0.2
acetic acid	Fisher <sup>b</sup>	3.9	0.2	132	117	75, 45	0.3
lactic acid	Sigma- Aldrich <sup>c</sup>	12.3	0.5	230	191	147, 117	0.2
oxalic acid	Sigma- Aldrich	13.6	0.6	230	190	219, 147	0.2
3-hydroxybutyric acid	Sigma- Aldrich	13.8	0.6	244	191	233, 117	0.04
butanediol	Sigma- Aldrich	13.9	0.6	234	177	147, 116	0.02
benzoic acid	Sigma- Aldrich	15.3	0.7	192	179	135, 105	0.4
glycerol	Fisher	15.7	0.7	308	205	218, 117	0.2
proline	Sigma- Aldrich	15.9	0.7	259	142	216, 73	0.1
malic acid	Sigma- Aldrich	18.5	0.8	344	233	245, 147	0.04
phthalic acid	Sigma- Aldrich	20.8	0.9	310	295	147, 73	0.1
xylitol	Supelco <sup>d</sup>	21.0	0.9	502	307	319, 217	0.04
arabitol	Supelco	21.1	0.9	502	307	319, 217	0.02
ribitol	Supelco	21.2	0.9	502	319	307, 217	0.06
citric acid	Sigma- Aldrich	22.2	1.0	480	273	465, 73	0.03
glucose	Supelco	23.1	1.0	530	204	191, 147	0.02
sucrose	Supelco	29.8	1.3	902	361	217, 73	19

<sup>a</sup> Fluka – St. Louis, MO, USA; <sup>b</sup> Fisher – Waltham, MA, USA; <sup>c</sup> Sigma-Aldrich – St. Louis, MO, USA; <sup>d</sup> Supelco – St. Louis, MO, USA

### II.2.3 Sample preparation

*Direct BSTFA derivatization.* Samples (1.0 mg) were directly mixed with 50 µL BSTFA and derivatized overnight at 60 °C. The amount of BSTFA was calculated to be in a 20-fold molar excess, considering the amounts of succinic acid in the samples. Samples were diluted to 200 µL using DCM together with 5.0 µL of an internal standard (IS, *o*-terphenyl) to control the volume changes, and analyzed in vials with 400 µL inserts.

*Extraction.* Bioproduced succinic acid samples ( $1.00 \pm 0.05$  g) were sonicated overnight with 1 mL of ACN. After sonication, the samples were filtered through some purified glass wool inserted into a Pasteur pipette.

*BSTFA derivatization.* Filtered ACN extracts (100  $\mu$ L aliquot) were mixed with 50  $\mu$ L BSTFA (99% + 1% TMCS), then derivatized for 1 h at 60 °C. Alternatively, samples were derivatized for 18 h at 70 °C in order to achieve a complete derivatization of saccharides and polyalcohols.

*BSTFA derivatization with ACN.* Acid and saccharides standards (100  $\mu$ L) were dried and subsequently mixed with 50  $\mu$ L BSTFA and 100  $\mu$ L ACN and derivatized for 18 h at 70 °C.

*BSTFA derivatization with pyridine.* Filtered ACN extracts (100  $\mu$ L aliquot) were mixed with 60  $\mu$ L BSTFA (99% + 1% TMCS) and 60  $\mu$ L of pyridine and derivatized for 18 h at 70 °C.

*MSTFA derivatization.* Acid and saccharides standards (100  $\mu$ L) were mixed with 50  $\mu$ L MSTFA and derivatized for 18 h at 70 °C.

*Calibration.* Stock solutions of individual compounds were prepared and combined into two mixtures, i.e., acids (the final concentration ca. 0.5 mg/mL per analyte) and saccharides (the final concentration ca. 0.2 mg/mL per analyte). The calibration range was between 0.001–50  $\mu$ g/mL, where the highest calibration point corresponded to ca. 30  $\mu$ moles of carboxylic or hydroxy groups. The list of compounds with their retention times, target and confirmation ions used for data processing is provided in Table II.1.

Prior to the analysis an IS (*o*-terphenyl, 10  $\mu$ L, ca. 1 mg/mL), was added to all samples, and the solution was diluted to 1.0 mL using DCM unless stated otherwise.

## II.2.4 Instrumentation

GC analyses were performed using a 5890 GC with 5972 MS equipped with an autosampler (6890 series, Agilent Technologies, Santa Clara, CA, USA). Injections were performed in the splitless mode for 0.50 min at 250 °C and the injection volume was 1 µL. The separation was performed using a 52-m long DB-5MS capillary column, with 0.25 mm internal diameter (I.D.) and 0.25 µL film thickness (J&W Scientific, Folsom, CA, USA). A constant flow of the carrier gas (helium) at a flow rate of 1.0 mL/min was maintained during the analysis. The temperature program used was adapted from previous work [27,28], and started at 35 °C held for 5 min, followed by a gradient of 15 °C/min to 300 °C and held for 1 min. The MS data in total ion chromatograms (TIC) were acquired in the mass range of  $m/z$  of 35–1000 at a scan rate 2.66 scan/s using the EI of 70 eV. The MS was turned off to eliminate the signal from the derivatization agents and their by-products in periods determined by observing the increase of pressure in MS. Namely, for BSTFA with pyridine, the MS was off for the first 2.5 min, 2.90–3.60 min, 4.40–7.00 min, 8.00–8.70 min; for MSTFA, the MS was off for the first 4 min.

## II.2.5 Data processing

GC-MS data were processed using ChemStation (version E.02.02.1431) and AMDIS software (Automated Mass Spectral Deconvolution and Identification System, version 2.71) [29]. Compounds' identification was based on confirmation with the corresponding analytical standard, or as isomers of standards with similar mass spectra and/or using NIST 05 Mass Spectra library.

AMDIS software was used for the deconvolution of MS ion spectra and tentative identification of impurities for which the analytical standards are not available. The tentative

identification was based primarily on the reversed match of >80% (described in Appendix A) and compared to the weighted match requiring at least 80% for both matching methods. Peaks found in the pure succinic acid standard and in the BSTFA blank were not considered. Based on TIC, the AMDIS program provided a percent response, which allowed for semi-quantification of impurities (Table II.2) and their comparison between the samples, by normalizing to the response of the IS. The protocol developed for AMDIS processing is included in Appendix A.

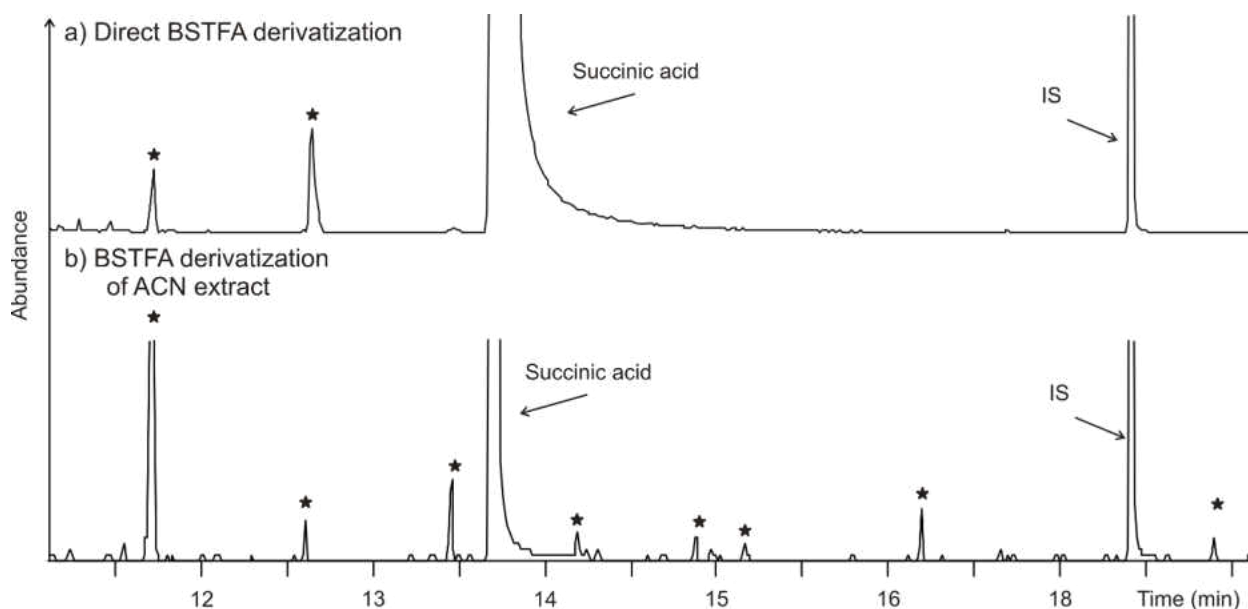
The limits of detection and quantification (LODs and LOQs) were determined using the target ions, which were selected based on the highest signal-to-noise ratio (ions listed in Table II.1). The instrumental LODs were calculated from calibration curves (within one order of magnitude of LOD) using the formula  $LOD=3.3*s_y/k$ , where k is a slope of the calibration curve and  $s_y$  is the standard error of the predicted y-value for each x-value;  $s_y$  was obtained by a least square linear regression. In order to report the low amounts of impurities we have used for quantification, lower limits of quantification were defined as  $LOQ=5* s_y/k$ .

The repeatability of the quantification method was evaluated using a representative sample of bioproduced succinic acid (C), which was chosen on the basis of preliminary testing. The sample was prepared in triplicate and analyzed in the following ways: 1) the same sample was analyzed three times in a row to assess the intraday GC repeatability; 2) the same sample was analyzed throughout the sequence on two consecutive days, to evaluate the interday GC repeatability; and 3) the extraction triplicate was analyzed to assess the extraction repeatability.

## II.3. RESULTS AND DISCUSSION

### II.3.1 Extraction vs direct analysis

The selection of a sample preparation method strongly affects the impurities detected. Thus, we first compared the extraction using ACN followed by BSTFA derivatization with direct BSTFA derivatization (no extraction). Figure II.1 shows that the ACN extraction was essential for characterization of impurities. A range of peaks representing impurities was observed in the majority of ACN extracted and BSTFA derivatized samples (Fig. II.1b, Table II.2). We expected enhanced derivatization when eliminating the extraction step and using BSTFA in molar excess; however no additional impurities were found when the direct analysis was applied (Fig. II.1a). The higher responses observed after extraction could be explained by a higher solubility of impurities in ACN than in the derivatization agent alone, combined with a lower solubility of succinic acid in ACN.



**Figure II.1** GC-MS analyses following a) direct BSTFA derivatization and b) derivatization of ACN extracted bacterial sample F. Stars mark the peaks of impurities in observed in bacterial samples. Chromatograms are scaled to the internal standard height. All acronyms are defined in the list of abbreviations.



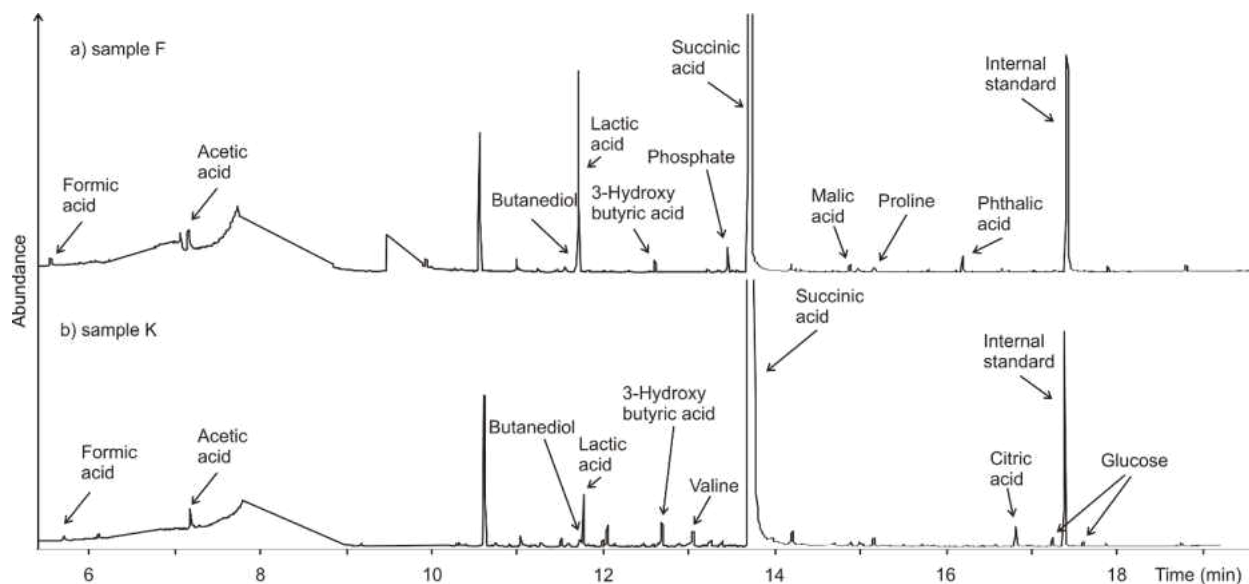
### II.3.2 Initial identification of impurities

The initial method of analysis was adapted from our previous work [27] allowing for quantification of a wide range of mono- and di-carboxylic acids. Over 120 peaks were observed in the initial process bacterial succinic acid samples upon derivatization with BSTFA. Table II.2 shows the normalized data for the most abundant species (the detailed list is in Appendix A Table A.3). The common impurities of higher abundance in the bacterial samples were formic, acetic, lactic and malic acids, butanediol and valine (Fig. II.2). Using this screening method, we also observed incompletely derivatized saccharides. Other compounds found in a lower abundance were oxalic, benzoic, phthalic, hexadecanoic, and octadecanoic acids (Table II.3). These acids might be from the sample preparation contamination, however their abundance in controls (experiment performed without analytes) seemed to be lower.

**Table II.2 Contaminants and their percent responses, with respect to an internal standard, observed upon BSTFA derivatization of an ACN extract of petroleum produced succinic acid and initial process bio-based succinic acid samples.**

$r_{12}$	Identified compounds	A (petroleum)	F (bacteria)	K (bacteria)	Confirmed <sup>a</sup>
0.319	formic acid	0.01	0.03	0.03	*
0.406	acetic acid	0.02	0.12	0.17	*
0.570	methyl-propanoic acid		0.03		
0.604	alanine			0.03	
0.608	dimethylsulfone			0.01	*
0.631	ethanediol	0.04			*
0.663	butanediol		0.02	0.03	*
0.672	lactic acid		0.74	0.30	*
0.694	alanine			0.01	
0.715	methyl butanol	0.01			
0.720	3-hydroxybutyric acid			0.02	*
0.722	oxypentanoic acid			0.02	
0.724	hydroxymethylbutyric acid		0.05		
0.736	pentenoic acid			0.03	
0.747	L-valine (bisTMS)			0.08	*
0.759	ethyl succinate			0.04	*
0.770	glycerol			0.04	*
0.773	phosphoric acid		0.10		
0.792	methyl succinic acid	0.03			
0.798	pyrimidine			0.02	
0.815	malic acid		0.03	0.08	
0.821	pentanedioic acid			0.02	*
0.854	malic acid	5.40	0.03	0.02	
0.860	hexanedioic acid		0.01		*
0.930	phthalic acid	0.03	0.05		
0.967	citric acid			0.07	*
0.992	heptanol derivative			0.04	
<b>1.000</b>	<b>o-terphenyl (IS)</b>	<b>1.00</b>	<b>1.00</b>	<b>1.00</b>	<b>IS</b>
1.012	glucose			0.02	

<sup>a</sup> Confirmed using the analysis of standard.



**Figure II.2 Comparison of GC-MS chromatograms of analysis BSTFA derivatization of ACN extracted bioproduced succinic acid samples, normalized to the same percent response of internal standard. Samples F(a) and K(b) were initial process samples.**

The screening results showed primarily acids, saccharides and polyalcohols, which are essential for production control on a large scale [2,7], and thus, the further quantification efforts targeted these species.

### II.3.3 Development of quantification method for analysis of acids and saccharides as the most abundant impurities

Based on our previous work [27] and reported data, several trimethylsilylation methods were compared to determine the most efficient approach for a simultaneous derivatization of saccharides and acids. These methods included the derivatization with MSTFA in the presence of ACN, and BSTFA (1% TMCS) with/without ACN or pyridine. The application of these derivatization agents to saccharides resulted in only an incomplete derivatization in MSTFA with or without ACN and in BSTFA without either pyridine or ACN (Figs. II.3a,b). Xue *et al.* [30] reported multiple peaks for glucose derivatized with MSTFA, however, it was not addressed. By contrast, BSTFA in the presence of either ACN or pyridine resulted in a complete derivatization of saccharides and

polyalcohols (Fig. II.3c,d). Nevertheless, further tests of derivatization evaluation of BSTFA with ACN and pyridine resulted in higher peaks or glucose in presence of pyridine (Fig. II.4). The comparison of extracted ion chromatograms of acetic acid (ion 117, [M-15]<sup>+</sup>) demonstrates that the MSTFA (Fig. II.5a) and BSTFA derivatization with ACN (Fig. II.5c) resulted in higher peaks compared to the derivatization using BSTFA with pyridine. Perhaps pyridine had a negative effect on the transfer of volatile analytes from the GC injection port to the column due to its relatively high boiling point and tendency to bind acids due to the formation of pyridinium salts. Therefore, the derivatization using BSTFA with ACN seemed to be optimal for acids, while BSTFA with pyridine was more effective for saccharides (Figs. II.3-5). We also tested the separation of succinic acid and its isomer, methylmalonic acid. Those compounds were completely separated as shown in Figure A.1.

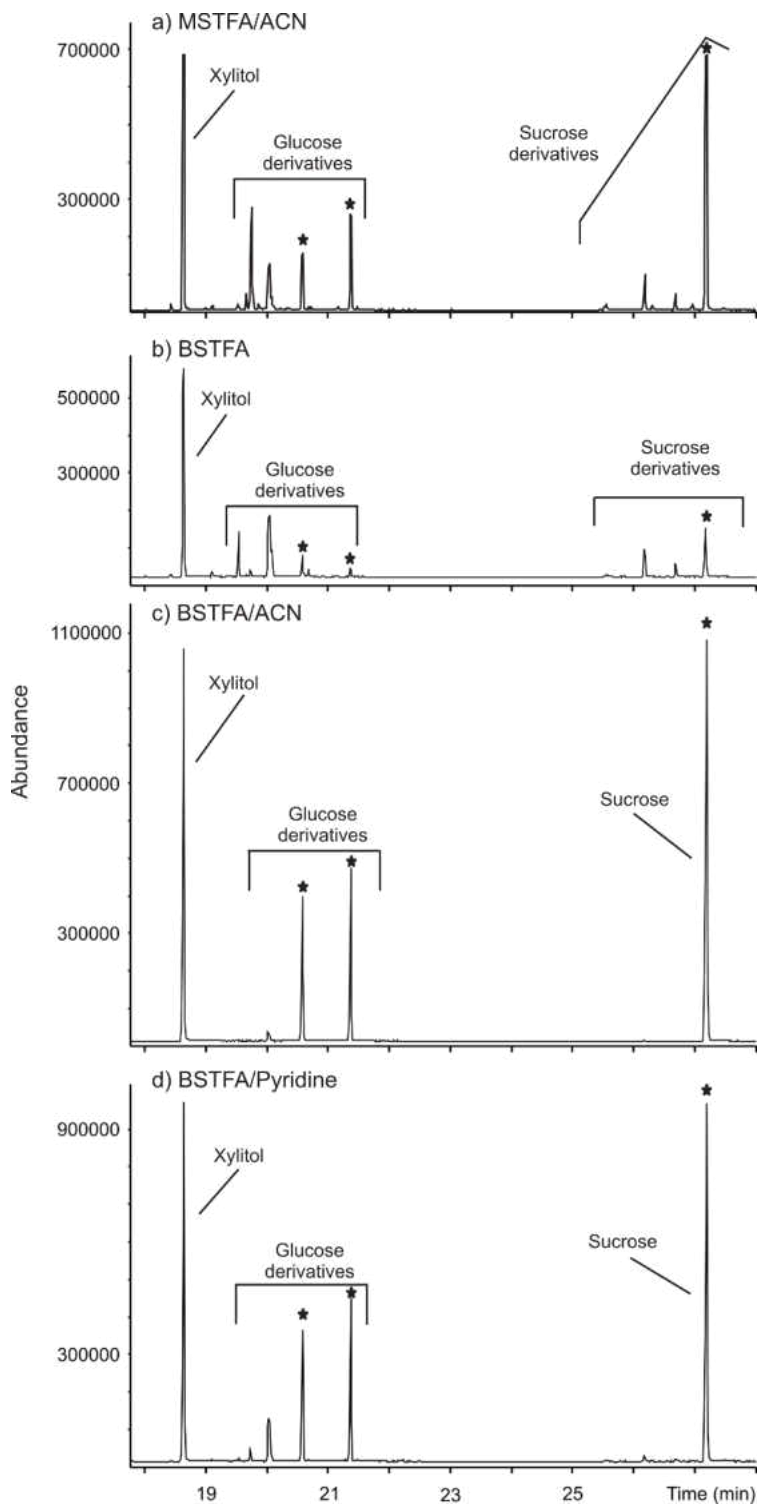


Figure II.3 GC-MS extracted ion chromatograms ( $m/z = 217$ ) of a mixture of standard saccharides and polyalcohols upon derivatization (18 h at 70 °C) with a) MSFTA with ACN, b) BSTFA (1%TMCS), c) BSTFA 1% TMCS with ACN, d) BSTFA (1% TMCS) with pyridine. The stars mark peaks of the completely derivatized sucrose and glucose. The scale is the same for all parts of the figure.

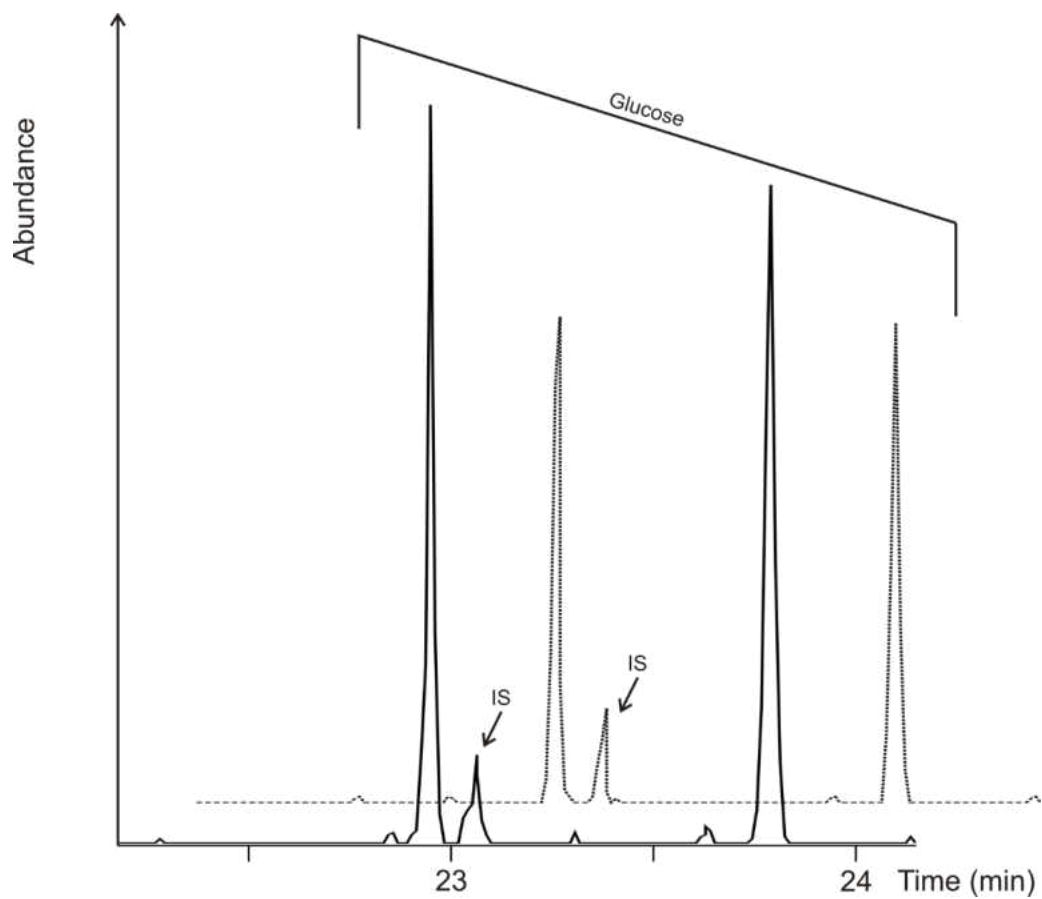


Figure II.4 GC-MS extracted ion 204 chromatograms of bio-produced succinic acid (sample F) upon derivatization with various derivatization agents for 18 hours at 70 °C. Derivatization with pyridine (solid line) provided higher response than derivatization with ACN (dashed line). The IS co-elutes with other derivatized hexose which is believed to be an impurity in the glucose standard.

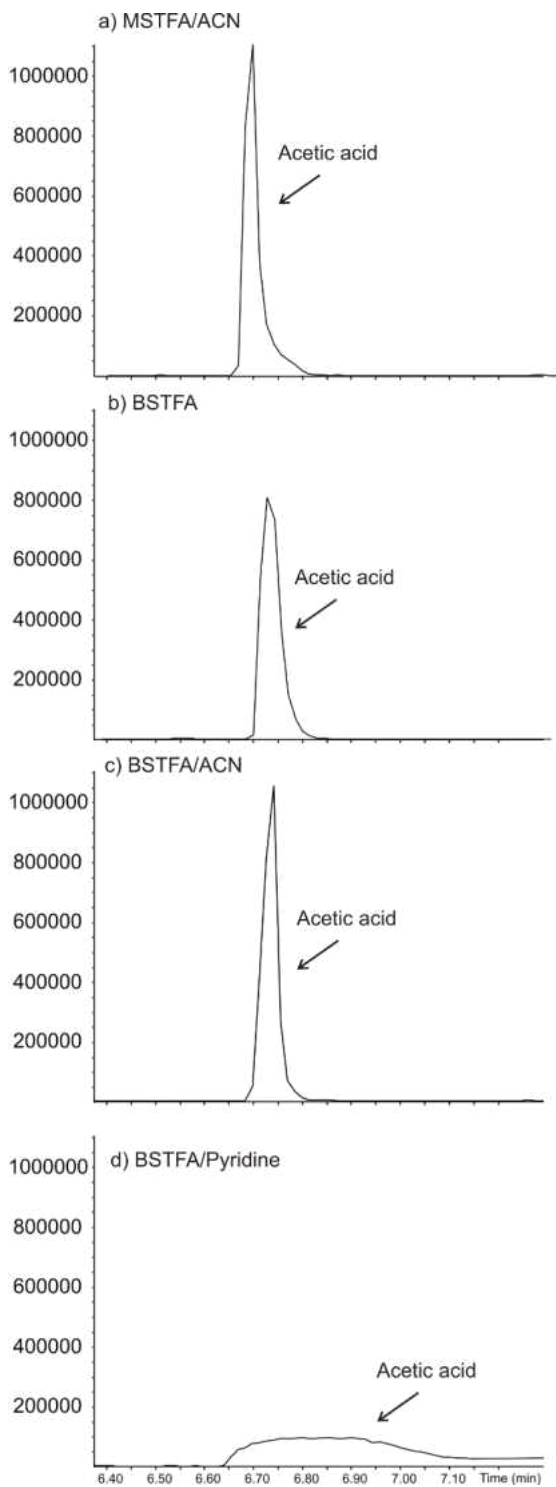


Figure II.5 GC-MS extracted ion chromatograms ( $m/z = 117$ ) of an acetic acid standard upon derivatization (18 h at 70 °C) with a) MSFTA with ACN, b) BSTFA (1%TMCS), c) BSTFA 1% TMCS with ACN, d) BSTFA 1% TMCS with pyridine.

### II.3.4 Limits of detection and repeatability

Table II.1 lists the obtained instrumental LODs, which were in a range of 0.03–0.6 ng for acids and 0.03–0.2 ng for saccharides and polyalcohols. The values obtained for acids are comparable to those reported in our previous study [27], while we achieved tenfold lower values for sugars than in the study of Adams *et al.* [14], where HMDS was used as a derivatization agent, possibly due to a more effective derivatization or broader calibration range. LOD's in other studies [15,17,19] were not comparable because they have been reported in different units, e.g. Pietrogrande and Bacco [15] reported them as air volume concentrations.

The repeatability of the developed quantification method on representative sample C is demonstrated in Table V.3. The GC intra- and interday repeatability as well as sample preparation were similar, with the relative standard deviation (RSD) <10%, with the exception of glycerol, for which the intraday reproducibility was 12%

**Table II.3 GC intra, interday, and extraction method repeatability for a bioprocessed sample of succinic acid (sample C) reported as a mean value (in µg/g) ± one standard deviation (n=3)**

Analyte	GC intraday			GC interday			Extraction		
lactic acid	6.3	±	0.5	6.2	±	0.4	6.0	±	0.1
benzoic acid	0.63	±	0.02	0.67	±	0.06	0.61	±	0.03
glycerol	0.12	±	0.01	0.11	±	0.01	0.12	±	0.01
glucose	0.08	±	0.01	0.08	±	0.01	0.071	±	0.004

### II.3.5 Characterization of succinic acid samples

The developed quantification method was applied to bioproduced succinic acid samples, as an application for monitoring the product quality. The targeted compounds were the most abundant acids, , i.e., formic, acetic, lactic, oxalic, 3-hydroxybutyric, benzoic, malic, phthalic and citric acids, as well as saccharides, and polyalcohols, i.e. butanediol, glycerol, xylitol, arabitol,



glucose, and sucrose (Table II.2). Due to the low concentrations of some of these compounds in the samples, quantification is reported only for a narrower range of these compounds featuring the concentrations above the corresponding LODs (Table II.4).

**Table II.4 Concentrations of acids and saccharides in bioprocessed succinic acid samples reported as a mean value (in µg/g) ± one standard deviation (n=3).**

Analyte	A		F		K		G		L	
	(petroleum)		(initial process)		(initial process)		(final process)		(final process)	
formic acid	15	± 5	5	± 2	1.1	± 0.03	1	± 0.06	1.5	± 0.8
acetic acid	Below LOQ		13	± 3	20	± 6	3.2	± 0.6	3.9	± 0.8
oxalic acid	8	± 5	Below LOQ <sup>a</sup>		Below LOQ		ND <sup>b</sup>		ND	
lactic acid	ND		186	± 19	27	± 4	ND		ND	
3-hydroxybutyric acid	Below LOQ		Below LOQ		1.1	± 0.1	ND		ND	
butanediol	Below LOQ		5.1	± 0.3	3.6	± 0.1	ND		ND	
benzoic acid	2.00	± 3	Below LOQ		ND		ND		0.2	± 0.0
glycerol	ND		0.49	± 0.06	ND		ND		3	± 3
malic acid	9	± 24	10	± 2	Below LOQ		Below LOQ		Below LOQ	
phthalic acid	7	± 2	ND		ND		ND		ND	
citric acid	ND		Below LOQ		8	± 1	ND		ND	
glucose	Below LOQ		3.1	± 0.2	0.07	± 0.01	0.0	± 0.00	2	± 1

### II.3.5.1 Abundance of acids, saccharides, and polyalcohols

Quantification confirmed the occurrence of all tested acids and glucose (Tables II.2 and II.4). The polyalcohols in samples were found as well but xylitol, arabitol and ribitol were below their LOD.

As mentioned above, acids were the prevailing impurities in the bacterial samples. Acetic acid is a common contaminant of biologically produced succinic acid [2], and for its unpleasant smell was an undesirable impurity. It was abundant in samples F and K (13 µg/g and 20 µg/g,

respectively), but its concentration decreased in purified sample G (3  $\mu\text{g/g}$ ). Formic acid, which also has an undesirable odor, was determined in all samples between 1  $\mu\text{g/g}$  in samples K, L, and M (Table II.5) and 16  $\mu\text{g/g}$  in samples A (petroleum-based sample). Similarly to acetic acid, formic acid concentration decreased after purification from 5  $\mu\text{g/g}$  (sample F) to 1  $\mu\text{g/g}$  (sample G). Malic acid, also used in industry for polymer production [7], was the major impurity in sample A (1.2 mg/g) and lactic acid was found in samples F and K (0.2 mg/g and 27  $\mu\text{g/g}$ , respectively).

Polyalcohols found in the samples were glycerol and butanediol (Table II.4). Glycerol was found in samples F and L (0.5 and 0.3  $\mu\text{g/g}$ , respectively). Butanediol was also found in sample F (5  $\mu\text{g/g}$ ) and sample K (4  $\mu\text{g/g}$ ). Ethanediol was observed petroleum based sample but it was not quantified in other samples. Sugar polyalcohols were not detected, with exception of arabitol, which was detected in sample N, but it was below its limit of quantification. Glucose was only representative of saccharides with its concentration up to 8  $\mu\text{g/g}$  in sample K (Table II.4).

The effect of production media on the purity of succinic acid was evaluated for samples K–O comparing the product produced by bacteria in a defined medium (sample K) and in corn steep liquor (samples M, N, O). Corn steep liquor is less expensive as it is a by-product of corn wet milling and so it is preferred in industry; however, the product obtained using this complex organic mixture was expected to contain more impurities. In contrast to this expectation, samples M, N, and O and other initial process samples contained similar impurities (formic acid, acetic acid and glucose), suggesting that the production medium had a lower impact on generation of the observed impurities than the production microorganism. Only oxalic acid was observed in a 4-fold higher abundance in sample M with corn steep, compared to sample K produced using a defined medium.

### II.3.5.2 Final Bacterial Process Samples

The effectiveness of the product purification was evaluated by the comparison of samples F and K (initial process), and G and L (final product) where G was purified F. While most of the targeted compounds were detected in the initial process samples, only formic and acetic acids were quantified in purified sample G, showing a decrease from 0.13  $\mu\text{g/g}$  to 0.06  $\mu\text{g/g}$  for formic acid and from 0.3  $\mu\text{g/g}$  to 0.1  $\mu\text{g/g}$  for acetic acid. Sample L showed also some glycerol present. Lactic and malic acids were both detected in the initial process samples, but were not found in refined samples (Table II.4). Thus, the developed method was demonstrated to be suitable for the quality control of the process and demonstrated purity of the final products.

## II.4 CONCLUSIONS

We developed a protocol for characterization and quality control of bioproduced succinic acid. A prior ACN extraction was found to be essential to detect impurities. The optimization of derivatization was critical for low molecular weight polar acids as well as saccharides; a procedure using BSTFA with pyridine as a catalyst was determined to be suitable for both polyalcohols and saccharides whereas the BSTFA with ACN treatment was found to be the most suitable for quantification of low molecular weight carboxylic acids. The presence of short chain monocarboxylic acids, i.e. formic and acetic acid, has an effect on the odor of the final product, which is undesirable in the industrial process. The presence of saccharides might lead to caramelization or Maillard reactions, resulting in coloring the final product. We achieved LODs as low as 0.02 ng for saccharides and 0.03 ng for acids, which makes the quantification method advantageous for detection of trace-level impurities even in the presence of one major

compound at a high concentration, e.g., succinic acid. The final process samples showed removal or decrease of all quantified compounds.

### III. CHAPTER

## CHARACTERIZATION OF BIOLOGICALLY ACTIVE MOLECULES IN PULICARIA JAUBERTII EXTRACTS USING GAS AND LIQUID CHROMATOGRAPHY AND MASS SPECTROMETRY

### III.1. BACKGROUND

In the Middle East, levels of obesity are growing along with the predicted consequences like insulin resistance [31,32]. This has resulted in increased attention towards the identification of the anti-obesogenic properties of traditional Middle Eastern herbal medicines. Species of the genus *Pulicaria* are widespread throughout the Mediterranean, Middle East, and Asia [33]. *Pulicaria jaubertii* Gamal-Eldin (PJ) is a traditional Yemeni flavorant and is used in the traditional medicines, as is typical of the genus *Pulicaria* [33–35]. The extracted oils of PJ are known to have cytotoxic effects towards breast cancer cells and moderate antimicrobial activities [36]. The extent to which PJ may contain phytochemicals with anti-obesogenic properties has not been explored.

Thus, a methanolic extract of PJ and its fractions were characterized to identify the possible active compounds. In this case, combining both GC-MS and LC-ESI-HRMS is taking advantage of both the EI spectral library and accurate molecular mass determination, respectively.

## III.2. MATERIALS AND METHODS

### III.2.1 Plant collection

PJ plant leaves and flowers were collected from Sana`a, Yemen by Dr. Al-Naqeb [37]. The plant was identified and authenticated by a plant taxonomist at the Department of Botany, Faculty of Agriculture, Sana`a University, Yemen. The plant material was air-dried being protected from light. Dried plant material was stored at 4 °C and protected from light prior to further use.

### III.2.2 Chemicals

MeOH (LC-MS Optima grade), and DCM (GC quality) were purchased from Fisher Scientific. *n*-Hexane (LC-MS grade) was obtained from JT Baker, USA. BSTFA (99%) with 1% TMCS was purchased from Sigma-Aldrich (St. Louis, MO, USA) and used to form trimethylsilyl (TMS) derivatives.

### III.2.3 Preparation of the PJ extract and its fractionation.

Dried PJ was finely ground using an electric grinder (Ika Labortechnik M 20 Brand). The resulting powder was extracted with MeOH with a 1:5 powder:MeOH (w/v) ratio for 48h, stirred under dark conditions. The resulting extract was filtered and the filtrate was concentrated by a rotary evaporation at 40 °C. The final extract was transferred into glass amber bottles and stored at 4 °C for subsequent analyses. A 5% yield of the final methanolic PJ extract, denoted PJ<sub>M</sub>, relative to starting powder was obtained.

For liquid-liquid fractionation, twelve grams of PJ<sub>M</sub> were mixed with *n*-hexane at a 1:5 w/v ratio and 100 mL of methanol: water (80:20 v/v) was added. The mixture was shaken in a separatory funnel and the *n*-hexane layer was collected. This step was repeated once more. DCM was added into the remaining aqueous residue and the process was repeated. The resulting DCM

and hexane fractions were concentrated to dryness using a rotary evaporator. The aqueous phase was subjected to freeze drying. The yields obtained for each PJ fraction with respect to the initial methanolic extract were: *n*-hexane (denoted PJ<sub>H</sub>) 5.0 g (41%), DCM (denoted PJ<sub>D</sub>) 1.8 g (16%) and residual MeOH:aqueous fraction (denoted PJ<sub>A</sub>) 1.2 g (8%).

#### III.2.4 Chemical characterization of PJ fractions.

For GC-MS analysis, the methanolic extract, PJ<sub>M</sub>, and each fraction (PJ<sub>H</sub>, PJ<sub>D</sub>, PJ<sub>A</sub>) were analyzed in the amounts proportional to the weight of corresponding fraction obtained from the extract (e.g., 5.0 mg of PJ<sub>H</sub>, 1.8 mg of PJ<sub>D</sub>). Samples were dissolved in 1.0 mL DCM with and without TMS derivatization with BSTFA. Prior to GC-MS analyses, 25 µL of IS (*o*-terphenyl, 1.4 mg/mL) was added to control volume changes in each sample. The tentative identification of observed compounds was based on comparison with the NIST 05 Mass Spectra library.

For TMS derivatization, appropriate amounts of the methanol extract and its fractions were weighed, dried, and reconstituted with and 100 µL of BSTFA and 50 µL pyridine. The solution was heated at 70 °C for 18 h. After derivatization 25 µL of IS (*o*-terphenyl) were added together with 0.85 mL of DCM.

GC-MS analyses were performed using a 6890N GC with 5975C MS (Agilent Technologies, Santa Clara, CA, USA) equipped with a Gerstel MPS2 autosampler (Gerstel, Baltimore, MD, USA). Injections (1 µL) were performed in a splitless mode for 0.40 min at 250 °C. Separation was performed using a DB-5MS capillary column (30 m), with 0.25 mm internal diameter (I.D.) and 0.25 µm film thickness (J&W Scientific, Folsom, CA, USA). A constant carrier gas (helium) flow rate of 1 mL/min was maintained during the analysis. The temperature program started at 35 °C held for 5 min, followed by a gradient of 10 °C/min to 300 °C and held for 1 min. The MS data in TIC

mode were acquired in the mass range of  $m/z$  of 35–1000 at a scan rate of 2.66 scan/s using an EI of 70 eV. The duration of the solvent delay was based on the elution of the derivatization agent, their by-products, and solvent retention times, measured by observing the vacuum change. Namely, for BSTFA with pyridine, the MS was off for the first 2.5 min, 2.90–3.60 min, 4.40–7.00 min, 8.00–8.70 min; for samples without derivatization, the solvent delay was 2.5 minutes.

For LC-MS analyses, a stock solution of each sample (P<sub>JM</sub>, P<sub>JH</sub>, P<sub>JD</sub>, P<sub>JA</sub>) was prepared in methanol in a concentration of 2–3 mg/mL. Stocks were further diluted to a final concentration of 10 – 16 ppm in ACN and water (50:50 v/v) with ammonium acetate (a final concentration of ca. 5 mM). LC-ESI-HRMS analyses were carried out using the electrospray ionization with time of flight mass spectrometer (G1969A, Agilent, Santa Clara, CA, USA) coupled to an Agilent LC 1100 LC) The column was a C<sub>18</sub> Zorbax Eclipse plus (2.1 x 150 mm with 3.5 $\mu$ m particle size) with a 1.2 cm guard column (Agilent). For the chromatographic separations, the mobile phase solutions consisted of 1.0 mM ammonium acetate in water:ACN (95:5, v/v) as solvent A and 1.0 mM ammonium acetate in ACN as solvent B. The flow rate was 0.2 mL/min, and the injection volume was 50  $\mu$ L with an injector needle wash program to avoid cross-contamination. The gradient elution program started isocratically at 0% B for 2 min, followed by a linear gradient to 80% B from 2 min to 30 min with maintenance of 80% B for 5 min. Following a sharp gradient to 100% A from 35 to 36 min, the column was re-equilibrated with 100% solvent A from 36 to 56 min. The column temperature was maintained at 30 °C. ESI was performed in negative mode with an electrospray voltage of 4500 V, a fragmentor voltage of 175 V, a nebulization pressure of 25 psig, a drying gas flow rate of 12 L/min, and a drying gas temperature of 350 °C.



### III.3. RESULTS AND DISCUSSION

#### III.3.1 Determination of bioactive fractions

PJ<sub>M</sub> was fractionated in the order of increasing solvent polarity into *n*-hexane (PJ<sub>H</sub>), DCM (PJ<sub>D</sub>) and aqueous (PJ<sub>A</sub>) fractions. Several methods were used to determine bioactivity by Dr. Al-Naqeb [37] including inhibition of TG accumulation. The bioactivity results (Appendix Table B.1) showed that the PJ<sub>D</sub> (i.e., the fraction recovered in DCM) but not the PJ<sub>H</sub> or PJ<sub>A</sub> fractions significantly inhibited TG accumulation.

#### III.3.2 Chemical characterization of PJ fractions

The PJ<sub>M</sub>, PJ<sub>H</sub>, PJ<sub>D</sub>, and PJ<sub>A</sub> fractions were analyzed by GC-MS and LC-ESI-HRMS in order to characterize the bioactive compounds present. GC-MS analyses were performed with and without the formation of TMS derivatives. The formation of TMS derivatives allows for analysis of compounds with limited volatility. Direct GC-MS analysis (without TMS derivatization) (Figure III.1) of PJ fractions showed that most fractions contained carvotanacetone, with the highest abundance in hexane fraction, i.e. PJ<sub>H</sub>. Other compounds were observed in limited abundance and the data are further detailed in Appendix B (Table B.2). These profiles are in agreement with prior reports on the chemical composition of other *Pulicaria* species [34,36,38,39].

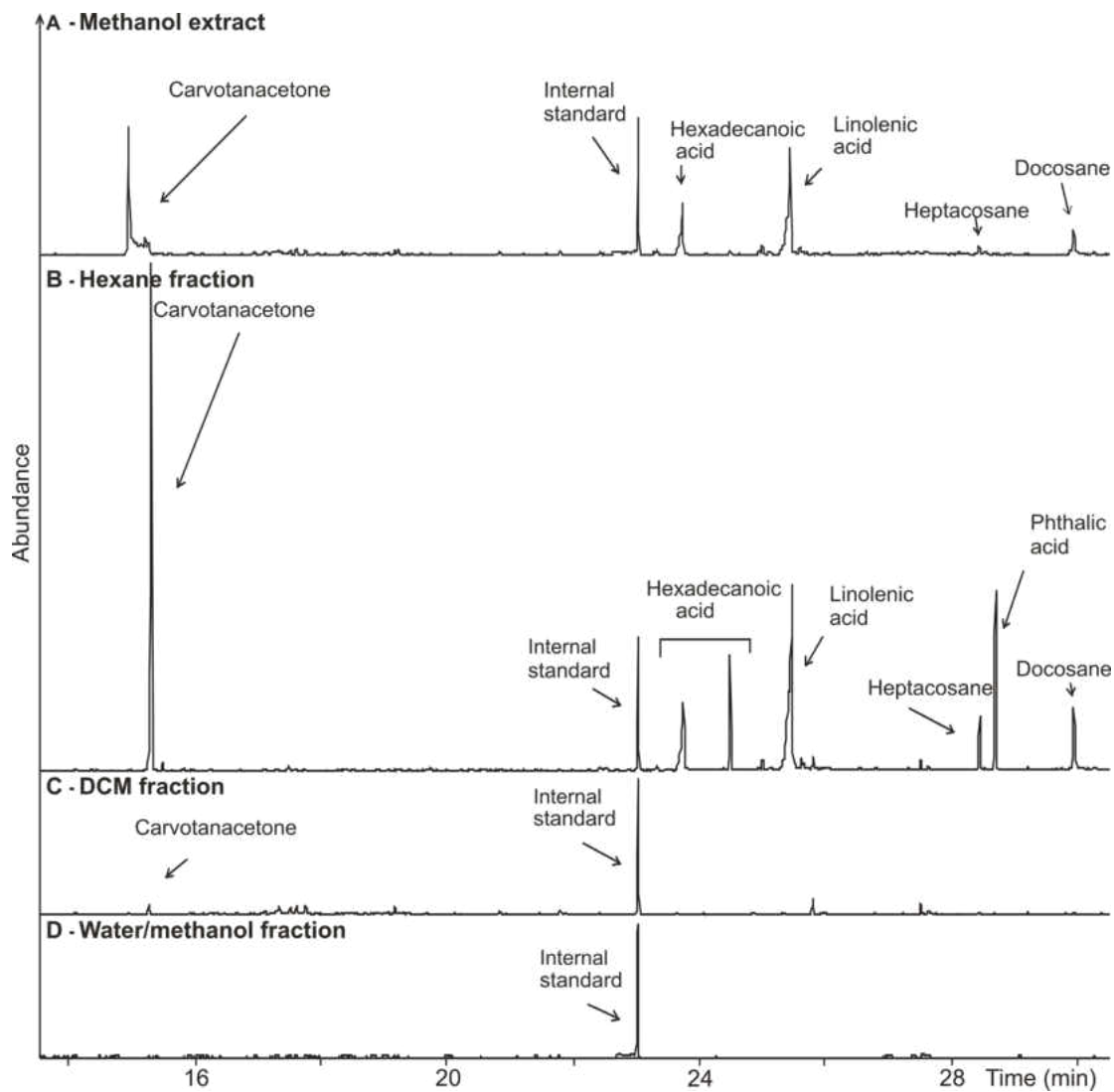


Figure III.1 GC-MS total ion current chromatograms of methanol extract and its fractions without TMS derivatization. (A) methanol extract (P<sub>JM</sub>), (B) DCM fraction (P<sub>JD</sub>), (C) n-hexane fraction (P<sub>JH</sub>), (D) water/methanol fraction (P<sub>JA</sub>). All chromatograms are normalized to the response of internal standard, thus providing proportional response based on quantities extracted.

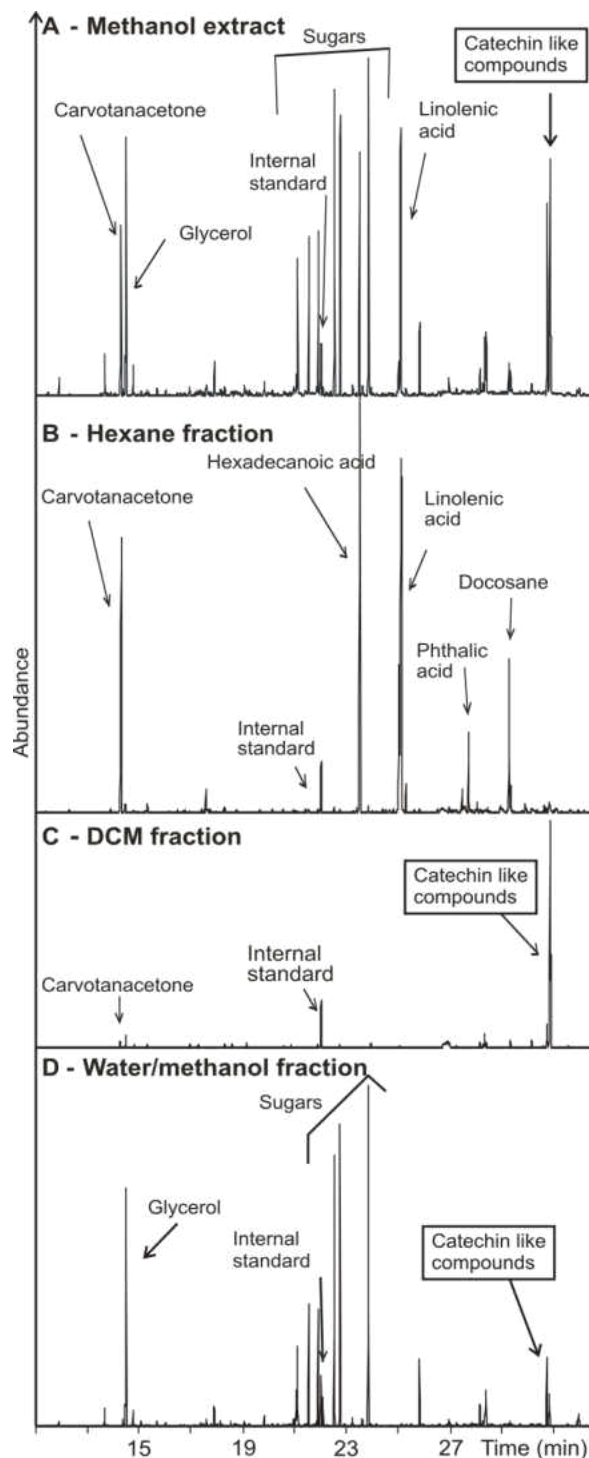
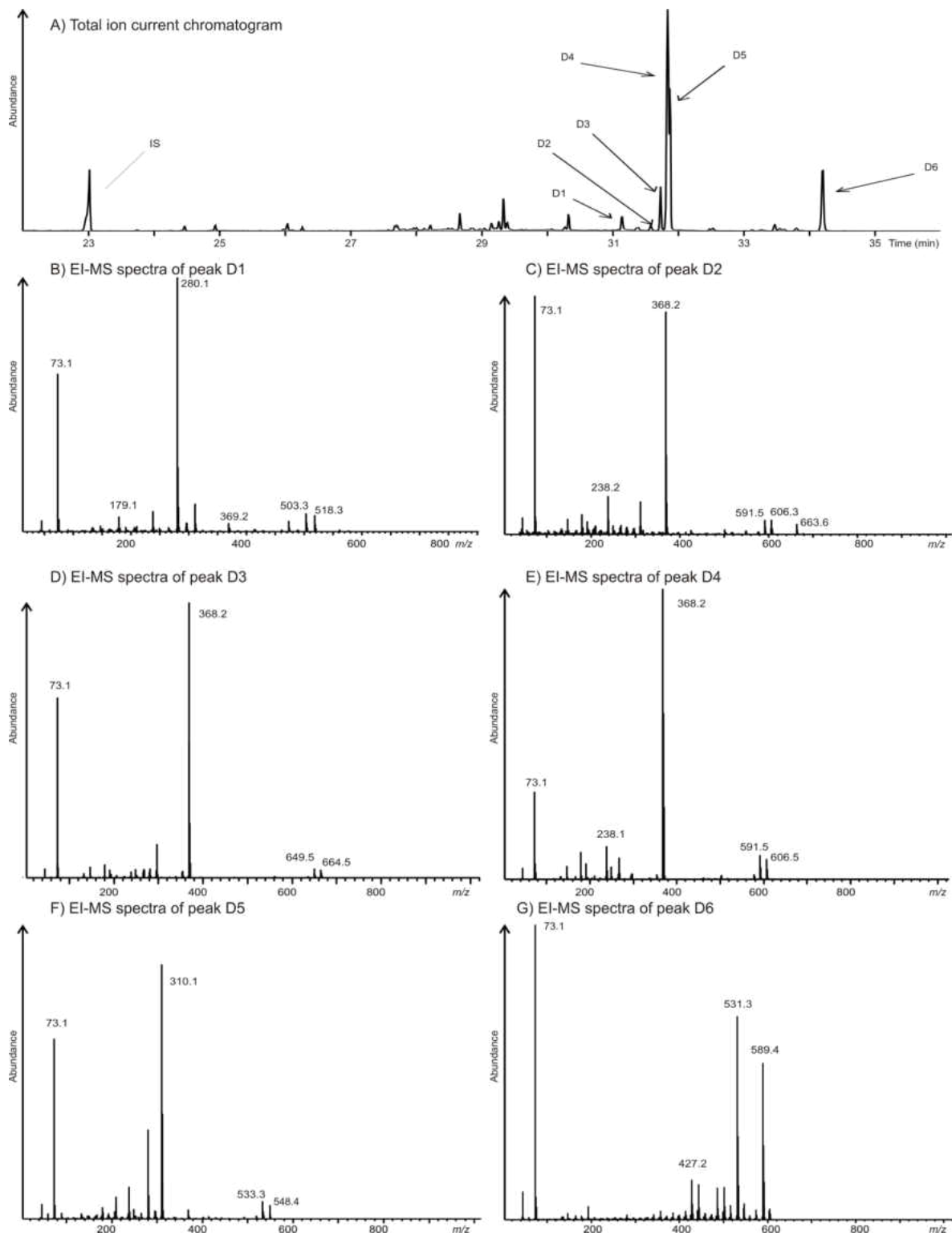


Figure III.2 GC-MS total ion current chromatograms of methanol extract and its fractions with TMS derivatization. (A) methanol extract ( $P_{JM}$ ), (B) DCM fraction ( $P_{JD}$ ), (C) n-hexane fraction ( $P_{JH}$ ), (D) water/methanol fraction ( $P_{JA}$ ). Note that analysis of TMS derivatives allowed for enhanced characterization of the fractions and allowed for identification of catechin-like compounds in the methanol extract and the DCM fraction. All chromatograms are normalized to the response of internal standard, thus providing proportional response based on quantities extracted.



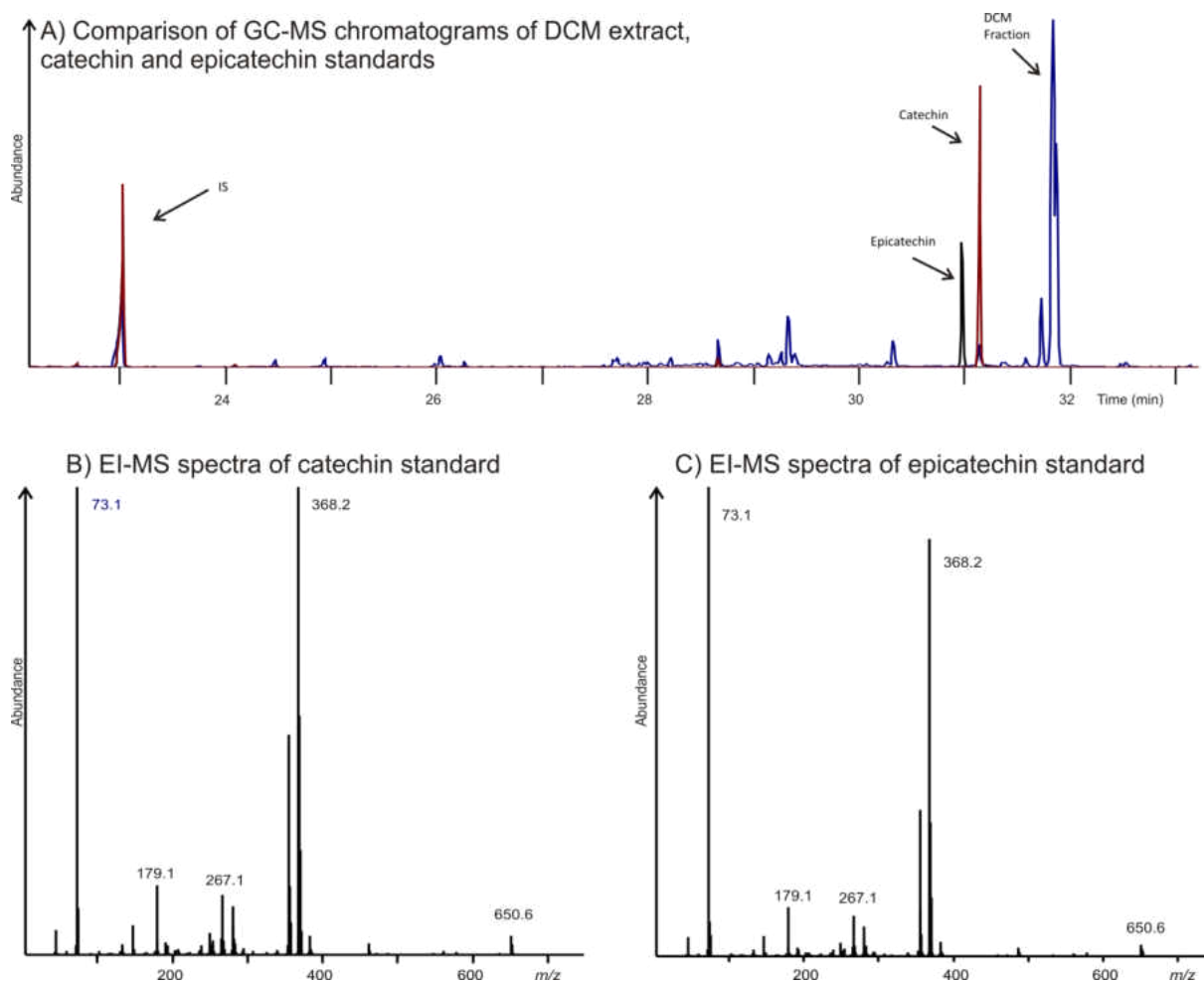
**Figure III.3** GC-MS characterization of DCM fraction (PJ<sub>b</sub>) and EI-MS spectrum of most abundant catechin-like compounds. (A) Total ion current chromatogram (B-G) EI-MS spectra of peaks D1-D6. Compounds D2, D3, D4 showed high identity (> 80%) with the EI/MS NIST library for catechin. Compounds were analyzed as TMS derivatives.

In order to further characterize less volatile, polar components by GC-MS, TMS derivatization was performed (Fig. III.2). Based upon the match with the NIST mass spectra library, catechin-like compounds were found in high abundance in the polar fractions (P<sub>JM</sub> and the P<sub>JD</sub>, Fig. III.2A,C) and parallel the bioactivity of these two fractions. Several other compounds, including carvotanacetone, fatty acids and sugars were observed in the fractions analyzed and this information further detailed in supplementary data (Table B.3).

To investigate the potential source of antioxidant properties, further analysis of these catechin-like compounds was performed (Fig. III.3). Focusing on the relevant section of the chromatogram derived from GC-EI-MS of TMS-derivatized P<sub>JD</sub> fraction, six catechin-like compounds were observed (Fig. III.3A). Three of these compounds, peaks D2,D3, D4 (Fig. III.3B-D), had a characteristic common ion 368 *m/z* that matched the EI mass spectra of catechin and epi-catechin analytical standards (Fig. III.3E) [40]. However, the retention time of these catechin-like species did not match the retention times of the catechin and epicatechin standards (Fig. III.4). While catechins are mostly known as antioxidants, they also prevent the differentiation of adipocytes [41–44]. Catechins and related flavonoid phytochemicals have not been reported in previous analyses of PJ, likely as a result of using GC-MS without TMS derivatization. The low resolution of the EI-MS data prevented the confirmation of identification of these compounds.

The P<sub>JD</sub> fraction was analyzed using LC-ESI-HRMS. Similar to GC-MS, two peaks with ions of 289.07 *m/z* (corresponding to [M-H]<sup>-</sup> ion for catechin) were observed (Fig. III.5A), and similar to GC, they eluted at later retention times. The low mass accuracy error of 14 ppm supported the molecular structure of this ion as that of catechin (Fig. III.5A). The mass spectra of these peaks (Fig. III.5B,C) showed the most abundant fragments as 317.05 *m/z* and 359.19 *m/z*. The first peak

(L1,  $t_R$  19.15) with the ions of 289  $m/z$  and 317  $m/z$  may be related to GC-MS peaks D2 and D4 (Figure 7), respectively. The 317  $m/z$  corresponds to catechin with a CO group, with 40 ppm error. The second peak (L2) had an abundant ion of 359  $m/z$ , suggesting that the parent molecule possessed a mass of 360 with a proposed structure  $C_{20}H_{24}O_6$  and with a mass error of 111 ppm.



**Figure III.4** GC-MS characterization of catechin and epicatechin standards. (A) TMS-derivatives of catechin and epicatechin standards were analyzed by GC-MS in comparison to the TMS-derivatized DCM fraction,  $PJ_D$ . Note that the retention times for the standards do not match that of the compounds observed in the  $PJ_D$ . The EI-MS spectra of catechin and epicatechin are provided in (B) and (C). Note that of the 368.2 ions present in the standards is also enriched in the TMS-derivatized compounds observed in the DCM fraction detailed in Figure III.3.

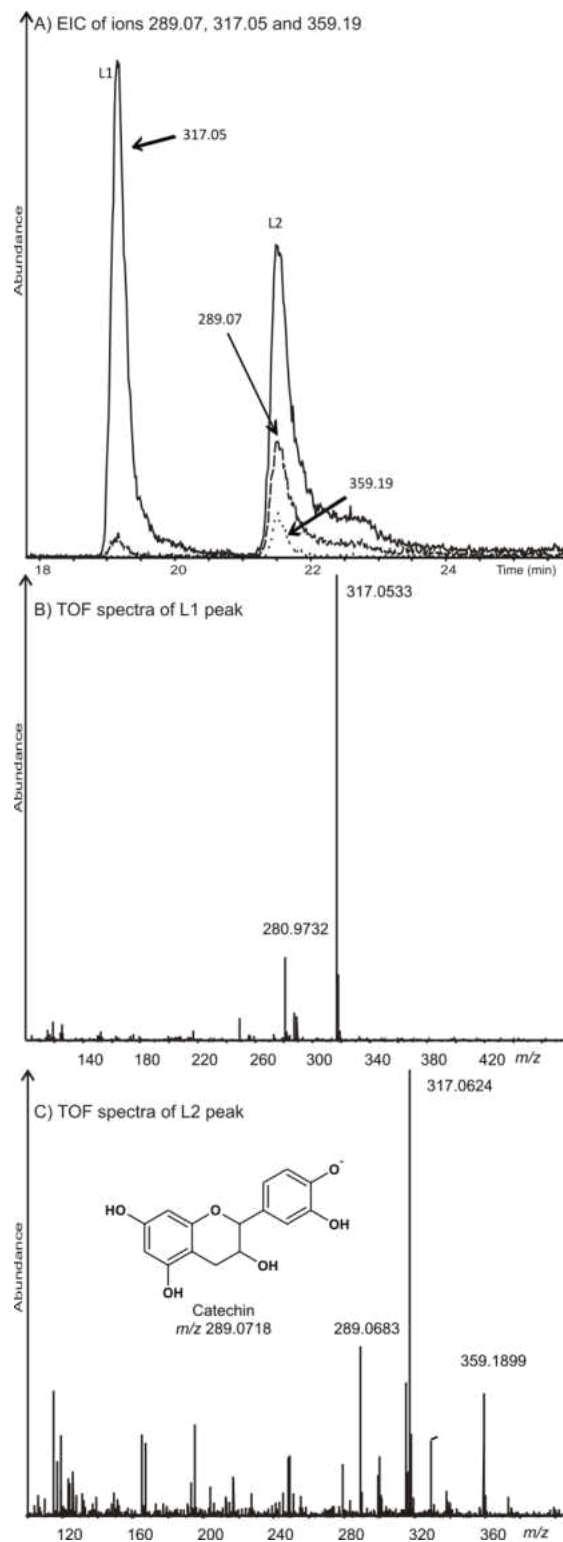


Figure III.5 Extracted ion chromatograms and mass spectra of LC-HR-MS analysis of the DCM fraction P<sub>J<sub>D</sub></sub>. (A) Extracted ion chromatogram (EIC) of ions 289.07, 317.05 and 359.19. (B) Time of flight (TOF) mass spectrum of L1 peak, (C) TOF mass spectrum of L2 peak and mass accuracy confirming the catechin-like structure. The structure of catechin ( $m/z$  289.0718) is provided for comparison.

### III.4 CONCLUSIONS

We have analyzed methanolic extract of *Pulicaria jaubertii* E.Gamal-Eldin and its fractions. Al-Naqeb *et al.* [37] showed that the methanol extract of PJ and its subsequent DCM fraction possessed bioactivity towards inhibiting TG accumulation. Our analysis revealed a high abundance of catechin-like compounds. Other compounds observed in higher abundance were carvotanacetone, fatty acids and sugars, however, these were not specific to the DCM fraction.



## IV. CHAPTER

### DETERMINATION OF *TRANS*-RESVERATROL AND ITS METABOLITES IN RAT SERUM USING LIQUID CHROMATOGRAPHY WITH HIGH-RESOLUTION TIME OF FLIGHT MASS SPECTROMETRY

#### IV.1. BACKGROUND

RES (3,5,4'-trihydroxy-*trans*-stilbene) is a polyphenol found in many foods, such as peanuts and berries, and red wine [1]. RES and its metabolites have been reported to exhibit anticancer, analgesic, cardioprotective, and neuroprotective effects [1]. Numerous animal studies have already been performed to evaluate the benefits of RES [45,46]. A majority of animal studies involving RES have employed rats [47,48], as reviewed by Park and Pezzuto [45], while use of other animals, such as pigs [49,50] and dogs [51] have been reported. The doses of RES in these studies varied greatly, between 1 to 1200 mg/kg/day [47–51]. The specific RES metabolites, R3G and R3S were shown to be the most abundant primary resveratrol metabolites in rat serum [49,52–54]. Long-term clinical studies are still necessary to investigate its effectiveness in humans.

Various LC-MS methods have been employed to detect and quantify RES and its metabolites in blood and tissue samples as summarized in Appendix Table C.1 [47–70]. The constituents of the mobile phase employed generally consisted of various mixtures of MeOH [55–62] or ACN [47–50,52–54,63–68] with water and electrolytes such as acetic acid [54,69,70], ammonium acetate [55,58,61,62,70], or formic acid [48–52,57,60,63]. For the MS analysis, ESI was typically used in negative mode, with voltages ranging from 2500 to 5000 V [49–52,54–67].

The limits of quantification were between 0.1 and 63 ng/mL [47,49,51,57,59–62,65,66,68,70]. The variety of conditions and matrices reported precludes the selection of the most sensitive method. Moreover, reasons for the selection of a particular electrolyte, its concentration, or the ESI voltages were generally not provided.

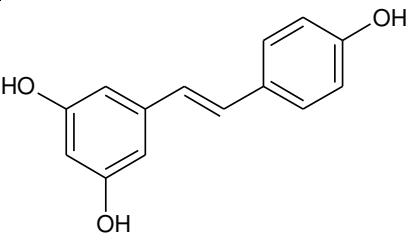
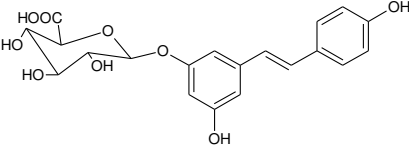
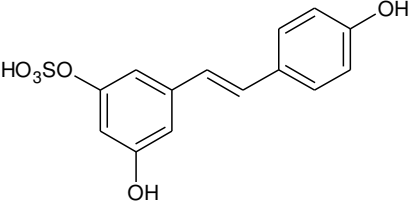
LC with tandem MS/MS has generally been employed for quantification and confirmation of the identity of various resveratrol species [47–54,56–58,60,62–66,68–70]. To our knowledge, LC-HRMS has not been used for quantification of resveratrol species, and only one study used LC-HRMS for identification of such compounds [49].

A variety of ISs have been used in the LC-MS analysis of RES and its metabolites. The ISs were often compounds of different chemical structure from RES [45,48,50,52,55,57,60–63,66], and only two studies reported the use of  $^{13}\text{C}_6$ -RES as an IS, which was added before extraction to correct the RES recoveries [51,61]. In these studies,  $^{13}\text{C}_6$ -RES was used as the IS for RES determination but not for its metabolites. The application of the  $^{13}\text{C}$  RES analog enables more accurate monitoring of RES behavior during sample processing but the cost is rather high and thus may be prohibiting. The application of a deuterated RES is more economical than that of the  $^{13}\text{C}$  RES analog, moreover, it has not previously been reported neither as an IS, nor as a possible recovery (surrogate) standard.

In this study, we optimized LC-ESI-HRMS method to determine levels of RES and its metabolites, R3G and *trans*-resveratrol-3-O-sulfate R3S (the target species are shown in Table IV.1). To increase the method precision and accuracy, deuterated standards of RES, R3G, and R3S were synthesized and used as RSs added prior to the sample preparation in combination with an IS (pinosylvin), which was added before injection. This combination of RSs and IS (used frequently

in environmental studies) allowed for an improved understanding of repeatability issues (i.e., whether the issues arise from sample preparation or analysis). The developed method was applied to rat serum samples following their exposure to RES.

**Table IV.1 Target analytes, their structures, the mass of the ions used for quantification, and determination of LODs.**

Compound	Formula	Structure	Quantification ion [M-H] <sup>-</sup> (m/z)	Confirmation ion (m/z)
<i>trans</i> -resveratrol (RES)	C <sub>14</sub> H <sub>12</sub> O <sub>3</sub>		227.07137	228.07765
<i>trans</i> -resveratrol-3-O-β-D-glucuronide (R3G)	C <sub>20</sub> H <sub>20</sub> O <sub>9</sub>		403.103456	227.07137
<i>trans</i> -resveratrol-3-O-sulfate (R3S)	C <sub>14</sub> H <sub>12</sub> O <sub>6</sub> S		307.028182	227.07137

## IV.2. MATERIALS AND METHODS

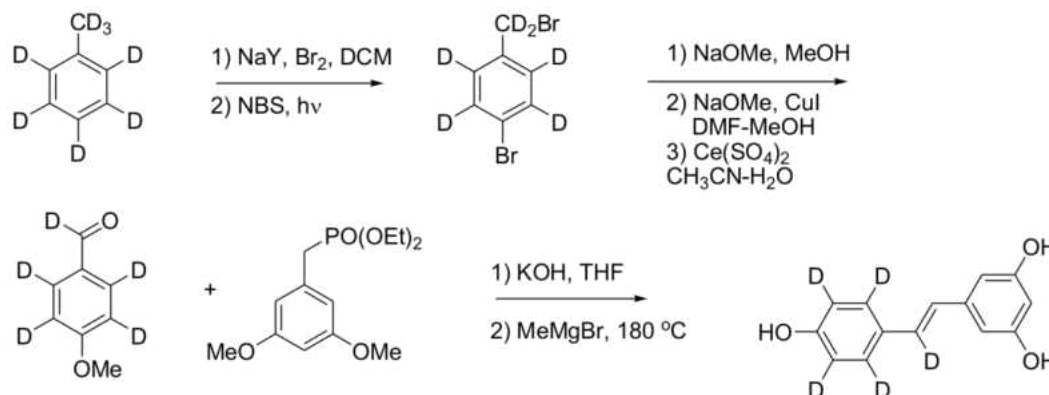
### IV.2.1 Materials

RES (≥99%), pinosylvin (97%) and ascorbic acid were purchased from Sigma-Aldrich (St. Louis, MO, USA). ACN, MeOH, acetic acid, and ammonium acetate (all LC-MS quality) were obtained from Fisher Scientific (Pittsburgh, PA, USA). Deionized water was obtained using a Direct-Q 3 UV water purification system (Millipore Corporation, Billerica, MA, USA). Toluene-d<sub>8</sub> was purchased from Cambridge Isotope Laboratories, other starting materials for the synthesis

(3,5-dihydroxybenzoic acid, iodomethane, triethylphosphite) were purchased from Sigma-Aldrich.

#### IV.2.2 Synthesis and purification of RES analogs and deuterated RSs

R3G and R3S were synthesized using a previously developed procedure for non-deuterated analogs [71]. Resveratrol- $d_5$  (RES- $d_5$ ), along with its conjugates (R3S- $d_5$  and R3G- $d_5$ ), were prepared using a modification of this procedure (described in detail in Appendix C), based on the condensation of 3,5-dimethoxybenzyl diethylphosphonate and anisaldehyde- $d_5$  (Fig. IV.1). Anisaldehyde- $d_5$  was prepared from readily available commercial toluene- $d_8$ , relying on the reported highly selective NaY zeolite catalyzed *para*-bromination, followed by radical benzylic bromination [72].



**Figure IV.1** Schematics of synthesis of RES- $d_5$ .

Synthesized R3G and RES- $d_5$  were purified using solid phase extraction (SPE), with a Waters Sep-Pak  $C_{18}$  cartridge. R3G, in 0.5 mM acetic acid, was eluted with 10% and 20% MeOH and RES- $d_5$ , in 90 mM acetic acid, was eluted with 40% ACN; their LC purity was 98% and 89%, respectively. Synthesized R3S, R3S- $d_5$ , and R3G- $d_5$  were dissolved in 100% MeOH, which resulted

in LC purity of 99%, 90%, and 86%, respectively. No non-deuterated compounds were observed in the mass spectra of the deuterated analogs.

#### IV.2.3 Sample preparation

Standards for the ESI optimization were solutions consisting of RES, R3G, or R3S (4 µg/mL each) in a range of electrolyte concentrations (0–10 mM ammonium acetate or 0–100 mM acetic acid) in 50% MeOH/H<sub>2</sub>O or 50% ACN/H<sub>2</sub>O. For the analysis of serum samples, calibration solutions were in the range 2 to 70 ng/mL of RES and R3S, and 0.2 to 6.7 µg/mL of R3G dissolved in the mobile phase. Calibration of RSs was in the range 2 to 125 ng/mL of RES-d<sub>5</sub> and R3S-d<sub>5</sub>, and 0.1 to 5.0 µg/mL of R3G-d<sub>5</sub> in the same solvent system.

Serum samples were obtained from ACI (August Copenhagen) rats, which spontaneously form mammary cancer when estradiol (E2) is delivered through slow release pellets [31]. Rats were subjected to one of four treatment regimens involving RES in a diet for 5.5 months (control, E2 only, E2 + low dose of RES (5 mg/kg/day), E2 + high dose of RES (25 mg/kg/day)). No animal died nor did any require euthanasia prior to study completion. By 21wk, some tumors were quite large and would soon require sacrifice. To maintain consistency, all rats were sacrificed at this time. Tissue was collected and processed as described by Qin et al. [73]. Blood was collected by a tail vein at the time of sacrifice in accord with a protocol approved by the UND animal care committee. Serum was extracted using a serum separator tube and centrifugation performed at 3000 rpm for 10 min. Samples were snap frozen at -80 °C until use.

The analyte extraction method was adapted from earlier reports [61,74], implementing the use of deuterated RSs. A serum aliquot (75 µL) was spiked with 10 µL of the RS solution, consisting of 2.8 µg/mL each of RES-d<sub>5</sub>, R3G-d<sub>5</sub> and R3S-d<sub>5</sub>, and mixed with 1.0 mL of ACN. The

solution was vortex-mixed for 2 min and centrifuged at 6,000 rpm for 10 min. The supernatant was filtered using a 0.2  $\mu\text{m}$  PTFE syringe filter and the extract was evaporated under a gentle stream of nitrogen after the addition of 10  $\mu\text{L}$  of 4 mg/mL (ca. 100  $\mu\text{M}$ ) ascorbic acid, which was added to prevent the degradation of RES and R3G, as suggested by Juan et al. [54]. The dried residue was redissolved in 250  $\mu\text{L}$  of mobile phase and 3  $\mu\text{L}$  IS (11.35  $\mu\text{g}/\text{mL}$  pinosylvin) were added to control for volume changes before LC-ESI-HRMS analysis. Blank serum samples (i.e., from rats not exposed to RES) spiked with 100 ng/mL each of RES, R3G, and R3S and the RSs were used for development of the extraction protocol. Three serum aliquots were used to prepare the samples for triplicate analysis and determination of mean values and standard deviations.

#### IV.2.4 Instrumentation

All determinations were carried out using ESI-TOF-MS (G1969A, Agilent, Santa Clara, CA, USA) coupled to an Agilent LC 1100 LC. The column was a  $\text{C}_{18}$  Zorbax Eclipse plus (2.1 x 150 mm with 3.5  $\mu\text{m}$  particle size) with a 1.2 cm guard column (both Agilent). Because ions corresponding to R3S and R3G were not detected in the positive mode, the ESI negative ion mode was used for all experiments.

#### IV.2.5 ESI optimization

All optimized conditions are summarized in Table IV.2 and details are provided in Appendix Tables C.2-7. All conditions were evaluated independently using flow injection analysis (FIA) employing a multi-level full factorial design of experiments (DOE). This design allows for three or more levels per factor while analyzing all the combinations of factors. We first evaluated ionization and fragmentor voltages as well as nebulization conditions, which do not seem to be affected by other parameters [75]. The solvent evaluation was performed in 50% MeOH/ $\text{H}_2\text{O}$  and

50% ACN/H<sub>2</sub>O. The ACN system produced approximately 1.5-fold higher analyte responses; therefore, it was used for all subsequent experiments. Preliminary screening showed that the peak area of RES was much lower when formic acid was present, compared with ammonium acetate and acetic acid. Our experiments and previous work showed significant interactions between the type of electrolyte and its concentration [75]; thus, DOE was performed evaluating ammonium acetate and acetic acid added to the samples (Table IV.2). The final concentrations of electrolytes in the mobile phase, considering 50  $\mu$ L injection volume at a flow rate of 0.2 mL/min, were 0.025–10 mM ammonium acetate and 0.025–100 mM acetic acid (i.e., four-fold lower than the prepared solutions).

The effect of the serum matrix on ionization was evaluated using control serum samples, where RES or its metabolites were below their limits of detection. Samples were spiked with RES, R3G, and R3S (with a final concentration of ca. 100 ng/mL of each analyte). The spiked serum samples were purified using the protocol described in the sample preparation section and analyzed using LC-ESI-HRMS. Several mobile phase solvent systems containing various electrolytes (0.025, 0.25, 0.50, and 1.0 mM ammonium acetate and 0.25 and 1.0 mM acetic acid) were evaluated.

**Table IV.2 Summary of experimental conditions used for flow injection analysis of individual target analytes with ESI in negative mode with 50% MeOH or 50% ACN as the mobile phase. All experiments were run in two blocks.**

Factors	No. of levels	Levels
<b>Optimization of ESI voltages</b> (drying gas: 350 °C and 12 L/min; nebulization pressure 25 psig)		
Capillary (V)	3	3500
		4000
		4500
Fragmentor (V)	4	125
		150
		175
		200
<b>Optimization of ESI nebulization conditions</b> (capillary voltage of 4500 V, fragmentor voltage of 175 V)		
Drying gas temperature (°C)	4	200
		250
		300
		350
Nebulizer pressure (psig)	3	15
		20
		25
Drying gas flow rate (L/min)	3	8
		10
		12
<b>Evaluation of mobile phase</b> (capillary voltage of 4500 V, fragmentor voltage of 175 V)		
Solvent	2	ACN
		MeOH
Electrolyte (0.1 mM)	3	none
		ammonium acetate
		acetic acid
<b>Optimization of electrolyte conditions</b> (capillary voltage of 4500 V, fragmentor voltage of 175 V)		
Electrolyte	2	ammonium acetate
		acetic acid
Electrolyte concentration (mM)	4	0
		0.1
		1
		10 <sup>a</sup>

<sup>a</sup> for acetic acids concentration of 100 and 400 mM was evaluated as well however the response was low and thus not reported.



#### IV.2.6 LC-ESI-HRMS conditions for serum analysis

For the final chromatographic separations, the flow rate was set to 0.2 mL/min, the injection volume was 50  $\mu$ L, and the column was equilibrated at 30 °C. The mobile phase solvent A consisted of 1.0 mM ammonium acetate in water:ACN (95:5, v/v) and solvent B of 1.0 mM ammonium acetate in ACN. The gradient elution program started isocratically at 0% B for 2 min followed by a linear gradient to 80% B from 2 to 15 min, and was maintained at 80% for 5 min. This was followed by a sharp gradient to 0% B from 20 to 21 min. To allow for column equilibration, the program was completed isocratically at 0% B from 21 to 40 min. The optimized ESI conditions employed for the analysis of serum samples were as follows: an electrospray voltage of 4500 V, fragmentor voltage of 175 V, nitrogen gas nebulization pressure of 25 psig, drying gas (nitrogen) flow rate of 12 L/min, and drying gas temperature of 350 °C.

#### IV.2.7 Data processing

The LC-ESI-HRMS data were processed using Analyst QS 1.1 (Applied Biosystems) and MassHunter Workstation Quantitative Analysis B.04.00 (Agilent Technologies). Target analytes were quantified using deprotonated molecular ions  $\pm 0.03$  Da and verified using confirmation ions (See Table IV.1 for masses and Appendix Fig. C.1 for mass spectra) and interpretation of the observed ions [64,68,76,77]. Minitab 16.1.1 and JMP software was used for statistical analysis. The analysis of variance (ANOVA) general linear model was used to analyze main factors and interactions in DOE, and any having a *p*-value less than 0.05 were considered to be significant. Chi-square test was used for comparing the numbers of rats between the low and high RES dose groups which developed tumors within 6 months. The serum concentrations of RES, R3G and R3S

were compared between groups using Wilcoxon Test. P values less than 0.05 were considered a statistically significant difference.

Instrumental LODs and LOQs were calculated from calibration curves of RES, R3G, and R3S using the equations  $LOD = 3.3 \times s_y/k$  and  $LOQ = 5 \times s_y/k$ , where  $k$  is the slope of the calibration curve and  $s_y$  is the standard error of the predicted y-value for each x-value. These values were obtained using linear least squares regressions. To determine the matrix LODs, control serum samples were spiked with RES, R3G, and R3S at concentrations within one order of magnitude of the LOD (4.9–32.1, 66.1–264.5, 9.8–63.8 ng/mL, respectively). The quantification of analyte concentrations in serum samples was based on the IS method of calibration, corrected with the recoveries of the deuterated RSs.

### IV.3. RESULTS AND DISCUSSION

#### IV.3.1 Evaluation of ESI conditions

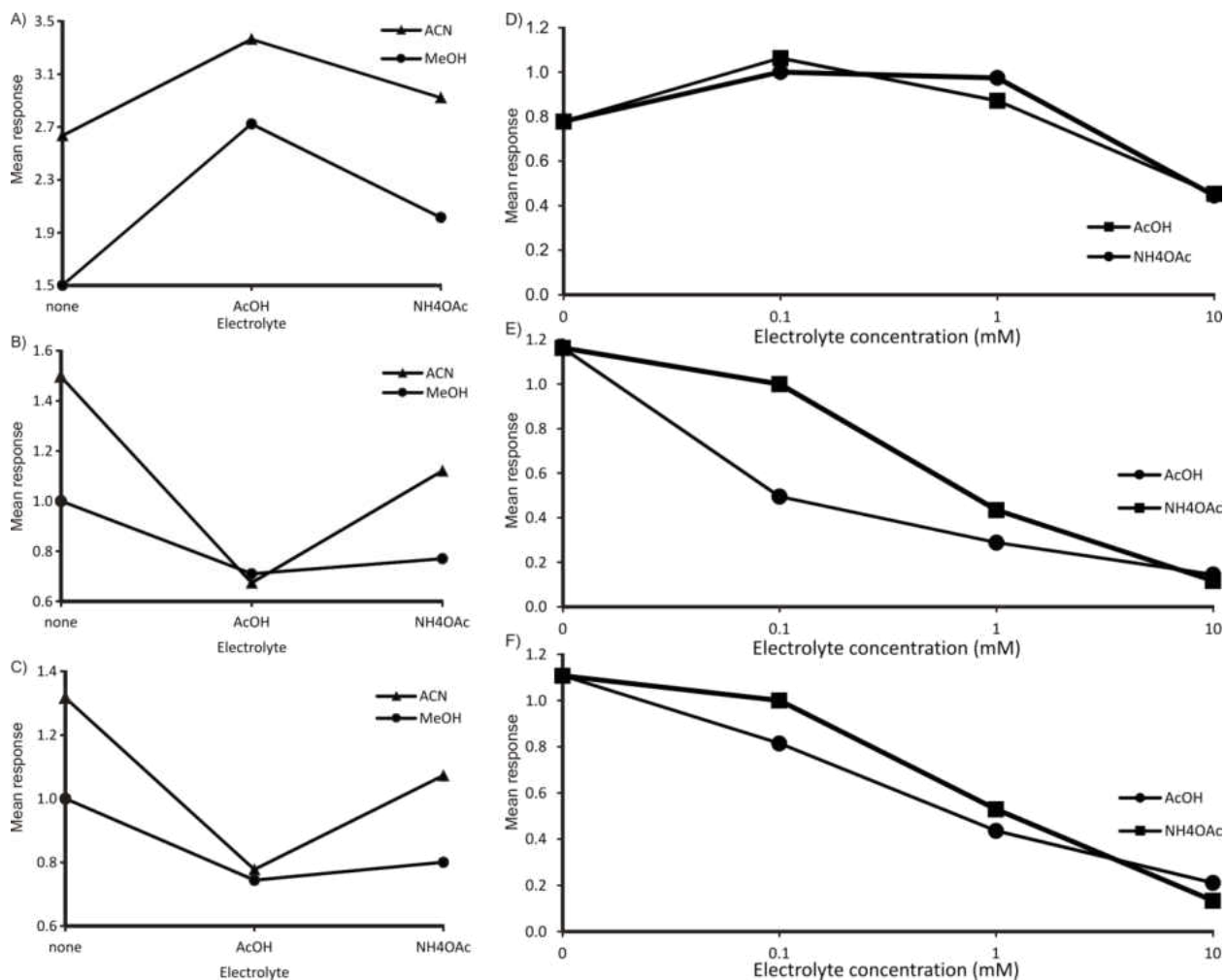
Both our previous work and preliminary screening suggested that electrospray and fragmentor voltages are independent of other factors such as the electrolyte and its concentration [75]. Thus, they were evaluated independently using flow injection analysis (FIA). The optimum conditions for ESI capillary and fragmentor were 4500 V and 175 V, respectively (Appendix Fig. C.2). Similarly, nebulization conditions were evaluated independently (Appendix Fig. C.3) showing as optimal a nebulization pressure of 25 psig, drying gas flow rate of 12 L/min, and drying gas temperature of 350 °C.

Comparison of two solvent systems showed that the application of 50% MeOH/H<sub>2</sub>O and 50% ACN/H<sub>2</sub>O resulted in similar mass spectra (the representative mass spectra are shown in

Appendix Fig. C.1); however, 50% ACN produced an overall higher response than MeOH, particularly in the presence of ammonium acetate (Fig. IV.2 A,B,C).

We confirmed that the concentration and selection of the electrolyte affected the ESI-MS response (Fig. IV.2D,E,F). This DOE was set up using FIA to introduce varying electrolyte concentrations into the mobile phase. A trend of decreasing response with increasing electrolyte concentration was observed for all analytes (Fig. IV.2D,E,F, data are shown up to 2.5 mM estimated final concentration).

The further evaluation of the ESI efficiency was performed on serum samples spiked with RES and R3S and their RSs (RES-d<sub>5</sub> and R3S-d<sub>5</sub>) to determine the impact of the matrix. The ionization of R3S was enhanced in the presence of purified serum with acetic acid. While this could be beneficial to increase analysis sensitivity towards this metabolite, our aim was to ensure a robust repeatable method. Among the tested electrolytes, the most consistent results were achieved for 1.0 mM ammonium acetate (Appendix Table C.8). Therefore, further determinations of RES and its metabolites in serum samples were performed using 1.0 mM ammonium acetate in an ACN/H<sub>2</sub>O solvent system.

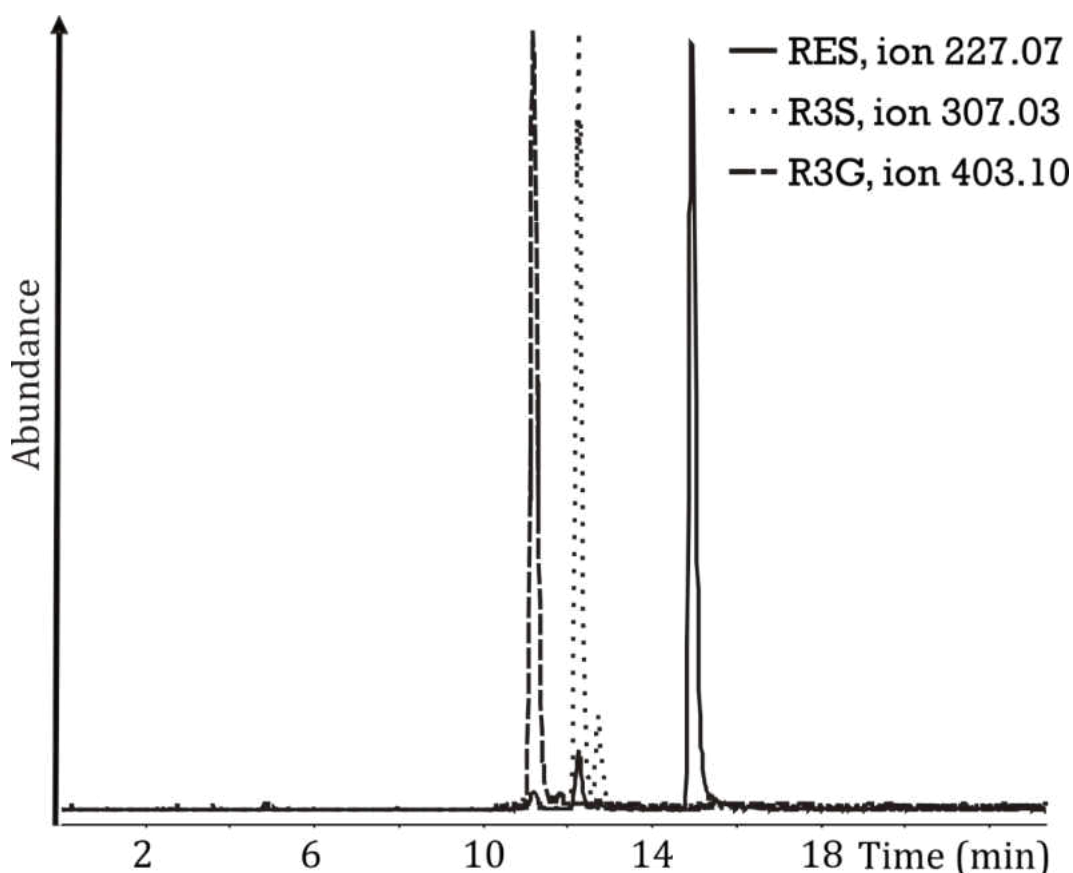


**Figure IV.2** ESI-MS normalized response for RES (A), R3G (B), and R3S (C), comparing the solvents 50% MeOH/H<sub>2</sub>O and 50% ACN/H<sub>2</sub>O, with no electrolyte, 0.1 mM AcOH, and 0.1 mM NH<sub>4</sub>OAc, determined using FIA in the negative mode (for RES: solvent  $p=0.288$ , for R3G: solvent  $p=0.065$ , for R3S: solvent  $p=0.045$ ). ESI-MS normalized response of RES (D), R3G (E), and R3S (F) in 50% ACN/H<sub>2</sub>O solutions with AcOH and NH<sub>4</sub>OAc (0–10 mM in sample) determined in the negative mode using FIA (for RES: concentration  $p<0.0005$ , electrolyte and concentration interaction  $p=0.012$ ; for R3G: electrolyte  $p=0.002$ , concentration  $p<0.0005$ , electrolyte and concentration interaction  $p=0.002$ ; for R3S: concentration  $p<0.0005$ )

#### IV.3.2 Calibration parameters and limits of detection

The calibration parameters and LODs for RES, R3G, and R3S are shown in Table IV.5. Instrumental LODs were determined to be 1.3, 4.4, and 1.6 ng/mL for RES, R3G, and R3S, respectively. LODs for the serum matrix spiked with target analytes and subjected to the full method were 9.7, 82.4, and 4.7 ng/mL for RES, R3G, and R3S, respectively (Appendix Table C.9). These LODs for LC-ESI-HRMS are similar to those reported in previous studies using LC-MS/MS

[49,51,57] and higher than those obtained by LC-MS [67]. Other studies [59,61,66,68,70] reported lower LOQs (Appendix Table C.1). These LOQs appear to be based on a signal intensity rather than the signal to noise ratio and thus these points may be at the level of LODs or even lower. It is of note that most of these studies succeed due to higher sample size [59,61,68,70], which is not always available. Perhaps we could improve our LODs if the ethylacetate extraction was used for sample purification was used [66] instead of typically employed SPE.



**Figure IV.3** Representative LC-ESI-HRMS extracted ion chromatograms (EIC) of control serum spiked with RES, R3G, R3S (0.32, 3.9, 0.48  $\mu\text{g}/\text{mL}$ , respectively; scaled to same peak height)

The selectivity of the developed LC-ESI-HRMS method, when applied to extracts of control spiked plasma samples, is demonstrated in the EIC chromatograms of deprotonated molecules

showing no interference for RES and its metabolites, R.S., and I.S. from the endogenous compounds (Fig. IV.3).

The repeatability of analysis was evaluated using the serum samples targeting the metabolites (as RES present only in trace concentrations) (Appendix Table C.10). The metabolites were determined with a 10% relative standard deviation for samples with a higher concentration of target analytes (200 ng/L) prepared in triplicate. For lower concentrations of sulfates, the RSD increased due to interference from the matrix (Table IV.3). The interday repeatability of the LC analysis was determined for analytes in two selected serum samples by measuring on two different days. The interday average concentrations for R3G and R3S were  $3689 \pm 313$  ng/mL, and  $55 \pm 3$  ng/mL, respectively (Appendix Table C.10).

#### IV.3.3 Concentration of RES and its metabolites in rat serum and their impact on tumor growth

The developed method was employed to evaluate serum samples from rats, which were subjected to a treatment involving either a low or high dose RES diet, allowing for determination of both RES and its metabolites (Table IV.3). It is of note that beside R3S we have also observed two other peaks characteristic for resveratrol sulfate ( $m/z$  of 307) eluting between 10–12 min (Fig. IV.4 and Appendix Fig. C.4 for mass spectra). We have attempted to identify both of these peaks assuming that, based on the isotopic lines and this ion, they must be resveratrol sulfate derivatives. The occurrence of the previously reported R4'S isomer was ruled out as its characteristic ion of 143 [78] was not present in the mass spectra of either of the peaks. The further MS interpretation of the first (smaller) peak (X1) was not possible due to its lower intensity. The mass spectrum of the second peak (X2) seemed to lack the corresponding pseudomolecular ion, which could not be assigned to ion 441, as the loss of 15.97 (from 441 to

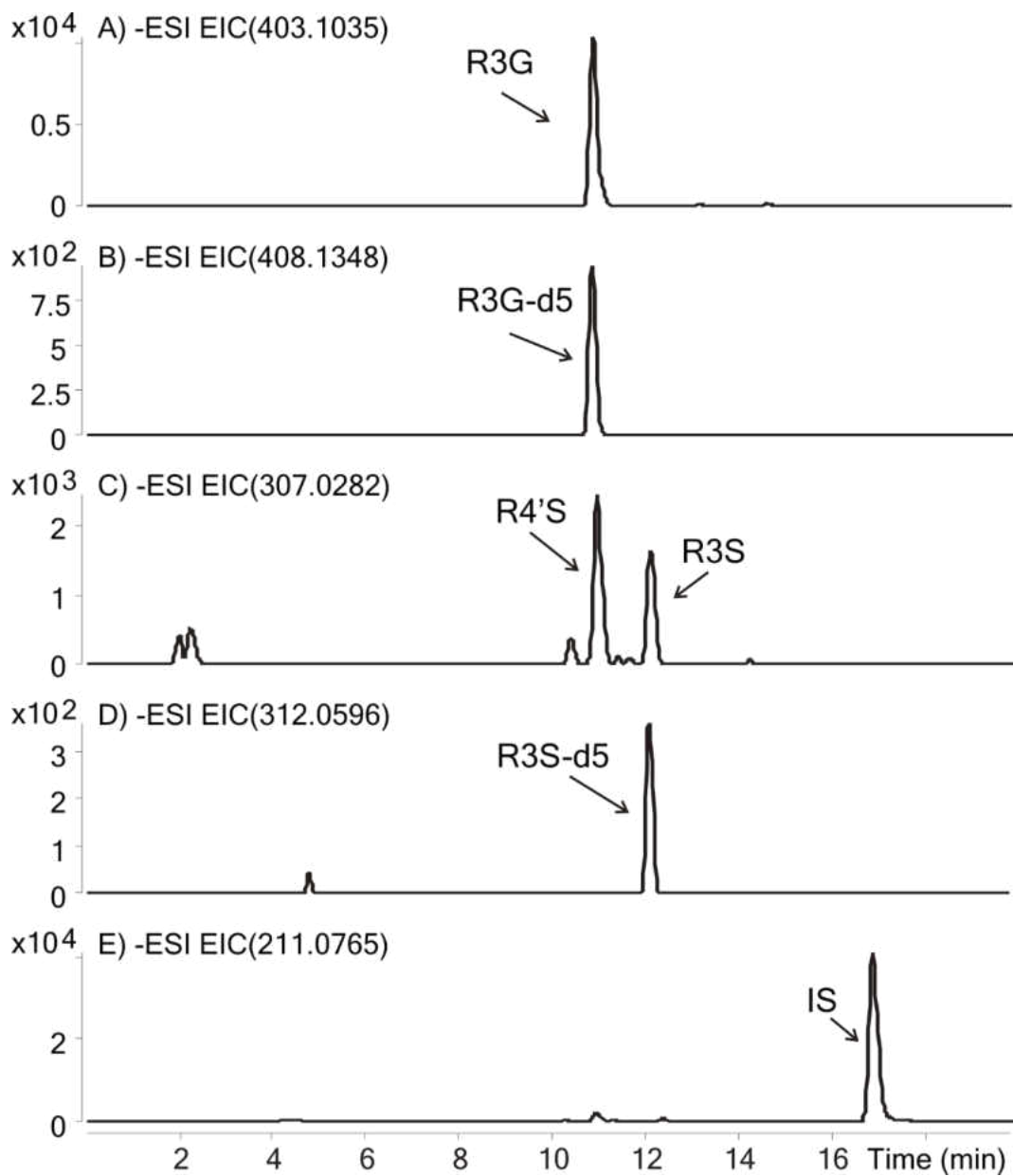
425) could not be attributed to either oxygen or CH<sub>3</sub> with a sufficient mass accuracy. The tentative identification of this ion was consistent with the loss of CO from resveratrol trisulfate (RtS) [M-CO]<sup>-</sup>, with a fairly low mass error (13 ppm), although we cannot explain the formation of such ions from RtS. Thus, the results suggest that X2 represents a higher MW RS derivative, possibly RtS. The X2 and R3S peaks were of the same order of magnitude in both types of samples (low and high dose).

**Table IV.3 Concentration (ng/mL) of RES and its metabolites in serum samples of rats exposed to RES. The data are presented as mean with one standard deviation (n=3).**

	RES		R3G		R3S		Resveratrol Sulfates <sup>a</sup>	
	Mean	SD	Mean	SD	Mean	SD	Mean	SD
<b>Low Dose (5 mg/kg/day)</b>								
171	2	4	4938	363	76	15	131	11
173	6	1	6391	390	314	93	626	181
175	6	1	6807	487	374	103	757	220
178	7	0.5	1950	232	216	12	418	26
179	ND		3775	313	61	9	117	7
181	2	0.3	4611	324	391	104	743	195
183	8	1	1924	109	256	5	490	15
186	1	0.3	5645	292	358	170	691	328
188	2	0.2	7335	169	272	139	539	271
<b>Mean</b>	<b>4</b>	<b>1<sup>b</sup></b>	<b>4801</b>	<b>317</b>	<b>268</b>	<b>94</b>	<b>501</b>	<b>183</b>
<b>High Dose (25 mg/kg/day)</b>								
148	31	1	8124	314	191	10	627	41
150	7	0.4	3476	53	395	7	676	10
152	22	2	3852	381	94	4	349	17
154	6	1	8111	155	275	80	372	54
156	8	0.2	11660	418	907	28	1774	55
158	7	1	3540	116	326	47	611	59
160	27	11	12553	195	349	17	959	33
162	20	4	11279	418	213	81	697	63
165	7	0.1	2756	167	336	11	578	16
168	8	0.2	2601	476	356	53	617	104
<b>Mean</b>	<b>16</b>	<b>3.8</b>	<b>6795</b>	<b>304</b>	<b>344</b>	<b>44</b>	<b>731</b>	<b>73</b>

<sup>a</sup> Represents sum of peaks observed as resveratrol sulfates

<sup>b</sup> Overall standard deviation was determined as pooled standard deviation of all sample analysis



**Figure IV.4** Representative LC-ESI-HRMS analysis of *in vivo* rat serum sample; extracted ion chromatogram (EIC) for R3G (A), EIC for R3G-d<sub>5</sub> (B), EIC for resveratrol sulfates (C), EIC for R3G-d<sub>5</sub> (D), EIC for internal standard (IS, E). Peaks X1 and X2 represent suspected derivatives of resveratrol sulfate

The observed RES concentrations were either low or at the limit of detection, but were nevertheless 4 times higher for the higher dose diet. By contrast, R3G (6.8 µg/mL and 4.8 µg/mL, high dose and low dose, respectively) and resveratrol sulfates (0.7 µg/mL and 0.5 µg/mL, respectively) were much more abundant. The resveratrol conjugates were found in all serum



samples with a 1.4 fold higher response in samples from rats receiving the high dose treatment. RES concentrations were significantly different between the high and low dose groups ( $p=0.0147$ ), but the concentrations for R3G and R3S were not significantly different with  $p$  values, 0.4963 and 0.7055, respectively (Fig. IV.5a). Two rats in the high dose group and six in the low dose group developed tumors within 6 months, which was not significantly different ( $p=0.0679$ ). Fewer rats developed tumors in the high dose resveratrol group than in the low dose group, however, the result was not significantly different. This lack of statistical significance is likely a result of limited sample size. Even though not statistically different ( $p=0.068$ ), the fact that only one third as many rats in the high RES group compared to the low RES group formed tumors, may be viewed as biologically significant, and consistent with a protective effect of active RES (but not the metabolites, which were not higher in tumor), on the development of mammary cancer formation. These tumors are hormone sensitive as are 70% of human breast cancers, suggesting that RES may also be useful in the prevention of the most common form of human breast cancer.

When the serum concentrations were compared, the RES concentrations were significantly lower in the rats with tumors than without tumors ( $p=0.0081$ ). The  $p$  values for R3G and R3S were both 0.2801 using nonparametric statistical tests (Fig. IV.5b). This result suggests that animals have differential responses to resveratrol doses and the serum resveratrol concentration is a better predictor of cancer onset than dietary dose.

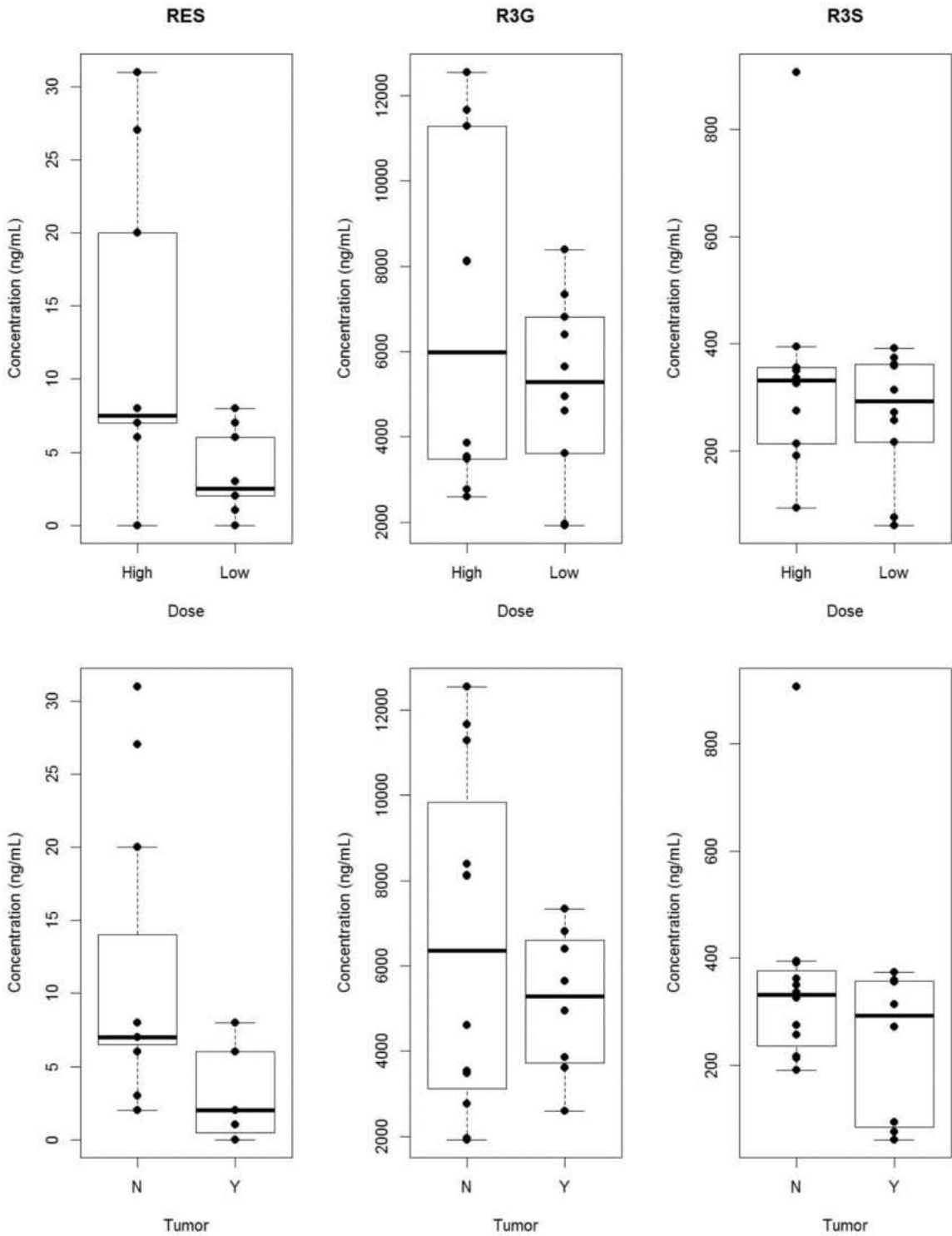


Figure IV.5 Boxplots representing measured concentrations (ng/mL) of RES, R3G and R3S in rat serum and tumor after exposure to RES after 21 weeks

#### IV.4. CONCLUSIONS

A sensitive method for the determination of RES and its two most abundant metabolites, R3G and R3S, in rat serum was developed using LC-ESI-HR-TOF MS suggesting that the RES serum concentration is of higher significance than its dietary dose. While the ESI response was highest at lower electrolyte concentrations, to achieve reproducible results it was necessary to use 1.0 mM ammonium acetate. Deuterated RSs were employed to account for analyte loss during sample preparation. LODs achieved in this way were similar to those reported for other methods using LC-MS. This method was used to determine levels of RES and its metabolites in rat serum samples after treatment with high (25 mg/kg/day) and low (5 mg/kg/day) dose of RES. R3G was the most abundant analyte with a concentration of 5–7  $\mu\text{g}/\text{mL}$  while resveratrol sulfates had a 10 fold lower concentration, i.e. 0.5–0.7  $\mu\text{g}/\text{mL}$ . Fewer rats developed tumors in the high dose resveratrol group than in the low dose group, however, the result was not significantly different. When the serum concentrations were compared, the RES concentrations were significantly lower in the rats with tumors than without tumors. To our best knowledge, levels of RES and its metabolites in human serum and occurrence of breast cancer were not correlated, however, preventive effect of RES dose on human breast cancer had been described in many studies, most recently reviewed by Kotecha et al. [46]. Thus, the sensitive method developed in this study provides a robust approach for monitoring serum resveratrol and its metabolites levels, which may contribute to cancer prevention.

## V. CHAPTER

### METHOD DEVELOPMENT FOR DETERMINATION OF TRACE CONCENTRATIONS OF ALDEHYDES AND CARBOXYLIC ACIDS IN PARTICULATE MATTER

#### V.1. BACKGROUND

Carboxylic and carbonyl compounds are significant constituents of atmospheric carbonaceous PM formed as a result of both primary emissions and secondary atmospheric reactions [3–5]. The observed variety of carboxylic and carbonyl compounds in PM includes linear monocarboxylic acids, dicarboxylic acids, aromatic polycarboxylic acids, polycyclic quinones, hydroxyacids, ketoacids, aldehydes, dialdehydes, ketones and multifunctional aliphatic and aromatic compounds [3,4]. Within secondary atmospheric reactions, aldehydes are readily oxidized to acids and also react with acids leading to the formation of polymers [3–5]. Owing to the hydrophilicity of acids and aldehydes, they are also suggested to serve as cloud condensation nuclei [3,79,80]. The high reactivity of these species in atmospheric processes warrants their accurate determination [3–5].

To investigate the occurrence of compounds with various polar functional groups, such as hydroxyl, carbonyl or carboxyl groups present in PM, a multi-step derivatization is often employed prior to their GC analysis [81–93]. The most common approach is the derivatization of carbonyl groups with PFBHA·HCl and then a separate derivatization of carboxylic and hydroxyl groups via either their BSTFA [81–91,93–97] or esterification with an alcohol, such as butanol or MeOH, in the presence of  $\text{BF}_3$  [84–86,88,92]. These studies summarized in Table V.1 pioneered the identification but quantified only few species and thus, as described below, not addressing potential quantification issues.

For determination of aldehydes and acids in PM using the PFBHA·HCl/BSTFA protocol (Table V.1), a Soxhlet extraction using either DCM or a mixture of DCM / ACN is frequently employed [81,85–87,98,99]. The next step in the typical PFBHA·HCl/BSTFA protocol involves derivatization with PFBHA in an aqueous solution [82,91,96,97], which is not miscible with DCM used for the initial extraction. As a result, this process requires a drying step prior to the PFBHA·HCl derivatization [82,85,86,96], which may lead to losses of volatile analytes. Moreover, due to the use of aqueous solutions, PFBHA oximes have to be extracted prior to BSTFA derivatization [83–86,88–90,93,95] thus adding another step potentially resulting in a further analyte loss. Another option (used in studies with PFBHA alone) is to carry out the derivatization with PFBHA dissolved in MeOH, thus combining the extraction from PM and derivatization step [100,101]. Perhaps due to the focus on aldehyde derivatization [100,101], to our knowledge, there have been no studies reporting the expected occurrence of methyl esters as a result of the acids' exposure to methanolic solutions in the presence of HCl (which is a part of the PFBHA·HCl molecule) or evaluating the effectiveness of such a derivatization.

**Table V.1 Comprehensive summary of derivatization protocols using sequential derivatization with PFBHA and BSTFA for determination of carboxylic and carbonyl compounds in atmospheric samples.**

Sample type	Compounds	Initial sample preparation	Derivatization reaction conditions		Analysis	Comments	Reference
			PFBHA	BSTFA			
Acids and aldehydes							
PM 2.5 <sup>a</sup>	hydroxyacids, ketoacids, dicarboxylic acids; carbonyls	Soxhlet, DCM/ACN (1:1, v/v), 24 h	350 $\mu$ L 160 mM PFBHA (in water); dried with N <sub>2</sub>	850 $\mu$ L DCM/hexane (1:2, v/v), 50 $\mu$ L BSTFA, 100 $\mu$ L pyridine, overnight stand (25 °C), then 70°C/120 min	GC-MS PCI (CH <sub>4</sub> )	IS: d <sub>5</sub> - benzaldehyde (prior derivatization)	[81]
Chamber experiments	pinic, pinonic, norpinic acid	flow through impinger with 500 mL ACN for 24 h, volume reduced to 300 mL	100 $\mu$ L PFBHA (19 mM in ACN/water), 16-18 h/ 25 °C, reduced to 5 mL by rotary evaporation, dried with N <sub>2</sub>	100 $\mu$ L hexane, 100 $\mu$ L DCM, 20 $\mu$ L BSTFA:TMSC (90:10, v/v), 70 °C/ 150 min	GC-MS PCI (CH <sub>4</sub> )	IS: nopinone (prior derivatization)	[82]
Model compounds	monocarboxylic, polycarboxylic, hydroxy and ketoacids; carbonyls	NA	1 mL water, 250 PFBHA (50 g/L in water), 24 h/ 25 °C, extraction with hexane/DCM (2:1, v/v), dried with N <sub>2</sub>	250 $\mu$ L BSTFA/TMCS (9:1, v/v), 100 $\mu$ L pyridine, 70 °C/ 120 min	GC-MS EI, PCI (CH <sub>4</sub> ), CID <sup>b</sup> (He)	other multi-derivatizations No IS/RS reported	[84]
PM 2.5, chamber experiments	substituted carboxylic acids and dicarboxylic acids	PM: Soxhlet, DCM/ACN (1:1, v/v), 24 h; chamber: Soxhlet, DCM, 6 h; both dried with N <sub>2</sub>	1 mL water, 250 PFBHA (50 g/L in water), 24 h/ 25 °C, extraction with hexane/DCM (2:1, v/v), dried with N <sub>2</sub>	250 $\mu$ L BSTFA/TMCS (9:1, v/v), 100 $\mu$ L pyridine, 70 °C/ 120 min	GC-MS EI, PCI (CH <sub>4</sub> ), CID (He)	other multi-derivatizations RS: cis-ketopinonic acid, d <sub>50</sub> -tetracosane; IS	[85]

Table V.1 Cont.

Sample type	Compounds	Initial sample preparation	Derivatization reaction conditions		Analysis	Comments	Reference
			PFBHA	BSTFA			
PM 2.5 chamber experiments	linear and substituted dicarboxylic acids	PM: Soxhlet, DCM/ACN (1:1, v/v), 24 h; chamber: Soxhlet, DCM, 6 h; both dried with N <sub>2</sub>	1 mL water, 250 PFBHA (50 g/L in water), 24 h/ 25 °C, extraction with hexane/DCM (2:1, v/v), dried with N <sub>2</sub>	250 µL BSTFA/TMCS (9:1, v/v), 100 µL pyridine, 70 °C/ 120 min	GC-MS EI, CI (CH <sub>4</sub> )	other multi-derivatizations RS: cis-ketopinic acid, d <sub>50</sub> -tetracosane; IS	[86]
PM 2.5 Gas phase	substituted (hydroxy, oxo) carboxylic acids	PM: Soxhlet, 24 h DCM or DCM/ACM (1:1, v/v) denuder: 2X 275 mL hexane/DCM/ACN (1:1:2, v/v) and extraction with MeOH	160 µL PFBHA in water PFBHA added, 24 h reaction time, dried with N <sub>2</sub>	50 µL BSTFA, 100 µL pyridine, 850 µL DCM/hexane (1:2, v/v), 65 °C/ 120 min	GC-MS PCI (CH <sub>4</sub> )	IS: d <sub>5</sub> -benzaldehyde (prior derivatization)	[87]
PM 2.5	dicarboxylic, substituted (hydroxy, oxo) carboxylic acids	Soxhlet, DCM/ACN (1:1, v/v), 24 h	1 mL water, 250 PFBHA (50 g/L in water), 24 h/ 25 °C, extraction with hexane/DCM (2:1, v/v), dried with N <sub>2</sub>	250 µL BSTFA/TMCS (9:1, v/v), 100 µL pyridine, 70 °C/ 120 min	GC-MS CI (CH <sub>4</sub> )	other multi-derivatizations RS: cis-ketopinic acid, d <sub>50</sub> -tetracosane; IS	[88]

Table V.1 Cont.

Sample type	Compounds	Initial sample preparation	Derivatization reaction conditions		Analysis	Comments	Reference
			PFBHA	BSTFA			
PM 2.5	substituted (hydroxy, oxo) carboxylic acids, carbonyls	Denuder impregnated with 40 mM PFBHA; particle phase: sonication in ice-bath, 15 min	Denuder: 3X extracted with 5 mL DCM/ACN (1:1, v/v), then 20 h/ 25 °C; particle phase: 30 µL PFBHA (40 mM), 24 h/ 25 °C	50 µL BSTFA, 100 µL DCM/hexane (1:1, v/v), 75 °C/ 150 min	GC-MS EI	IS: phenyldodecane (prior to analysis)	1- [93]
Chamber experiments, field samples	substituted (hydroxy, oxo) carboxylic acids, carbonyls	PFBHA coated denuder; gas: 3X5 mL DCM for 1 min; particles: 6 mL DCM, sonication in ice-bath, filtration, 2X rinse 3 mL DCM	30 µL PFBHA (40 mM), 20 h/ 25 °C, dried with N <sub>2</sub>	50 µL BSTFA:TMCS, 100 µL DCM/hexane (1:1, v/v), 75 °C/ 150 min	GC-MS EI	IS: phenyldodecane (prior to analysis)	1- [83]
PM 2.5	substituted (hydroxy, oxo) carboxylic acids	Extraction with PFBHA	0.1 M PFBHA in water; 24 h/ 25 °C, acidified with H <sub>2</sub> SO <sub>4</sub> , extraction to MTBE, dried with N <sub>2</sub>	200 µL BSTFA, 42 °C/ 12 h	GC-MS EI, CI (CH <sub>4</sub> , PFBOH <sup>c</sup> )	IS: fluorobenzaldehyde (prior to derivatization)	4- [89]



Table V.1 Cont.

Sample type	Compounds	Initial sample preparation	Derivatization reaction conditions		Analysis	Comments	Reference
			PFBHA	BSTFA			
Model compounds	pyruvic acid, substituted carbonyls	NA	10 mL PFBHA (2 mM in water), 24 h/ 25 °C, 2X extraction with 2 mL DCM, MTBE or hexane, evaporation	Evaporated to dryness with 100 µL BSTFA; 20 µL BSTFA (20 % in DCM), BSTFA:TMCS (99:1, v/v, 20% in DCM) or BSFTA:TMCS (90:10, v/v, 20% in DCM) into PFBHA derivatives in DCM	GC-MS CI (CH <sub>4</sub> )	different BSTFA derivatization protocols IS: 2,2'-difluorobiphenyl (prior to analysis)	[90]
Model compounds	monocarboxylic, dicarboxylic, hydroxy and ketoacids	NA	50 µL PFBHA (19 mM in ACN/water), 16-24 h/ 25 °C, evaporation	100 µL hexane/DCM (1:1, v/v), 20 µL BSTFA, 60 °C/ 40 min	GC-MS EI, CI (CH <sub>4</sub> )	No reported	IS/RS [91]
Chamber experiments	carbonyls	3 mL MeOH, 200 µL PFBHA (20 mM in ACN), dried and reconstituted with 100 µL MeOH	200 µL PFBHA (20 mM in ACN), overnight at 25 °C	20 µL BSTFA, 60 °C/ 45 min	GC-MS EI, CI (ACN)	No reported	IS/RS [96]
Chamber experiments	carbonyls	flow through impinger containing 4 mL ACN, 250 µL PFBHA (0.02 M in ACN)	4 mL ACN, 250 µL PFBHA (0.02 M in ACN), 24-48 h/ 25 °C, dried with N <sub>2</sub>	150 µL BSTFA, 70 °C/ 60 min	GC-MS EI, CI (CH <sub>4</sub> )	No reported	IS/RS [97]

<sup>a</sup> PM 2.5 – particulate matter with diameter less than 2.5 µm; <sup>b</sup> CID – collisionally activated dissociation; <sup>c</sup> PFBOH – pentafluorobenzyl alcohol

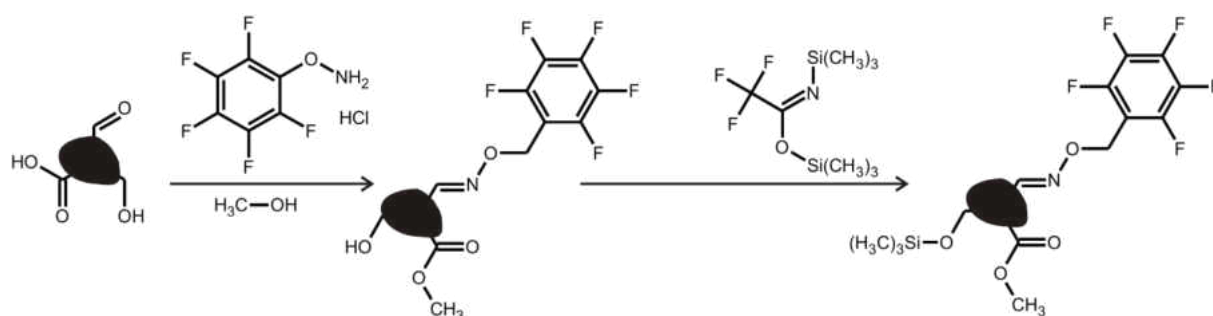
Another technique that may be coupled with PFBHA·HCl derivatization is the esterification of carboxylic acids in the presence of a strong mineral acid using an alcohol, such as BF<sub>3</sub>/butanol or MeOH [84–86,92]. This method is generally used for monocarboxylic [99,102–105] and dicarboxylic acids [85,98,103,104,106–114]. Successful derivatization of aromatic acids [102–104,107,108,110,112], hydroxyacids [104,107,108,112] and ketoacids [86,99,102–104,106,107,110,112,113] was also reported.

Besides the combined derivatization protocols, a number of studies focused on improvement of individual derivatization steps. MeOH in combination with DCM and ACN was used to extract samples from PM matrices and derivatize aldehydes in one step [100,101]. Temime et al. [100] compared the PFBHA aldehyde derivatization efficiencies in several solvent systems including MeOH, water/ACN (9.875:0.125 v/v) and ACN/DCM/MeOH (1:8.5:0.5 v/v/v) and reported similar derivatization yields. The advantage of this approach of using organic rather than aqueous solvents was a facile removal of the precipitated PFBHA residue, thus making the subsequent extraction of PFBHA oximes unnecessary. However to our knowledge, these protocols using organic solvents have not been used in sequence with a BSTFA derivatization [100,101].

As mentioned above, the BSTFA derivatization used either in a single step or following a PFBHA derivatization is commonly employed for determination of carboxylic and hydroxy groups. It has been used either in a mixture with a catalyst, TMCS, their ratio varying between 99:1 (v/v) [90] and 90:10 (v/v) [82,84–86,88,95], or with the addition of pyridine [81,84–88].

Previous studies focused on extensive identification of a broad range of compounds in PM with a variety of functional groups (Table V.1), which limited the quantification to only a few compounds [83,89,93] or to the quantification using direct silylation or esterification in the presence of BF<sub>3</sub> [27,84–86]. The majority of quantification studies employed a single IS,

which was added either prior to the analysis or prior to the derivatization. (Table V.1). RS sometimes called surrogate standards (e.g., isotope-labeled standards added prior to the extraction) were only used in several studies, however only 1–2 of the used RSs were representative for multiple compounds and the actual recoveries were not reported [85–87].



**Figure V.1** The proposed derivatization scheme using PFBHA·HCl with BSTFA for derivatization of aldehydic, carboxylic and hydroxylic groups on air PM.

The aim of this study was to develop a sample preparation method involving a two-step derivatization followed by GC-MS for determination of a broad range of oxygenated compounds including monocarboxylic, dicarboxylic, aromatic acids, ketoacids and hydroxyacids in PM. Our goal was to first extract and derivatize aldehydes to stabilize them prior to further derivatization. We have evaluated two solvent systems used previously for extraction, ACN/DCM/MeOH and MeOH alone. An advantage of the use of MeOH in the presence of a BF<sub>3</sub> salt was the concomitant methylation of carboxylic acids. Thus, in addition, we evaluated the influence of the methylation reaction conditions on the process efficiency and compared that to the methylation with BF<sub>3</sub> and silylation with BSTFA. Figure V.1 is showing the proposed new derivatization pathway. The efficiency of the proposed extraction method was studied using wood smoke (WS) PM, which has a higher abundance of organic compounds. The concentrations of acids and aldehydes were compared for two common PM matrices: WS and urban air (UA) standard reference material (SRM) PM.

## V.2. MATERIALS AND METHODS

### V.2.1 Materials

ACN (LCMS Optima grade), MeOH (99.9% Purge and Trap grade) and DCM (GC quality) were purchased from Fisher Scientific (Waltham, MA, USA); *n*-hexane (GC quality) was from Sigma-Aldrich (St. Louis, MO, USA). Water was purified using a Direct-Q3 water purification system with an incorporated dual wavelength UV lamp (Millipore, Billerica, MA, USA) to assure a low total carbon content (the manufacturer claimed this impurity to be less than 5 ng/g).

The derivatization agents, PFBHA·HCl (>99%), BSTFA (1% TMCS; 10% TMCS) and BF<sub>3</sub>/methanol (10% w/w) were purchased from Sigma-Aldrich, pyridine (>99%) was purchased from Alfa Aesar (Ward Hill, MA, USA). The information on aldehydes and acids considered in this study is provided in Tables V.2 and V.3, respectively including suppliers, relative retention and ions (*m/z*) used in the GC-MS analysis.

Model mixtures (Table V.3) of stock solutions representing different classes of carboxylic acids were prepared, including long chain monocarboxylic acids (ca. 0.5 mg/mL per analyte in DCM), dicarboxylic acids (ca. 1.5 mg/mL per analyte in ACN), aromatic acids (ca. 0.2 mg/mL per analyte in ACN), ketoacids and hydroxyacids (ca. 1 mg/mL per analyte in ACN and MeOH), and stored at -18 °C. Stock solutions of single representatives of each group (ca. 0.5-5 mg/mL) were also prepared.

*Calibration solutions.* The aldehyde calibration solution was prepared in a concentration range of 0.03–50 µg/mL with the addition of a recovery standard mixture (Table V.2, the concentration range 0.03–30 µg/mL). The acid calibration solution was prepared by mixing acid standard mixtures (within a concentration range of 0.02–100 µg/mL) with acid

recovery standards (Table V.3; concentration range 0.01–50 µg/mL). The solutions were derivatized according to the PFBHA derivatization protocol (MeOH only). The calibration mixture for hydroxy and aromatic acids was prepared separately and was subjected to the sequential PFBHA/BSTFA derivatization protocol. Two ISs were employed to correct for the injection volume, *o*-terphenyl for acids and octafluoronaphthalene (OFN) for aldehydes (suitable for NCI).

Two bulk PM samples (WS and UA PM) were used for this study. Bulk WS PM was collected from a chimney that vented an airtight wood stove burning a mix of hardwoods [115,116]. The UA PM used in this study was NIST SRM 1648b.

## V.2.2 Sample preparation

### V.2.2.1 Evaluation of derivatization conditions

Five model mixtures (Table V.3) of stock solutions representing different classes of carboxylic acids were prepared, including long chain monocarboxylic acids (~0.5 mg/mL per analyte in DCM), dicarboxylic acids (~1.5 mg/mL per analyte in ACN), aromatic acids (~0.2 mg/mL per analyte in ACN), ketoacids and hydroxyacids (~1 mg/mL per analyte in ACN and MeOH), and stored at -18 °C. Stock solutions of single representative of each group (~0.5-5 mg/mL) were also prepared.

*PFBHA-HCl derivatization.* Two different solvents systems were evaluated for PFBHA derivatization developed in previous studies [100,101], derivatization 1) in the presence of MeOH and 2) in the solvent system containing ACN, DCM and MeOH. The acid samples (with a final concentration of ~100 ppm) were mixed with PFBHA dissolved in MeOH (40 mg/mL) allowing for at least a 10-fold excess in the moles of PFBHA to the moles of acids present in the solvent system containing either ACN, DCM, and MeOH (1.0:8.5:0.5, v/v/v, the final

volume 1.0 mL), or just MeOH (0.10 mL). The acids were derivatized for either 1, 3 or 18 hours using sonication for agitation. Alternatively, the acids were stirred by a magnetic stir bar while heated to 50 °C for 18 hours to evaluate the effect of sonication. After cooling, the solution in the second solvent system was evaporated to 50 µL and DCM was added in the 0.5:9.5 ratio (MeOH/DCM, v/v, the final volume 1.0 mL), while ACN/DCM/MeOH solutions were left intact. The solutions were filtered using a 0.2 µm PTFE filter to remove excess precipitated PFBHA from the solution.

*BF<sub>3</sub>/alcohol derivatization.* For esterification of carboxylic acids with methanol in the presence of BF<sub>3</sub>, an adopted protocol [106,107] was used. The acid samples (the final concentration ~100 ppm) were added to 50 µL of a BF<sub>3</sub>/methanol solution and heated to 60 °C for 60 minutes. After cooling to room temperature, 0.5 mL of a saturated NaCl solution in water were added and methyl esters were extracted three times with *n*-hexane. The fractions were combined (the total volume 2.0 mL) and the solution was filtered through anhydrous Na<sub>2</sub>SO<sub>4</sub> to remove residual water.

*Sequential PFBHA·HCl /BSTFA derivatization.* The acid samples (the final concentration ~100 ppm) were first derivatized as described in the PFBHA·HCl or BF<sub>3</sub>/methanol derivatization protocols. After drying the filtered solution, 50 µL BSTFA was added and the mixture was held at 60 °C for 60 minutes. Subsequently, DCM was added up to 1.0 mL volume. Alternatively, a BSTFA solution with 10% of TMCS was used with/without the addition of pyridine (50 µL).

All samples were spiked with 5.0 µL of IS (*o*-terphenyl) prior to the analysis to control the volume changes.

### V.2.2.2 Extraction and derivation of PM samples

*PM samples.* PM samples (~2.5-5 mg) were spiked with recovery standards (~10-20 µg/mL), extracted with 5 mL of a tested solvent system and derivatized using the optimized protocol, i.e., with PFBHA·HCl (200 µL of 40 mg/mL of PFBHA·HCl in MeOH) for 18 hours and agitation by sonication. After cooling to room temperature, samples were evaporated to 50 µL, spiked with both ISSs, and then DCM was added in the 0.5:9.5 ratio (MeOH/DCM, v/v, the final volume 1 mL). Samples were processed according to the sequential PFBHA·HCl /BSTFA protocol.

Alternatively, 2 mg of WS PM was first extracted and derivatized using 9.5 mL of MeOH and 0.5 mL of PFBHA (10 mg/mL) in MeOH for 18 hours and agitation by sonication. WS PM was filtered out using filtration paper and further extracted and derivatized using ACN/DCM/MeOH procedure. Finally, WS PM residue was extracted on the Soxhlet for 18 hours with MeOH. All extraction fractions were analyzed separately.

### V.2.3 Instrumentation

Analyses were performed using a GC-MS (6890N GC, 5975 MS; Agilent Technologies, Santa Clara, CA, USA) equipped with a Gerstel MPS2 autosampler (Gerstel, Baltimore, MD, USA). Injections were performed in a splitless mode for 0.5 min at 250 °C, injection volume was 1 µL. The separation was performed using a 30-m long DB-5 capillary column, with 0.25 mm internal diameter (I.D.) and 0.25 µL film thickness (J&W Scientific, Folsom, CA, USA). A constant carrier gas (helium) flow rate of 1.0 mL/min was maintained during the analysis. The temperature program used started at 35 °C held for 1 min, followed by a gradient of 20 °C/min to 85 °C, followed by a second ramp of 5 °C/min to 320 °C and held for 2 min. The MS analysis was performed in the selected ion-total ion (SITI) mode. The ions used for selected ion monitoring (SIM, within SITI) are specified in Tables 2 and 3 with a typical dwell time of 50 ms,

the TIC mass range of  $m/z$  50–600. The EI was used with an ionization energy of 70 eV. The temperatures of MS-NCI source, mass analyzer, and the transfer line were 155 °C, 150 °C and 280 °C respectively. The reagent gas used for NCI ionization was methane with a flow rate of 3 mL/min and ionization energy of 230 eV.

#### V.2.4 Data processing

MSD Chemstation E.02.00.147 software was employed for the GC-MS data acquisition and processing. Quantification was performed using the IS calibration method using the area of the target ion (Tables V.2 and V.3) obtained in the SIM mode (within SITI method). The recovery standards were used to correct recoveries of native aldehydes and aldehydes extracted from PM. Thus, a least square calibration curve was obtained for each recovery standard using Microsoft Office Excel to obtain calibration curve parameters. The instrumental LODs were calculated from the calibration curves using the formula  $LOD=3.3*s_y/k$ , where  $k$  is a slope of the calibration curve and  $s_y$  is the standard error of the predicted  $y$ -value for each  $x$ -value;  $s_y$  was obtained by a least square linear regression. From the acquired calibration profiles, the points within one order of magnitude of the LOD were used for the LOD calculations.



**Table V.2 List of aldehydes studied with their supplier, the corresponding GC-MS relative retention, target and confirmation ions and their relative abundance (listed in parenthesis) used for data acquisition and processing.**

Label	Aldehyde	Supplier	MW g/mol	EI			NCI			r <sub>12</sub>
				Target ion	Confirmation ions	LOD ng	Target ion	Confirmation ions	LOD ng	
AL1	Formaldehyde	Fisher Scientific <sup>a</sup>	225	181 (100)	195 (10), 225 (1)	NA	225 (50)	205 (100)	1.02	0.76
AL2	Acetaldehyde	Sigma Aldrich <sup>b</sup>	239	181 (100)	209 (10), 239 (5)	0.22	239 (100)	218 (15)	0.24	0.98
AL3	Propanal	Sigma-Aldrich	253	181 (100)	223 (5), 236 (10)	0.15	253 (100)	233 (50)	0.08	1.16
AL4	Acrolein	Sigma-Aldrich	251	181 (100)	221 (5), 251 (20)	1.13	231 (70)	201 (100)	0.12	1.17
AL5	Isobutanal	Sigma Aldrich	267	181 (100)	250 (10)	0.18	178 (100)	247 (10), 267 (10)	0.06	1.25
AL6	Butanal	Fluka <sup>c</sup>	267	181 (100)	239 (15)	0.20	247 (100)	267 (50)	0.08	1.35
AL7	Crotonal	Chem Service <sup>d</sup>	265	181 (100)	195 (5), 250 (25)	0.21	245 (100)	215 (80)	0.07	1.47
AL8	Pentanal	Sigma Aldrich	281	181(100)	207 (5), 239 (20)	0.21	178 (100)	261 (20), 231 (15)	0.03	1.54
AL9	Hexanal	Sigma Aldrich	295	181 (100)	239 (25), 295 (5)	0.19	178 (100)	248 (30), 275 (20)	0.03	1.72
AL10	Furaldehyde	Sigma Aldrich	271	291 (50)	248(20), 181(100)	0.15	241 (100)	271 (80)	0.10	1.79
AL11	<i>trans</i> -2-Hexenal	Sigma Aldrich	293	181 (100)	250 (20), 293 (5)	0.16	273 (100)	243 (80)	0.05	1.85
AL12	Heptanal	Sigma Aldrich	309	181 (100)	207 (5), 239 (30)	0.19	178 (100)	289 (40)	0.02	1.90
AL13	Octanal	Sigma Aldrich	323	181 (100)	239 (30), 323 (1)	0.18	178 (100)	276 (10)	0.02	2.07
AL14	Benzaldehyde	Sigma Aldrich	301	301 (100)	271 (50)	0.11	281 (100)	251 (60)	0.07	2.12
AL15	Phenylacetaldehyde	Sigma Aldrich	315	181 (100)	91 (50), 315 (10)	0.09	178 (100)	205(50)	0.07	2.20
AL16	Nonanal	Fluka	337	181 (100)	239 (30)	0.14	178 (100)	317 (25)	0.02	2.24
AL17	<i>m</i> -Tolualdehyde	Sigma Aldrich	315	181 (100)	91 (15), 315 (30)	0.05	295 (100)	265 (40), 167 (25)	0.10	2.29
AL18	<i>o</i> -Tolualdehyde	Sigma Aldrich	315	181 (100)	91 (15), 315 (30)	0.07	295 (100)	265 (50), 167 (60)	0.10	2.29
AL19	Hydrocinnamaldehyde	Sigma Aldrich	329	181 (100)	271 (10), 329 (20)	0.16	178 (100)	309 (30)	0.06	2.35
AL20	<i>trans</i> -2-Nonenal	Sigma Aldrich	335	181 (100)	250 (25), 335 (5)	0.12	315 (100)	285 (30)	0.08	2.37
AL21	2-Hydroxy benzaldehyde	Chem Service	317	181 (100)	300 (15), 317 (40)	0.14	136 (100)	280 (5)	0.12	2.46
AL22	Decanal	Sigma Aldrich	351	181 (100)	239 (30), 351 (1)	0.14	178 (100)	331 (30), 196 (50)	0.03	2.40

Table V.1. cont.

Label	Aldehyde	Supplier	MW g/mol	EI			NCI			r <sub>12</sub>
				Target ion	Confirmation ions	LOD ng	Target ion	Confirmation ions	LOD ng	
AL23	2,5-Dimethylbenzaldehyde	Sigma Aldrich	329	181 (100)	286 (10), 329 (50)	0.14	309 (100)	279 (40)	0.04	2.43
AL24	5-Hydroxymethylfurfural	Sigma Aldrich	321	181 (100)	291 (15), 321 (50)	0.11	271 (100)	285 (25), 301 (40)	0.13	2.47
AL25	2,4-Nonadienal	Sigma Aldrich	333	181 (100)	276 (70), 333 (15)	0.16	283 (100)	167 (50)	0.13	2.49
AL26	Glyoxal	Sigma Aldrich	448	181 (100)	418 (1), 448 (5)	0.16	267 (100)	167 (35)	0.11	2.53
AL27	Anisaldehyde	Chem Service	331	331 (100)	181 (90), 288 (20)	0.11	311 (100)	281 (40)	0.07	2.57
AL28	Methylglyoxal	Sigma Aldrich	462	181 (100)	432 (1), 462 (5)	0.14	281 (100)	167 (20), 392 (10)	0.08	2.59
AL29	4-Hydroxybenzaldehyde	Chem Service	317	181 (100)	274 (10), 317 (40)	0.35	297 (100)	267 (40)	0.15	2.66
AL30	Dodecanal	Sigma Aldrich	379	181 (100)	239 (35)	0.10	178 (100)	332 (10), 359 (30)	0.23	2.69
AL31	Glutaraldehyde	Sigma Aldrich	490	181 (100)	293 (5), 490 (1)	0.22	178 (100)	450 (20)	0.22	2.85
AL32	Syringaldehyde	Chem Service	377	377 (100)	181 (70)	0.24	357 (100)	327 (20)	0.13	2.94
<b>Recovery Standards</b>										
	Formaldehyde- <sup>13</sup> C-d <sub>2</sub>	Isotec <sup>e</sup>	227	181(100)	198 (95)	NA	228(50)	208(100)	NA	0.76
	Acetaldehyde-d <sub>4</sub>	CDN Isotopes <sup>f</sup>	243	181(100)	213(10)	NA	243(90)	222(100)	NA	0.98
	Propanal-d <sub>2</sub>	CDN Isotopes	255	181(100)	238(15), 225(10)	NA	255(100)	235(60)	NA	1.16
	Butanal-d <sub>2</sub>	CDN Isotopes	269	181(100)	241(10)	NA	269(75)	221(100)	NA	1.35
	Furaldehyde-d <sub>4</sub>	CDN Isotopes	275	181(100)	295(30), 251(5)	NA	245(100)	275(50)	NA	1.79
	Octanal-d <sub>16</sub>	CDN Isotopes	329	181(100)	243(20), 339(5)	NA	319(100)	289(20)	NA	2.07
	Benzaldehyde-d <sub>6</sub>	CDN Isotopes	307	181(100)	307(25), 277(15)	NA	287(100)	257(70)	NA	2.12
	p-Anisaldehyde-d <sub>3</sub>	CDN Isotopes	334	181(100)	334(80)	NA	314(100)	284(35)	NA	2.57
	4-Hydroxybenzaldehyde-d <sub>4</sub>	CDN Isotopes	321	181(100)	321(70)	NA	301(100)	271(40)	NA	2.66

<sup>a</sup>(Pittsburgh, PA,USA); <sup>b-c</sup>(St. Louis, MO, USA); <sup>d</sup>(West Chester, PA, USA); <sup>e</sup>(Champaign, IL, USA); <sup>f</sup>(Pointe-Claire, Quebec, Canada)

**Table V.3 List of carboxylic acids studied with their supplier, the corresponding GC-MS relative retention, target and confirmation ions and their relative abundance (listed in parenthesis) used for data acquisition and processing.**

Label	Acid	Supplier	MW g/mol	Target ion	Confirmation ions	LOD ng	r <sub>12</sub>
<b>Monocarboxylic Acids</b>							
MA1	Valeric	Sigma Aldrich <sup>a</sup>	116	74 (100)	87(40) 57(50)	0.12	0.16
MA2	Hexanoic	Acros <sup>b</sup>	130	74(100)	87(60) 99(30)	0.12	0.19
MA3	Heptanoic	Acros	144	74(100)	113(40) 87(30)	0.22	0.25
MA4	Octanoic	Acros	158	74(100)	87(50) 127(30)	0.23	0.32
MA5	Nonanoic	Sigma Aldrich	172	74(100)	87(50) 141(20)	0.21	0.41
MA6	Decanoic	Acros	186	74(100)	87(50) 143(20) 155(15)	0.15	0.50
MA7	Undecanoic	Acros	200	74(100)	143(20) 169(20)	0.13	0.60
MA8	Dodecanoic	Sigma Aldrich	214	74(100)	143(20) 171(20)	0.15	0.69
MA9	Tridecanoic	Sigma Aldrich	228	74(100)	143(20) 228(10)	0.12	0.78
MA10	Tetradecanoic	Sigma Aldrich	242	74(100)	143(20) 242(10)	0.17	0.87
MA11	Pentadecanoic	Acros	256	74(100)	143(20) 256(20)	0.07	0.95
MA12	Hexadecanoic	Acros	270	74(100)	143(30) 270 (20)	0.16	1.03
MA13	Heptadecanoic	Sigma Aldrich	284	74(100)	143(30) 284(20)	0.15	1.11
MA14	Octadecanoic	Acros	298	74(100)	298(30) 143(30)	0.27	1.18
MA15	Oleic	Sigma Aldrich	296	74(100)	143(10) 87(40)	0.24	1.16
MA16	Nonadecanoic	Sigma Aldrich	312	74(100)	143(30) 87(80)	0.03	1.25
MA17	Eicosanoic	Acros	326	74(100)	143(30) 87(80)	0.04	1.32
MA18	Docosanoic	Sigma Aldrich	354	74(100)	143(30) 87(80)	0.04	1.45
MA19	Tricosanoic	Sigma Aldrich	368	74(100)	143(40) 87(80)	0.04	1.51
MA20	Tetracosanoic	Fisher Scientific <sup>b</sup>	382	74(100)	143(40) 87(90)	0.02	1.57
MA21	Heneicosanoic	Sigma Aldrich	340	74(100)	143(30) 87(80)	0.05	1.38
MA22	Octacosanoic	Sigma Aldrich	438	74(100)	143(50) 87(90)	0.05	1.78
<b>Dicarboxylic Acids</b>							
DA1	Oxalic	Sigma Aldrich	118	59(100)	118(5)	0.18	0.15
DA2	Malonic	Sigma Aldrich	132	101(100)	74(50) 59(90)	0.13	0.19
DA3	Succinic	Sigma Aldrich	146	115(100)	87(20) 55(60)	0.22	0.25
DA4	Glutaric	Sigma Aldrich	160	59(100)	100(80) 129(60)	0.14	0.33
DA5	Adipic	Sigma Aldrich	174	114(100)	143(70) 59(100)	0.27	0.42
DA6	Pimelic	Sigma Aldrich	188	115(100)	157(50) 125(50)	0.27	0.52
DA7	Methyl Malonic	Sigma Aldrich	146	115(50)	87(40) 59(100)	0.32	0.30
DA8	Methyl Succinic	Fluka <sup>a</sup>	160	129(50)	101(40) 87(20)	0.19	0.28
DA9	Methyl Glutaric	Fluka	174	114(100)	143(50) 99(50)	0.14	0.36
DA10	Maleic	Sigma Aldrich	144	113(100)	85(40) 59(40)	0.5	0.25
DA11	Fumaric	Fluka	144	113(100)	85(60) 59(30)	0.5	0.25
DA12	Methyl Maleic	Sigma Aldrich	158	127(100)	99(30) 59(40)	0.25	0.21
DA13	Suberic	Sigma Aldrich	202	171(70)	138(100) 129(90)	0.16	0.62
DA14	Azelaic	Sigma Aldrich	216	185(60)	152(100) 143(40)	0.19	0.71
DA15	Sebacic	Sigma Aldrich	230	199(70)	166(50) 157(60)	0.06	0.80

Table V.3 cont.

Label	Acid	Supplier	MW g/mol	Target ion	Confirmation ions	LOD ng	r <sub>12</sub>
<b>Dicarboxylic Acids</b>							
DA16	Undecanedioic	Sigma Aldrich	244	213(70)	171(50) 139(70)	0.11	0.60
DA17	Dodecanedioic	Sigma Aldrich	258	227(60)	185(40) 98(100)	0.19	0.97
DA18	Tridecanedioic	Acros	272	241(50)	199(40) 98(100)	0.09	1.05
DA19	Tetradecanedioic	Sigma Aldrich	286	255(60)	213(40) 181(30)	0.03	1.13
DA20	Pinic	Sigma Aldrich	214	128(50)	154(30) 115(100)	0.15	0.61
<b>Ketoacids</b>							
KA1	Pyruvic	Fisher	297	195(10)	181(100) 297(1)	0.17	0.59
KA2	Glyoxylic	Fisher	283	195(10)	181(100) 283(5)	0.24	0.55
KA3	4-Oxopentanoic	Acros	325	294(30)	181(100) 195(10)	0.28	0.75
KA4	Oxaloacetic	Sigma Aldrich	355	293(10)	181(100) 195(10)	0.24	0.85
KA5	2-Ketoglutaric	Acros	369	352(20)	181(100) 195(5)	0.16	0.93
KA6	4-Ketopimelic	Sigma Aldrich	397	366(20)	181(100) 397(10)	0.1	1.08
KA7	<i>cis</i> -Pinonic	Sigma Aldrich	393	212(50)	266(40) 181(100)	0.21	1.05
<b>Hydroxyacids</b>							
HA1	Malic	Sigma Aldrich	350	335(10)	245(20) 233(25)	0.21	0.43
HA2	Tartaric	Sigma Aldrich	439	423(10)	292(30) 219(20)	0.59	0.62
HA3	Vanillic	Sigma Aldrich	312	312(80)	297(90) 267(100)	1.14	0.72
HA4	Annisic	Sigma Aldrich	224	209(100)	179(30) 193(20)	14	0.57
HA5	Homovanillic	Sigma Aldrich	308	293(100)	308(70) 219(80)	0.57	0.83
HA6	Syringic	Sigma Aldrich	342	342(70)	327(100) 312(70)	1.14	1.01
<b>Aromatic Acids</b>							
AA1	Benzoic	Sigma Aldrich	194	194(10)	179(100) 135(40)	0.8	0.43
AA2	Salicylic	Sigma Aldrich	282	267(100)	209(10) 193(10)	0.1	0.67
AA3	Mandelic	Sigma Aldrich	296	253(20)	281(5) 179(100)	0.04	0.57
AA4	3-Nitrobenzoic	Sigma Aldrich	239	224(100)	178(30) 150(20)	0.05	0.79
AA5	Phthalic	Sigma Aldrich	310	295(30)	310(10) 221(10)	0.16	0.84
AA6	4-Methylphthalic	Sigma Aldrich	324	309(40)	250(50) 237(40)	0.03	0.93
<b>Recovery Standards</b>							
	Malonic acid-d <sub>4</sub>	Sigma Aldrich	134	103(30)	134(5) 59(100)	NA	0.15
	Nonanoic acid-d <sub>17</sub>	CDN Isotopes <sup>e</sup>	189	77(100)	91(50) 50(15)	NA	0.41
	Dodecanodioic acid-d <sub>4</sub>	CDN Isotopes	258	231(70)	187(40) 155(40)	NA	0.97
	Phthalic acid-d <sub>4</sub>	Isotec <sup>d</sup>	314	299(30)	314(10)	NA	0.84

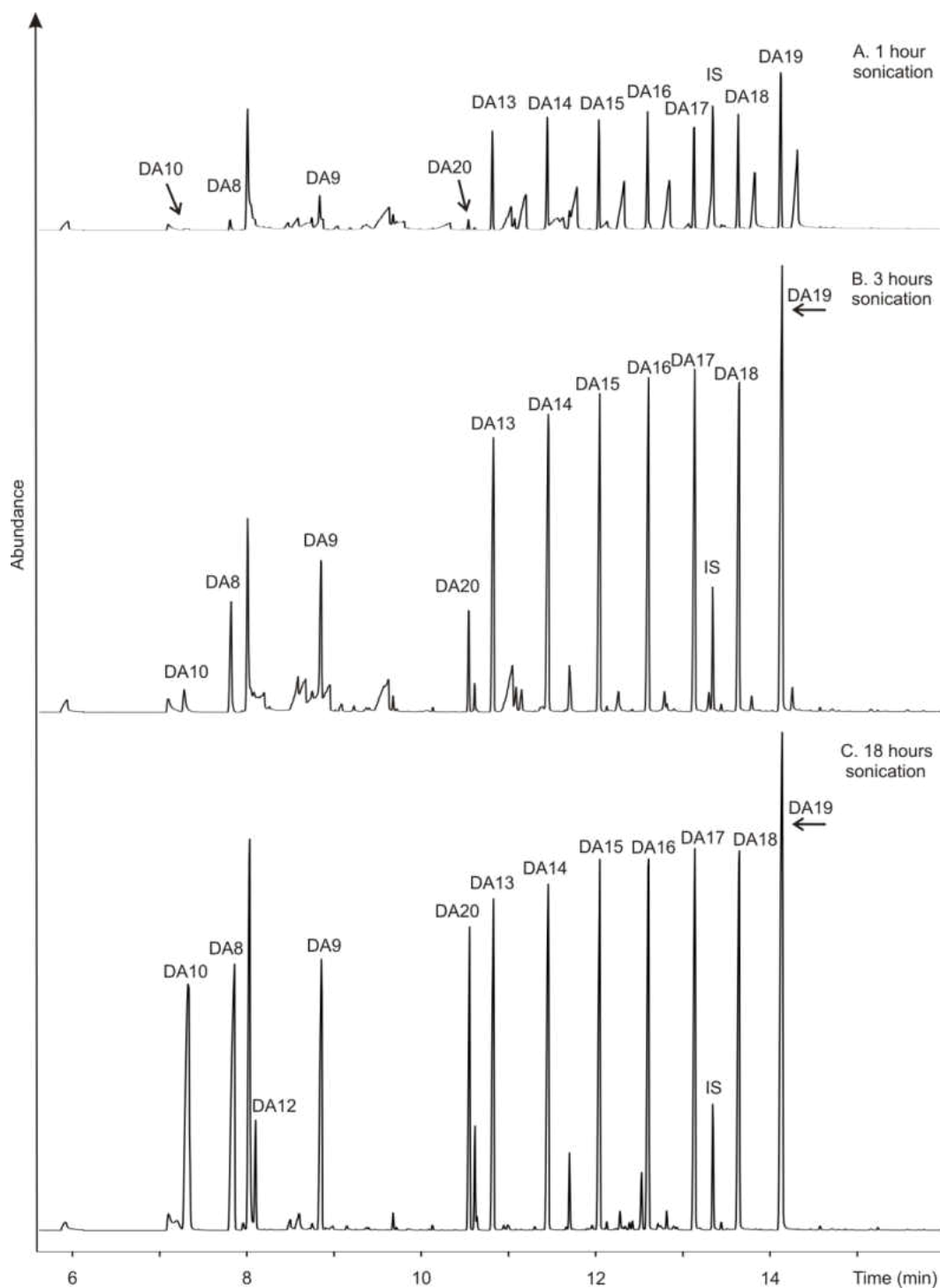
<sup>a</sup>(St. Louis, MO, USA); <sup>b</sup>(Pittsburgh, PA, USA); <sup>c</sup>(Pointe-Claire, Quebec, Canada); <sup>d</sup>(Champaign, IL, USA)

### V.3. RESULTS AND DISCUSSION

#### V.3.1 Evaluation of derivatization and extraction

A typical protocol was previously developed for derivatization and extraction of aldehydes with PFBHA·HCl [100]. It was also shown that both MeOH and ACN/DCM/MeOH derivatization systems are effective for derivatization of aldehydes [100]. Previous studies also employed sonication to enhance extraction, but not derivatization [81,93,101,117]. Following on this study, we have confirmed effectiveness of this system and observed that sonication improved the derivatization recoveries of aldehydes (Analysis performed by Mr. Chintapalli [118], Appendix Fig. D.1). Further, to promote the esterification reaction along with the formation of methoximes from carbonyls (Fig. V.1), we evaluated the effect of sonication time in MeOH (Fig. V.2). As shown for dicarboxylic acids (Fig. V.2) and similar to aldehydes, 18 hours of sonication were required for derivatization of the majority of tested acids with the exception of aromatic acids. After 3 hours, long monocarboxylic acids were completely methylated, however, dicarboxylic acids and ketoacids were derivatized only partially (presented in Fig. V.2 for dicarboxylic acids only). When the time of sonication was decreased to 1 hour, we observed an incomplete esterification for all tested acids.

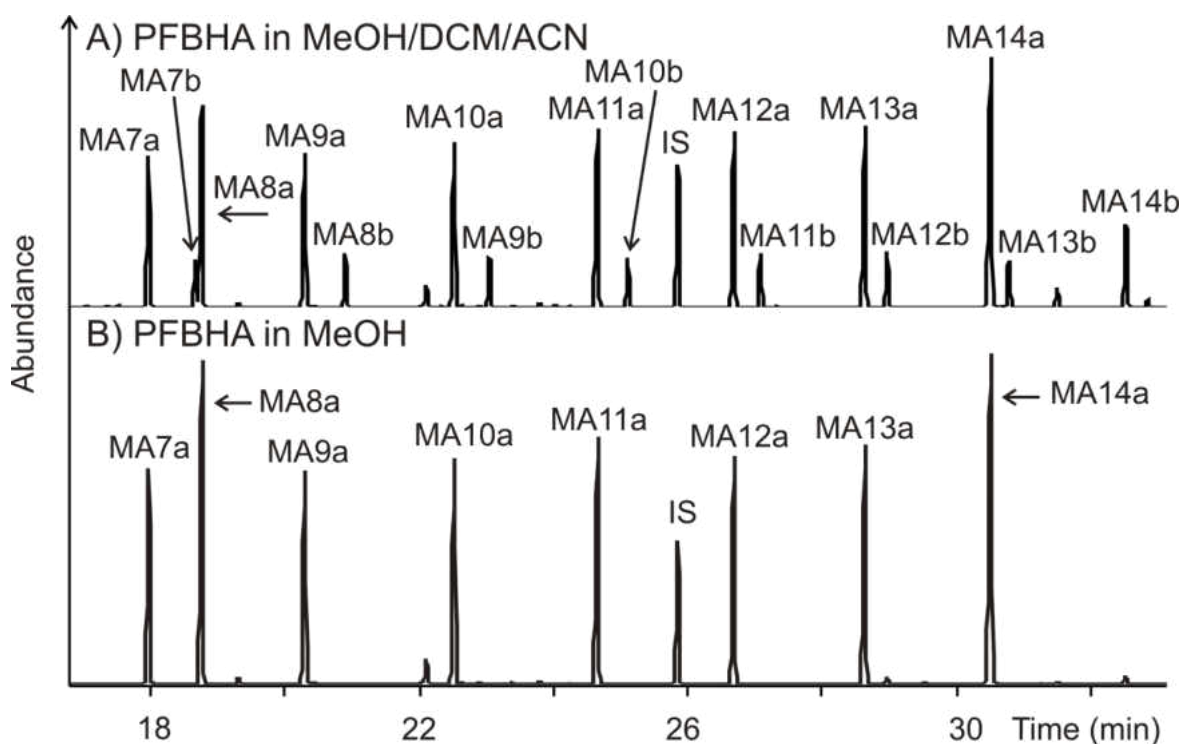
Since heat is released during the sonication (the temperature in a sonication bath reached 50 °C), we have explored whether the higher derivatization efficiency was due to the temperature (or if sonication was essential). The comparison for C<sub>8</sub>-C<sub>14</sub> dicarboxylic acids derivatized while being either sonicated or heated on a hot plate (with the mixing by a magnetic stirrer for 18 hours) has demonstrated an incomplete derivatization of the heated sample showing both monomethyl and dimethyl esters. By contrast, the derivatization in sonicated samples was complete, showing dimethyl esters as single reaction products (Fig. D.2).



**Figure V.2** The effect of time on methylation of dicarboxylic acids with PFBHA-HCl in MeOH. A) 1 h, B) 3 h, C) 18 h. The acids labels are provided in Table V.2.

To align our study with typical conditions for aldehydes' derivatization [100], we also explored the use of an ACN/DCM/MeOH solvent system. The reaction completeness was confirmed by a subsequent BSTFA derivatization. In the ACN/DCM/MeOH solvent system, the

methylation of the majority of acids was incomplete showing the occurrence of both methyl and trimethylsilyl esters, the latter obtained by the sequential derivatization with BSTFA (Fig. V.3 A, shown for monocarboxylic acids), while a complete methylation was achieved for model compounds using MeOH as a single solvent (Fig V.3 B).



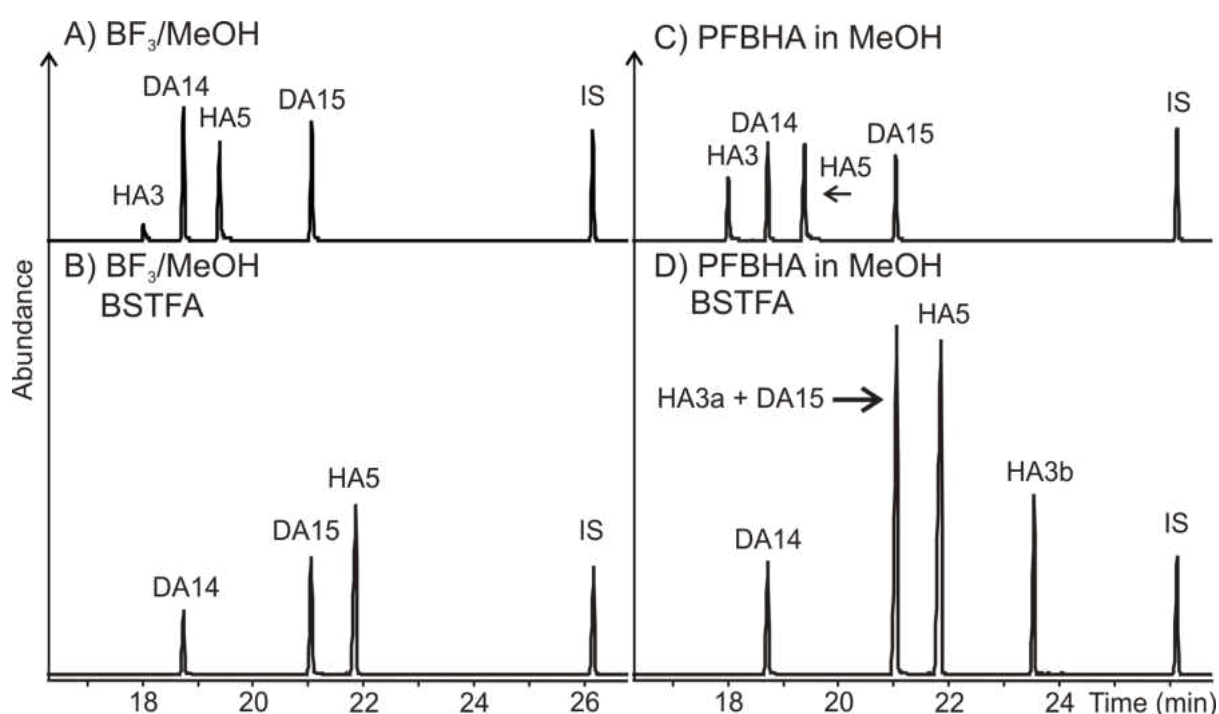
**Figure V.3** Demonstration of derivatization efficiency of monocarboxylic acid with 18 h sonication in two solvent systems A) PFBHA in ACN/DCM/MeOH and B) PFBHA in MeOH. The acids labels are provided in Table V.2. Denotation “a” stands for methyl ester, “b” stands for trimethylsilyl ester. The acids labels are provided in Table V.2.

### V.3.1.1 Efficiency of esterification of aromatic acids

As shown in the previous section, the esterification reaction was not complete for aromatic acids even after 18 hour of sonication. In order to complete their derivatization, we attempted to enhance the methylation by increasing both the MeOH and PFBHA·HCl concentrations; however, no increase in the abundance of methyl esters was observed (Fig. D.3).

We have compared the developed PFBHA/MeOH protocol to a common  $\text{BF}_3/\text{MeOH}$  method [84–86,88,92] with the goal to address the derivatization of all acids including

aromatic. This method was chosen because it was previously reported that butylation in presence of  $\text{BF}_3$  yielded similar or even lower LODs to those obtained by trimethylsilylation with BSTFA for mono- and dicarboxylic acids [27,98]. Methylation was selected as opposed to butylation because it yields the same products as in our method. Esterification was tested using a mixture consisting of two aromatic acids with hydroxyl groups (vanillic and homovanillic) and two dicarboxylic acids (azelaic and sebacic) were used as reference compounds.



**Figure V.4 Comparison of  $\text{BF}_3/\text{MeOH}$  with PFBHA methylation protocols each followed by BSTFA trimethylsilylation shown for representative model acid mixture: A)  $\text{BF}_3/\text{MeOH}$ , B)  $\text{BF}_3/\text{MeOH}$  with subsequent BSTFA, C) PFBHA·HCl in MeOH, and D) PFBHA·HCl in MeOH with subsequent BSTFA The acids labels are provided in Table V.2. Denotation “a” stands for methyl ester, “b” stands for trimethylsilyl ester.**

While the reaction was complete for dicarboxylic acids and homovanillic acid (Fig. V.4A–D), an incomplete derivatization was still observed for vanillic acid. In the case of vanillic acid, the corresponding methyl ester was observed in both  $\text{BF}_3/\text{MeOH}$  and PFBHA·HCl in MeOH (Fig. V.4A, C), although the response in the second system was significantly higher



(using the 95% confidence interval). A subsequent derivatization with BSTFA showed the vanillic acid methyl ester, now with the trimethylsilylated hydroxy group, in both systems, albeit with a lower abundance in the  $\text{BF}_3$  reaction. Vanillic acid with two trimethylsilyl groups was observed only in the PFBHA·HCl system (Fig. V.4D). This observation suggests that the non-derivatized vanillic acid was not extracted during the  $\text{BF}_3/\text{MeOH}$  derivatization procedure. Thus, the esterification with MeOH in the presence of PFBHA·HCl has a clear advantage in determination of aromatic acids, because samples were evaporated to prevent the potential losses from incomplete extraction.

#### V.3.1.2. Trimethylsilylation of aromatic acids

The complete methylation of aromatic acids could not be achieved with the exception of homovanillic acid (Fig. V.4). Thus, we evaluated a possible quantification of aromatic acids as trimethylsilyl (TMS) esters following the PFBHA·HCl step.

The PFBHA·HCl step resulted in a partial methylation of aromatic acids, thus we have attempted to enhance the following BSTFA derivatization (transesterification) with an increased TMCS content and with/without the presence of pyridine (Fig. V.5A). However, no significant difference was observed in the response of TMS derivatives of aromatic acids (Fig. V.5B) suggesting that the achieved partial methylation is irreversible under the tested conditions.

Nevertheless, we observed that the TMS derivatives of aromatic acids were of significant abundance, and we have confirmed their abundance increased proportionally with concentration (Fig. V.5C).

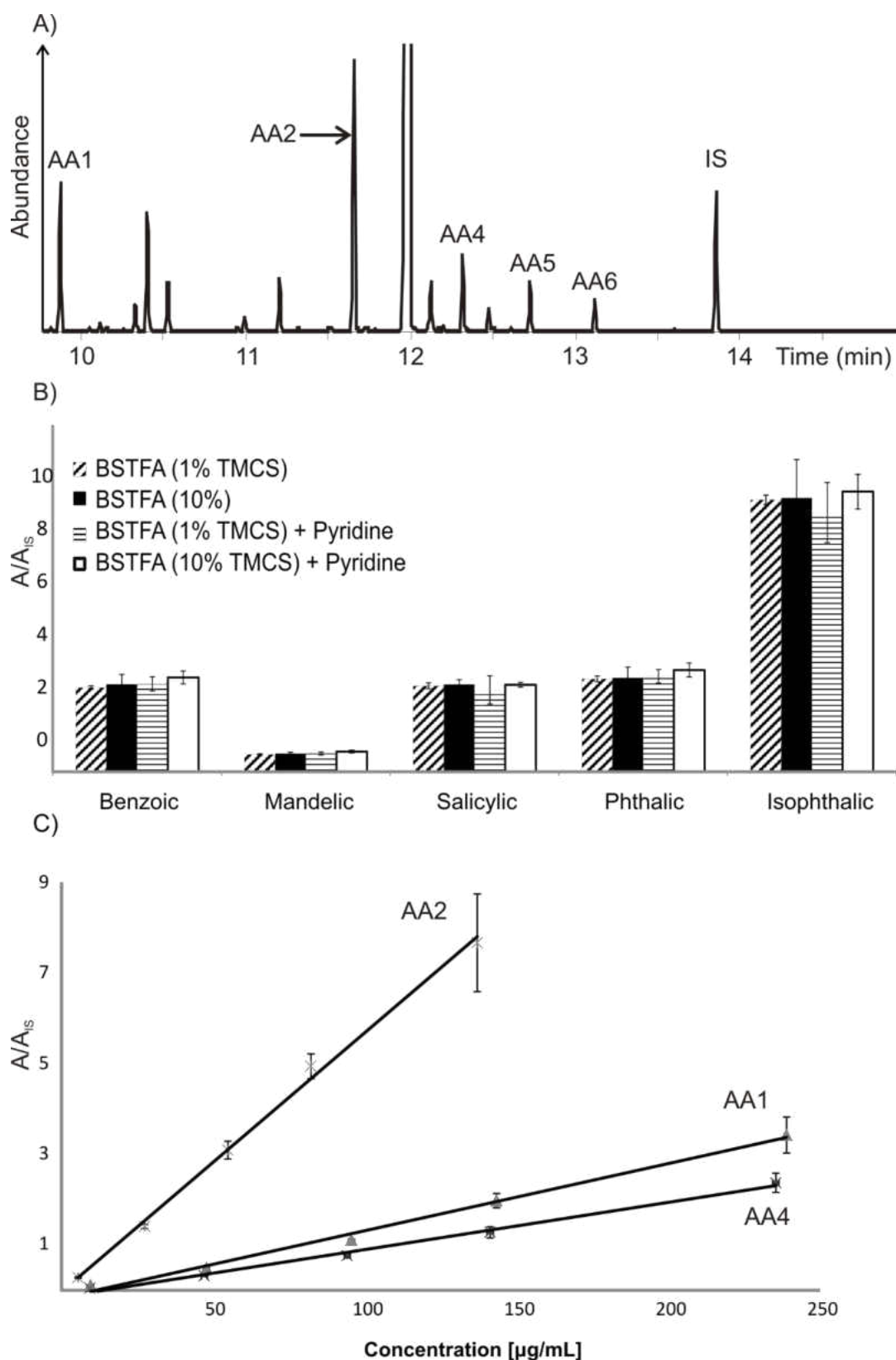
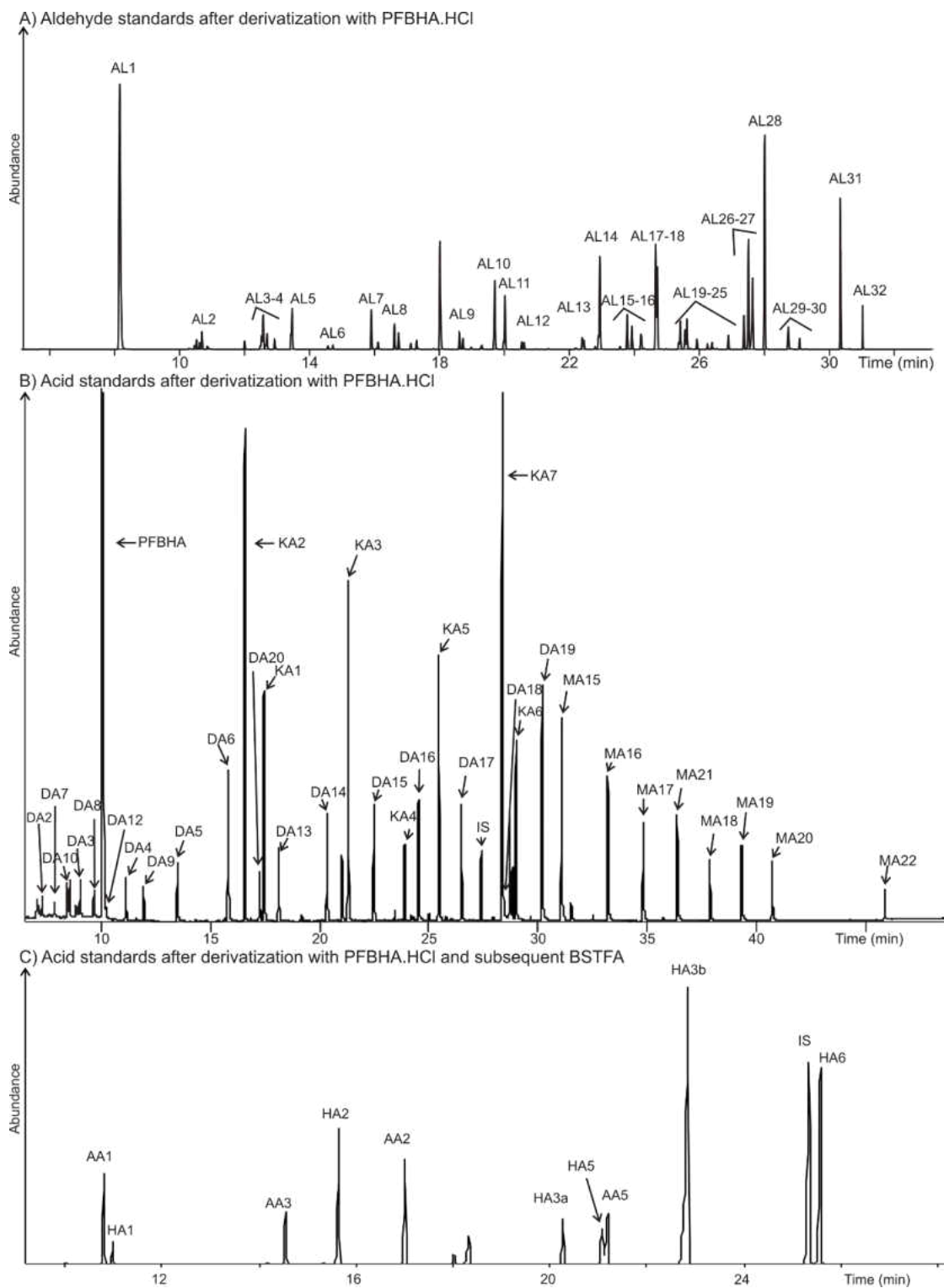


Figure V.5 The efficiency of trimethylsilylation of aromatic acids: A) GC-MS TIC chromatogram with TMS derivatives following using PFBHA·HCl/BSTFA protocol; B) Efficiency of derivatization of aromatic acids with different catalyst system of subsequent BSTFA; C) Calibration curves obtained for trimethylsilyl esters of aromatic acids prepared with PFBHA/BSTFA protocol. The acids labels are provided in Table V.2.

### V.3.1.3. Quantification of aldehydes and acids and calibration parameters

The developed method allows for quantification of 61 acids and 32 aldehydes shown in chromatograms (Fig. V.6). The calibration parameters for all acids and aldehydes are provided in Table S.2. Tables V.2-3 summarize the instrumental LODs obtained with the developed methodology. The majority of aldehydes (Fig. V.6A) were observed within a range of 0.05  $\mu\text{g/mL}$  – 0.35  $\mu\text{g/mL}$  in EI mode compared to 0.02  $\mu\text{g/mL}$  – 0.12  $\mu\text{g/mL}$  in NCI mode, with the exception of formaldehyde (1  $\mu\text{g/mL}$  in NCI). These values were comparable to the work of others [119–121]. It is worth noting that the protocols employing a solid phase micro-extraction tend to report lower LODs for carbonyls [122–124], however, these reports were not targeting acids, either as trimethylsilyl derivatives or as methyl esters.

Methylated acids (Fig. V.6B) were recovered in a range of 0.02 – 0.3  $\mu\text{g/mL}$ , while the aromatic and hydroxyacids (Fig. V.6C) were determined in a somewhat broader range of 0.03 – 1  $\mu\text{g/mL}$ . The achieved LODs were either comparable or lower than those reported in recent papers [92,125].

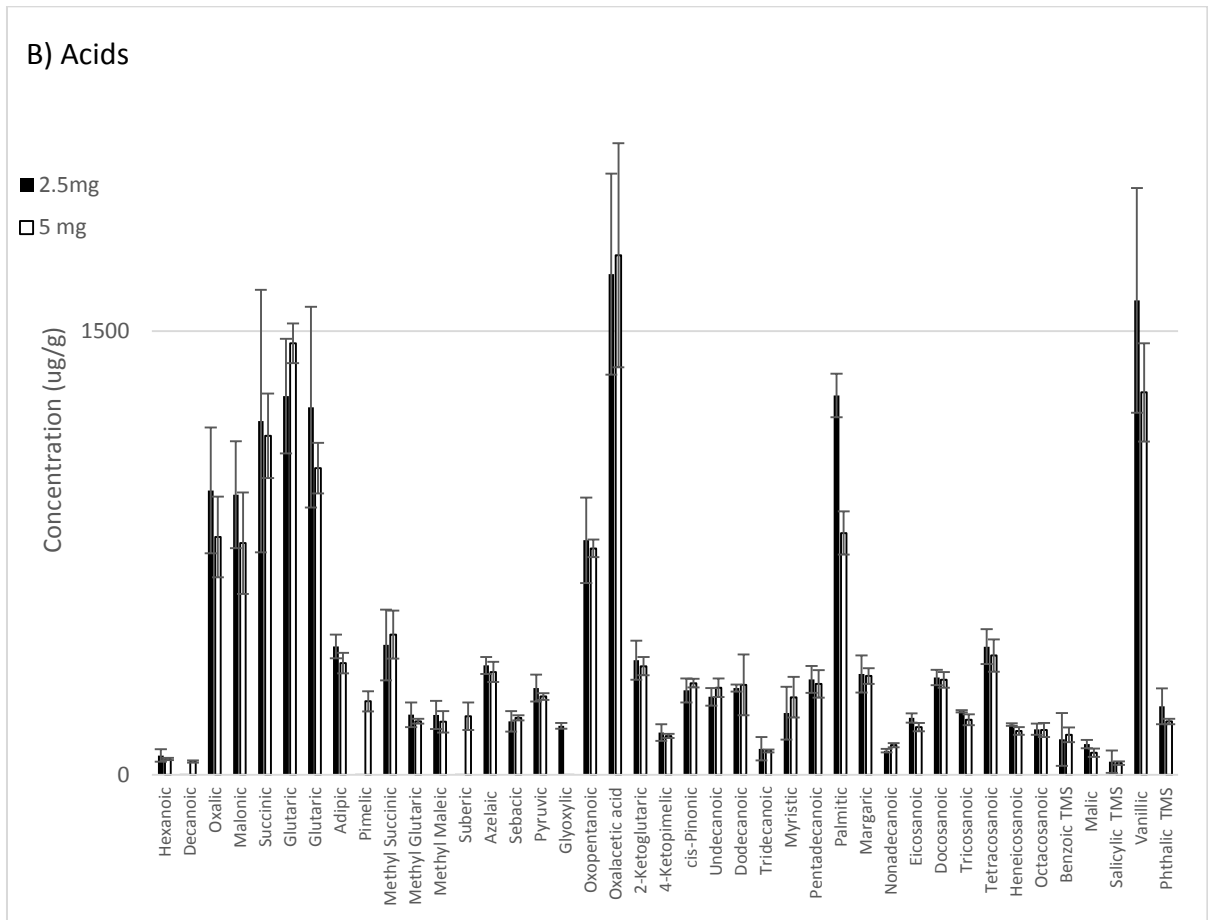
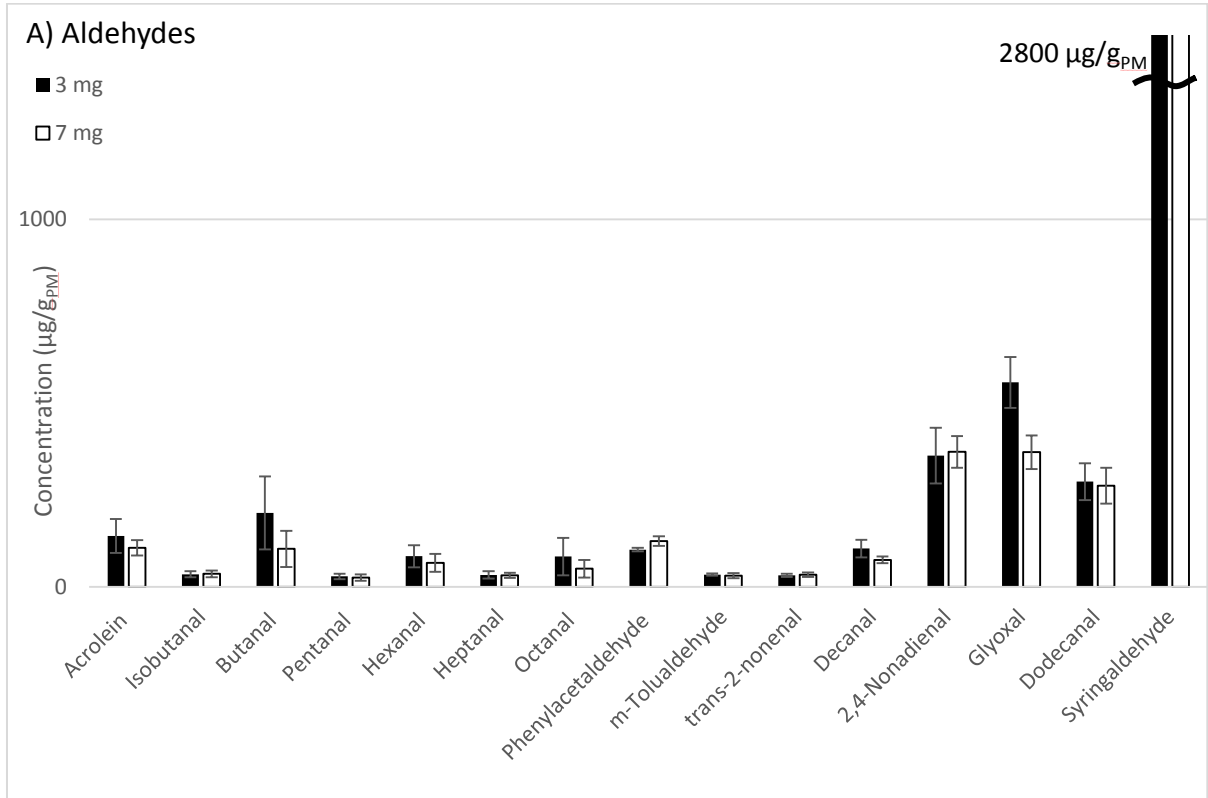


**Figure V.6 GC-MS TIC analysis of A) Aldehyde standards after derivatization with PFBHA·HCl, B) Acid standards (dicarboxylic acids, ketoacids and long monocarboxylic acids) after derivatization with PFBHA·HCl, and C) (hydroxy and aromatic acids) after esterification with MeOH in presence of PFBHA·HCl and subsequent BSTFA trimethylsilylation. The acids labels are provided in Table V.2. “HA3a” stands for vanillic acid methyl ester, “HA3b” stands for vanillic acid trimethylsilyl ester.**

### V.3.2 Determination of acids and aldehydes in PM samples

The developed method was used to extract and derivatize two representative PM samples of a significantly different organic carbon content; WS PM was chosen because of its high organic carbon content (61%); while UA has a lower organic content (13%) and is used as SRM [126]. For aldehydes, the extraction with ACN/DCM/MeOH was previously accomplished [100]. The efficiency of the extraction in the MeOH system was confirmed by sequential extraction of WS PM, which demonstrated full aldehyde recoveries in the first sonication step, and with no aldehyde shown in consecutive steps, i.e., ACN/DCM/MeOH sonication, and Soxhlet extraction (Analysis performed by Mr. Chintapalli [118], Fig. D.4A).

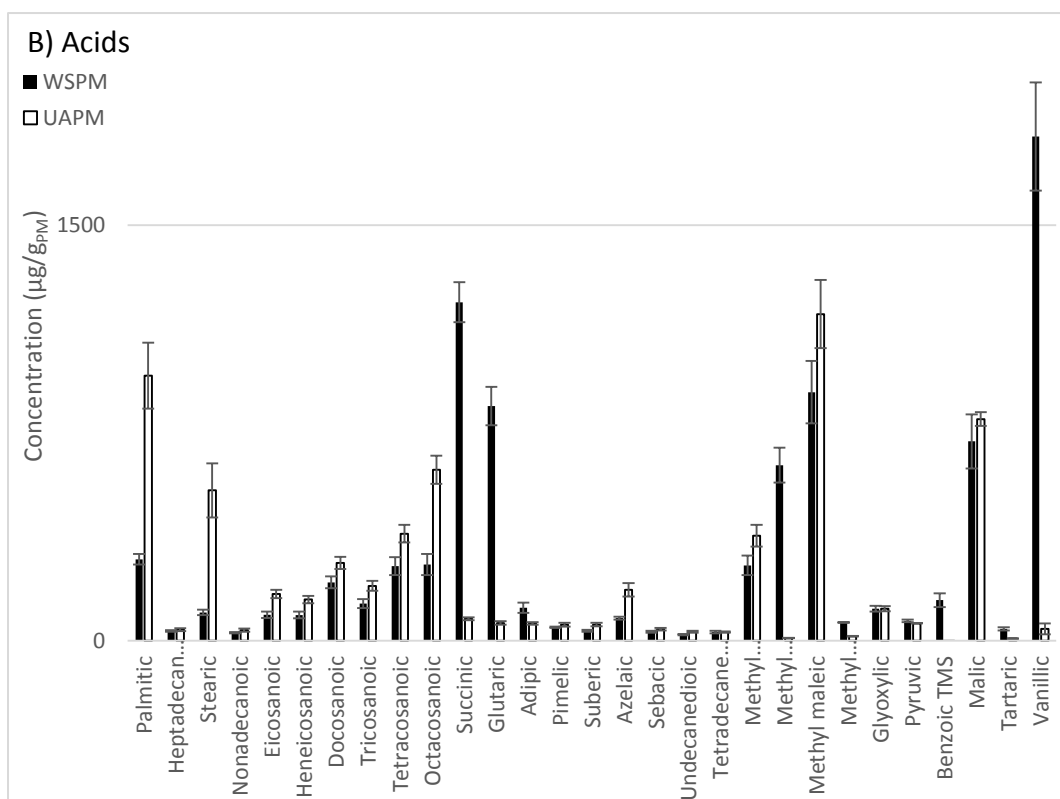
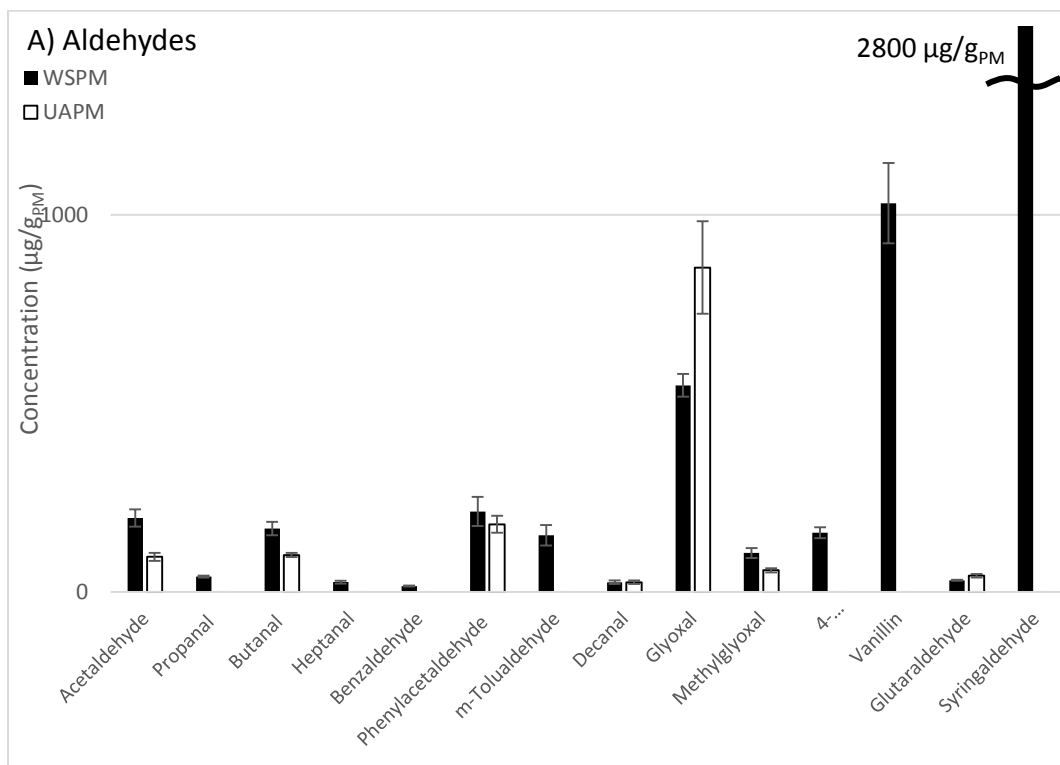
Furthermore, we extracted different amounts of WS PM to evaluate the extraction recoveries of aldehydes and acids (Fig V.7A, B, respectively) ensuring sufficient capacity. Similar recoveries were achieved for both PM loadings, although, some of the acids (decanoic, pimelic, and suberic) were below the limit of detection in the samples of lower loadings.



**Figure V.7 Occurrence of aldehydes (A) and acids (B) determined in different amounts of WS PM using the developed PFBHA·HCl /BSTFA protocol. Aldehydes analysis performed by Mr. Chintapalli [118]**

The concentration and occurrence of acids and aldehydes in WS PM was then compared to UA PM (Fig. V.8, Table D.2). A lower organic carbon content in UA PM [126], was most likely the reason for the observed lower concentration of target compounds (both acids and aldehydes) compared to WS PM. The most abundant acids in both PM samples were short-chain dicarboxylic acids ( $\leq C_{10}$ ), while WS PM had a high abundance of hydroxyacids (vanillic and malic acid), as well as ketoacids (glutaric and oxalacetic), and UA PM had a high abundance of long-chain monocarboxylic acid ( $\geq C_{16}$ ). It is worth noting that azelaic acid concentration was higher in the UA rather than WS PM. This could be possibly due to azelaic acid resulting from secondary emission as suggested for other urban sites in Gent, Belgium [127], Ulaanbaatar, Mongolia [128] and Research Triangle Park, NC [88].

The most abundant compounds in the WS PM were related to lignin pyrolysis, such as vanillin, syringaldehyde ( $\sim 1$  and  $3$  mg/g<sub>PM</sub>, respectively; Fig. V.8A), as well as vanillic acid ( $\sim 1.5$  mg/g<sub>PM</sub>; Fig. V.8B). Other abundant observed compounds were dicarboxylic acids, such as succinic, methyl succinic and glutaric acid (all  $\sim 1$  mg/g<sub>PM</sub>), that were related to oxidation of terpenes [88]. UA PM featured higher concentrations of palmitic and stearic acids ( $1$  and  $0.5$  mg/g<sub>PM</sub>, respectively; Fig. V.8B) and glyoxal ( $0.8$  mg/g<sub>PM</sub>; Fig. V.8A). Studies of urban sampling sites report similar long-chain mono carboxylic acids ( $\geq C_{16}$ ) and short-chain dicarboxylic acids ( $\leq C_{10}$ ), as well as dialdehydes (glyoxal and methylglyoxal) [88,127–130]. To our knowledge, there was no other study providing a full profile of aldehydes and carboxylic acids in SRM 1648b (UA PM).



**Figure V.8 Occurrence of aldehydes (A) and acids (B) determined in WS PM and UA PM using the developed PFBHA-HCl /BSTFA protocol.**



#### V.4. CONCLUSIONS

We have developed a new protocol employing a sequential PFBHA·HCl/BSTFA derivatization. In the first step using PFBHA·HCl in methanol, complete methylation was achieved for the majority of carboxylic acids, allowing for easier MS interpretation without the interference from hydroxy groups. This method was shown to be effective for hydroxyacids, providing the methylation of carboxylic groups in the first step and derivatization of the hydroxyl groups in the second step using BSTFA.

An overnight (18 hours) derivatization with sonication was essential in order to achieve a complete methylation of all tested acids with the exception of aromatic acids.

Aromatic acids were only partially derivatized (methylated), we were unable to enhance the reaction either towards methylation or trimethylsilylation. However, we demonstrated the feasibility of quantification based on trimethylsilyl esters.

The developed method was applied to two types of PM, wood smoke and urban air. The observed aldehydes were in concentrations 10–3000  $\mu\text{g}/\text{g}_{\text{PM}}$  in WS PM and 10–900  $\mu\text{g}/\text{g}_{\text{PM}}$  in UA PM, while the observed acids were in concentrations 20–1800  $\mu\text{g}/\text{g}_{\text{PM}}$  in WS PM and 15–1200  $\mu\text{g}/\text{g}_{\text{PM}}$  in UA PM. The most prominent aldehydes were syringaldehyde and vanillin in the WS PM and glyoxal in UA PM. The most abundant acids in both PM samples were short-chain dicarboxylic acids ( $\leq\text{C}_{10}$ ), while WS PM had a high abundance of hydroxyacids (vanillic and malic acid), as well as ketoacids (glutaric and oxalacetic), and UA PM had a high abundance of long-chain monocarboxylic acid ( $\geq\text{C}_{16}$ ).

## APPENDICES

## APPENDIX A

### **Application of AMDIS for the automatized interpretation of GC-MS data**

The following protocol describes the identification of multiple species in GC-MS chromatogram using AMDIS deconvolution software and MS library resulting in the identification report. The advantage of this setup over the traditional use of MS library is that the AMDIS software deconvolutes, which MS ions truly belong the peak and which belong to the background. AMDIS allows to provide two options of matching with MS library where reverse matching seems to be better. It also allows to setup number of parameters to get optimal results. The data files can be processed either as a single files or in batch.

*The overall process consist from 3 major steps, deconvolution, identification, and generation of report. The deconvolution can be performed either one-by-one (single data file) or as a batch (multiple files).*

#### 1. Deconvolution

##### Single data file

**File -> Open (pick data file to process)**

**Analyze -> Analyze GC-MS data (finds all the peaks in the data file)**

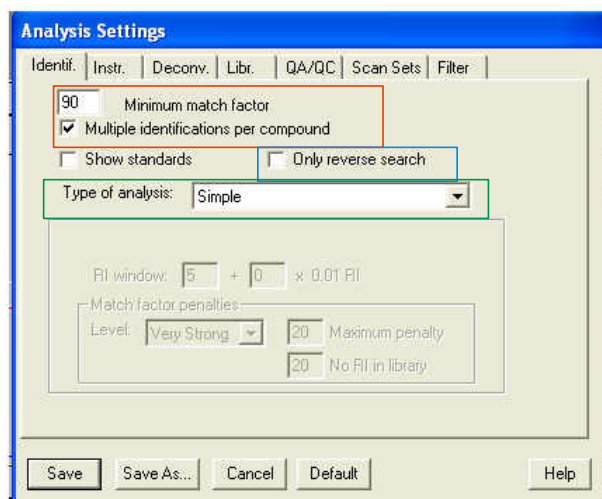
Analysis Settings:

*Identif. pane* offers matching with library, it seems the reverse search<sup>1</sup> provides higher quality data and applies to library matching

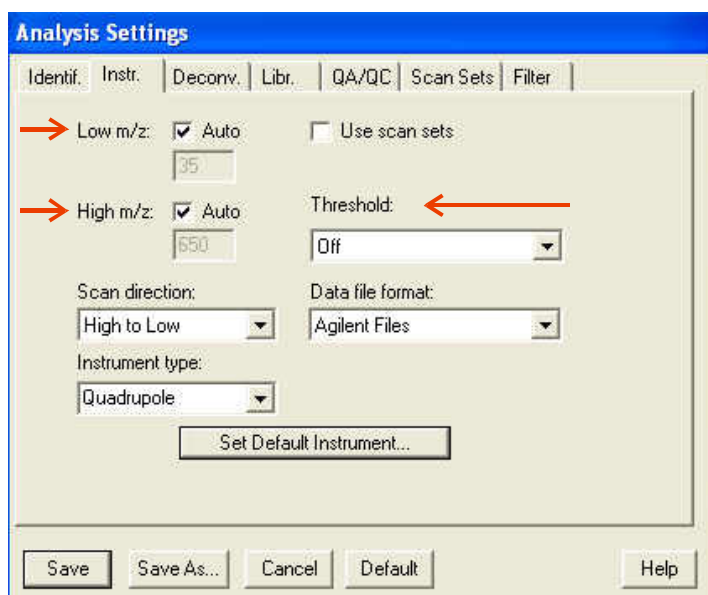
– *Type of analysis* allows to use retention indexes. We use “Simple”, because we don’t use retention indexes

---

<sup>1</sup> Reverse Match Factor (RMF) is the normalized dot product with square-root scaling of the submitted mass spectrum and the library mass spectrum, but the elements that are not present in the library mass spectrum are not included.



The *instr. pane* sets the instrumental parameters, such as  $m/z$  range, which ensures only mass range available is used for matching. *Threshold* is a basic parameter for discriminating peaks by size. The selecting of “Low, Medium or High” setting automatically determines, which noise level will be utilized. For “Low setting” the signal threshold will then be set slightly lower than the determined noise level. For “Medium setting” it will be set at or near to the noise level and for “High” it will be a little above. With the default value of “Off”, the analysis will use the signal threshold value stored in the data file.



We left other settings unaltered.

The deconvolution pane offers omitting certain  $m/z$  values. Adjacent peak subtraction (None, One, Two) – sets whether subtraction from one side or from both sides, default value is “One”. Resolution (Low, Medium, High), Sensitivity (Very High, High, Medium, Low, Very Low) and Shape requirements (High, Medium, Low) set those parameters, while higher setting leads to significant increase of processing time and number of targets per peak. The default values are “Medium” for all three of them. We generally use default settings, e.i. “One, Medium, Medium, Medium), with threshold either “Low”, or “Medium”

The library panel allows to choose from pre-defined RI libraries.

The QA/QC pane allows to insert typical values for solvent tailing and column bleed.

The scan sets pane covers the possibility of different scan sets in the analysis, to use, the box in instrument panel has to be checked (USE SCAN SETS).

The filter pane covers filters for the analysis of chromatogram.

*Save*

**Pressing “Run” analyzes the file based on last saved settings**

Multiple files

**File -> Batch job -> Create and Run Job**

**It uses the last saved settings for analyzing (described under single files)**

This is particularly useful for analysis of more samples where we want to process them all by one method.

2. MS analysis

After the chromatogram is deconvoluted, we can proceed to identification of the peaks using full NIST library.

**Analyze -> Search NIST library**

The red box – how many hits program reports, either based on concrete number, minimal match factor (i.e. if we want only hits more than 75%) or probability<sup>2</sup>

The blue box – there is possibility to omit already identified compounds from the first step, however, it is better to analyze everything again, because the NIST library offers better hits.

The green box – here either exact number of peaks is analyzed or peaks above the threshold. Zero means all the compounds, however, it's possible to discriminate peaks based on their size.

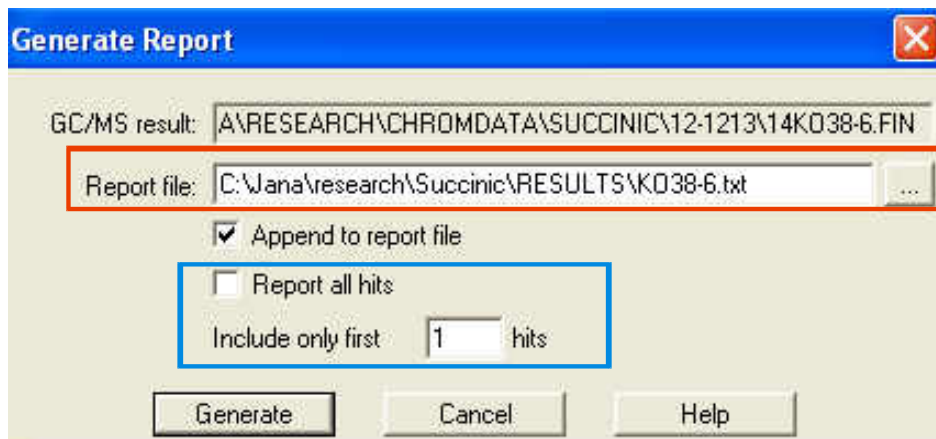
The yellow box – library can be chosen here.

---

<sup>2</sup> percentage probability threshold that hits must exceed to be reported (not sure what it actually does, may have connection with RI related search)

### 3. Generating report

**File -> Generate Report ...**



It creates a txt file with all the information found about the compound – including data file name, CAS number, tentative identification and the information in the red box on figure below. There is possibility to save all the generated hits, or just the first.

**Table A.1 Summary of previous studies focusing on simultaneous GC-MS determination of acids, saccharides and polyalcohols in various sample matrices.**

Sample matrix	Target analytes				Concentration range	Sample preparation			Ref.
	Acids	Saccharides	Polyalcohols	Derivatization		Pre-treatment	Method analysis		
apricots	phosphoric, succinic, palmitic, galacturonic, quinic, tartaric	fructose, maltose, sucrose, raffinose, galactose	turanose, glucose, trehalose, xylose	mannitol, sorbitol, inositol	2.52500 µg/mL	hydroxylamine in pyridine HMDS with TFA	evaporation	GC-IT-MS	[1]
plant tissue	lactic, pyruvic, ascorbic	malic, citric, fructose, sucrose	glucose	pinitol, mannitol, sorbitol, inositol	25125 µM LOD: 3-76 ng	hydroxylamine in ACN HMDS with TFA	SPE	GC-FID	[2]
apricots	ascorbic, malic, tartaric, succinic	citric, quinic, fructose, raffinose, xylose	maltose, trehalose	inositol, mannitol, sorbitol	0.014 mg/mL	pyridine HMDS TMCS	evaporation	GLC-FID	[3]
sour cherry apple ber fruit	succinic, malic, quinic, stearic	decanoic, tartaric, citric, galacturonic	fructose, sucrose, rhamnase, raffinose	glucose, xylose, inositol, sorbitol	2.52500 µg/mL	hydroxylamine in pyridine HMDS with TFA	evaporation	GC-IT-MS	[4]
	fumaric, malonic, oxalic, tartaric; capric, nonadecanoic, palmitic, stearic	maleic, malic, succinic, arachidic, myristic, oleic	arabinose, glucose, maltose, ribose, xylose	galactose, lactose, mannose	erythritol, glycerol, inositol, mannitol	methoxylamine HCl in pyridine BSTFA (1% TMCS)	evaporation	GCxGC-TOF-MS	[5]



Table A.1 cont.

Sample matrix	Target analytes			Concentration range	Sample preparation			Ref.
	Acids	Saccharides	Polyalcohols		Derivatization	Pre-treatment	Method analysis	
soil	NR <sup>b</sup>	ribose, rhamnose, arabinose, xylose, fructose, mannose, glucose, galactose	NR	10800 µg/mL	hydroxylamine and 4-dimethylamine in pyridine-methanol	hydrolysis	GC-FID	[6]
atmospheric aerosol	Glycolic, malonic, succinic, mandelic, hydroxybenzoic, pimelic, suberic, azelaic	maleic, glutaric, malic, adipic, phthalic, arabinose, mannose, galactose, glucose, levoglucosan, trehalose, maltose	NR	0.515 µg/L LOD: 17 ng/m <sup>3</sup>	BSTFA (1% TMCS) with pyridine		GC-MS	[7]
urine atmospheric aerosol	oxalic, methylmalonic, malonic, methylsuccinic, fumaric, glutaric, pimelic, suberic, azelaic, oleic, linoleic, sebacic	maleic, succinic, adipic, phthalic, rhamnose, arabinose, xylose, mannose, glucose, levoglucosan, sucrose, maltose, lactose, mezitose	xylitol, arabitol, mannitol, inositol	NR	BSTFA/MTBSTFA		GC-MS	[8]
bacteria	citric, malic, pyruvic, ascorbic, fumaric, benzoic, citric, fumaric, glyceric, benzoic, isocitric, malic, nicotinic, pyruvic, succinic, tartaric	lactic, oxaloacetate, fructose, glucose, ribose	xylitol	0.250 µg/mL LOQ <sup>c</sup> : 0.10.7 mmol/g	ethoxylamine in pyridine, MSTFA with pyridine		GC-MS	[9]
rye grass		NA	NR	50 mg/L	BSA, TMCS, TMSI with pyridine	dried @50C for 60h	GCxGC-TOF-MS	[10]

Table A.1 cont.

Sample matrix	Target analytes			Concentration range	Sample preparation			Ref.
	Acids	Saccharides	Polyalcohols		Derivatization	Pre-treatment	Method analysis	
basidiomycetes	Uronic	arabinose, ribose, fructose, galactose, glucose, disaccharides	NA	NR	hydroxylamine in pyridine HMDS with TFA	evaporation	GC-IT-MS	[11]
flour	NR	NR	NR	NR	TMSI with pyridine		GC-MS	[12]
fruit pulp	NR	arabinose, xylose, fructose, glucose, sucrose	NR	NR	BSTFA with pyridine BSTFA with aniline BSTFA with ACN	evaporation	GC-MS	[13]
parsley leaves	quinic	apinose, arabinose, fructose, glucose, sucrose, raffinose, melezitose	sorbitol, inositol, chrysoeriol, stigmasterol, sitosterol	580 ng/μL	hydroxylamine in pyridine HMDS with TFA	evaporation	GC-IT-MS	[14]
fruits atmospheric aerosol soil sediment	NR	glucose, levoglucosan, sucrose	sorbitol	1.2120 μg/mL LOD: 130360 ng/mL	BSTFA with pyridine	evaporation	GC-MS	[15]
honey	Benzoic, phosphoric, succinic, malic, shikimic, citric, isocitric, quinic, margaric, stearic	NR	Hydromethyl-furfurol	0.54 mg/mL	hydroxylamine in pyridine HMDS with TFA	evaporation	GC-MS	[16]
orange juice	oxalic, succinic, fumaric, malic, tartaric, citric, quinic, glutaric, galacturonic	xylose, arabinose, ribose, rhamnase, fructose, glucose, sucrose, maltose, raffinose	sorbitol, mannitol, inositol	80110 μg/mL	methoxylamine HCl in pyridine MSTFA	evaporation	GC-MS	[17]

Table A.2 Optical microscope images of succinic acid samples

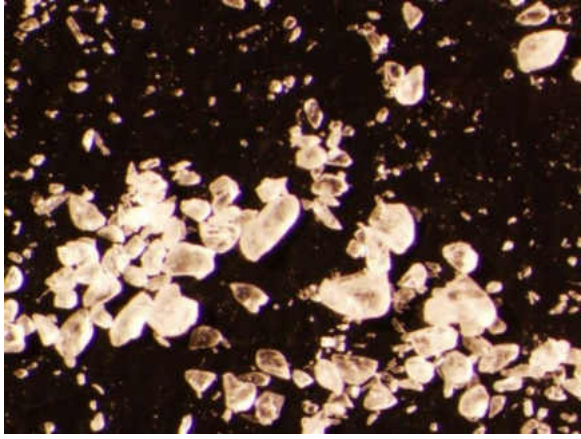
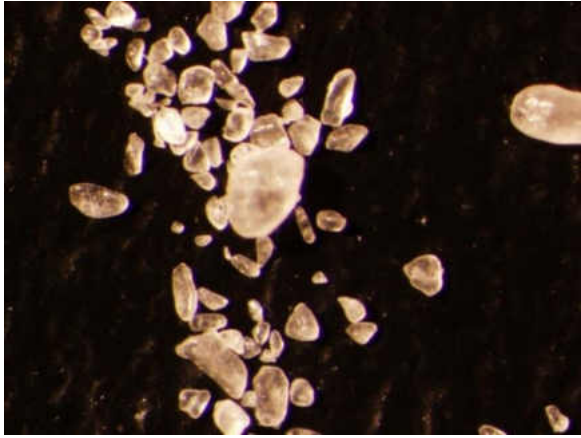
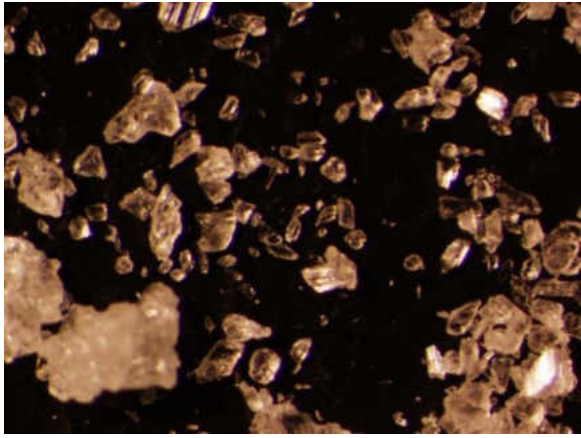
Image	Description
	<p>JR96-1</p> <p>A – Kawasaki Obtained: 6/22/2012 White small grains</p>
	<p>JR96-2</p> <p>B – Myriant Obtained: 6/22/2012 White medium grains</p>
	<p>JR96-3</p> <p>C – Rick 18 Obtained: 6/22/2012 White huge grains Unpleasant odor</p>

Table A.2 cont.


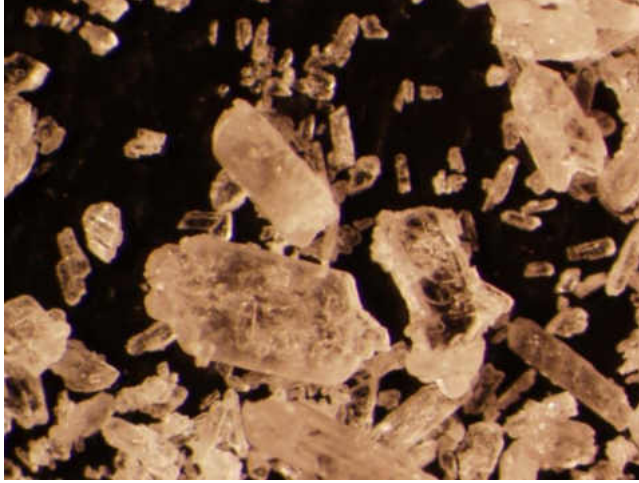
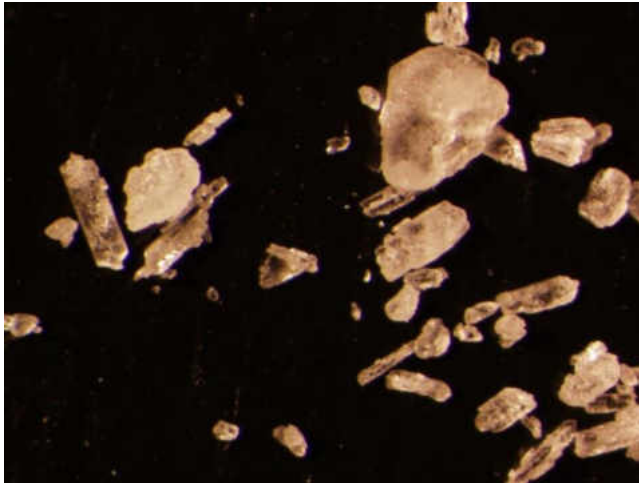
	<p>JR96-4</p> <p>D – Rick 20 Obtained: 6/22/2012 White medium grains</p>
	<p>JR96-5</p> <p>E – 11007 Obtained: 6/22/2012 White medium flakes Unpleasant odor</p>
	<p>JR96-6</p> <p>F – 11006 Obtained: 2/28/2012 White small grains Unpleasant odor</p>

Table A.2 cont.


	<p>JR96-7</p> <p>G – 111101A Obtained: 2/28/2012 White small grains Unpleasant odor</p>
	<p>JR96-8</p> <p>H – E. coli Obtained: 12/7/2012 Yellow small flakes Unpleasant odor</p>
	<p>JR96-11</p> <p>K – 120303 Obtained: 12/7/2012 White small flakes Unpleasant odor</p>

Table A.2 cont.

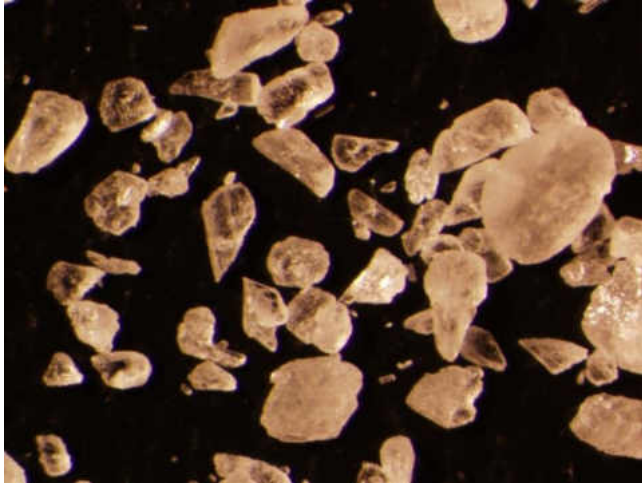
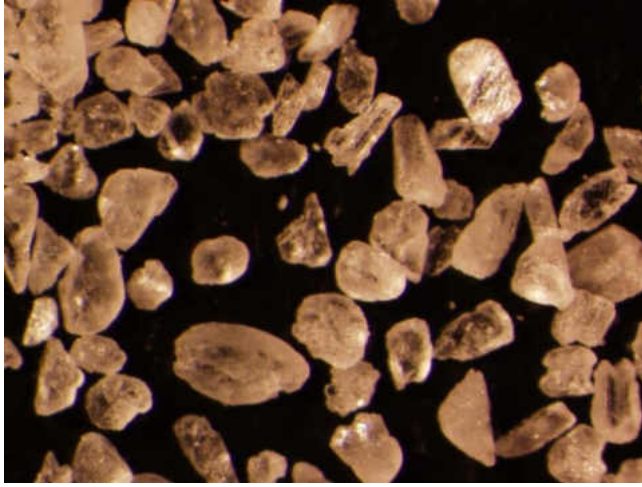
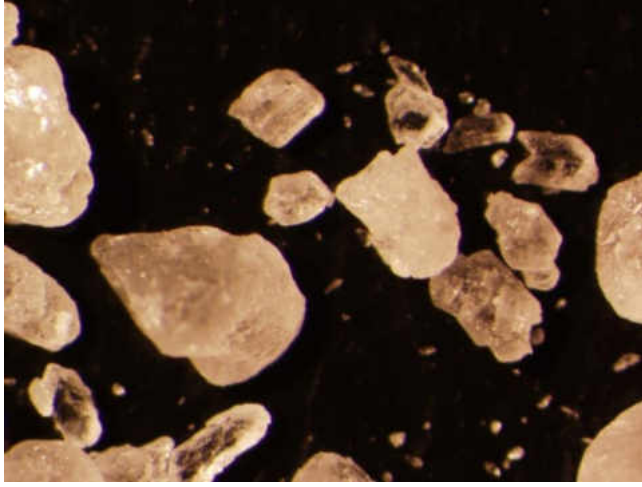
	<p>JR96-12</p> <p>L – 111001A</p> <p>Obtained: 12/7/2012</p> <p>White medium grains</p>
	<p>JR96-13</p> <p>M – 10018</p> <p>Obtained: 12/7/2012</p> <p>White small grains</p> <p>Unpleasant odor</p>
	<p>JR96-14</p> <p>N – 10022</p> <p>Obtained: 12/7/2012</p> <p>White medium grains</p>

Table A.2 cont.

 A micrograph showing numerous small, irregular, light-colored grains against a dark background. The grains vary in size and shape, with some appearing more rounded and others more angular. The overall appearance is that of a fine-grained material.	<p>JR96-15</p> <p>O – 10023</p> <p>Obtained: 12/7/2012</p> <p>White small grains</p>
 A micrograph showing numerous small, irregular, light-colored grains against a dark background. The grains are similar in appearance to those in the first image, with varying sizes and shapes, some appearing more rounded and others more angular.	<p>JR96-16</p> <p>P – 120401</p> <p>Obtained: 12/15/2012</p> <p>White small grains</p>

Microscope used to obtain images was Olympus SZX12 with Fiber Optics lenses (Olympus Corporation, Japan), with 450x magnification. Image was captured with DP-70 camera (Olympus Corporation, Japan)

**Table A.3 Contaminants observed upon BSTFA derivatization of ACN extract of petroleum based and initial processed succinic acid samples.**

t <sub>r12</sub>	name	A - Petroleum				K - initially processed				Confirmed
		Percent response <sup>c</sup>	Adjusted Per. Resp. <sup>d</sup>	MS match <sup>e</sup>	lib. R <sup>f</sup>	Percent response	Adjusted Per. Resp.	MS match <sup>e</sup>	lib. R <sup>f</sup>	
0.316	formic acid	0.01%	<b>0.015</b>	87	87	0.05%	<b>0.035</b>	94	94	*
0.403	acetic acid	0.02%	<b>0.024</b>	89	91	0.26%	<b>0.172</b>	91	92	*
0.517	methyl ester hexanoic acid					0.01%	<b>0.007</b>	35	43	
0.571	methyl-propanoic acid	0.0004%	<b>0.0005</b>	67	78					
0.585	alanine					0.04%	<b>0.026</b>	66	72	
0.589	dimethylsulfone					0.02%	<b>0.013</b>	84	89	*
0.610	benzotriazol-5-amine, 1-phenyl-					0.03%	<b>0.020</b>	53	84	
0.631	ethanediol	0.04%	<b>0.043</b>	92	93					*
0.629	1,2-benzenedicarbonitrile					0.01%	<b>0.008</b>	63	69	
0.635	silane, (2-furanylmethoxy)trimethyl-					0.01%	<b>0.006</b>	56	64	
0.658	aminoethanol	0.003%	<b>0.004</b>	59	80					
0.660	butanediol					0.04%	<b>0.026</b>	86	91	*
0.671	lactic acid	0.004%	<b>0.005</b>	76	77	0.45%	<b>0.304</b>	94	94	*
0.680	glycolic acid	0.003%	<b>0.004</b>	83	83					*
0.689	indene					0.00%	<b>0.002</b>	73	88	
0.692	alanine					0.02%	<b>0.015</b>	88	88	
0.703	butanediol					0.00%	<b>0.001</b>	63	75	
0.706	oxalic acid	0.004%	<b>0.005</b>	86	90					*
0.715	methyl butanol	0.01%	<b>0.015</b>	69	70					
0.718	hydroxybutyric acid					0.02%	<b>0.016</b>	90	91	*
0.722	oxypentanoic acid					0.02%	<b>0.016</b>	75	76	
0.730	phenol, 2-amino-4,6-bis(1,1-dimethylethyl)-					0.00%	<b>0.003</b>	39	58	



Table A.3 cont.

t <sub>r12</sub>	name	A - Petroleum				K - initially processed				Confirmed
		Percent response <sup>c</sup>	Adjusted Per. Resp. <sup>d</sup>	MS match W <sup>e</sup>	lib. R <sup>f</sup>	Percent response	Adjusted Per. Resp.	MS match W	lib. R	
0.736	pentenoic acid					0.04%	<b>0.027</b>	57	67	
	hydroxylamine, (pentafluorobenzyl)-N-									
0.743	(trimethylsilyl)-					0.72%	<b>0.483</b>	83	85	
0.746	L-valine (bisTMS)					0.12%	<b>0.081</b>	78	78	*
0.747	10-nonadecanamine					0.002%	<b>0.001</b>	67	74	
0.753	hydroxymethylpentanoic acid					0.01%	<b>0.004</b>	68	71	
0.757	ethyl succinate					0.06%	<b>0.043</b>	80	80	*
0.763	benzoic acid	0.01%	<b>0.008</b>	90	90					*
0.765	glycerol					0.06%	<b>0.041</b>	60	62	
0.770	glycerol	0.001%	<b>0.001</b>	70	70	0.01%	<b>0.010</b>	83	87	*
0.774	hydroxyhexanoic acid					0.01%	<b>0.005</b>	39	52	
0.778	butanetriol					0.01%	<b>0.006</b>	78	79	
0.784	diphenoxybenzene					0.004%	<b>0.003</b>	50	64	
0.789	3,4-dimethoxymandelic acid					0.01%	<b>0.008</b>	48	72	
0.792	methyl succinic acid	0.03%	<b>0.033</b>	82	84					
0.793	dihydroxypropanoic acid					0.003%	<b>0.002</b>	54	57	
0.798	pyrimidine					0.02%	<b>0.015</b>	67	68	
0.814	malic acid isomer					0.12%	<b>0.077</b>	55	55	
0.821	pentanedioic acid	0.000%	<b>0.0004</b>	48	77	0.03%	<b>0.021</b>	74	75	*
0.842	357(10),181(60),176(50),147(100)					1.44%	<b>0.966</b>			
0.851	hydroxypentanoic acid					0.01%	<b>0.003</b>	44	44	
0.854	malic acid	4.49%	<b>5.403</b>	91	94	0.03%	<b>0.022</b>	85	91	

Table A.3. cont.

t <sub>r12</sub>	name	A - Petroleum				K - initially processed				Confirmed
		Percent response <sup>c</sup>	Adjusted Per. Resp. <sup>d</sup>	MS match <sup>e</sup>	lib. R <sup>f</sup>	Percent response	Adjusted Per. Resp.	MS match <sup>e</sup>	lib. R	
0.860	hexanedioic acid	0.003%	<b>0.004</b>	61	63					*
0.860	acetamide, N,N-dimethyl-(4-phenyl)diphenyl-					0.02%	<b>0.012</b>	63	82	
0.862	threitol					0.01%	<b>0.008</b>	55	57	
0.870	2,9-dimethyl-3,4,5,10-tetrahydro-2H-azepinol[3,4-b]indol-1-one					0.08%	<b>0.050</b>	53	55	
0.872	proline	0.001%	<b>0.001</b>	79	82					
0.877	pentitol					0.00%	<b>0.003</b>	57	57	
0.884	dihydroxypentanedioic acid					0.002%	<b>0.001</b>	47	48	
0.892	glyceric acid	0.004%	<b>0.005</b>	79	80					
0.902	hexanoic acid derivative					0.01%	<b>0.010</b>	58	77	
0.903	phenylpyridine					0.01%	<b>0.005</b>	42	83	
0.907	succinyl lactate	0.003%	<b>0.003</b>	72	74	0.01%	<b>0.004</b>	54	70	
0.910	xylonic acid					0.003%	<b>0.002</b>	55	58	
0.925	octanedioic acid	0.001%	<b>0.001</b>	48	48					*
0.930	phthalic acid	0.03%	<b>0.031</b>	91	93					
0.933	heptulose					0.01%	<b>0.005</b>	71	74	
0.953	arabinoic acid lactone					0.01%	<b>0.007</b>	62	71	
0.959	terephthalic acid	0.00001	<b>0.001</b>	84	84					
0.960	arabinose					0.001%	<b>0.001</b>	56	61	
0.967	citric acid					0.10%	<b>0.066</b>	48	51	
0.971	tetradecanoic acid	0.00001	<b>0.001</b>	41	43					*
0.975	arabinose					0.01%	<b>0.003</b>	68	76	

Table A.3 cont.

t <sub>r12</sub>	name	A - Petroleum				K - initially processed				Confirmed
		Percent response <sup>c</sup>	Adjusted Per. Resp. <sup>d</sup>	MS match <sup>e</sup>	lib. R <sup>f</sup>	Percent response	Adjusted Per. Resp.	MS match	lib. R	
0.978	glucose					0.01%	<b>0.005</b>	72	74	
0.992	heptanol derivative					0.05%	<b>0.035</b>	83	88	
0.995	arabinose					0.002%	<b>0.002</b>	67	73	
1.000	<b><i>o</i>-terphenyl (IS)</b>	0.83%	<b>1.000</b>	90	90	1.49%	<b>1.000</b>	79	79	<b>IS</b>
1.006	lyxose					0.001%	<b>0.001</b>	58	71	
1.013	glucose					0.03%	<b>0.021</b>	74	84	
1.028	hexadecanoic acid	0.02%	<b>0.023</b>	89	91	0.01%	<b>0.007</b>	72	75	*
1.080	octadecanoic acid	0.03%	<b>0.036</b>	83	85	0.01%	<b>0.009</b>	68	72	*

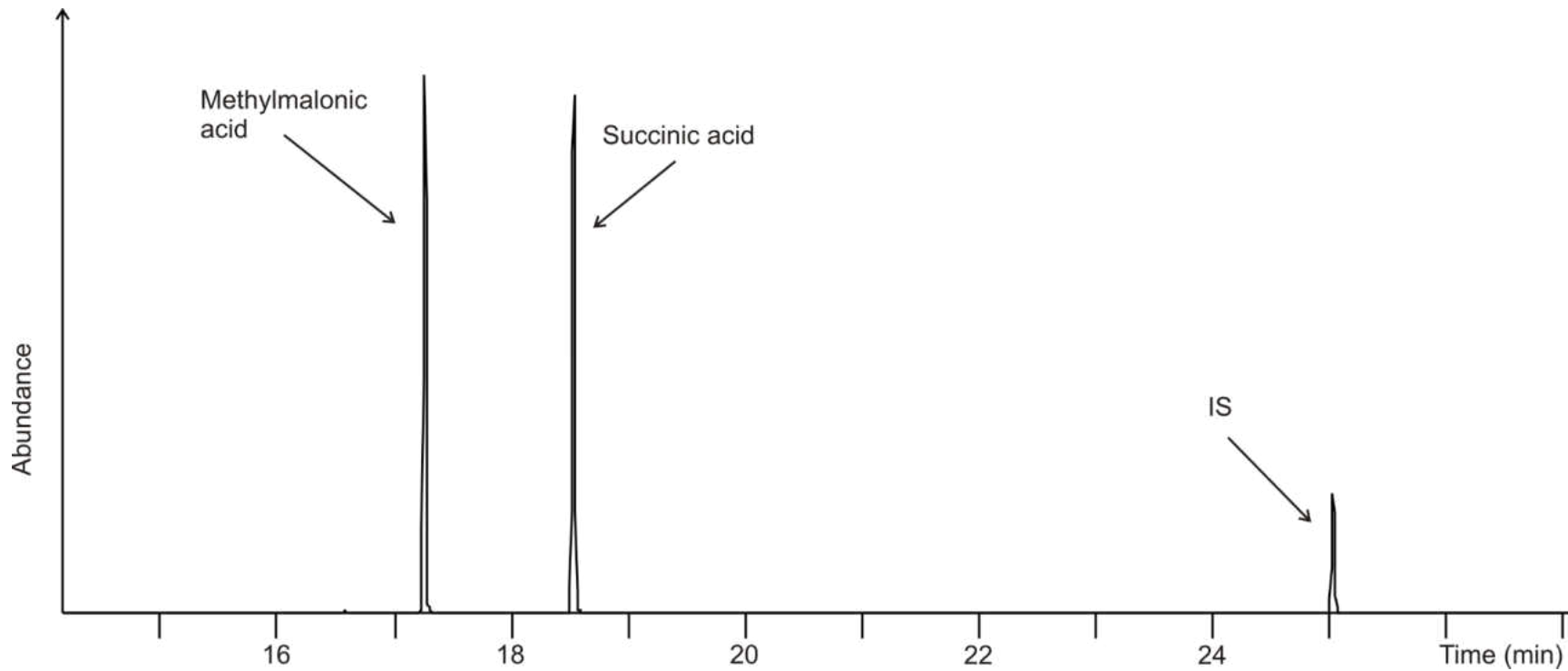


Figure A.0.1 Comparison of elution of succinic acid and its isomer methylsuccinic acid using developed GC-MS program

## APPENDIX B

**Table B.1 Determination of bioactive fractions of *Pulicaria jaubertii***

<u>Endpoint</u>	Fraction <sup>1</sup>				
	Control	PJ <sub>M</sub>	PJ <sub>H</sub>	PJ <sub>D</sub>	PJ <sub>A</sub>
Triacylglyceride <sup>2</sup> (mg/mg protein)	1.45 (0.18)	0.61 (0.15)*	1.15 (0.24)	0.90 (0.07)*	1.01 (0.27)
GSH <sup>3</sup> (nmol/mg protein)	28.5 (2.3)	10.9 (1.2)*	14.2 (2.5) <sup>a</sup>	12.2 (3.7)*	24.5 (4.4)
GSSG <sup>3</sup> (nmol/mg protein)	0.53 (0.12)	0.95 (0.29)	1.03 (0.24)	1.01 (0.22)	0.65 (0.18)
<u>Gene Expression<sup>4</sup></u>					
NQO1	1.00	6.2 (0.8)*	2.4 (0.5)	7.6 (0.8)*	1.6 (0.1)
GR	1.00	2.7 (0.1)*	1.7 (0.1)	3.3 (0.5)*	1.3 (0.1)
GCLc	1.00	5.7 (0.1)*	1.6 (0.5)	7.1 (1.2)*	1.4 (0.4)
GPx1	1.00	1.2 (0.2)	1.1 (0.1)	1.5 (0.6)	1.5 (0.7)
GPx3	1.00	7.0 (0.5)*	5.7 (0.1)*	12.2 (0.9)*	1.4 (0.1)
GPx4	1.00	1.6 (0.2)*	1.3 (0.2)	1.7 (0.2)*	1.6 (0.0)
Catalase	1.00	3.2 (0.3)*	2.8 (0.7)*	2.9 (0.3)*	1.6 (0.0)
SOD1	1.00	1.4 (0.5)	1.5 (0.5)	1.1 (0.4)	1.6 (0.1)
SOD2	1.00	1.5 (0.4)	1.5 (0.2)	1.5 (0.1)	1.1 (0.1)

\* significantly ( $p \leq 0.05$ ) different from the Control (vehicle only) treatment using one way ANOVA.

<sup>1</sup> *Pulicaria jaubertii* methanol fraction (PJ<sub>M</sub>); PJ hexane fraction (PJ<sub>H</sub>); PJ dichloromethane fraction (PJ<sub>D</sub>); PJ aqueous fraction (PJ<sub>A</sub>); NADPH;Quinone Oxidoreductase 1 (NQO1); Glutathione reductase (GR); glutamate cysteine ligase catalytic unit (GCLc); Glutathione peroxidase (GPx); Superoxide dismutase (SOD); <sup>2</sup>Triacylglyceride content was measured after treating 3T3-L1 preadipocytes with the fractions following the seven-day differentiation regimen. Data are the mean  $\pm$  the SD for three independent experiments ( $n = 3$ ); <sup>3</sup> GSH and GSSG were measured following a 6 hr exposure of 3T3-L1 preadipocytes to the fractions. Data are the mean  $\pm$  the SD for three independent experiments ( $n = 3$ ); <sup>4</sup> Gene expression analysis was performed on 3T3-L1 preadipocytes 48 hrs following a single exposure to the fractions. Data are the mean  $\pm$  the SD for three independent experiments ( $n = 3$ ).

**Table B.2 Compounds observed in *Pulicaria* extract and its fractions using GC-MS. Amount is reported as percentage of TIC together with amount normalized by internal standard amount. Only compounds with amount higher than 0.5% were reported.**

Name	MeOH crude extract			Hexane fraction			DCM fraction			Water-methanol fraction			MS match	library
	r <sub>12</sub>	Amount <sup>a</sup>	% of IS	r <sub>12</sub>	Amount	% of IS	r <sub>12</sub>	Amount	% of IS	r <sub>12</sub>	Amount	% of IS	W <sup>b</sup>	R <sup>c</sup>
Carvotanacetone	0.661	0.59%	4%	0.665	30.98%	376%	0.663	4.23%	7%				91	92
Octanoic acid, 4-methyl-, methyl ester							0.743	1.28%	2%				60	62
2H-Pyran-2-one, 5,6-dihydro-4,6,6-trimethyl-							0.752	3.52%	6%				66	84
Cyclohexanone, 2-pentyl-							0.760	2.72%	5%				64	66
Cyclohexanone, 2-ethyl-							0.764	3.02%	5%				70	74
8-Hydroxycarvotanacetone							0.771	3.58%	6%				87	88
3-Cyclohexene-1-carboxylic acid, 4-methyl-2-oxo-, methyl ester							0.832	2.58%	4%				71	72
<i>o</i> -Terphenyl (IS)	1.000	14.82%	100%	1.000	8.23%	100%	1.000	59.87%	100%	1.000	92.30%	100%		
n-Hexadecanoic acid	1.031	12.01%	81%	1.031	7.99%	97%	1.120	6.05%	10%				90	90
n-Hexadecanoic acid				1.063	5.36%	65%							91	95
2-Cyclopentene-1-tridecanoic acid				1.103	3.15%	38%							60	62
α-Linolenic acid	1.105	27.69%	187%	1.106	25.32%	308%							87	88
Octadecanoic acid							1.194	4.23%	7%				81	81
Pregnane derivative										1.206	1.25%	1%	37	54
Pentacosane				1.235	2.76%	34%							88	88
1,2-Benzenedicarboxylic acid, mono(2-ethylhexyl) ester				1.246	9.63%	117%							94	95
1-Docosene	1.299	3.14%	21%	1.300	3.18%	39%							76	83

<sup>a</sup>"amount" denotes normalized percent of TIC, <sup>b</sup>"W" denotes weighted library match; <sup>c</sup>"R" denotes reversed library match

**Table B.3 Compounds observed in Pulicaria extract and its fractions using GC-MS after derivatization with BSTFA. Amount is reported as percentage of TIC together with amount normalized by internal standard amount. Only compounds with amount higher than 0.5% were reported**

Name	MeOH crude extract			Hexane fraction			DCM fraction			Water-methanol fraction			MS library match	
	r <sub>12</sub>	Amount <sup>a</sup>	% of IS	r <sub>12</sub>	Amount	% of IS	r <sub>12</sub>	Amount	% of IS	r <sub>12</sub>	Amount	% of IS	W <sup>b</sup>	R <sup>c</sup>
Carvotanacetone	0.665	5.36%	336%	0.666	18.77%	1418%	0.663	1.59%	15%				91	91
Glycerol	0.674	7.09%	444%				0.673	3.05%	28%	0.674	12.64%	473%	93	93
Butanoic acid, 4-amino-										0.821	1.02%	38%	85	91
D-Fructose										0.958	1.50%	56%	81	88
D-Fructose	0.961	3.81%	238%							0.961	3.89%	146%	91	94
Pregnane derivative	0.980	3.69%	231%							0.979	5.19%	194%	56	60
D-Glucose	0.995	3.70%	231%							0.995	4.92%	184%	92	97
<i>o</i> -Terphenyl (IS)	1.000	1.60%	100%	1.000	1.32%	100%	1.000	10.72%	100%	1.000	2.67%	100%	93	93
Inositol	1.022	8.16%	510%							1.022	14.95%	560%	86	86
Inositol	1.022	3.43%	215%										54	55
Talose	1.032	7.96%	498%							1.032	12.59%	471%	92	93
Hexadecanoic acid	1.064	6.96%	435%	1.065	20.25%	1529%							89	95
Inositol	1.079	10.17%	636%				1.083	0.99%	9%	1.079	17.56%	657%	88	89
Linoleic acid				1.130	8.41%	635%							89	92
$\alpha$ -Linolenic acid	1.132	9.16%	573%	1.134	22.43%	1694%							91	97
Glycerol galactoside	1.164	1.93%	121%							1.164	3.02%	113%	81	94
Pregnane derivative							1.212	2.95%	27%				60	77
Estratriene derivative	1.274	1.11%	69%				1.274	2.74%	26%	1.276	2.71%	102%	90	92
Adenosine	1.277	1.51%	94%							1.277	1.63%	61%	80	89
Tricosanoic acid				1.315	5.00%	378%							86	87
Catechin-like compound	1.378	5.70%	356%				1.378	5.79%	54%	1.378	3.25%	122%	74	80
Cinnamic acid	1.382	1.29%	81%				1.382	7.94%	74%				46	59
Catechin-like compound	1.383	7.36%	460%				1.383	41.16%	384%				58	70
Cinnamic acid	1.384	1.23%	77%				1.384	16.81%	157%	1.382	1.48%	55%	57	71

<sup>a</sup>"amount" denotes normalized percent of TIC, <sup>b</sup>"W" denotes weighted library match; <sup>c</sup>"R" denotes reversed library match

## APPENDIX C

### Preparation of RES-d<sub>5</sub>, R3G-d<sub>5</sub>, and R3S-d<sub>5</sub>.

**R3G-d<sub>5</sub>** and **R3S-d<sub>5</sub>** were prepared from **RES-d<sub>5</sub>** as described for the non-deuterated analogs.<sup>3,4</sup> **RES-d<sub>5</sub>** was prepared from toluene-d<sub>8</sub>, as shown in Fig 1, relying on the previously developed condensation of 3,5-dimethoxybenzyl diethylphosphonate with anisaldehyde.<sup>3</sup> **4-Bromotoluene-d<sub>7</sub>** and **1-bromo-4-(bromomethyl)benzene-d<sub>6</sub>** were prepared from toluene-d<sub>8</sub> according to the reported method,<sup>5</sup> relying on the highly *para*-selective electrophilic bromination in presence of NaY zeolite.<sup>6</sup> Thus, obtained **1-bromo-4-(bromomethyl)benzene-d<sub>6</sub>** was converted to **anisaldehyde-d<sub>6</sub>** as follows.

**1-Bromo-4-(methoxymethyl)benzene -d<sub>6</sub>**. A round bottom flask was charged with sodium methoxide (5 M in methanol, 2.06 mL) and anhydrous methanol (5 mL). **1-Bromo-4-(bromomethyl)benzene-d<sub>6</sub>** (875 mg, 3.41 mmol) in methanol (10 mL) was then added and the resulting reaction mixture was stirred at room temperature under nitrogen for 15 h. Methanol was evaporated under reduced pressure and the obtained residue was diluted with ethyl acetate (15 mL). The organic layer was washed subsequently with 1N HCl (15 mL), water (15 mL) and with brine (15 mL). The resulted organic layer was dried with anhydrous magnesium sulfate, filtered and volatiles were evaporated under reduced pressure. The residue was purified by column a quick chromatography on silica gel (1:9, EtOAc/hexane), and immediately used in the next step. Yield: 566 mg (80%). *R<sub>f</sub>* = 0.4 (1:7, EtOAc/hexane). <sup>1</sup>H NMR (CDCl<sub>3</sub>, 500 MHz): δ 3.38 (s, 3H). <sup>13</sup>C NMR (CDCl<sub>3</sub>, 125 MHz): δ 137.0, 131.2 (t, *J*<sub>CD</sub> = 25 Hz), 129.0 (t, *J* = 25 Hz), 121.3, 73.1 (nonet, *J*<sub>CD</sub> = 21 Hz), 58.2.

**1-Methoxy-4-(methoxymethyl)benzene-d<sub>6</sub>**. To the solution of sodium methoxide (5 M in methanol, 26.5 mL) anhydrous dimethylformamide (15 mL) was added under nitrogen. After stirring the mixture for 10 min at room temperature (rt), copper(I) iodide (1.95 g, 10.2 mmol) was added and stirred at 90 °C until the solution turned to pale yellow. A solution of **1-bromo-4-(methoxymethyl)benzene -d<sub>6</sub>** (450 mg, 2.56 mmol) in

---

<sup>3</sup> Jungong CS, Novikov A V (2012) Practical Preparation of Resveratrol 3-O-B-D-Glucuronide. *Synth Commun* 42:3589–3597.

<sup>4</sup> Hoshino J, Park EJ, Kondratyuk TP, Marler L, Pezzuto JM, van Breemen RB, Mo S, Li Y, Cushman M (2010) Selective Synthesis and Biological Evaluation of Sulfate-Conjugated Resveratrol Metabolites. *J. Med Chem.* 53: 5033–5043.

<sup>5</sup> Wacker SA, Kashyap S, Li X, Kapoor TM (2011) Examining the Mechanism of Action of a Kinesin Inhibitor Using Stable Isotope Labeled Inhibitors for Cross-Linking (SILIC) . *J. Am. Chem. Soc.* 133: 12386-12389.

<sup>6</sup> Smith K, El-Hiti GA, Hammond MEW, Bahzad D, Li Z, Siquet C (2000) Highly Efficient and Selective Electrophilic and Free Radical Catalytic Bromination Reactions of Simple Aromatic Compounds in the Presence of Reusable Zeolites. *J. Chem. Soc. Perkin Trans. 1* 2745–2752.



dimethylformamide (10 mL) was then added, and stirred for additional 5.5 h at 100 °C. Upon completion, the reaction mixture was brought to rt and quenched with ethyl acetate followed by 1N HCl. The product was extracted to diethyl ether (15 mL) and washed the organic layer with 1 N HCl (15 mL), water (15 mL) and brine (15 mL) followed by drying with anhydrous magnesium sulfate and filtering. Volatiles were removed under reduced pressure and purification of the crude product was performed by column chromatography on silica gel (1:5, EtOAc/hexane). The pure product was obtained as a pale yellow liquid with 265 g (77%).  $R_f = 0.30$  (1:3, EtOAc/hexane):  $^1\text{H NMR}$  ( $\text{CDCl}_3$ , 500 MHz):  $\delta$  3.82 (s, 3H), 3.37 (s, 3H).  $^{13}\text{C NMR}$  ( $\text{CDCl}_3$ , 125 MHz):  $\delta$  159.6, 130.4, 129.4 (t,  $J_{\text{CD}} = 24$  Hz), 113.8 (t,  $J = 24$  Hz), 73.9 (nonet,  $J_{\text{CD}} = 21$  Hz), 58.1, 55.7. HRMS (ESI) calculated for  $\text{C}_9\text{H}_7\text{D}_6\text{O}_2$  [M+H] 159.1286, found 159.1273.

**Anisaldehyde- $\text{d}_5$ .** A round bottom flask was charged with **1-methoxy-4-(methoxymethyl)benzene- $\text{d}_6$**  (200 mg, 1.26 mmol) in 5 mL of acetonitrile/water (1:2). Ceric ammonium nitrate (1.39 g, 2.53 mmol) was then added to the reaction mixture and stirred for 6 h at rt. Upon completion, the reaction mixture was diluted with water (10 mL) and the product was extracted to dichloromethane (3 x 10 mL). The combined organic layers were dried with anhydrous magnesium sulfate, filtered and concentrated under vacuum. Purification by chromatography on silica gel (1:7, EtOAc/hexane) provided the product with 150 mg (84%) as colorless viscous oil.  $^1\text{H NMR}$  ( $\text{CDCl}_3$ , 500 MHz):  $\delta$  3.88 (s, 3H).  $^{13}\text{C NMR}$  ( $\text{CDCl}_3$ , 125 MHz):  $\delta$  190.9 (t,  $J_{\text{CD}} = 26$  Hz), 165.0, 132.0 (t,  $J_{\text{CD}} = 24$  Hz), 130.1, 114.3 (t,  $J = 24$  Hz), 56.0. HRMS (ESI) calculated for  $\text{C}_8\text{H}_4\text{D}_5\text{O}_2$  [M+H] 142.0910, found 142.0869.

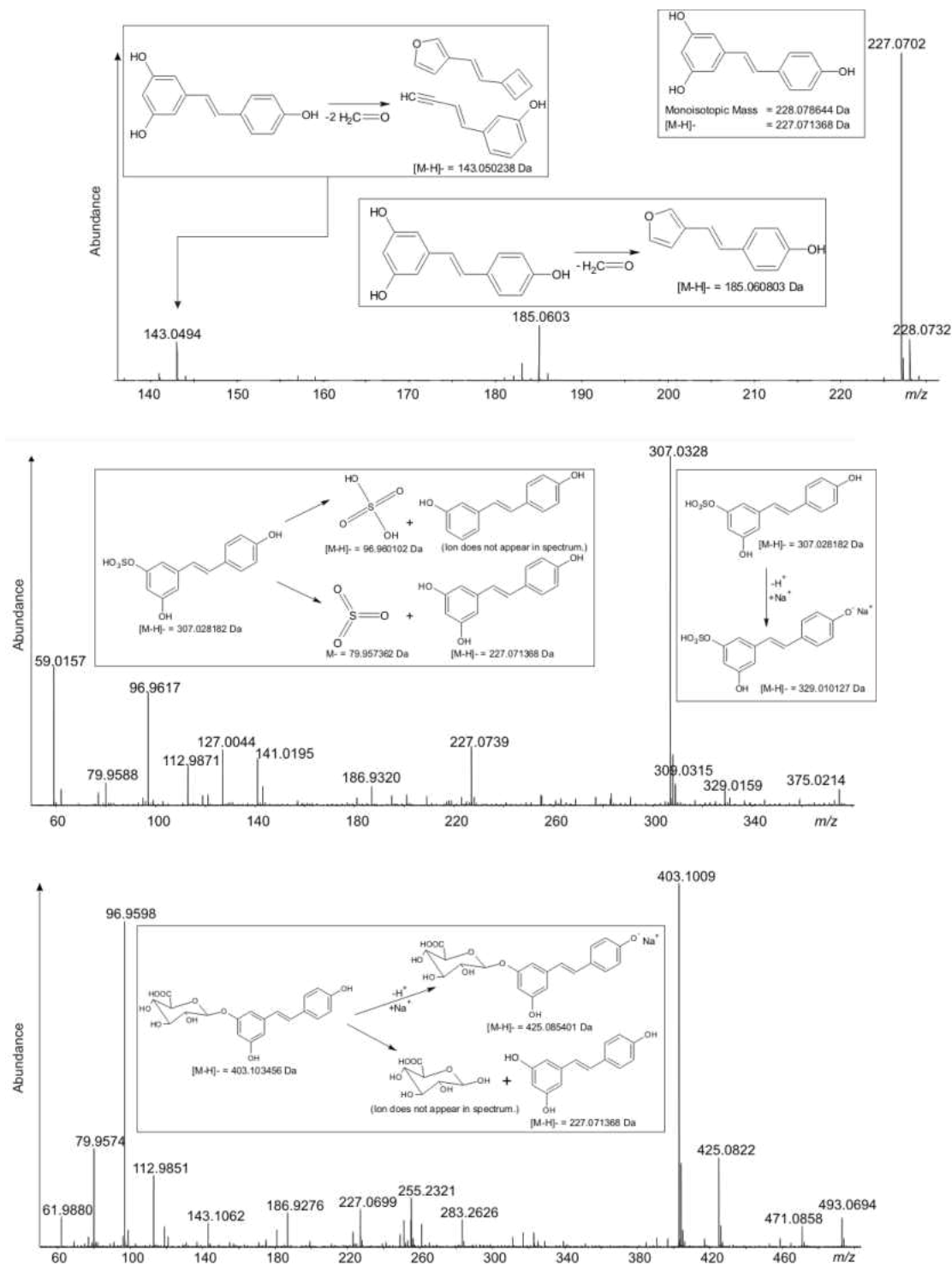


Figure C.1 ESI-TOF-MS spectrum acquired using FIA in negative mode for RES, showing deprotonated molecular ion 227.07137 and confirmation ion 228.07765 (electrolyte: 0.1 mM acetic acid; fragmentor: 225 V; capillary: 3500 V) (A), R3G, showing deprotonated molecular ion 403.103456 and confirmation ion 227.07137 (no electrolyte; fragmentor: 200 V; capillary: 4500 V) (B), and R3S, showing deprotonated molecular ion 307.028182 and confirmation ion 227.07137 (electrolyte: 1 mM ammonium acetate; fragmentor: 175 V; capillary: 4500 V) (C), with proposed fragmentation pathways inset, with all but the sodium adducts confirming previous interpretations [64,68,76,77].

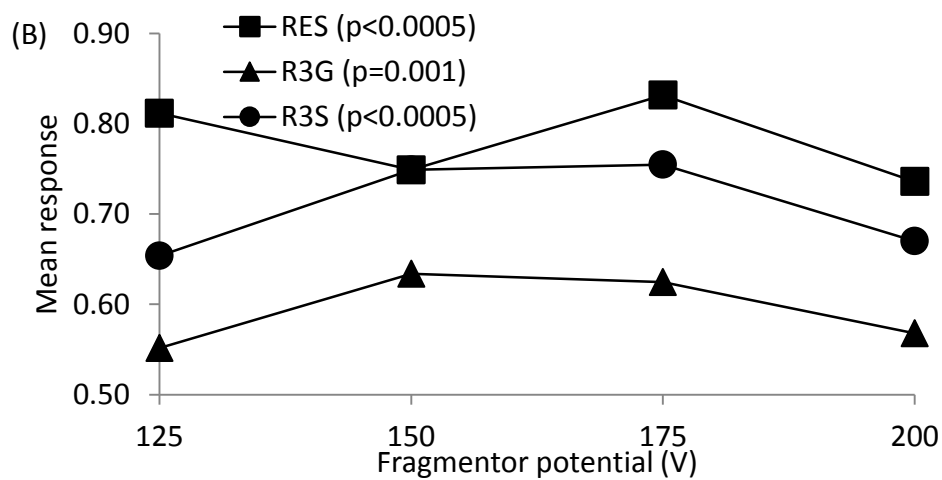
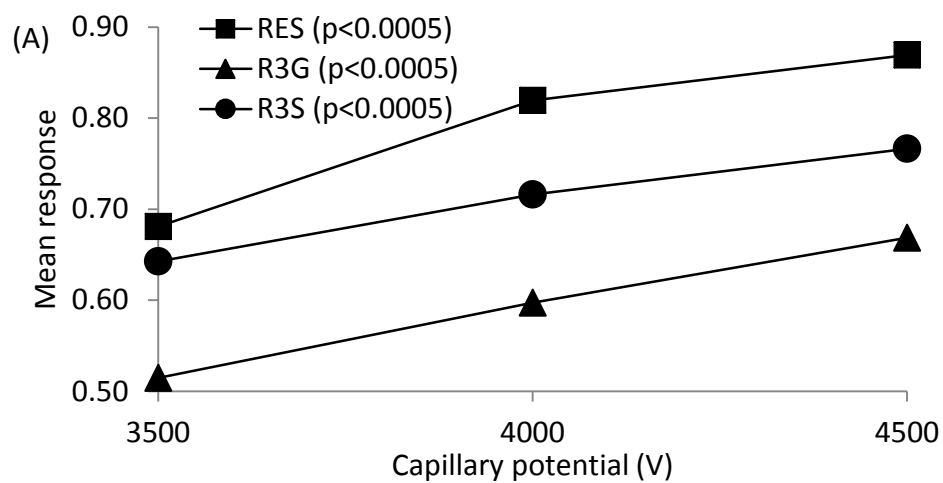


Figure C.2 Response (based on MS peak area) of RES, R3G, and R3S deprotonated ions at three capillary voltages (A) and four fragmentor voltages (B), determined in the negative mode using FIA with 50% MeOH/H<sub>2</sub>O solvent. (For RES, R3G, and R3S, fragmentor and capillary  $p < 0.0005$ .)

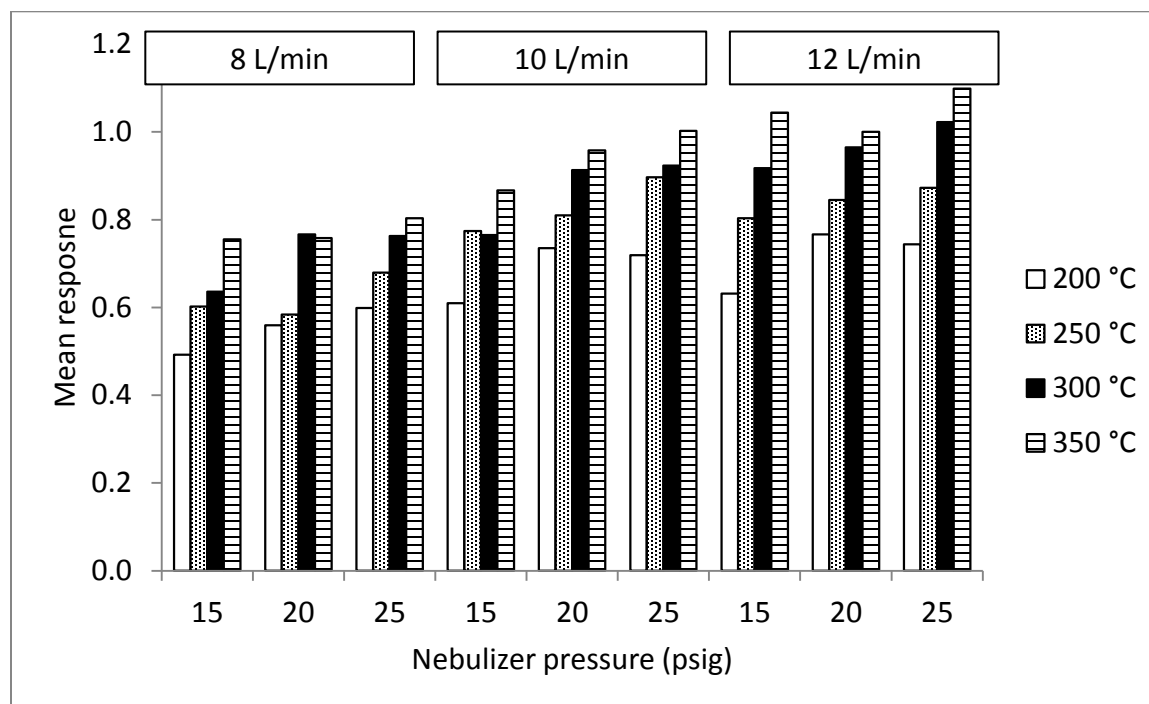


Figure C.3 Response (based on MS peak area) of deprotonated RES ions, from DOE optimization of nebulization conditions, determined in the negative mode using FIA with 50% MeOH/H<sub>2</sub>O solvent. (For gas temperature, nebulization pressure, and flow rate:  $p < 0.0005$ ; gas temperature and nebulizer pressure  $p = 0.001$ , gas temperature and flow rate  $p = 0.001$ , nebulizer pressure and flow rate  $p = 0.033$ .)

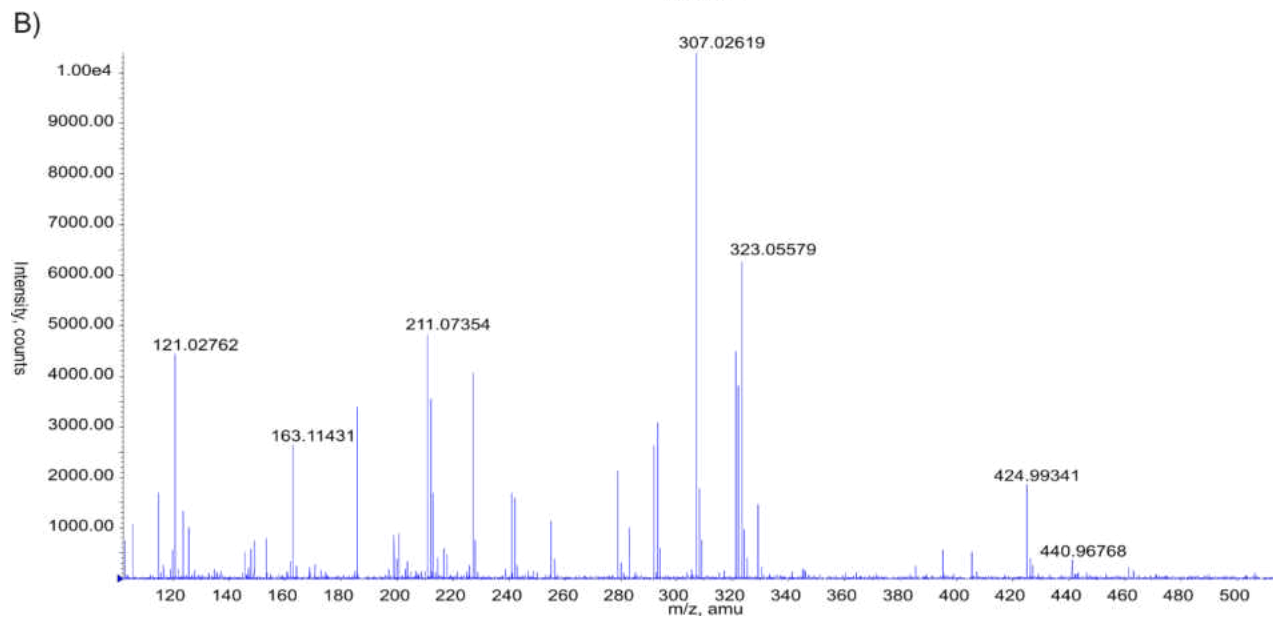
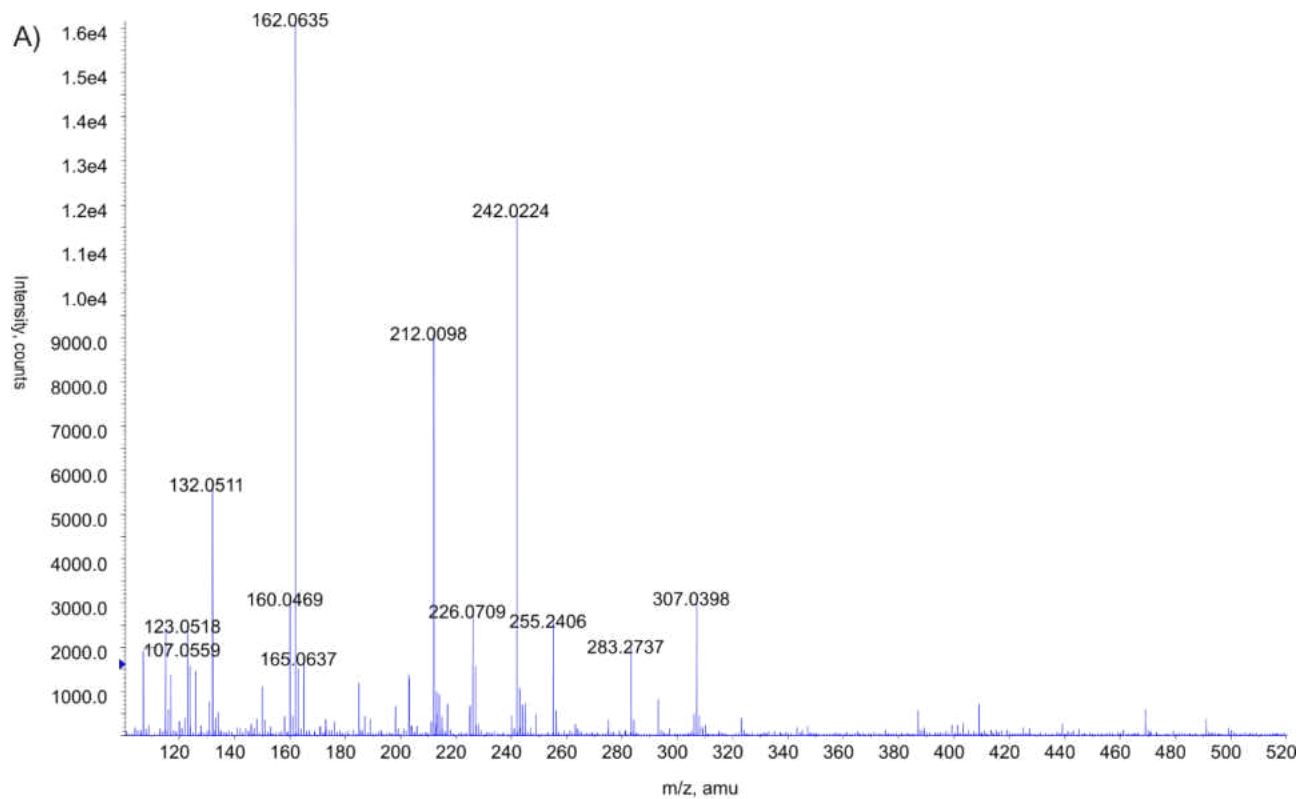


Figure C.4 ESI-TOF-MS spectrum of suspected resveratrol sulfate derivatives X1 (A) and X2(B) acquired using in negative mode.

**Table C.1: Summary of LC-MS methods previously used for detection of RES and its metabolites in blood and tissue matrices**

Sample matrix	Target analytes <sup>a</sup>	Sample preparation	Analysis method	LC conditions	Ionization	Quantification	Reference
rat plasma	t-RES, t-RES-gluc	centrifugation and vortexing with IS	LC-MS/MS	column: C <sub>18</sub> ; flow rate: 1.0 mL/min; injection volume: 20 µL; isocratic mobile phase with 25 mM ammonium acetate/65% MeOH	ESI; negative	calibration range: 5–5000 ng/mL (plasma); IS: naringenin	Marier 2002 [12]
mouse serum	t-RES, c-RES, t-R3G, c-R3G, t-R3S, t-R4'G, t-R4'S	centrifugation and vortexing with ACN	LC-MS, LC-MS/MS	column: C <sub>18</sub> ; flow rate: 0.2 mL/min; injection volume: 10 µL; gradient mobile phase with A: 26.5 mM formic acid, B: ACN	ESI; negative	IS: naringenin; calibration range: NR <sup>c</sup>	Yu et al. 2002 [2]
human, mice, rat plasma	t-RES, c-RES, t-RES-gluc, t-RES-sulf	extraction with ethyl acetate, evaporation, reconstitution in 20% MeOH	LC-MS/MS	column: C <sub>18</sub> ; flow rate: 0.2 mL/min; injection volume: 50 µL; mobile phase with A: 10% MeOH, B: 70% MeOH	ESI; negative	NR	Meng et al. 2004 [13]
human serum	t-RES, t-R3G, t-R4'G	extraction with ethyl acetate in presence of NaH <sub>2</sub> PO <sub>3</sub> , centrifugation with IS, filtration, evaporation, , reconstitution in MeOH	LC-MS/MS	column: C <sub>18</sub> ; flow rate: 0.2 mL/min; gradient mobile phase with A: 26.5 mM formic acid, B: 26.5 mM formic acid/MeOH	ESI; negative	calibration range: 2.5–2500 ng/mL (MeOH); LOD: 1 ng/mL; IS: carbamezepine	Vitaglione et al. 2005 [14]

Table C.1 cont.

Sample matrix	Target analytes <sup>a</sup>	Sample preparation	Analysis method	LC conditions	Ionization	Quantification	Reference	
human plasma	t-RES, digluc, gluc, disulf, sulf, sulfogluc	t-RES- t-RES- t-RES- t-RES- t-RES-	acidification, vortexing, evaporation, reconstitution in MeOH/H <sub>2</sub> O	LC-MS/MS	column: C <sub>18</sub> ; flow rate: 0.249 mL/min; injection volume: 30 µL; gradient mobile phase with A: 5 mM ammonium acetate/isopropanol, B: MeOH/2% isopropanol	ESI; negative	NR	Boocock et al. 2007 [15]
human plasma	t-RES, t-R3S, t-R3,4'S, t-R3,5'S, t-R3G, t-R4'G, t-R2,4'G, t-R2,4G	extraction with ACN, centrifugation, evaporation, reconstitution in MeOH	LC-MS/MS	column: C <sub>18</sub> ; flow rate not reported; injection volume: 80 µL (plasma); gradient mobile phase with A: 26.5 mM formic acid, B: ACN	ESI; positive	NR	Burkon & Somoza 2008 [3]	

Table C.1. cont.

Sample matrix	Target analytes <sup>a</sup>	Sample preparation	Analysis method	LC conditions	Ionization	Quantification	Reference
rat plasma, tissues	t-RES, t-RES-gluc, t-RES-sulf	plasma: SPE with MeOH, tissue: homogenized with MeOH, vortexed, extraction, centrifugation, evaporation	LC-MS/MS	column: C <sub>18</sub> ; flow rate: 1.5 mL/min; injection volume: 100 µL; gradient mobile phase with A: 524 mM acetic acid, B: 20% phase A/80%ACN	ESI; negative	NR	Juan et al. 2010 [4]
mouse plasma	t-RES, c-RES, t-RES-gluc, c-RES-gluc, t-RES-sulf, c-RES-sulf, t-RES-sulfogluc, c-RES-sulfogluc, RES-digluc	vortexed with ACN and supernatant mixed with water	LC-MS/MS	column: C <sub>18</sub> ; flow rate: 0.3 mL/min; injection volume: 15 µL; gradient mobile phase with A: 26.5 mM formic acid, B: ACN	ESI; negative	NR	Raal et al. 2009 [20]
rat tissue	t-RES, t-RES-gluc, t-RES-sulf	homogenization with MeOH, vortexed, centrifugation, evaporation, reconstituted in MeOH	LC-MS/MS	column: C <sub>18</sub> ; flow rate: 1.0 mL/min; injection volume: 20 µL; gradient mobile phase with A: 10% ACN, B: 80% ACN	ESI; negative	IS: naproxen	Wang et al. 2008 [21]



Table C.1 cont.

Sample matrix	Target analytes <sup>a</sup>	Sample preparation	Analysis method	LC conditions	Ionization	Quantification	Reference
human plasma	t-RES	vortexed with IS, SPE with 50% MeOH/THF	LC-MS	column: C <sub>18</sub> ; flow rate not reported; injection volume: 5 µL; gradient mobile phase with A: water, B: MeOH	ESI; negative	calibration range: 0.5–100 ng/mL; LOQ: 0.5 ng/mL; IS: naringenin	Nunes et al. 2009 [16]
rat serum, liver	t-RES	liver: ground in MeOH, filtration, evaporatation, reconstituted in MeOH; plasma: centrifugation with ethyl acetate, evaporation, reconstitution in MeOH	LC-MS/MS	column: C <sub>18</sub> ; flow rate: 0.2 mL/min; gradient mobile phase with A: 26.5 mM formic acid, B: 26.5 mM formic acid/MeOH	ESI; negative	LOD: ppb (specific number NR)	Vitaglione et al. 2009 [17]
rat plasma, small intestine, liver	t-RES, t-R3G, t-R4'G	extraction with IS and ethyl acetate, evaporation, reconstitution in MeOH	LC-MS/MS	column: C <sub>18</sub> ; flow rate: 0.2 mL/min; injection volume: 20 µL; gradient mobile phase with A: ACN, B: water	ESI; negative	LOQ: 0.4 ng/mL; IS: genistein	Zhou et al. 2009 [22]
pig plasma	t-RES, t-RES-digluc, t-R3G, t-RES-sulf, t-RES-sulfogluc,	vortexed and centrifuged with ACN, evaporation, reconstitution in MeOH/ water, filtration	LC-MS/MS	column: C <sub>18</sub> ; flow rate: 1.0 mL/min; injection volume: 50 µL; gradient mobile phase with A: 265 mM formic acid, B: ACN	ESI; negative	NR	Azorín-Ortuño et al. 2010 [10]

Table C.1 cont.

Sample matrix	Target analytes <sup>a</sup>	Sample preparation	Analysis method	LC conditions	Ionization	Quantification	Reference
rat tissues	t-RES, t-RES-gluc, t-RES-sulf	extraction with ethyl acetate and IS, vortexed, centrifugation, evaporation, reconstitution in MeOH	LC-MS/MS	column: C <sub>18</sub> ; flow rate: 0.2 mL/min; injection volume not reported; isocratic mobile phase with 60% ACN	ESI; negative	calibration range: 0.1–100.0 ng/mL (tissue homogenates); LOQ: 0.1 ng/mL; IS: apigenin	Liu et al. 2010 [23]
pig tissues, organs, fluids	t-RES, c-RES, t-R3G, t-R4'G, t-RES-digluc, t-RES-disulf, t-RES-sulf, t-RES-sulfogluc, t-RES-trisulf, DHR, DHR3G, DHR-digluc, DHR-disulf, DHR-sulf, DHR-sulfogluc, DHR-trisulf	vortexed and centrifuged with ACN, evaporation, reconstitution in MeOH and acidified water, filtration	LC-MS/MS	column: C <sub>18</sub> ; flow rate: 1.0 mL/min; injection volume: 50–80 µL; gradient mobile phase with A: 265 mM formic acid, B: ACN	ESI; negative	calibration range: 0.05–10 µM (in organs and fluids); LOD: 0.025 µM (5.7 ng/mL RES)–0.05 µM (DHR); LOQ: 0.05 µM (11.4 ng/mL RES)–0.25 (DHR) µM; IS: quercetin	Azorín-Ortuño et al. 2011 [5]
mouse serum	t-RES, t-R3G	vortexed with acid and MeOH, incubation, centrifugation, SPE with MeOH and acetic acid, evaporation, reconstitution in ACN/water	LC-MS	column: C <sub>18</sub> ; flow rate not reported; injection volume: 10 µL; gradient mobile phase with A: 1 mM ammonium bicarbonate/2% isopropanol; B: ACN/2% isopropanol	negative	calibration range: 10–10,000 ng/mL, 33.3–33,333 ng/mL; LOD: 21 ng/mL (RES), 10 ng/ml (R3G); IS: naproxen	Johnson et al. 2011 [24]

Table C.1 cont.

Sample matrix	Target analytes <sup>a</sup>	Sample preparation	Analysis method	LC conditions	Ionization	Quantification	Reference
rat plasma	t-RES	vortexed with IS, MeOH, and ethyl acetate, centrifugation, evaporation, reconstitution in MeOH	LC-MS/MS	column: C <sub>18</sub> ; flow rate: 1.0 mL/min; injection volume: 20 µL; isocratic mobile phase with 48% ACN	APCI; negative	calibration range: 0.1–500 ng/mL (plasma); LOQ: 0.1 ng/mL; IS: daidzein	Su et al. 2011 [25]
rat plasma	t-RES, t-RES-gluc, t-RES-sulf	vortexed with ACN, centrifugation, evaporation, reconstituted in MeOH, vortexed and centrifuged with water	LC-MS/MS	column: C <sub>18</sub> ; flow rate: 0.25 mL/min; injection volume not reported; gradient mobile phase A: 5 mM ammonium acetate/2% isopropanol, B: MeOH/2% isopropanol	ESI; negative	calibration range: 5–1000 ng/mL (plasma); LOQ: 5 ng/mL IS: <sup>13</sup> C <sub>6</sub> -RES	Kapetanovic et al. 2011 [18]
dog plasma	t-RES, t-R3G, t-R3S	vortexed with IS and ACN, centrifugation, evaporation, reconstituted in MeOH or ACN/MeOH, vortexed and centrifuged with water	LC-MS/MS	column: C <sub>18</sub> ; flow rate: 0.25 mL/min; injection volume: 25 µL; gradient mobile phase (for resveratrol) with A: 5 mM ammonium acetate/2% isopropanol, B: MeOH/2% isopropanol; gradient mobile phase (for metabolites) with A: 26.5 mM formic acid, B: 26.5 mM formic acid/ ACN	ESI; negative (t-RES, t-R3S) and positive (t-R3G)	calibration range: 5–1000 ng/mL (RES and R3G in plasma), 10–2000 ng/mL (R3S in plasma); LOQ: 5 ng/mL RES and R3G), 10 ng/mL (R3S); IS: trans-resveratrol- <sup>13</sup> C <sub>6</sub>	Muzzio et al. 2012 [11]

Table C.1 cont.

Sample matrix	Target analytes <sup>a</sup>	Sample preparation	Analysis method	LC conditions	Ionization	Quantification	Reference
mouse plasma	t-RES, t-R3G, t-R4'G, t-R3S, t-R4'S	vortexed with ascorbic acid and IS, centrifugation	LC-MS/MS	column: C18; flow rate: 1.0 mL/min; injection volume: 10 µL; gradient mobile phase with A: 5 mM ammonium acetate, B: MeOH	ESI; negative	calibration range: 10–10,000 ng/mL (RES, R3G, R4'G in plasma); 3.57–3570 ng/mL (R4'S in plasma), 2.46–2460 ng/mL (R3S in plasma); LOQ: 3.57 ng/ml (R4'S), 2.46 ng/ml (R3S), 10 ng/ml (R4'G, R3G and RES); IS: acetaminophen	Iwuchukwu et al. 2012 [19]
human plasma	t-RES, c-RES, t-R3G, c-R3G, t-R3S, c-R3S, t-R4'G, c-R4'G, t-R4'S, c-R4'S, DHR3G, DHR3S, DHR4'G, DHR4'S	SPE with acidified MeOH and ethyl acetate, evaporation, reconstitution in mobile phase	LC-MS/MS	column: C <sub>18</sub> ; flow rate: 0.5 mL/min; injection volume: 15 µL; gradient mobile phase with A: 8.73 mM acetic acid, B: 70% acetone/30% ACN/6.99 mM acetic acid	ESI; negative	NR	Rotches-Ribalta et al. 2012 [26]

Table C.1. cont.

Sample matrix	Target analytes <sup>a</sup>	Sample preparation	Analysis method	LC conditions	Ionization	Quantification	Reference
human urine	t-RES, c-RES, t-R3G, c-R3G, t-R3S, c-R3S, t-R4'G, c-R4'G, t-R4'S, c-R4'S, DHR-gluc, DHR-sulf, t-RES-disulf, c-RES-disulf, t-RES-sulfogluc	SPE with acidified MeOH, ethyl acetate and ammonia (5%) in MeOH, evaporation, reconstitution in mobile phase	UPLC-MS/MS	Column: C <sub>18</sub> ; flow rate: 1 mL/min; injection volume: 5 µL; gradient mobile phase with A: 8.33 mM acetic acid or 10 mM ammonium acetate in water, B: 70% acetone/30% ACN	ESI; negative	Calibration range: 1-1000 ng/mL (urine); LLOQ: 0.48 ng/mL (t-RES), 1.41 ng/mL (t-R3G), 0.36 ng/mL (t-R3S); IS: trans-resveratrol- <sup>13</sup> C <sub>6</sub> , taxifolin	Rotches-Ribalta et al. 2012 [27]
rat plasma and urine	t-RES, t-RES-gluc, t-RES-sulf	Extraction with ACN, centrifugation, evaporation and reconstitution with mobile phase	LC-MS/MS	Column: C <sub>18</sub> ; flow rate: 1 mL/min; injection volume: 5 µL; gradient mobile phase with A: 0.1 % phosphoric acid in water, B: 0.1 % phosphoric acid in ACN	ESI; negative	Calibration range: 0.2-10 µM (45-228 ng/mL t-RES); LOD: 0.1 µM (22.8 ng/mL t-RES)	Setoguchi et al. 2014 [8]

Table C.1 cont.

Sample matrix	Target analytes <sup>a</sup>	Sample preparation	Analysis method	LC conditions	Ionization	Quantification	Reference
rat hearth tissue and urine	t-RES, t-R3S, t-R3G	Precipitation with trifluoroacetic acid, extraction with MeOH, vortexed and centrifuged, evaporated and reconstituted with 1% formic acid in 50% MeOH	UPLC-MS <sup>n</sup>	Column: C <sub>18</sub> ; flow rate: 0.2 mL/min; gradient mobile phase with A: 0.1 % formic acid in water, B: 0.1 % formic acid in ACN	ESI; negative	NR	Bresciani et al. 2014 [9]

<sup>a</sup>analyte abbreviations: t=*trans*, c=*cis*, RES=resveratrol, R3G=resveratrol-3-O-glucuronide, R4'G=resveratrol-4'-O-glucuronide, gluc=glucuronide, R3S=resveratrol-3-sulfate, R4'S=resveratrol-4'-sulfate, sulf=sulfate, digluc=diglucurnoide, disulf= disulfate, sulfogluc=sulfoglucuronide, trisulf=trisulfate, DHR=dihydroresveratrol, R3,4'S=resveratrol-3,4'-disulfate; t-R3,5'S=resveratrol-3,5'-disulfate, R2,4'G=resveratrol-2-C-β-D-/4'-O-β-D-diglucuronide, R2,4G=resveratrol-2-C-β-D-/4-O-β-D-diglucuronide

**Table C.2 ESI conditions for RES samples introduced to TOF-MS via LC for DOE optimization in negative mode (FIA, 50% MeOH/H<sub>2</sub>O solvent, drying gas at 350 °C and 10 L/min; nebulization pressure at 25 psig).**

Block	Run	Electrolyte	Capillary voltage	Fragmentor voltage
1	1*	none**	3500	125
1	1	none	3500	150
1	1	none	3500	175
1	1	none	3500	200
1	2	none	4000	125
1	2	none	4000	150
1	2	none	4000	175
1	2	none	4000	200
1	3	none	4500	125
1	3	none	4500	150
1	3	none	4500	175
1	3	none	4500	200
1	4	0.1 mM acetic acid	3500	125
1	4	0.1 mM acetic acid	3500	150
1	4	0.1 mM acetic acid	3500	175
1	4	0.1 mM acetic acid	3500	200
1	5	0.1 mM acetic acid	4000	125
1	5	0.1 mM acetic acid	4000	150
1	5	0.1 mM acetic acid	4000	175
1	5	0.1 mM acetic acid	4000	200
1	6	0.1 mM acetic acid	4500	125
1	6	0.1 mM acetic acid	4500	150
1	6	0.1 mM acetic acid	4500	175
1	6	0.1 mM acetic acid	4500	200
1	7	0.55 mM acetic acid	3500	125
1	7	0.55 mM acetic acid	3500	150
1	7	0.55 mM acetic acid	3500	175
1	7	0.55 mM acetic acid	3500	200
1	8	0.55 mM acetic acid	4000	125
1	8	0.55 mM acetic acid	4000	150
1	8	0.55 mM acetic acid	4000	175
1	8	0.55 mM acetic acid	4000	200
1	9	0.55 mM acetic acid	4500	125
1	9	0.55 mM acetic acid	4500	150
1	9	0.55 mM acetic acid	4500	175
1	9	0.55 mM acetic acid	4500	200
1	10	1 mM acetic acid	3500	125

**Table C.2 cont.**

Block	Run	Electrolyte	Capillary voltage	Fragmentor voltage
1	10	1 mM acetic acid	3500	150
1	10	1 mM acetic acid	3500	175
1	10	1 mM acetic acid	3500	200
1	11	1 mM acetic acid	4000	125
1	11	1 mM acetic acid	4000	150
1	11	1 mM acetic acid	4000	175
1	11	1 mM acetic acid	4000	200
1	12	1 mM acetic acid	4500	125
1	12	1 mM acetic acid	4500	150
1	12	1 mM acetic acid	4500	175
1	12	1 mM acetic acid	4500	200
1	13	0.1 mM ammonium acetate	3500	125
1	13	0.1 mM ammonium acetate	3500	150
1	13	0.1 mM ammonium acetate	3500	175
1	13	0.1 mM ammonium acetate	3500	200
1	14	0.1 mM ammonium acetate	4000	125
1	14	0.1 mM ammonium acetate	4000	150
1	14	0.1 mM ammonium acetate	4000	175
1	14	0.1 mM ammonium acetate	4000	200
1	15	0.1 mM ammonium acetate	4500	125
1	15	0.1 mM ammonium acetate	4500	150
1	15	0.1 mM ammonium acetate	4500	175
1	15	0.1 mM ammonium acetate	4500	200
1	16	0.55 mM ammonium acetate	3500	125
1	16	0.55 mM ammonium acetate	3500	150
1	16	0.55 mM ammonium acetate	3500	175
1	16	0.55 mM ammonium acetate	3500	200
1	17	0.55 mM ammonium acetate	4000	125
1	17	0.55 mM ammonium acetate	4000	150
1	17	0.55 mM ammonium acetate	4000	175
1	17	0.55 mM ammonium acetate	4000	200
1	18	0.55 mM ammonium acetate	4500	125
1	18	0.55 mM ammonium acetate	4500	150
1	18	0.55 mM ammonium acetate	4500	175
1	18	0.55 mM ammonium acetate	4500	200
1	19	1 mM ammonium acetate	3500	125
1	19	1 mM ammonium acetate	3500	150
1	19	1 mM ammonium acetate	3500	175



**Table C.2 cont.**

Block	Run	Electrolyte	Capillary voltage	Fragmentor voltage
1	19	1 mM ammonium acetate	3500	200
1	20	1 mM ammonium acetate	4000	125
1	20	1 mM ammonium acetate	4000	150
1	20	1 mM ammonium acetate	4000	175
1	20	1 mM ammonium acetate	4000	200
1	21	1 mM ammonium acetate	4500	125
1	21	1 mM ammonium acetate	4500	150
1	21	1 mM ammonium acetate	4500	175
1	21	1 mM ammonium acetate	4500	200
2	1	none	4500	125
2	1	none	4500	150
2	1	none	4500	175
2	1	none	4500	200
2	2	none	3500	125
2	2	none	3500	150
2	2	none	3500	175
2	2	none	3500	200
2	3	none	4000	125
2	3	none	4000	150
2	3	none	4000	175
2	3	none	4000	200
2	4	0.1 mM acetic acid	4500	125
2	4	0.1 mM acetic acid	4500	150
2	4	0.1 mM acetic acid	4500	175
2	4	0.1 mM acetic acid	4500	200
2	5	0.1 mM acetic acid	4000	125
2	5	0.1 mM acetic acid	4000	150
2	5	0.1 mM acetic acid	4000	175
2	5	0.1 mM acetic acid	4000	200
2	6	0.1 mM acetic acid	3500	125
2	6	0.1 mM acetic acid	3500	150
2	6	0.1 mM acetic acid	3500	175
2	6	0.1 mM acetic acid	3500	200
2	7	0.55 mM acetic acid	3500	125
2	7	0.55 mM acetic acid	3500	150
2	7	0.55 mM acetic acid	3500	175
2	7	0.55 mM acetic acid	3500	200
2	8	0.55 mM acetic acid	4500	125

**Table C.2 cont.**

Block	Run	Electrolyte	Capillary voltage	Fragmentor voltage
2	8	0.55 mM acetic acid	4500	150
2	8	0.55 mM acetic acid	4500	175
2	8	0.55 mM acetic acid	4500	200
2	9	0.55 mM acetic acid	4000	125
2	9	0.55 mM acetic acid	4000	150
2	9	0.55 mM acetic acid	4000	175
2	9	0.55 mM acetic acid	4000	200
2	10	1 mM acetic acid	4000	125
2	10	1 mM acetic acid	4000	150
2	10	1 mM acetic acid	4000	175
2	10	1 mM acetic acid	4000	200
2	11	1 mM acetic acid	3500	125
2	11	1 mM acetic acid	3500	150
2	11	1 mM acetic acid	3500	175
2	11	1 mM acetic acid	3500	200
2	12	1 mM acetic acid	4500	125
2	12	1 mM acetic acid	4500	150
2	12	1 mM acetic acid	4500	175
2	12	1 mM acetic acid	4500	200
2	13	0.1 mM ammonium acetate	4000	125
2	13	0.1 mM ammonium acetate	4000	150
2	13	0.1 mM ammonium acetate	4000	175
2	13	0.1 mM ammonium acetate	4000	200
2	14	0.1 mM ammonium acetate	4500	125
2	14	0.1 mM ammonium acetate	4500	150
2	14	0.1 mM ammonium acetate	4500	175
2	14	0.1 mM ammonium acetate	4500	200
2	15	0.1 mM ammonium acetate	3500	125
2	15	0.1 mM ammonium acetate	3500	150
2	15	0.1 mM ammonium acetate	3500	175
2	15	0.1 mM ammonium acetate	3500	200
2	16	0.55 mM ammonium acetate	4500	125
2	16	0.55 mM ammonium acetate	4500	150
2	16	0.55 mM ammonium acetate	4500	175
2	16	0.55 mM ammonium acetate	4500	200
2	17	0.55 mM ammonium acetate	3500	125
2	17	0.55 mM ammonium acetate	3500	150

**Table C.2 cont.**

Block	Run	Electrolyte	Capillary voltage	Fragmentor voltage
2	17	0.55 mM ammonium acetate	3500	175
2	17	0.55 mM ammonium acetate	3500	200
2	18	0.55 mM ammonium acetate	4000	125
2	18	0.55 mM ammonium acetate	4000	150
2	18	0.55 mM ammonium acetate	4000	175
2	18	0.55 mM ammonium acetate	4000	200
2	19	1 mM ammonium acetate	3500	125
2	19	1 mM ammonium acetate	3500	150
2	19	1 mM ammonium acetate	3500	175
2	19	1 mM ammonium acetate	3500	200
2	20	1 mM ammonium acetate	4000	125
2	20	1 mM ammonium acetate	4000	150
2	20	1 mM ammonium acetate	4000	175
2	20	1 mM ammonium acetate	4000	200
2	21	1 mM ammonium acetate	4500	125
2	21	1 mM ammonium acetate	4500	150
2	21	1 mM ammonium acetate	4500	175
2	21	1 mM ammonium acetate	4500	200

\*The fragmentor was set to 125, 150, 175, and 200 V, in that order, during each run.

\*\*In all statistical analyses of ESI conditions, the runs with no electrolyte were entered twice.

**Table C.3 ESI conditions for R3G samples introduced to TOF-MS via LC for DOE optimization in negative mode (FIA, 50% MeOH/H<sub>2</sub>O solvent, drying gas at 350 °C and 10 L/min; nebulization pressure at 25 psig).**

Block	Run	Electrolyte	Capillary voltage	Fragmentor voltage
1	1	none	3500	125
1	1	none	3500	150
1	1	none	3500	175
1	1	none	3500	200
1	2	none	4000	125
1	2	none	4000	150
1	2	none	4000	175
1	2	none	4000	200
1	3	none	4500	125
1	3	none	4500	150
1	3	none	4500	175
1	3	none	4500	200
1	4	0.1 mM acetic acid	3500	125
1	4	0.1 mM acetic acid	3500	150
1	4	0.1 mM acetic acid	3500	175
1	4	0.1 mM acetic acid	3500	200
1	5	0.1 mM acetic acid	4000	125
1	5	0.1 mM acetic acid	4000	150
1	5	0.1 mM acetic acid	4000	175
1	5	0.1 mM acetic acid	4000	200
1	6	0.1 mM acetic acid	4500	125
1	6	0.1 mM acetic acid	4500	150
1	6	0.1 mM acetic acid	4500	175
1	6	0.1 mM acetic acid	4500	200
1	7	0.55 mM acetic acid	3500	125
1	7	0.55 mM acetic acid	3500	150
1	7	0.55 mM acetic acid	3500	175
1	7	0.55 mM acetic acid	3500	200
1	8	0.55 mM acetic acid	4000	125
1	8	0.55 mM acetic acid	4000	150
1	8	0.55 mM acetic acid	4000	175
1	8	0.55 mM acetic acid	4000	200
1	9	0.55 mM acetic acid	4500	125
1	9	0.55 mM acetic acid	4500	150
1	9	0.55 mM acetic acid	4500	175
1	9	0.55 mM acetic acid	4500	200
1	10	1 mM acetic acid	3500	125

**Table C.3 cont.**

Block	Run	Electrolyte	Capillary voltage	Fragmentor voltage
1	10	1 mM acetic acid	3500	150
1	10	1 mM acetic acid	3500	175
1	10	1 mM acetic acid	3500	200
1	11	1 mM acetic acid	4000	125
1	11	1 mM acetic acid	4000	150
1	11	1 mM acetic acid	4000	175
1	11	1 mM acetic acid	4000	200
1	12	1 mM acetic acid	4500	125
1	12	1 mM acetic acid	4500	150
1	12	1 mM acetic acid	4500	175
1	12	1 mM acetic acid	4500	200
1	13	0.1 mM ammonium acetate	3500	125
1	13	0.1 mM ammonium acetate	3500	150
1	13	0.1 mM ammonium acetate	3500	175
1	13	0.1 mM ammonium acetate	3500	200
1	14	0.1 mM ammonium acetate	4000	125
1	14	0.1 mM ammonium acetate	4000	150
1	14	0.1 mM ammonium acetate	4000	175
1	14	0.1 mM ammonium acetate	4000	200
1	15	0.1 mM ammonium acetate	4500	125
1	15	0.1 mM ammonium acetate	4500	150
1	15	0.1 mM ammonium acetate	4500	175
1	15	0.1 mM ammonium acetate	4500	200
1	16	0.55 mM ammonium acetate	3500	125
1	16	0.55 mM ammonium acetate	3500	150
1	16	0.55 mM ammonium acetate	3500	175
1	16	0.55 mM ammonium acetate	3500	200
1	17	0.55 mM ammonium acetate	4000	125
1	17	0.55 mM ammonium acetate	4000	150
1	17	0.55 mM ammonium acetate	4000	175
1	17	0.55 mM ammonium acetate	4000	200
1	18	0.55 mM ammonium acetate	4500	125
1	18	0.55 mM ammonium acetate	4500	150
1	18	0.55 mM ammonium acetate	4500	175
1	18	0.55 mM ammonium acetate	4500	200
1	19	1 mM ammonium acetate	3500	125
1	19	1 mM ammonium acetate	3500	150

**Table C.3 cont.**

Block	Run	Electrolyte	Capillary voltage	Fragmentor voltage
1	19	1 mM ammonium acetate	3500	175
1	19	1 mM ammonium acetate	3500	200
1	20	1 mM ammonium acetate	4000	125
1	20	1 mM ammonium acetate	4000	150
1	20	1 mM ammonium acetate	4000	175
1	20	1 mM ammonium acetate	4000	200
1	21	1 mM ammonium acetate	4500	125
1	21	1 mM ammonium acetate	4500	150
1	21	1 mM ammonium acetate	4500	175
1	21	1 mM ammonium acetate	4500	200
2	1	none	4000	125
2	1	none	4000	150
2	1	none	4000	175
2	1	none	4000	200
2	2	none	3500	125
2	2	none	3500	150
2	2	none	3500	175
2	2	none	3500	200
2	3	none	4500	125
2	3	none	4500	150
2	3	none	4500	175
2	3	none	4500	200
2	4	0.1 mM acetic acid	4500	125
2	4	0.1 mM acetic acid	4500	150
2	4	0.1 mM acetic acid	4500	175
2	4	0.1 mM acetic acid	4500	200
2	5	0.1 mM acetic acid	3500	125
2	5	0.1 mM acetic acid	3500	150
2	5	0.1 mM acetic acid	3500	175
2	5	0.1 mM acetic acid	3500	200
2	6	0.1 mM acetic acid	4000	125
2	6	0.1 mM acetic acid	4000	150
2	6	0.1 mM acetic acid	4000	175
2	6	0.1 mM acetic acid	4000	200
2	7	0.55 mM acetic acid	3500	125
2	7	0.55 mM acetic acid	3500	150
2	7	0.55 mM acetic acid	3500	175

**Table C.3 cont.**

Block	Run	Electrolyte	Capillary voltage	Fragmentor voltage
2	7	0.55 mM acetic acid	3500	200
2	8	0.55 mM acetic acid	4500	125
2	8	0.55 mM acetic acid	4500	150
2	8	0.55 mM acetic acid	4500	175
2	8	0.55 mM acetic acid	4500	200
2	9	0.55 mM acetic acid	4000	125
2	9	0.55 mM acetic acid	4000	150
2	9	0.55 mM acetic acid	4000	175
2	9	0.55 mM acetic acid	4000	200
2	10	1 mM acetic acid	4000	125
2	10	1 mM acetic acid	4000	150
2	10	1 mM acetic acid	4000	175
2	10	1 mM acetic acid	4000	200
2	11	1 mM acetic acid	4500	125
2	11	1 mM acetic acid	4500	150
2	11	1 mM acetic acid	4500	175
2	11	1 mM acetic acid	4500	200
2	12	1 mM acetic acid	3500	125
2	12	1 mM acetic acid	3500	150
2	12	1 mM acetic acid	3500	175
2	12	1 mM acetic acid	3500	200
2	13	0.1 mM ammonium acetate	4000	125
2	13	0.1 mM ammonium acetate	4000	150
2	13	0.1 mM ammonium acetate	4000	175
2	13	0.1 mM ammonium acetate	4000	200
2	14	0.1 mM ammonium acetate	4500	125
2	14	0.1 mM ammonium acetate	4500	150
2	14	0.1 mM ammonium acetate	4500	175
2	14	0.1 mM ammonium acetate	4500	200
2	15	0.1 mM ammonium acetate	3500	125
2	15	0.1 mM ammonium acetate	3500	150
2	15	0.1 mM ammonium acetate	3500	175
2	15	0.1 mM ammonium acetate	3500	200
2	16	0.55 mM ammonium acetate	4500	125
2	16	0.55 mM ammonium acetate	4500	150
2	16	0.55 mM ammonium acetate	4500	175
2	16	0.55 mM ammonium acetate	4500	200

**Table C.3 cont.**

Block	Run	Electrolyte	Capillary voltage	Fragmentor voltage
2	17	0.55 mM ammonium acetate	4000	125
2	17	0.55 mM ammonium acetate	4000	150
2	17	0.55 mM ammonium acetate	4000	175
2	17	0.55 mM ammonium acetate	4000	200
2	18	0.55 mM ammonium acetate	3500	125
2	18	0.55 mM ammonium acetate	3500	150
2	18	0.55 mM ammonium acetate	3500	175
2	18	0.55 mM ammonium acetate	3500	200
2	19	1 mM ammonium acetate	3500	125
2	19	1 mM ammonium acetate	3500	150
2	19	1 mM ammonium acetate	3500	175
2	19	1 mM ammonium acetate	3500	200
2	20	1 mM ammonium acetate	4000	125
2	20	1 mM ammonium acetate	4000	150
2	20	1 mM ammonium acetate	4000	175
2	20	1 mM ammonium acetate	4000	200
2	21	1 mM ammonium acetate	3500	125
2	21	1 mM ammonium acetate	3500	150
2	21	1 mM ammonium acetate	3500	175
2	21	1 mM ammonium acetate	3500	200
3	1	none	4000	125
3	1	none	4000	150
3	1	none	4000	175
3	1	none	4000	200
3	2	none	3500	125
3	2	none	3500	150
3	2	none	3500	175
3	2	none	3500	200
3	3	none	4500	125
3	3	none	4500	150
3	3	none	4500	175
3	3	none	4500	200
3	4	0.1 mM acetic acid	3500	125
3	4	0.1 mM acetic acid	3500	150
3	4	0.1 mM acetic acid	3500	175
3	4	0.1 mM acetic acid	3500	200
3	5	0.1 mM acetic acid	4000	125



**Table C.3 cont.**

Block	Run	Electrolyte	Capillary voltage	Fragmentor voltage
3	5	0.1 mM acetic acid	4000	150
3	5	0.1 mM acetic acid	4000	175
3	5	0.1 mM acetic acid	4000	200
3	6	0.1 mM acetic acid	4500	125
3	6	0.1 mM acetic acid	4500	150
3	6	0.1 mM acetic acid	4500	175
3	6	0.1 mM acetic acid	4500	200
3	7	0.55 mM acetic acid	4000	125
3	7	0.55 mM acetic acid	4000	150
3	7	0.55 mM acetic acid	4000	175
3	7	0.55 mM acetic acid	4000	200
3	8	0.55 mM acetic acid	4500	125
3	8	0.55 mM acetic acid	4500	150
3	8	0.55 mM acetic acid	4500	175
3	8	0.55 mM acetic acid	4500	200
3	9	0.55 mM acetic acid	3500	125
3	9	0.55 mM acetic acid	3500	150
3	9	0.55 mM acetic acid	3500	175
3	9	0.55 mM acetic acid	3500	200
3	10	1 mM acetic acid	4500	125
3	10	1 mM acetic acid	4500	150
3	10	1 mM acetic acid	4500	175
3	10	1 mM acetic acid	4500	200
3	11	1 mM acetic acid	3500	125
3	11	1 mM acetic acid	3500	150
3	11	1 mM acetic acid	3500	175
3	11	1 mM acetic acid	3500	200
3	12	1 mM acetic acid	4000	125
3	12	1 mM acetic acid	4000	150
3	12	1 mM acetic acid	4000	175
3	12	1 mM acetic acid	4000	200
3	13	0.1 mM ammonium acetate	3500	125
3	13	0.1 mM ammonium acetate	3500	150
3	13	0.1 mM ammonium acetate	3500	175
3	13	0.1 mM ammonium acetate	3500	200
3	14	0.1 mM ammonium acetate	4500	125
3	14	0.1 mM ammonium acetate	4500	150

**Table C.3 cont.**

Block	Run	Electrolyte	Capillary voltage	Fragmentor voltage
3	14	0.1 mM ammonium acetate	4500	175
3	14	0.1 mM ammonium acetate	4500	200
3	15	0.1 mM ammonium acetate	4000	125
3	15	0.1 mM ammonium acetate	4000	150
3	15	0.1 mM ammonium acetate	4000	175
3	15	0.1 mM ammonium acetate	4000	200
3	16	0.55 mM ammonium acetate	4000	125
3	16	0.55 mM ammonium acetate	4000	150
3	16	0.55 mM ammonium acetate	4000	175
3	16	0.55 mM ammonium acetate	4000	200
3	17	0.55 mM ammonium acetate	4500	125
3	17	0.55 mM ammonium acetate	4500	150
3	17	0.55 mM ammonium acetate	4500	175
3	17	0.55 mM ammonium acetate	4500	200
3	18	0.55 mM ammonium acetate	3500	125
3	18	0.55 mM ammonium acetate	3500	150
3	18	0.55 mM ammonium acetate	3500	175
3	18	0.55 mM ammonium acetate	3500	200
3	19	1 mM ammonium acetate	4000	125
3	19	1 mM ammonium acetate	4000	150
3	19	1 mM ammonium acetate	4000	175
3	19	1 mM ammonium acetate	4000	200
3	20	1 mM ammonium acetate	3500	125
3	20	1 mM ammonium acetate	3500	150
3	20	1 mM ammonium acetate	3500	175
3	20	1 mM ammonium acetate	3500	200
3	21	1 mM ammonium acetate	4500	125
3	21	1 mM ammonium acetate	4500	150
3	21	1 mM ammonium acetate	4500	175
3	21	1 mM ammonium acetate	4500	200

**Table C.4 ESI conditions for R3S samples introduced to TOF-MS via LC for DOE optimization in negative mode (FIA, 50% MeOH/H<sub>2</sub>O solvent, drying gas at 350 °C and 10 L/min; nebulization pressure at 25 psig).**

Block	Run	Electrolyte	Capillary voltage	Fragmentor voltage
1	1	none	4000	125
1	1	none	4000	150
1	1	none	4000	175
1	1	none	4000	200
1	2	none	3500	125
1	2	none	3500	150
1	2	none	3500	175
1	2	none	3500	200
1	3	none	4500	125
1	3	none	4500	150
1	3	none	4500	175
1	3	none	4500	200
1	4	0.1 mM acetic acid	4000	125
1	4	0.1 mM acetic acid	4000	150
1	4	0.1 mM acetic acid	4000	175
1	4	0.1 mM acetic acid	4000	200
1	5	0.1 mM acetic acid	4500	125
1	5	0.1 mM acetic acid	4500	150
1	5	0.1 mM acetic acid	4500	175
1	5	0.1 mM acetic acid	4500	200
1	6	0.1 mM acetic acid	3500	125
1	6	0.1 mM acetic acid	3500	150
1	6	0.1 mM acetic acid	3500	175
1	6	0.1 mM acetic acid	3500	200
1	7	0.55 mM acetic acid	4500	125
1	7	0.55 mM acetic acid	4500	150
1	7	0.55 mM acetic acid	4500	175
1	7	0.55 mM acetic acid	4500	200
1	8	0.55 mM acetic acid	3500	125
1	8	0.55 mM acetic acid	3500	150
1	8	0.55 mM acetic acid	3500	175
1	8	0.55 mM acetic acid	3500	200
1	9	0.55 mM acetic acid	4000	125
1	9	0.55 mM acetic acid	4000	150
1	9	0.55 mM acetic acid	4000	175
1	9	0.55 mM acetic acid	4000	200
1	10	1 mM acetic acid	3500	125

**Table C.4 cont.**

Block	Run	Electrolyte	Capillary voltage	Fragmentor voltage
1	10	1 mM acetic acid	3500	150
1	10	1 mM acetic acid	3500	175
1	10	1 mM acetic acid	3500	200
1	11	1 mM acetic acid	4000	125
1	11	1 mM acetic acid	4000	150
1	11	1 mM acetic acid	4000	175
1	11	1 mM acetic acid	4000	200
1	12	1 mM acetic acid	4500	125
1	12	1 mM acetic acid	4500	150
1	12	1 mM acetic acid	4500	175
1	12	1 mM acetic acid	4500	200
1	13	0.1 mM ammonium acetate	4000	125
1	13	0.1 mM ammonium acetate	4000	150
1	13	0.1 mM ammonium acetate	4000	175
1	13	0.1 mM ammonium acetate	4000	200
1	14	0.1 mM ammonium acetate	3500	125
1	14	0.1 mM ammonium acetate	3500	150
1	14	0.1 mM ammonium acetate	3500	175
1	14	0.1 mM ammonium acetate	3500	200
1	15	0.1 mM ammonium acetate	4500	125
1	15	0.1 mM ammonium acetate	4500	150
1	15	0.1 mM ammonium acetate	4500	175
1	15	0.1 mM ammonium acetate	4500	200
1	16	0.55 mM ammonium acetate	4500	125
1	16	0.55 mM ammonium acetate	4500	150
1	16	0.55 mM ammonium acetate	4500	175
1	16	0.55 mM ammonium acetate	4500	200
1	17	0.55 mM ammonium acetate	4000	125
1	17	0.55 mM ammonium acetate	4000	150
1	17	0.55 mM ammonium acetate	4000	175
1	17	0.55 mM ammonium acetate	4000	200
1	18	0.55 mM ammonium acetate	3500	125
1	18	0.55 mM ammonium acetate	3500	150
1	18	0.55 mM ammonium acetate	3500	175
1	18	0.55 mM ammonium acetate	3500	200
1	19	1 mM ammonium acetate	3500	125
1	19	1 mM ammonium acetate	3500	150
1	19	1 mM ammonium acetate	3500	175

**Table C.4 cont.**

Block	Run	Electrolyte	Capillary voltage	Fragmentor voltage
1	19	1 mM ammonium acetate	3500	200
1	20	1 mM ammonium acetate	4500	125
1	20	1 mM ammonium acetate	4500	150
1	20	1 mM ammonium acetate	4500	175
1	20	1 mM ammonium acetate	4500	200
1	21	1 mM ammonium acetate	4000	125
1	21	1 mM ammonium acetate	4000	150
1	21	1 mM ammonium acetate	4000	175
1	21	1 mM ammonium acetate	4000	200
2	1	none	3500	125
2	1	none	3500	150
2	1	none	3500	175
2	1	none	3500	200
2	2	none	4500	125
2	2	none	4500	150
2	2	none	4500	175
2	2	none	4500	200
2	3	none	4000	125
2	3	none	4000	150
2	3	none	4000	175
2	3	none	4000	200
2	4	0.1 mM acetic acid	3500	125
2	4	0.1 mM acetic acid	3500	150
2	4	0.1 mM acetic acid	3500	175
2	4	0.1 mM acetic acid	3500	200
2	5	0.1 mM acetic acid	4000	125
2	5	0.1 mM acetic acid	4000	150
2	5	0.1 mM acetic acid	4000	175
2	5	0.1 mM acetic acid	4000	200
2	6	0.1 mM acetic acid	4500	125
2	6	0.1 mM acetic acid	4500	150
2	6	0.1 mM acetic acid	4500	175
2	6	0.1 mM acetic acid	4500	200
2	7	0.55 mM acetic acid	4000	125
2	7	0.55 mM acetic acid	4000	150
2	7	0.55 mM acetic acid	4000	175
2	7	0.55 mM acetic acid	4000	200
2	8	0.55 mM acetic acid	4500	125

**Table C.4 cont.**

Block	Run	Electrolyte	Capillary voltage	Fragmentor voltage
2	8	0.55 mM acetic acid	4500	150
2	8	0.55 mM acetic acid	4500	175
2	8	0.55 mM acetic acid	4500	200
2	9	0.55 mM acetic acid	3500	125
2	9	0.55 mM acetic acid	3500	150
2	9	0.55 mM acetic acid	3500	175
2	9	0.55 mM acetic acid	3500	200
2	10	1 mM acetic acid	4500	125
2	10	1 mM acetic acid	4500	150
2	10	1 mM acetic acid	4500	175
2	10	1 mM acetic acid	4500	200
2	11	1 mM acetic acid	3500	125
2	11	1 mM acetic acid	3500	150
2	11	1 mM acetic acid	3500	175
2	11	1 mM acetic acid	3500	200
2	12	1 mM acetic acid	4000	125
2	12	1 mM acetic acid	4000	150
2	12	1 mM acetic acid	4000	175
2	12	1 mM acetic acid	4000	200
2	13	0.1 mM ammonium acetate	3500	125
2	13	0.1 mM ammonium acetate	3500	150
2	13	0.1 mM ammonium acetate	3500	175
2	13	0.1 mM ammonium acetate	3500	200
2	14	0.1 mM ammonium acetate	4500	125
2	14	0.1 mM ammonium acetate	4500	150
2	14	0.1 mM ammonium acetate	4500	175
2	14	0.1 mM ammonium acetate	4500	200
2	15	0.1 mM ammonium acetate	4000	125
2	15	0.1 mM ammonium acetate	4000	150
2	15	0.1 mM ammonium acetate	4000	175
2	15	0.1 mM ammonium acetate	4000	200
2	16	0.55 mM ammonium acetate	4000	125
2	16	0.55 mM ammonium acetate	4000	150
2	16	0.55 mM ammonium acetate	4000	175
2	16	0.55 mM ammonium acetate	4000	200
2	17	0.55 mM ammonium acetate	3500	125
2	17	0.55 mM ammonium acetate	3500	150
2	17	0.55 mM ammonium acetate	3500	175

**Table C.4 cont.**

Block	Run	Electrolyte	Capillary voltage	Fragmentor voltage
2	17	0.55 mM ammonium acetate	3500	200
2	18	0.55 mM ammonium acetate	4500	125
2	18	0.55 mM ammonium acetate	4500	150
2	18	0.55 mM ammonium acetate	4500	175
2	18	0.55 mM ammonium acetate	4500	200
2	19	1 mM ammonium acetate	4500	125
2	19	1 mM ammonium acetate	4500	150
2	19	1 mM ammonium acetate	4500	175
2	19	1 mM ammonium acetate	4500	200
2	20	1 mM ammonium acetate	4000	125
2	20	1 mM ammonium acetate	4000	150
2	20	1 mM ammonium acetate	4000	175
2	20	1 mM ammonium acetate	4000	200
2	21	1 mM ammonium acetate	3500	125
2	21	1 mM ammonium acetate	3500	150
2	21	1 mM ammonium acetate	3500	175
2	21	1 mM ammonium acetate	3500	200
3	1	none	4000	125
3	1	none	4000	150
3	1	none	4000	175
3	1	none	4000	200
3	2	none	4500	125
3	2	none	4500	150
3	2	none	4500	175
3	2	none	4500	200
3	3	none	3500	125
3	3	none	3500	150
3	3	none	3500	175
3	3	none	3500	200
3	4	0.1 mM acetic acid	4500	125
3	4	0.1 mM acetic acid	4500	150
3	4	0.1 mM acetic acid	4500	175
3	4	0.1 mM acetic acid	4500	200
3	5	0.1 mM acetic acid	4000	125
3	5	0.1 mM acetic acid	4000	150
3	5	0.1 mM acetic acid	4000	175
3	5	0.1 mM acetic acid	4000	200
3	6	0.1 mM acetic acid	3500	125

**Table C.4 cont.**

Block	Run	Electrolyte	Capillary voltage	Fragmentor voltage
3	6	0.1 mM acetic acid	3500	150
3	6	0.1 mM acetic acid	3500	175
3	6	0.1 mM acetic acid	3500	200
3	7	0.55 mM acetic acid	3500	125
3	7	0.55 mM acetic acid	3500	150
3	7	0.55 mM acetic acid	3500	175
3	7	0.55 mM acetic acid	3500	200
3	8	0.55 mM acetic acid	4500	125
3	8	0.55 mM acetic acid	4500	150
3	8	0.55 mM acetic acid	4500	175
3	8	0.55 mM acetic acid	4500	200
3	9	0.55 mM acetic acid	4000	125
3	9	0.55 mM acetic acid	4000	150
3	9	0.55 mM acetic acid	4000	175
3	9	0.55 mM acetic acid	4000	200
3	10	1 mM acetic acid	4000	125
3	10	1 mM acetic acid	4000	150
3	10	1 mM acetic acid	4000	175
3	10	1 mM acetic acid	4000	200
3	11	1 mM acetic acid	3500	125
3	11	1 mM acetic acid	3500	150
3	11	1 mM acetic acid	3500	175
3	11	1 mM acetic acid	3500	200
3	12	1 mM acetic acid	4500	125
3	12	1 mM acetic acid	4500	150
3	12	1 mM acetic acid	4500	175
3	12	1 mM acetic acid	4500	200
3	13	0.1 mM ammonium acetate	4500	125
3	13	0.1 mM ammonium acetate	4500	150
3	13	0.1 mM ammonium acetate	4500	175
3	13	0.1 mM ammonium acetate	4500	200
3	14	0.1 mM ammonium acetate	4000	125
3	14	0.1 mM ammonium acetate	4000	150
3	14	0.1 mM ammonium acetate	4000	175
3	14	0.1 mM ammonium acetate	4000	200
3	15	0.1 mM ammonium acetate	3500	125
3	15	0.1 mM ammonium acetate	3500	150
3	15	0.1 mM ammonium acetate	3500	175



**Table C.4 cont.**

Block	Run	Electrolyte	Capillary voltage	Fragmentor voltage
3	15	0.1 mM ammonium acetate	3500	200
3	16	0.55 mM ammonium acetate	3500	125
3	16	0.55 mM ammonium acetate	3500	150
3	16	0.55 mM ammonium acetate	3500	175
3	16	0.55 mM ammonium acetate	3500	200
3	17	0.55 mM ammonium acetate	4500	125
3	17	0.55 mM ammonium acetate	4500	150
3	17	0.55 mM ammonium acetate	4500	175
3	17	0.55 mM ammonium acetate	4500	200
3	18	0.55 mM ammonium acetate	4000	125
3	18	0.55 mM ammonium acetate	4000	150
3	18	0.55 mM ammonium acetate	4000	175
3	18	0.55 mM ammonium acetate	4000	200
3	19	1 mM ammonium acetate	4000	125
3	19	1 mM ammonium acetate	4000	150
3	19	1 mM ammonium acetate	4000	175
3	19	1 mM ammonium acetate	4000	200
3	20	1 mM ammonium acetate	4500	125
3	20	1 mM ammonium acetate	4500	150
3	20	1 mM ammonium acetate	4500	175
3	20	1 mM ammonium acetate	4500	200
3	21	1 mM ammonium acetate	3500	125
3	21	1 mM ammonium acetate	3500	150
3	21	1 mM ammonium acetate	3500	175
3	21	1 mM ammonium acetate	3500	200

**Table C.5 Nebulization ESI conditions in negative mode for samples introduced to TOF-MS via LC for DOE optimization of nebulization conditions for RES (FIA, 50% MeOH/H<sub>2</sub>O solvent, fragmentor at 175 V; capillary at 4500 V, electrolyte: 0.1 mM acetic acid in mobile phase).**

Replicate	Run	Drying gas temp (°C)	Drying gas flow rate (L/min)	Nebulizer pressure (psig)
1	1	200	8	15
2	2	200	8	15
1	3	200	10	15
2	4	200	10	15
1	5	200	12	15
2	6	200	12	15
1	7	200	12	20
2	8	200	12	20
1	9	200	10	20
2	10	200	10	20
1	11	200	8	20
2	12	200	8	20
1	13	200	8	25
2	14	200	8	25
1	15	200	10	25
2	16	200	10	25
1	17	200	12	25
2	18	200	12	25
1	19	250	12	25
2	20	250	12	25
1	21	250	10	25
2	22	250	10	25
1	23	250	8	25
2	24	250	8	25
1	25	250	8	20
2	26	250	8	20
1	27	250	10	20
2	28	250	10	20
1	29	250	12	20
2	30	250	12	20
1	31	250	12	15
2	32	250	12	15
1	33	250	10	15
2	34	250	10	15
1	35	250	8	15

Table C.5 cont.

Replicate	Run	Drying gas temp (°C)	Drying gas flow rate (L/min)	Nebulizer pressure (psig)
2	36	250	8	15
1	37	300	8	15
2	38	300	8	15
1	39	300	10	15
2	40	300	10	15
1	41	300	12	15
2	42	300	12	15
1	43	300	12	20
2	44	300	12	20
1	45	300	10	20
2	46	300	10	20
1	47	300	8	20
2	48	300	8	20
1	49	300	8	25
2	50	300	8	25
1	51	300	10	25
2	52	300	10	25
1	53	300	12	25
2	54	300	12	25
1	55	350	12	25
2	56	350	12	25
1	57	350	10	25
2	58	350	10	25
1	59	350	8	25
2	60	350	8	25
1	61	350	8	20
2	62	350	8	20
1	63	350	10	20
2	64	350	10	20
1	65	350	12	20
2	66	350	12	20
1	67	350	12	15
2	68	350	12	15
1	69	350	10	15
2	70	350	10	15
1	71	350	8	15
2	72	350	8	15

**Table C.6 Solvents and electrolytes employed for solvent optimization (FIA, negative mode, drying gas at 350 °C and 12 L/min; nebulization pressure at 25 psig, capillary at 4000 V, fragmentor at 175 V).**

Block	Analyte	Solvent	Electrolyte
1	RES	50% ACN/H2O	none
1	RES	50% ACN/H2O	0.1 mM acetic acid
1	RES	50% ACN/H2O	0.1 mM ammonium acetate
1	RES	50% MeOH/H2O	none
1	RES	50% MeOH/H2O	0.1 mM acetic acid
1	RES	50% MeOH/H2O	0.1 mM ammonium acetate
2	RES	50% ACN/H2O	none
2	RES	50% ACN/H2O	0.1 mM acetic acid
2	RES	50% ACN/H2O	0.1 mM ammonium acetate
2	RES	50% MeOH/H2O	none
2	RES	50% MeOH/H2O	0.1 mM acetic acid
2	RES	50% MeOH/H2O	0.1 mM ammonium acetate
1	R3G	50% ACN/H2O	none
1	R3G	50% ACN/H2O	0.1 mM acetic acid
1	R3G	50% ACN/H2O	0.1 mM ammonium acetate
1	R3G	50% MeOH/H2O	none
1	R3G	50% MeOH/H2O	0.1 mM acetic acid
1	R3G	50% MeOH/H2O	0.1 mM ammonium acetate
2	R3G	50% ACN/H2O	none
2	R3G	50% ACN/H2O	0.1 mM acetic acid
2	R3G	50% ACN/H2O	0.1 mM ammonium acetate
2	R3G	50% MeOH/H2O	none
2	R3G	50% MeOH/H2O	0.1 mM acetic acid
2	R3G	50% MeOH/H2O	0.1 mM ammonium acetate
1	R3S	50% ACN/H2O	none
1	R3S	50% ACN/H2O	0.1 mM acetic acid
1	R3S	50% ACN/H2O	0.1 mM ammonium acetate
1	R3S	50% MeOH/H2O	none
1	R3S	50% MeOH/H2O	0.1 mM acetic acid
1	R3S	50% MeOH/H2O	0.1 mM ammonium acetate
2	R3S	50% ACN/H2O	none
2	R3S	50% ACN/H2O	0.1 mM acetic acid
2	R3S	50% ACN/H2O	0.1 mM ammonium acetate
2	R3S	50% MeOH/H2O	none
2	R3S	50% MeOH/H2O	0.1 mM acetic acid
2	R3S	50% MeOH/H2O	0.1 mM ammonium acetate

**Table C.7 Effect of electrolyte concentrations of 0–400 mM acetic acid and 0–40 mM ammonium acetate in injected sample (FIA, ACN/H<sub>2</sub>O solvent, negative mode, drying gas at 350 °C and 12 L/min; nebulization pressure at 25 psig, capillary at 4000 V, fragmentor at 175 V).**

Block	Analyte	Electrolyte	Concentration (mM)
1	RES	acetic acid	0
1	RES	acetic acid	0.1
1	RES	acetic acid	1
1	RES	acetic acid	10
1	RES	acetic acid	100
1	RES	acetic acid	400
1	RES	ammonium acetate	0
1	RES	ammonium acetate	0.1
1	RES	ammonium acetate	1
1	RES	ammonium acetate	10
1	RES	ammonium acetate	20
1	RES	ammonium acetate	40
2	RES	acetic acid	0
2	RES	acetic acid	0.1
2	RES	acetic acid	1
2	RES	acetic acid	10
2	RES	acetic acid	100
2	RES	acetic acid	400
2	RES	ammonium acetate	0
2	RES	ammonium acetate	0.1
2	RES	ammonium acetate	1
2	RES	ammonium acetate	10
2	RES	ammonium acetate	20
2	RES	ammonium acetate	40
1	R3G	acetic acid	0
1	R3G	acetic acid	0.1
1	R3G	acetic acid	1
1	R3G	acetic acid	10
1	R3G	acetic acid	100
1	R3G	acetic acid	400
1	R3G	ammonium acetate	0
1	R3G	ammonium acetate	0.1
1	R3G	ammonium acetate	1
1	R3G	ammonium acetate	10
1	R3G	ammonium acetate	20
1	R3G	ammonium acetate	40

**Table C.7 cont.**

Block	Analyte	Electrolyte	Concentration (mM)
2	R3G	acetic acid	0
2	R3G	acetic acid	0.1
2	R3G	acetic acid	1
2	R3G	acetic acid	10
2	R3G	acetic acid	100
2	R3G	acetic acid	400
2	R3G	ammonium acetate	0
2	R3G	ammonium acetate	0.1
2	R3G	ammonium acetate	1
2	R3G	ammonium acetate	10
2	R3G	ammonium acetate	20
2	R3G	ammonium acetate	40
1	R3S	acetic acid	0
1	R3S	acetic acid	0.1
1	R3S	acetic acid	1
1	R3S	acetic acid	10
1	R3S	acetic acid	100
1	R3S	acetic acid	400
1	R3S	ammonium acetate	0
1	R3S	ammonium acetate	0.1
1	R3S	ammonium acetate	1
1	R3S	ammonium acetate	10
1	R3S	ammonium acetate	20
1	R3S	ammonium acetate	40
2	R3S	acetic acid	0
2	R3S	acetic acid	0.1
2	R3S	acetic acid	1
2	R3S	acetic acid	10
2	R3S	acetic acid	100
2	R3S	acetic acid	400
2	R3S	ammonium acetate	0
2	R3S	ammonium acetate	0.1
2	R3S	ammonium acetate	1
2	R3S	ammonium acetate	10
2	R3S	ammonium acetate	20
2	R3S	ammonium acetate	40

**Table C.8 Recoveries of spiked RES and R3S from control serum samples following the SPE purification method and LC-ESI-HRMS analysis using different electrolytes as the mobile phase.**

Electrolyte	Conc. (mM)	RES recovery (%)		Corrected RES recovery (%) <sup>a</sup>		R3S recovery (%)		Corrected R3S recovery (%)	
		Mean	SD	Mean	SD	Mean	SD	Mean	SD
ammonium acetate	0.025	28	18	121	25	132	36	102	8
ammonium acetate	0.25	135	37	86	3	173	52	107	6
ammonium acetate	0.5	119	16	79	7	94	14	78	6
ammonium acetate	1.0	82	7	86	7	91	4	92	4
acetic acid	0.25	91	30	79	6	323	76	97	2
acetic acid	1.0	94	16	73	5	304	20	101	0.5

<sup>a</sup>The corrected values were obtained using the deuterated RSs.

**Table C.9 Calibration parameters and LODs of RES, R3G, and R3S obtained using a linear least square regression. The internal standard was pinosylvin with a final concentration of 11.35 µg/mL.**

Analyte	RES	R3G	R3S
Calibration linear Range (ng/mL)	2.5–46.5	198.1–6737.1	6.6–69.3
Slope	0.006	0.00031	0.001
Intercept	-0.021	-0.139	0.005
S <sub>y</sub>	0.0092	0.079	0.0017
R <sup>2</sup>	0.9903	0.9940	0.9904
Instrumental LOD (ng/mL) <sup>a</sup>	1.3	4.4	1.6
Serum matrix LOD (ng/mL)	3.7	82	4.7

<sup>a</sup> Injection volume was 50 µL.

**Table C.10 Interday and intraday repeatability of RES, R3G, and R3S concentrations (ng/mL) in a representative serum sample. The data are presented as mean with one standard deviation (n=3).**

	Intraday	Interday
RES	ND	ND
R3S	3775±174	3689±313
R3G	61±9	55±3

## APPENDIX D

**Table D.1 Calibration parameters of aldehydes as PFBHA oximes and acids as methyl esters or trimethylsilyl esters (denoted TMS). All areas were normalized to area of internal standard (aldehydes – octafluoronaphthalene, acids – *o*-terphenyl)**

Aldehydes	k	intercept	S <sub>y</sub>
Formaldehyde	0.089	1.662	0.0122
Acetaldehyde	0.012	0.050	0.0006
Propanal	0.014	0.024	0.0003
Acrolein	0.003	0.002	0.0001
Isobutyraldehyde	0.016	0.014	0.0002
Butyraldehyde	0.031	0.014	0.0002
Crotonaldehyde	0.015	0.013	0.0009
Pentanal	0.018	0.013	0.0001
Hexanal	0.029	0.008	0.0002
Furaldehyde	0.016	0.009	0.0002
<i>trans</i> -Hexenal	0.040	0.015	0.0002
Heptanal	0.030	0.006	0.0003
Octanal	0.039	0.006	0.0003
Benzaldehyde	0.070	0.014	0.0004
Phenylacetaldehyde	0.014	0.007	0.0002
Nonanal	0.060	0.001	0.0003
<i>m</i> -Tolualdehyde	0.104	-0.084	0.0023
Hydrocinnamaldehyde	0.009	0.003	0.00005
<i>trans</i> -2-Nonenal	0.040	0.007	0.0001
Decanal	0.033	0.004	0.0002
Dimethylbenzaldehyde	0.061	0.022	0.0003
2,4-Nonadienal	0.013	-0.0001	0.0001
Glyoxal	0.019	-0.050	0.0005
Anisaldehyde	0.088	0.084	0.0009
Methylglyoxal	0.024	0.054	0.0005
4-Hydroxybenzaldehyde	0.099	-0.070	0.0006
Dodecanal	0.031	0.007	0.0002
Vanillin	0.006	-0.022	0.0004
Glutaraldehyde	0.014	0.051	0.0003
Syringaldehyde	0.070	-1.035	0.0003
Acids			
Hexanoic	0.081	-0.021	0.0024
Heptanoic	0.163	-0.607	0.0025
Octanoic	0.209	-0.908	0.0030
Nonanoic	0.295	-1.105	0.0065
Decanoic	0.189	-0.126	0.0065



**Table D.1 cont.**

Aldehydes	k	intercept	S <sub>y</sub>
Undecanoic	0.199	-0.059	0.0028
Dodecanoic	0.223	-0.067	0.0022
Tridecanoic	0.120	-0.005	0.0031
Tetradecanoic	0.110	-0.002	0.0029
Pentadecanoic	0.127	-0.005	0.0012
Palmitic	0.516	-0.529	0.0112
Heptadecanoic	0.090	-0.003	0.0009
Stearic	0.280	-0.060	0.0128
Nonadecanoic	0.327	-0.013	0.0015
Eicosanoic	0.595	-0.074	0.0019
Heneicosanoic	0.437	-0.042	0.0023
Docosanoic	0.416	-0.049	0.0025
Tricosanoic	0.313	-0.034	0.0035
Tetracosanoic	0.547	-0.075	0.0024
Octacosanoic	0.108	-0.009	0.0036
Oxalic	0.090	-0.083	0.0290
Malonic	0.070	-0.080	0.0123
Succinic	0.063	-0.115	0.0029
Glutaric	0.041	-0.028	0.0040
Adipic	0.033	-0.020	0.0013
Pimelic	0.064	-0.058	0.0018
Suberic	0.029	-0.007	0.0017
Azelaic	0.035	-0.012	0.0027
Sebacic	0.105	-0.037	0.0033
Undecanedioic	0.064	-0.075	0.0218
Dodecanedioic	0.046	-0.038	0.0027
Tridecanedioic	0.272	-0.293	0.0005
Tetradecanedioic	0.080	-0.223	0.0002
Methyl malonic	0.026	-0.181	0.0003
Maleic	0.031	-0.024	0.0001
Methyl succinic	0.014	-0.008	0.0006
Methyl maleic	0.009	-0.003	0.0007
Methyl glutaric	0.034	-0.012	0.0018
Glyoxylic	0.036	-0.005	0.0039
Pyruvic	0.030	-0.018	0.0014
Oxopentanoic	0.159	-0.118	0.0032
Oxalacetic	0.024	-0.018	0.0029
Ketoglutaric	0.013	-0.007	0.0006
<i>cis</i> -Pinonic	0.037	-0.008	0.0030
Ketopimelic	0.009	-0.002	0.0002
Benzoic TMS	0.054	0.022	0.0019

**Table D.1 cont.**

Aldehydes	k	intercept	S <sub>y</sub>
Malic	0.035	-0.004	0.0005
Annisic	0.0003	-0.006	0.0003
Mandelic	0.106	0.001	0.0006
Tartaric	0.072	0.110	0.0030
Salicylic TMS	1.954	-0.100	0.0154
Vanillic TMS	0.016	-0.008	0.0020
Homovanillic	0.398	-0.149	0.0107
Syringic TMS	0.091	0.033	0.0046

**Table D.2 Aldehydes and acids observed in WS and UA PM**

Aldehyde	WS ( $\mu\text{g}/\text{g}_{\text{PM}}$ )		UA ( $\mu\text{g}/\text{g}_{\text{PM}}$ )	
	mean	S.D.	mean	S.D.
Propanal	41	3	ND	
Acrolein	ND		ND	
Isobutanal	16	4	ND	
Butanal	168	18	98	6
Crotonal	ND		ND	
Pentanal	10	2	16	1
Hexanal	11	2	20	1
Furaldehyde	33	3	ND	
Heptanal	26	4	ND	
Octanal	ND		ND	
Benzaldehyde	16	1	ND	
Phenylacetaldehyde	214	39	180	22
Nonanal	8	1	44	14
<i>m</i> -Tolualdehyde	150	27	ND	
Hydrocinnamaldehyde	31	4	ND	
<i>trans</i> -2-Nonenal	ND		ND	
Decanal	26	5	26	5
2,5-Dimethylbenzaldehyde	ND		ND	
2,4-Nonadienal	ND		ND	
Glyoxal	548	30	860	123
Anisaldehyde	ND		ND	
Methylglyoxal	103	13	58	6
4-Hydroxybenzaldehyde	157	14	ND	
Vanillin	1031	106	ND	
Glutaraldehyde	31	1	43	4

**Table D.2 cont.**

Aldehyde	WS ( $\mu\text{g/gPM}$ )		UA ( $\mu\text{g/gPM}$ )	
	mean	S.D.	mean	S.D.
Syringaldehyde	2786	286	ND	
<b>Acid</b>				
Hexanoic	ND		ND	
Heptanoic	ND		ND	
Octanoic	ND		ND	
Nonanoic	30	5	ND	
Decanoic	ND		ND	
Undecanoic	18	2	ND	
Dodecanoic	19	3	ND	
Tridecanoic	ND		ND	
Tetradecanoic	34	4	ND	
Pentadecanoic	30	3	ND	
Palmitic	294	19	957	120
Heptadecanoic	35	3	40	5
Stearic	102	10	542	97
Nonadecanoic	29	2	38	5
Eicosanoic	93	12	169	15
Heneicosanoic	93	12	149	13
Docosanoic	211	21	281	22
Tricosanoic	134	16	198	18
Tetracosanoic	269	32	386	32
Octacosanoic	275	38	617	51
Succinic	1222	72	79	5
Glutaric	847	69	64	6
Adipic	119	18	63	5
Pimelic	48	2	57	7
Suberic	36	4	58	7
Azelaic	81	5	184	24
Sebacic	32	4	41	5
Undecanedioic	22	2	32	3
Dodecanedioic	ND		ND	
Tridecanedioic	ND		ND	
Tetradecanedioic	31	5	31	2
Methyl malonic	272	35	379	40
Maleic	151	19	ND	
Methyl succinic	633	63	10	1
Methyl maleic	897	112	1179	123

**Table D.2 cont.**

Acid	WS ( $\mu\text{g/gPM}$ )		UA ( $\mu\text{g/gPM}$ )	
	mean	S.D.	mean	S.D.
Methyl glutaric	66	1	16	1
Glyoxylic	115	10	115	9
Pyruvic	72	5	63	1
Oxopentanoic	203	19	ND	
Oxalacetic	168	20	ND	
Ketoglutaric	118	6	ND	
<i>cis</i> -Pinonic	87	8	ND	
Ketopimelic	91	9	ND	
Benzoic	146	24	ND	
Malic	719	98	800	25
Annisic	ND		ND	
Mandelic	ND		ND	
Tartaric	42	6	7	2
Salicylic	38	15	ND	
Vanillic	1820	195	42	19
Homovanillic	874	92	ND	
Syringic	711	116	ND	

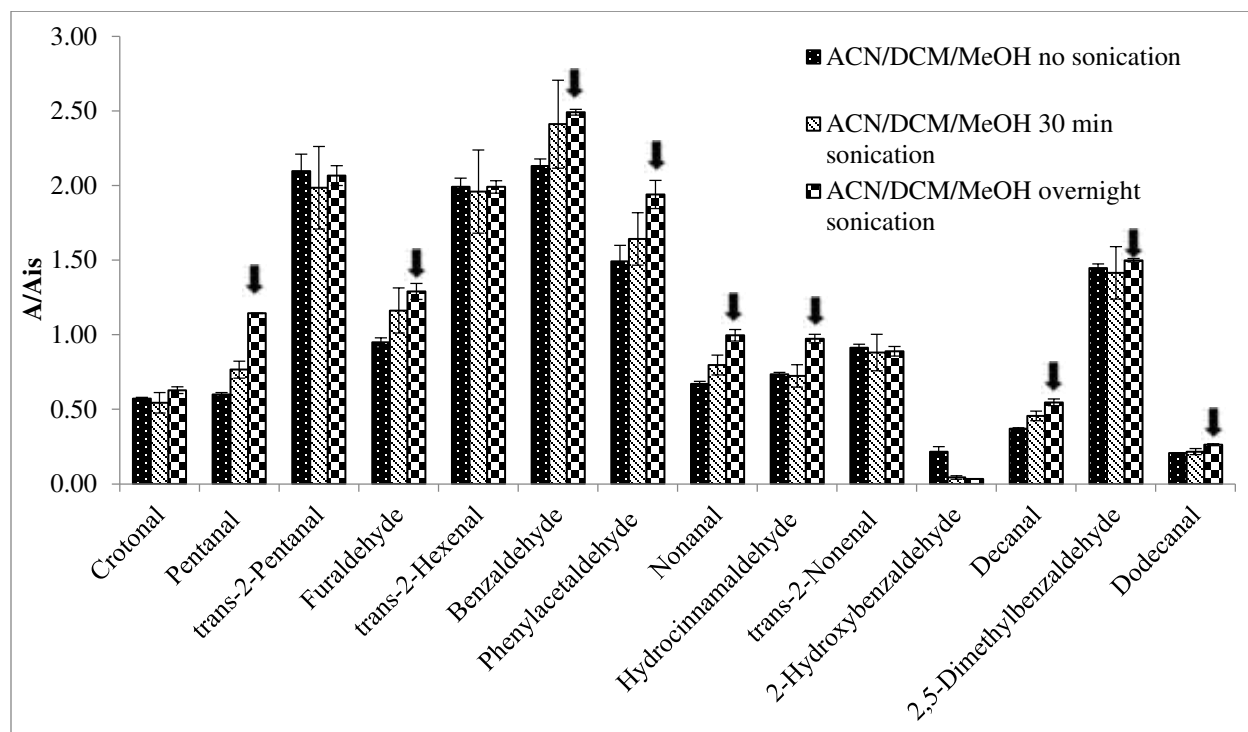
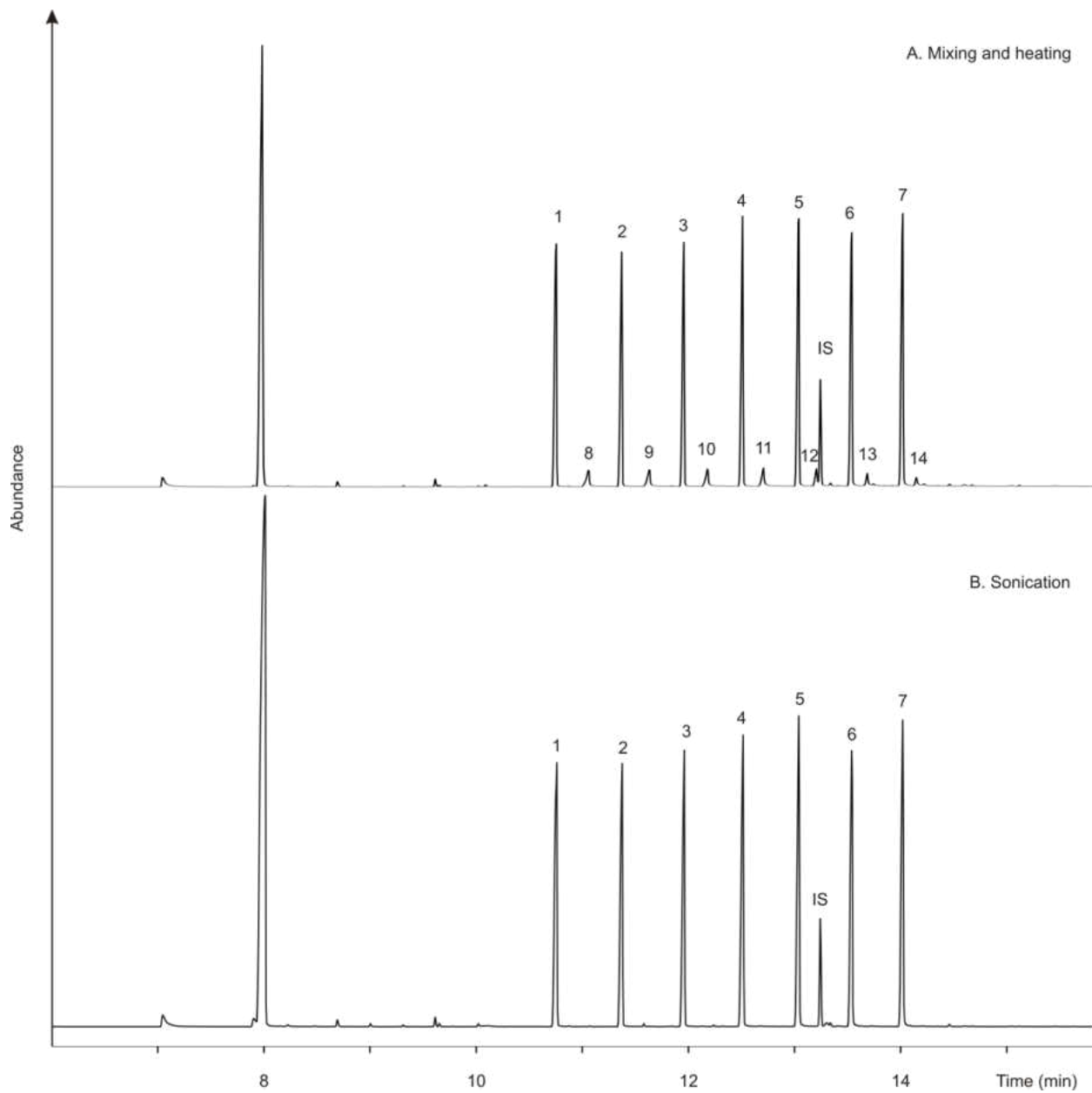


Figure D.1 Effect of sonication on derivatization of aldehydes with ACN/DCM/MeOH (1:8.5:0.5 v/v/v). The arrow denotes statistically significant difference between no sonication and overnight sonication (t-test at 95 % confidence level). Analysis performed by Mr. Chintapalli [118]



**Figure D.2** The effect of heat and mixing compared to sonication. A) mixing and heating, b) sonication. Peaks 1-7 correspond to dimethyl esters of dicarboxylic acids in following order: suberic, azelaic, sebacic, undecanedioic, dodecanedioic, tridecanedioic, tetradecanedioic, respectively. Peaks 8-14 correspond to monomethyl esters of dicarboxylic acids in following order: suberic, azelaic, sebacic, undecanedioic, dodecanedioic, tridecanedioic, tetradecanedioic, respectively.

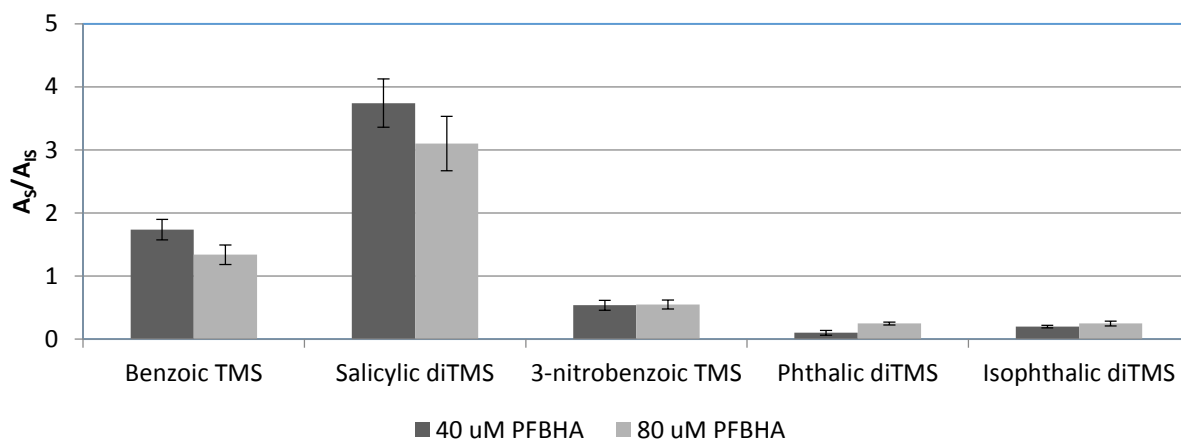


Figure D.3 The comparison of normalized peak area of TMS derivatives of aromatic acids in system with initial and increased content of PFBHA.HCl and methanol.

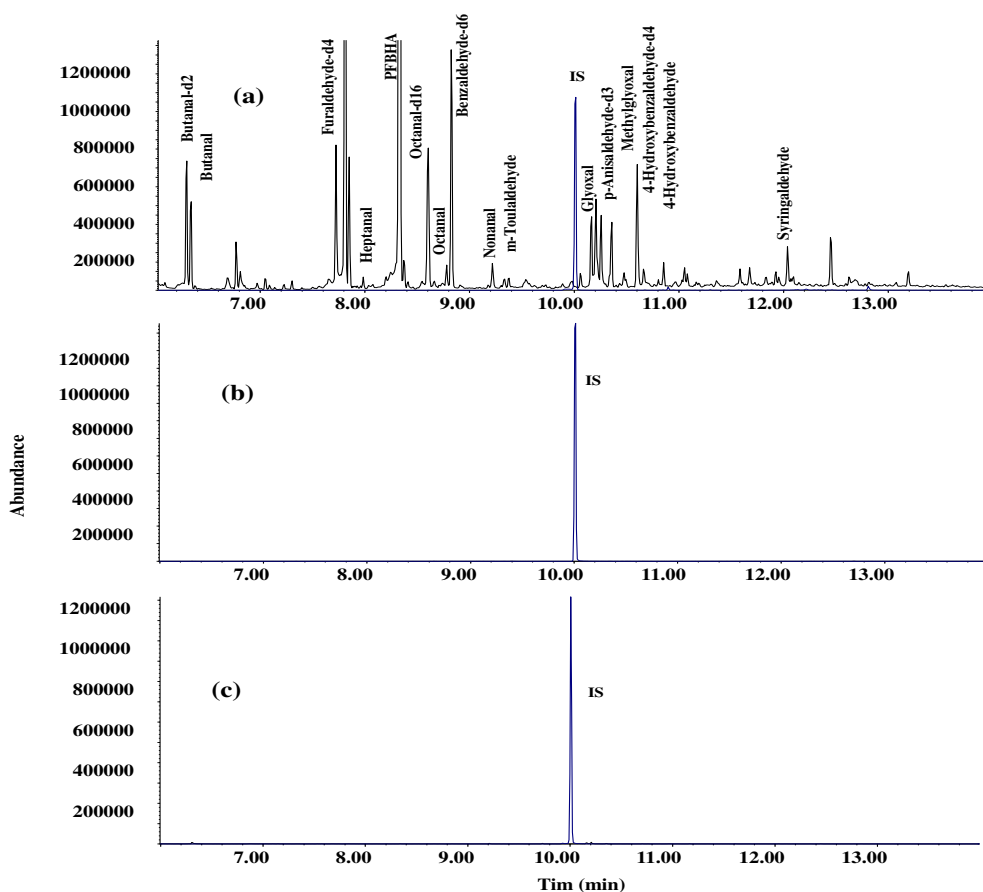


Figure D.4 GC-MS chromatograms showing composition of extracts obtained by sequential extraction of aldehydes from WS PM (2 mg) a) Sonication with MeOH in the presence of 2 mg WS PM under sonication b) Extraction from ACN/DCM/MeOH under sonication c) Soxhlet extraction with MeOH for 18h. Analysis performed by Mr. Chintapalli [118].

## REFERENCES

- [1] J.A. Baur, D. a Sinclair, Therapeutic potential of resveratrol: the in vivo evidence., *Nat. Rev. Drug Discov.* 5 (2006) 493–506. doi:10.1038/nrd2060.
- [2] J. McKinlay, C. Vieille, J.G. Zeikus, Prospects for a bio-based succinate industry, *Appl. Microbiol. Biotechnol.* 76 (2007) 727–740. doi:10.1007/s00253-007-1057-y.
- [3] J.H. Seinfeld, S.N. Pandis, *Atmospheric Chemistry and Physics - From Air Pollution to Climate Change* (2nd Edition), John Wiley & Sons, n.d. [http://www.knovel.com/web/portal/browse/display?\\_EXT\\_KNOVEL\\_DISPLAY\\_bookid=2126](http://www.knovel.com/web/portal/browse/display?_EXT_KNOVEL_DISPLAY_bookid=2126).
- [4] K. a Prather, C.D. Hatch, V.H. Grassian, Analysis of atmospheric aerosols., *Annu. Rev. Anal. Chem.* (Palo Alto. Calif). 1 (2008) 485–514. doi:10.1146/annurev.anchem.1.031207.113030.
- [5] U. Pöschl, Atmospheric aerosols: composition, transformation, climate and health effects., *Angew. Chem. Int. Ed. Engl.* 44 (2005) 7520–40. doi:10.1002/anie.200501122.
- [6] T. Willke, K.D. Vorlop, Industrial bioconversion of renewable resources as an alternative to conventional chemistry, *Appl. Microbiol. Biotechnol.* 66 (2004) 131–142. doi:10.1007/s00253-004-1733-0.
- [7] M. Sauer, D. Porro, D. Mattanovich, P. Branduardi, Microbial production of organic acids: expanding the markets, *Trends Biotechnol.* 26 (2008) 100–108.



doi:<http://dx.doi.org/10.1016/j.tibtech.2007.11.006>.

- [8] I. Molnár-Perl, Role of chromatography in the analysis of sugars, carboxylic acids and amino acids in food, *J. Chromatogr. A.* 891 (2000) 1–32. doi:[http://dx.doi.org/10.1016/S0021-9673\(00\)00598-7](http://dx.doi.org/10.1016/S0021-9673(00)00598-7).
- [9] Z.F. Katona, P. Sass, I. Molnár-Perl, Simultaneous determination of sugars, sugar alcohols, acids and amino acids in apricots by gas chromatography-mass spectrometry, *J. Chromatogr. A.* 847 (1999) 91–102. doi:[10.1016/s0021-9673\(99\)00333-7](https://doi.org/10.1016/s0021-9673(99)00333-7).
- [10] Z. Füzfai, Z.F. Katona, E. Kovács, I. Molnár-Perl, Simultaneous identification and quantification of the sugar, sugar alcohol, and carboxylic acid contents of sour cherry, apple, and berry fruits, as their trimethylsilyl derivatives, by gas chromatography-mass spectrometry, *J. Agric. Food Chem.* 52 (2004) 7444–7452. doi:[10.1021/jf040118p](https://doi.org/10.1021/jf040118p).
- [11] M.M. Ačanski, D.N. Vujić, Comparing sugar components of cereal and pseudocereal flour by GC–MS analysis, *Food Chem.* 145 (2014) 743–748. doi:<http://dx.doi.org/10.1016/j.foodchem.2013.08.138>.
- [12] I. Boldizsár, Z. Füzfai, I. Molnár-Perl, Characterization of the endogenous enzymatic hydrolyses of *Petroselinum crispum* glycosides: Determined by chromatography upon their sugar and flavonoid products, *J. Chromatogr. A.* 1293 (2013) 100–106. doi:<http://dx.doi.org/10.1016/j.chroma.2013.03.037>.
- [13] K. Horváth, I. Molnár-Perl, Simultaneous GC-MS quantitation of o-phosphoric, aliphatic and aromatic carboxylic acids, proline, hydroxymethylfurfural and sugars as their TMS derivatives: In honeys, *Chromatographia.* 48 (1998) 120–126. doi:[10.1007/bf02467527](https://doi.org/10.1007/bf02467527).
- [14] M.A. Adams, Z. Chen, P. Landman, T.D. Colmer, Simultaneous determination by capillary

- gas chromatography of organic acids, sugars, and sugar alcohols in plant tissue extracts as their trimethylsilyl derivatives, *Anal. Biochem.* 266 (1999) 77–84. doi:10.1006/abio.1998.2906.
- [15] M.C. Pietrogrande, D. Bacco, GC-MS analysis of water-soluble organics in atmospheric aerosol: Response surface methodology for optimizing silyl-derivatization for simultaneous analysis of carboxylic acids and sugars, *Anal. Chim. Acta.* 689 (2011) 257–264. doi:10.1016/j.aca.2011.01.047.
- [16] C. Schummer, O. Delhomme, B.M.R. Appenzeller, R. Wennig, M. Millet, Comparison of MTBSTFA and BSTFA in derivatization reactions of polar compounds prior to GC/MS analysis, *Talanta.* 77 (2009) 1473–1482. doi:10.1016/j.talanta.2008.09.043.
- [17] M.M. Koek, B. Muilwijk, M.J. van der Werf, T. Hankemeier, Microbial Metabolomics with Gas Chromatography/Mass Spectrometry, *Anal. Chem.* 78 (2006) 1272–1281. doi:10.1021/ac051683+.
- [18] E. Rojas-Escudero, A.L. Alarcón-Jiménez, P. Elizalde-Galván, F. Rojo-Callejas, Optimization of carbohydrate silylation for gas chromatography, *J. Chromatogr. A.* 1027 (2004) 117–120. doi:http://dx.doi.org/10.1016/j.chroma.2003.10.131.
- [19] P.M. Medeiros, B.R.T. Simoneit, Analysis of sugars in environmental samples by gas chromatography–mass spectrometry, *J. Chromatogr. A.* 1141 (2007) 271–278. doi:http://dx.doi.org/10.1016/j.chroma.2006.12.017.
- [20] M. Cerdán-Calero, J.M. Sendra, E. Sentandreu, Gas chromatography coupled to mass spectrometry analysis of volatiles, sugars, organic acids and aminoacids in Valencia Late orange juice and reliability of the Automated Mass Spectral Deconvolution and

- Identification System for their automatic identifica, *J. Chromatogr. A.* 1241 (2012) 84–95.  
doi:<http://dx.doi.org/10.1016/j.chroma.2012.04.014>.
- [21] F.O. Silva, V. Ferraz, Microwave-assisted preparation of sugars and organic acids for simultaneous determination in citric fruits by gas chromatography, *Food Chem.* 88 (2004) 609–612. doi:10.1016/j.foodchem.2004.05.002.
- [22] S. Rodríguez-Sánchez, O. Hernández-Hernández, A.I. Ruiz-Matute, M.L. Sanz, A derivatization procedure for the simultaneous analysis of iminosugars and other low molecular weight carbohydrates by GC-MS in mulberry (*Morus sp.*), *Food Chem.* 126 (2011) 353–359. doi:10.1016/j.foodchem.2010.10.097.
- [23] D.J. Harvey, Derivatization of carbohydrates for analysis by chromatography; electrophoresis and mass spectrometry, *J. Chromatogr. B.* 879 (2011) 1196–1225. doi:<http://dx.doi.org/10.1016/j.jchromb.2010.11.010>.
- [24] M. Correia-da-Silva, E. Sousa, B. Duarte, F. Marques, L.M. Cunha-Ribeiro, M.M.M. Pinto, Dual anticoagulant/antiplatelet persulfated small molecules., *Eur. J. Med. Chem.* 46 (2011) 2347–58. doi:10.1016/j.ejmech.2011.03.016.
- [25] I. Boldizsár, K. Horváth, G. Szedlay, I. Molnár-Perl, Simultaneous GC-MS quantitation of acids and sugars in the hydrolyzates of immunostimulant, water-soluble polysaccharides of basidiomycetes, *Chromatographia.* 47 (1998) 413–419. doi:10.1007/bf02466472.
- [26] D. Glassner, P. Elankovan, D. Beacom, K. Berglund, Purification process for succinic acid produced by fermentation, *Appl. Biochem. Biotechnol.* 51–52 (1995) 73–82. doi:10.1007/BF02933412.
- [27] J. Šťábová, J. Beránek, E.P. Nelson, B.A. Diep, A. Kubátová, Limits of detection for the

- determination of mono- and dicarboxylic acids using gas and liquid chromatographic methods coupled with mass spectrometry, *J. Chromatogr. B Anal. Technol. Biomed. Life Sci.* 879 (2011) 1429–1438. doi:10.1016/j.jchromb.2010.11.027.
- [28] S.E. Stein, No Title, *J. Am. Soc. Mass. Spectrom.* 10 (1999) 770.
- [29] AMDIS, (n.d.). <http://chemdata.nist.gov/mass-spc/amdis/>.
- [30] R. Xue, S. Zhang, C. Deng, L. Dong, T. Liu, J. Wang, H. Wu, J. Gu, X. Shen, Simultaneous determination of blood glucose and isoleucine levels in rats after chronic alcohol exposure by microwave-assisted derivatization and isotope dilution gas chromatography/mass spectrometry, *Rapid Commun. Mass Spectrom.* 22 (2008) 245–252. doi:10.1002/rcm.3350.
- [31] M. Ng, T. Fleming, M. Robinson, B. Thomson, N. Graetz, C. Margono, E.C. Mullany, S. Biryukov, C. Abbafati, S.F. Abera, J.P. Abraham, N.M.E. Abu-Rmeileh, T. Achoki, F.S. AlBuhairan, Z.A. Alemu, R. Alfonso, M.K. Ali, R. Ali, N.A. Guzman, W. Ammar, P. Anwari, A. Banerjee, S. Barquera, S. Basu, D.A. Bennett, Z. Bhutta, J. Blore, N. Cabral, I.C. Nonato, J.-C.J.-C. Chang, R. Chowdhury, K.J. Courville, M.H. Criqui, D.K. Cundiff, K.C. Dabhadkar, L. Dandona, A. Davis, A. Dayama, S.D. Dharmaratne, E.L. Ding, A.M. Durrani, A. Esteghamati, F. Farzadfar, D.F.J. Fay, V.L. Feigin, A. Flaxman, M.H. Forouzanfar, A. Goto, M.A. Green, R. Gupta, N. Hafezi-Nejad, G.J. Hankey, H.C. Harewood, R. Havmoeller, S. Hay, L. Hernandez, A. Hussein, B.T. Idrisov, N. Ikeda, F. Islami, E. Jahangir, S.K. Jassal, S.H. Jee, M. Jeffreys, J.B. Jonas, E.K. Kabagambe, S.E.A.H.S.E.A.H. Khalifa, A.P. Kengne, Y.S. Khader, Y.-H.Y.-H. Khang, D. Kim, R.W. Kimokoti, J.M. Kinge, Y. Kokubo, S. Kosen, G. Kwan, T. Lai, M. Leinsalu, Y. Li, X. Liang, S. Liu, G. Logroscino, P.A. Lotufo, Y. Lu, J. Ma, N.K. Mainoo, G.A. Mensah, T.R.

- Merriman, A.H. Mokdad, J. Moschandreas, M. Naghavi, A. Naheed, D. Nand, K.M.V. Narayan, E.L. Nelson, M.L. Neuhouser, M.I. Nisar, T. Ohkubo, S.O. Oti, A. Pedroza, D. Prabhakaran, N. Roy, U. Sampson, H. Seo, S.G. Sepanlou, K. Shibuya, R. Shiri, I. Shiue, G.M. Singh, J.A. Singh, V. Skirbekk, N.J.C. Stapelberg, L. Sturua, B.L. Sykes, M. Tobias, B.X. Tran, L. Trasande, H. Toyoshima, S. Van De Vijver, T.J. Vasankari, J.L. Veerman, G. Velasquez-Melendez, V.V. Vlassov, S.E. Vollset, T. Vos, C. Wang, X. Wang, E. Weiderpass, A. Werdecker, J.L. Wright, Y.C. Yang, H. Yatsuya, J. Yoon, S.-J.S.-J. Yoon, Y. Zhao, M. Zhou, S. Zhu, A.D. Lopez, C.J.L. Murray, E. Gakidou, Global, regional, and national prevalence of overweight and obesity in children and adults during 1980–2013: a systematic analysis for the Global Burden of Disease Study 2013, *Lancet*. 384 (2014) 766–781. doi:10.1016/S0140-6736(14)60460-8.
- [32] B.M. Popkin, M.M. Slining, New dynamics in global obesity facing low- and middle-income countries, *Obes. Rev.* 14 (2013) 11–20. doi:10.1111/obr.12102.
- [33] L.-L. Liu, J.-L. Yang, Y.-P. Shi, Phytochemicals and biological activities of *Pulicaria* species, *Chem. Biodivers.* 7 (2010) 327–349. doi:10.1002/cbdv.200900014.
- [34] M.N. Algabr, S. Ameddah, A. Menad, R. Mekkiou, J.C. Chalchat, S. Benayache, F. Benayache, Essential oil composition of *Pulicaria jaubertii* from Yemen, *Int J Med Arom Plants.* 2 (2012) 688–690.
- [35] A.S. Dubaie, A.A. Al-Khulaida, Studies on the flora of Yemen on the flora of tihama plain, *J. Bot. Taxon. Geobot.* 104 (1993) 259–265.
- [36] G.A. Fawzy, H.Y. Al Ati, A.A. El Gamal, Chemical composition and biological evaluation of essential oils of *Pulicaria jaubertii*, *Pharmacogn. Mag.* 9 (2013) 28–32.

- [37] G. Al-Naqeb, J. Rousová, A. Kubátová, M.J. Picklo, *Pulicaria jaubertii* E. Gamal-Eldin reduces triacylglyceride content and modifies cellular antioxidant pathways in 3T3-L1 adipocytes, *Chem. Biol. Interact.* 253 (2016). doi:10.1016/j.cbi.2016.05.013.
- [38] N.A. Awadh Ali, F.S. Sharopov, M. Alhaj, G.M. Hill, A. Porzel, N. Arnold, W.N. Setzer, J. Schmidt, L. Wessjohann, Chemical composition and biological activity of essential oil from *Pulicaria undulata* from Yemen, *Nat. Prod. Commun.* 7 (2012) 257–260.
- [39] J. Sharifi-Rad, A. Miri, S.M. Hoseini-Alfatemi, M. Sharifi-Rad, W.N. Setzer, A. Hadjiakhoondi, Chemical composition and biological activity of *pulicaria vulgaris* essential oil from Iran, *Nat. Prod. Commun.* 9 (2014) 1633–1636.
- [40] C. Proestos, M. Komaitis, Analysis of naturally occurring phenolic compounds in aromatic plants by RP-HPLC coupled to diode array detector (DAD) and GC-MS after silylation, *Foods.* 2 (2013) 90–99.
- [41] H.-C. Ku, H.-H. Chang, H.-C. Liu, C.-H. Hsiao, M.-J. Lee, Y.-J. Hu, P.-F. Hung, C.-W. Liu, Y.-H. Kao, Green tea (-)-epigallocatechin gallate inhibits insulin stimulation of 3T3-L1 preadipocyte mitogenesis via the 67-kDa laminin receptor pathway, *Am. J. Physiol. - Cell Physiol.* 297 (2009) C121–C132. doi:10.1152/ajpcell.00272.2008.
- [42] N. Sakurai, K. Mochizuki, H. Kameji, M. Shimada, T. Goda, (-)-Epigallocatechin gallate enhances the expression of genes related to insulin sensitivity and adipocyte differentiation in 3T3-L1 adipocytes at an early stage of differentiation, *Nutrition.* 25 (2009) 1047–1056. doi:10.1016/j.nut.2009.02.012.
- [43] H. Lee, S. Bae, Y. Yoon, The anti-adipogenic effects of (-)-epigallocatechin gallate are dependent on the WNT/ $\beta$ -catenin pathway, *J. Nutr. Biochem.* 24 (2013) 1232–1240.

doi:10.1016/j.jnutbio.2012.09.007.

- [44] H.-S. Liu, Y.-H. Chen, P.-F. Hung, Y.-H. Kao, Inhibitory effect of green tea (-)-epigallocatechin gallate on resistin gene expression in 3T3-L1 adipocytes depends on the ERK pathway, *Am. J. Physiol. - Endocrinol. Metab.* 290 (2006) E273–E281. doi:10.1152/ajpendo.00325.2005.
- [45] E.J. Park, J.M. Pezzuto, The pharmacology of resveratrol in animals and humans, *Biochim. Biophys. Acta - Mol. Basis Dis.* 1852 (2015) 1071–1113. doi:10.1016/j.bbadis.2015.01.014.
- [46] R. Kotecha, A. Takami, J.L. Espinoza, Dietary phytochemicals and cancer chemoprevention: a review of the clinical evidence, *Oncotarget; Adv. Online Publ.* Page 2. 7 (2016). doi:10.18632/oncotarget.9593.
- [47] Y. Setoguchi, Y. Oritani, R. Ito, H. Inagaki, H. Maruki-Uchida, T. Ichiyanagi, T. Ito, Absorption and metabolism of piceatannol in rats, *J. Agric. Food Chem.* 62 (2014) 2541–2548. doi:10.1021/jf404694y.
- [48] L. Bresciani, L. Calani, L. Bocchi, F. Delucchi, M. Savi, S. Ray, F. Brighenti, D. Stilli, D. Del Rio, Bioaccumulation of resveratrol metabolites in myocardial tissue is dose-time dependent and related to cardiac hemodynamics in diabetic rats, *Nutr. Metab. Cardiovasc. Dis.* 24 (2014) 408–415. doi:10.1016/j.numecd.2013.09.008.
- [49] M. Azorín-Ortuño, M.J. Yáñez-Gascón, F. Vallejo, F.J. Pallarés, M. Larrosa, R. Lucas, J.C. Morales, F.A. Tomás-Barberán, M.T. García-Conesa, J.C. Espín, Metabolites and tissue distribution of resveratrol in the pig., *Mol. Nutr. Food Res.* 55 (2011) 1154–68. doi:10.1002/mnfr.201100140.
- [50] M. Azorín-Ortuño, M.J. Yáñez-Gascón, F.J. Pallarés, F. Vallejo, M. Larrosa, M.T. García-Conesa, F. Tomás-Barberán, J.C. Espín, Pharmacokinetic Study of trans-Resveratrol in Adult

- Pigs., *J. Agric. Food Chem.* (2010) 11165–11171. doi:10.1021/jf102799m.
- [51] M. Muzzio, Z. Huang, S.-C. Hu, W.D. Johnson, D.L. McCormick, I.M. Kapetanovic, Determination of resveratrol and its sulfate and glucuronide metabolites in plasma by LC-MS/MS and their pharmacokinetics in dogs., *J. Pharm. Biomed. Anal.* 59 (2012) 201–8. doi:10.1016/j.jpba.2011.10.023.
- [52] C. Yu, Y.G. Shin, A. Chow, Y. Li, J.W. Kosmeder, Y.S. Lee, W.H. Hirschelman, J.M. Pezzuto, R.G. Mehta, R.B. van Breemen, Human, rat, and mouse metabolism of resveratrol., *Pharm. Res.* 19 (2002) 1907–14. doi:10.1023/A:1021414129280.
- [53] A. Burkon, V. Somoza, Quantification of free and protein-bound trans-resveratrol metabolites and identification of trans-resveratrol-C/O-conjugated diglucuronides – Two novel resveratrol metabolites in human plasma, *Mol. Nutr. & Food Res.* 52 (2008) 549–557. doi:10.1002/mnfr.200700290.
- [54] M.E. Juan, M. Maijó, J.M. Planas, Quantification of trans-resveratrol and its metabolites in rat plasma and tissues by HPLC., *J. Pharm. Biomed. Anal.* 51 (2010) 391–8. doi:10.1016/j.jpba.2009.03.026.
- [55] J.J.-F. Marier, P. Vachon, A.R.I. Gritsas, J.I.E. Zhang, J. Moreau, M.P. Ducharme, M.D.S.P. Services, J.M. Canada, Metabolism and Disposition of Resveratrol in Rats: Extent of Absorption, Glucuronidation, and Enterohepatic Recirculation Evidenced by a Linked-Rat Model, *J. Pharmacol. Exp. Ther.* 302 (2002) 369–373. doi:10.1124/jpet.102.033340.
- [56] X. Meng, P. Maliakal, H. Lu, M.-J. Lee, C.S. Yang, Urinary and plasma levels of resveratrol and quercetin in humans, mice, and rats after ingestion of pure compounds and grape juice., *J. Agric. Food Chem.* 52 (2004) 935–42. doi:10.1021/jf030582e.



- [57] P. Vitaglione, S. Sforza, G. Galaverna, C. Ghidini, N. Caporaso, P.P. Vescovi, V. Fogliano, R. Marchelli, Bioavailability of trans-resveratrol from red wine in humans., *Mol. Nutr. Food Res.* 49 (2005) 495–504. doi:10.1002/mnfr.200500002.
- [58] D.J. Boocock, K.R. Patel, G.E.S. Faust, D.P. Normolle, T.H. Marczylo, J.A. Crowell, D.E. Brenner, T.D. Booth, A. Gescher, W.P. Steward, Quantitation of trans-resveratrol and detection of its metabolites in human plasma and urine by high performance liquid chromatography., *J. Chromatogr. B. Analyt. Technol. Biomed. Life Sci.* 848 (2007) 182–7. doi:10.1016/j.jchromb.2006.10.017.
- [59] T. Nunes, L. Almeida, J.-F. Rocha, A. Falcão, C. Fernandes-Lopes, A.I. Loureiro, L. Wright, M. Vaz-da-Silva, P. Soares-da-Silva, Pharmacokinetics of trans-resveratrol following repeated administration in healthy elderly and young subjects., *J. Clin. Pharmacol.* 49 (2009) 1477–82. doi:10.1177/0091270009339191.
- [60] P. Vitaglione, B. Ottanelli, S. Milani, F. Morisco, N. Caporaso, V. Fogliano, Dietary trans-resveratrol bioavailability and effect on CCl<sub>4</sub>-induced liver lipid peroxidation., *J. Gastroenterol. Hepatol.* 24 (2009) 618–22. doi:10.1111/j.1440-1746.2008.05598.x.
- [61] I.M. Kapetanovic, M. Muzzio, Z. Huang, T.N. Thompson, D.L. McCormick, Pharmacokinetics, oral bioavailability, and metabolic profile of resveratrol and its dimethylether analog, pterostilbene, in rats., *Cancer Chemother. Pharmacol.* 68 (2011) 593–601. doi:10.1007/s00280-010-1525-4.
- [62] O.F. Iwuchukwu, S. Sharan, D.J. Canney, S. Nagar, Analytical method development for synthesized conjugated metabolites of trans-resveratrol, and application to pharmacokinetic studies., *J. Pharm. Biomed. Anal.* 63 (2012) 1–8.

doi:10.1016/j.jpba.2011.12.006.

- [63] A. Raal, P. Pokk, A. Arend, M. Aunapuu, J. Jõgi, K. Õkva, T. Püssa, trans-resveratrol alone and hydroxystilbenes of rhubarb (*Rheum raphaniticum* L.) root reduce liver damage induced by chronic ethanol administration: a comparative study in mice, *Phyther. Res.* 23 (2009) 525–532. doi:10.1002/ptr.2665.
- [64] D. Wang, Y. Xu, W. Liu, Tissue distribution and excretion of resveratrol in rat after oral administration of *Polygonum cuspidatum* extract (PCE), *Phytomedicine.* 15 (2008) 859–66. doi:10.1016/j.phymed.2008.02.009.
- [65] S. Zhou, R. Yang, Z. Teng, B. Zhang, Y. Hu, Z. Yang, M. Huan, X. Zhang, Q. Mei, Dose-dependent absorption and metabolism of trans-polydatin in rats, *J. Agric. Food Chem.* (2009). doi:10.1021/jf803948g.
- [66] X. Liu, Z. Teng, Y. Zhang, M. Huan, S. Zhou, High Performance Liquid Chromatography—Tandem Mass Spectrometric Determination of Resveratrol and Its Metabolites in Rat Tissues, *Anal. Lett.* 43 (2010) 557–569. doi:10.1080/00032710903406938.
- [67] J.J. Johnson, M. Nihal, I.A. Siddiqui, C.O. Scarlett, H.H. Bailey, H. Mukhtar, N. Ahmad, Enhancing the bioavailability of resveratrol by combining it with piperine., *Mol. Nutr. Food Res.* 55 (2011) 1169–76. doi:10.1002/mnfr.201100117.
- [68] M. Su, B. Di, T. Hang, J. Wang, D. Yang, T. Wang, R. Meng, Rapid, Sensitive and Selective Analysis of trans-Resveratrol in Rat Plasma by LC–MS–MS, *Chromatographia.* 73 (2011) 1203–1210. doi:10.1007/s10337-011-2036-0.
- [69] M. Rotches-Ribalta, C. Andres-Lacueva, R. Estruch, E. Escribano, M. Urpi-Sarda, Pharmacokinetics of resveratrol metabolic profile in healthy humans after moderate

- consumption of red wine and grape extract tablets., *Pharmacol. Res.* 66 (2012) 375–382.  
doi:10.1016/j.phrs.2012.08.001.
- [70] M. Rotches-Ribalta, M. Urpi-Sarda, R. Llorach, M. Boto-Ordoñez, O. Jauregui, G. Chiva-Blanch, L. Perez-Garcia, W. Jaeger, M. Guillen, D. Corella, F.J. Tinahones, R. Estruch, C. Andres-Lacueva, Gut and microbial resveratrol metabolite profiling after moderate long-term consumption of red wine versus dealcoholized red wine in humans by an optimized ultra-high-pressure liquid chromatography tandem mass spectrometry method, *J. Chromatogr. A.* 1265 (2012) 105–113. doi:10.1016/j.chroma.2012.09.093.
- [71] C.S. Jungong, A. V Novikov, Practical Preparation of Resveratrol 3-O-B-D-Glucuronide., *Synth. Commun.* (2012). doi:10.1080/00397911.2011.585733.
- [72] K. Smith, G.A. El-Hiti, M.E.W. Hammond, D. Bahzad, Z. Li, C. Siquet, Highly efficient and selective electrophilic and free radical catalytic bromination reactions of simple aromatic compounds in the presence of reusable zeolites, *J. Chem. Soc. Perkin Trans. 1.* (2000) 2745–2752. doi:10.1039/B002157L.
- [73] W. Qin, K. Zhang, K. Clarke, T. Weiland, E.R. Sauter, Methylation and miRNA Effects of Resveratrol on Mammary Tumors vs. Normal Tissue, *Nutr. Cancer.* 66 (2014) 270–277. doi:10.1080/01635581.2014.868910.
- [74] E. Wenzel, T. Soldo, H. Erbersdobler, V. Somoza, Bioactivity and metabolism of trans-resveratrol orally administered to Wistar rats., *Mol. Nutr. Food Res.* 49 (2005) 482–94. doi:10.1002/mnfr.200500003.
- [75] N. Dongari, E.R. Sauter, B.M. Tande, A. Kubátová, Determination of Celecoxib in human plasma using liquid chromatography with high resolution time of flight-mass

- spectrometry., *J. Chromatogr. B.* (2014). doi:10.1016/j.jchromb.2014.02.012.
- [76] D. Wang, T. Hang, C. Wu, W. Liu, Identification of the major metabolites of resveratrol in rat urine by HPLC-MS/MS., *J. Chromatogr. B. Analyt. Technol. Biomed. Life Sci.* 829 (2005) 97–106. doi:10.1016/j.jchromb.2005.09.040.
- [77] X.-H. Shu, H. Li, Z. Sun, M.-L. Wu, J.-X. Ma, J.-M. Wang, Q. Wang, Y. Sun, Y.-S. Fu, X.-Y. Chen, Q.-Y. Kong, J. Liu, Identification of metabolic pattern and bioactive form of resveratrol in human medulloblastoma cells., *Biochem. Pharmacol.* 79 (2010) 1516–25. doi:10.1016/j.bcp.2010.01.022.
- [78] J. Hoshino, E.-J. Park, T.P. Kondratyuk, L. Marler, J.M. Pezzuto, R.B. van Breemen, S. Mo, Y. Li, M. Cushman, Selective synthesis and biological evaluation of sulfate-conjugated resveratrol metabolites., *J. Med. Chem.* 53 (2010) 5033–43. doi:10.1021/jm100274c.
- [79] J.N.P. Barbara J. Finlayson-Pitts, *Chemistry of the Upper and Lower Atmosphere*, 2000.
- [80] S. Bikkina, K. Kawamura, Y. Miyazaki, P. Fu, High abundances of oxalic, azelaic, and glyoxylic acids and methylglyoxal in the open ocean with high biological activity: Implication for secondary OA formation from isoprene, *Geophys. Res. Lett.* 41 (2014) 3649–3657. doi:10.1002/2014GL059913.
- [81] E.O. Edney, T.E. Kleindienst, T.S. Conner, C.D. McIver, E.W. Corse, W.S. Weathers, Polar organic oxygenates in PM<sub>2.5</sub> at a southeastern site in the United States, *Atmos. Environ.* 37 (2003) 3947–3965. doi:10.1016/s1352-2310(03)00461-8.
- [82] J. Fick, L. Pommer, C. Nilsson, B. Andersson, Effect of OH radicals, relative humidity, and time on the composition of the products formed in the ozonolysis of  $\alpha$ -pinene, *Atmos. Environ.* 37 (2003) 4087–4096. doi:10.1016/s1352-2310(03)00522-3.

- [83] R. Ortiz, K. Enya, K. Sekiguchi, K. Sakamoto, Experimental testing of an annular denuder and filter system to measure gas-particle partitioning of semivolatile bifunctional carbonyls in the atmosphere, *Atmos. Environ.* 43 (2009) 382–388. doi:10.1016/j.atmosenv.2008.09.074.
- [84] M. Jaoui, T.E. Kleindienst, M. Lewandowski, E.O. Edney, Identification and quantification of aerosol polar oxygenated compounds bearing carboxylic or hydroxyl groups. 1. Method development, *Anal. Chem.* 76 (2004) 4765–4778. doi:10.1021/ac049919h.
- [85] \*,† M. Jaoui, ‡ T. E. Kleindienst, ‡ M. Lewandowski, ‡ and J. H. Offenberg, E.O. Edney‡, Identification and Quantification of Aerosol Polar Oxygenated Compounds Bearing Carboxylic or Hydroxyl Groups. 2. Organic Tracer Compounds from Monoterpenes, 76 (2005) 5661–5673. doi:10.1021/ES048111B.
- [86] M. Jaoui, E. Corse, T.E. Kleindienst, J.H. Offenberg, M. Lewandowski, E.O. Edney, Analysis of secondary organic aerosol compounds from the photooxidation of d-limonene in the presence of NO<sub>x</sub> and their detection in ambient PM<sub>2.5</sub>, *Environ. Sci. Technol.* 40 (2006) 3819–3828. doi:10.1021/es052566z.
- [87] T.E. Kleindienst, T.S. Conver, C.D. McIver, E.O. Edney, Determination of secondary organic aerosol products from the photooxidation of toluene and their implications in ambient PM<sub>2.5</sub>, *J. Atmos. Chem.* 47 (2004) 79–100. doi:10.1023/b:joch.0000012305.94498.28.
- [88] M. Lewandowski, M. Jaoui, T.E. Kleindienst, J.H. Offenberg, E.O. Edney, Composition of PM<sub>2.5</sub> during the summer of 2003 in Research Triangle Park, North Carolina, *Atmos. Environ.* 41 (2007) 4073–4083. doi:10.1016/j.atmosenv.2007.01.012.
- [89] R.S. Spaulding, P. Frazey, X. Rao, M. Judith Charles, Measurement of hydroxy carbonyls

- and other carbonyls in ambient air using pentafluorobenzyl alcohol as a chemical ionization reagent, *Anal. Chem.* 71 (1999) 3420–3427. doi:10.1021/ac9900432.
- [90] R.S. Spaulding, M.J. Charles, Comparison of methods for extraction, storage, and silylation of pentafluorobenzyl derivatives of carbonyl compounds and multi-functional carbonyl compounds, *Anal. Bioanal. Chem.* 372 (2002) 808–816. doi:10.1007/s00216-002-1252-8.
- [91] J. Yu, H.E. Jeffries, K.G. Sexton, Atmospheric photooxidation of alkylbenzenes - I. Carbonyl product analyses, *Atmos. Environ.* 31 (1997) 2261–2280. doi:10.1016/S1352-2310(97)00011-3.
- [92] R.M. Flores, P. V. Doskey, Evaluation of multistep derivatization methods for identification and quantification of oxygenated species in organic aerosol, *J. Chromatogr. A.* 1418 (2015) 1–11. doi:10.1016/j.chroma.2015.09.041.
- [93] R. Ortiz, H. Hagino, K. Sekiguchi, Q. Wang, K. Sakamoto, Ambient air measurements of six bifunctional carbonyls in a suburban area, *Atmos. Res.* 82 (2006) 709–718. doi:10.1016/j.atmosres.2006.02.025.
- [94] P. Frazey, X. Rao, R. Spaulding, B. Beld, M.J. Charles, The power of pentafluorobenzyl alcohol chemical ionization/ion trap mass spectrometry to identify pentafluorobenzyl derivatives of oxygenated polar organics, *Int. J. Mass Spectrom.* 190–191 (1999) 343–357.
- [95] P.S. Chen, S.D. Huang, Coupled two-step microextraction devices with derivatizations to identify hydroxycarbonyls in rain samples by gas chromatography-mass spectrometry, *J. Chromatogr. A.* 1118 (2006) 161–167. doi:10.1016/j.chroma.2006.03.122.
- [96] J.E. Ham, J. Raymond Wells, Surface chemistry of dihydromyrcenol (2,6-dimethyl-7-octen-2-ol) with ozone on silanized glass, glass, and vinyl flooring tiles, *Atmos. Environ.* 43 (2009)

- 4023–4032. doi:10.1016/j.atmosenv.2009.05.007.
- [97] J.C. Harrison, J.R. Wells, Gas-phase chemistry of benzyl alcohol: Reaction rate constants and products with OH radical and ozone, *Atmos. Environ.* 43 (2009) 798–804. doi:10.1016/j.atmosenv.2008.11.001.
- [98] M.C. Pietrogrande, D. Bacco, M. Mercuriali, GC-MS analysis of low-molecular-weight dicarboxylic acids in atmospheric aerosol: Comparison between silylation and esterification derivatization procedures, *Anal. Bioanal. Chem.* 396 (2010) 877–885. <http://www.scopus.com/inward/record.url?eid=2-s2.0-76849113556&partnerID=40&md5=bc377c5d5bc86a003f69799e7e036f7f>.
- [99] Y.C. Li, J.Z. Yu, Simultaneous determination of mono- and dicarboxylic acids,  $\omega$ -oxo-carboxylic acids, midchain ketocarboxylic acids, and aldehydes in atmospheric aerosol samples, *Environ. Sci. Technol.* 39 (2005) 7616–7624. doi:10.1021/es050896d10.1029/2002GB001980; Miller, J.C., Miller, J.N., (1993) *Statistics for Analytical Chemistry*, 3rd Ed., pp. 115-117. , Ellis Horwood, Prentice-Hall: New York; Jang, M., Kamens, R.M., Atmospheric secondary aerosol formation by heterogeneous reactions of aldehydes in the presence of a sulfuric acid aerosol catalyst (2001) *Environ. Sci. Technol.*, 35, pp. 4758-4766; Liggo, J., Li, S.-M., McLaren, R., Heterogeneous reactions of glyoxal on particulate matter: Identification of acetals.
- [100] B. Temime, R.M. Healy, J.C. Wenger, A denuder-filter sampling technique for the detection of gas and particle phase carbonyl compounds, *Environ. Sci. Technol.* 41 (2007) 6514–6520. doi:10.1021/es070802v.
- [101] R.M. Healy, J.C. Wenger, A. Metzger, J. Duplissy, M. Kalberer, J. Dommen, Gas/particle

- partitioning of carbonyls in the photooxidation of isoprene and 1,3,5-trimethylbenzene, *Atmos. Chem. Phys.* 8 (2008) 3215–3230. doi:10.1029/2006GL026523; Edney, E.O., Driscoll, D.J., Weathers, W.S., Formation of polyketones in irradiated toluene/propylene/NO<sub>x</sub>/air mixtures (2001) *Aerosol Sci. Technol.* 35 (6), pp. 998-1008; Edney, E.O., Kleindienst, T.E., Jaoui, M., Formation of 2-methyl tetrols and 2-methylglyceric acid in secondary organic aerosol from laboratory irradiated isoprene/NO<sub>x</sub>/SO<sub>2</sub>/air mixtures and their detection in ambient PM<sub>2.5</sub> samples collected in the eastern United States (2005) *Atmos. Environ.* 39 (29), pp. 528.
- [102] C. Hallmann, B.G.K. van Aarssen, K. Grice, Relative efficiency of free fatty acid butyl esterification. Choice of catalyst and derivatisation procedure, *J. Chromatogr. A.* 1198–1199 (2008) 14–20. doi:10.1016/j.chroma.2008.05.030.
- [103] E. Dabek-Zlotorzynska, R. Aranda-Rodriguez, L. Graham, Capillary electrophoresis determinative and GC-MS confirmatory method for water-soluble organic acids in airborne particulate matter and vehicle emission, *J. Sep. Sci.* 28 (2005) 1520–1528. doi:10.1002/jssc.200400053.
- [104] J. Dron, G. Eyglunent, B. Temime-Roussel, N. Marchand, H. Wortham, Carboxylic acid functional group analysis using constant neutral loss scanning-mass spectrometry, *Anal. Chim. Acta.* 605 (2007) 61–69. doi:10.1016/j.aca.2007.10.020.
- [105] J.J. Jiménez, J.L. Bernal, M.J. del Nozal, M.T. Martín, J. Bernal, Sample preparation methods for beeswax characterization by gas chromatography with flame ionization detection, *J. Chromatogr. A.* 1129 (2006) 262–272. <http://www.scopus.com/inward/record.url?eid=2-s2.0-33748571924&partnerID=40&md5=06f517aca6d016add22b1802ee82e0b9>.



- [106] K. Kawamura, Identification of C2-C10  $\omega$ -oxocarboxylic acids, pyruvic acid, and C2-C3  $\alpha$ -dicarbonyls in wet precipitation and aerosol samples by capillary GC and GC/MS, *Anal. Chem.* 65 (1993) 3505–3511. doi:10.1021/ac00071a030.
- [107] K. Kawamura, T. Watanabe, Determination of stable carbon isotopic compositions of low molecular weight dicarboxylic acids and ketocarboxylic acids in atmospheric aerosol and snow samples, *Anal. Chem.* 76 (2004) 5762–5768. doi:10.1021/ac049491m.
- [108] J.B. Xiao, Identification of organic acids and quantification of dicarboxylic acids in Bayer process liquors by GC-MS, *Chromatographia.* 65 (2007) 185–190. doi:10.1365/s10337-006-0135-0.
- [109] K. Kawamura, L.A. Barrie, D. Toom-Saunty, Intercomparison of the measurements of oxalic acid in aerosols by gas chromatography and ion chromatography, *Atmos. Environ.* 44 (2010) 5316–5319. doi:10.1016/j.atmosenv.2010.08.051.
- [110] M. Tedetti, K. Kawamura, B. Charrièra, N. Chevalier, R. Sempéré, Determination of low molecular weight dicarboxylic and ketocarboxylic acids in seawater samples, *Anal. Chem.* 78 (2006) 6012–6018. <http://www.scopus.com/inward/record.url?eid=2-s2.0-33748500603&partnerID=40&md5=21dce812afae17cc28526c492b5d69be>.
- [111] N.K. Tran, S.M. Steinberg, B.J. Johnson, Volatile aromatic hydrocarbons and dicarboxylic acid concentrations in air at an urban site in the Southwestern US, *Atmos. Environ.* 34 (2000) 1845–1852. <http://www.scopus.com/inward/record.url?eid=2-s2.0-0033823895&partnerID=40&md5=4979a320ac725bfa92aace3ed4c3ccb5>.
- [112] H. Wang, K. Kawamura, K.F. Ho, S.C. Lee, Low molecular weight dicarboxylic acids, ketoacids, and dicarbonyls in the fine particles from a roadway tunnel: Possible secondary

- production from the precursors, *Environ. Sci. Technol.* 40 (2006) 6255–6260. doi:10.1021/es060732c.
- [113] G. Wang, M. Xie, S. Hu, S. Gao, E. Tachibana, K. Kawamura, Dicarboxylic acids, metals and isotopic compositions of C and N in atmospheric aerosols from inland China: Implications for dust and coal burning emission and secondary aerosol formation, *Atmos. Chem. Phys.* 10 (2010) 6087–6096. doi:10.5194/acp-10-6087-2010.1029/2007JD009365; Cao, J.J., Wu, F., Chow, J.C., Lee, S.C., Li, Y., Chen, S.W., An, Z.S., Liu, S.X., Characterization and source apportionment of atmospheric organic and elemental carbon during fall and winter of 2003 in Xi'an, China (2005) *Atmos. Chem. Phys.*, 5, pp. 3127-3137. , doi:10.5194/acp-5-3127-2005; Castro, L.M., Pio, C.A., Harrison, R.M., Smith, D.J.T., Carbonaceous aerosol in urban and rural European atmospheres: Estimation of secondary organic carbon conc.
- [114] Y. Zuo, K. Zhang, J. Wu, B. Men, M. He, Determination of o-phthalic acid in snow and its photochemical degradation by capillary gas chromatography coupled with flame ionization and mass spectrometric detection, *Chemosphere.* 83 (2011) 1014–1019. doi:10.1016/j.chemosphere.2011.02.008.
- [115] A. Kubátová, T.S. Steckler, J.R. Gallagher, S.B. Hawthorne, M.J. Picklo, Toxicity of wide-range polarity fractions from wood smoke and diesel exhaust particulate obtained using hot pressurized water, *Environ. Toxicol. Chem.* 23 (2004) 2243–2250. doi:10.1897/03-613.
- [116] S.B. Hawthorne, D.J. Miller, R.M. Barkley, M.S. Krieger, Identification of methoxylated phenols as candidate tracers for atmospheric wood smoke pollution, *Environ. Sci. Technol.* 22 (1988) 1191–1196. doi:10.1021/es00175a011.
- [117] C.A. Jakober, M.J. Charles, M.J. Kleeman, P.G. Green, LC-MS Analysis of Carbonyl

- Compounds and Their Occurrence in Diesel Emissions detection and sensitivity for many of the carbonyls inves-, Society. 78 (2006) 5086–5093. doi:10.1021/ac060301c.
- [118] M.R. Chintapalli, Determination of Aldehydes in Particulate Matter Using Gas Chromatography-Mass Spectrometry, 2015. <http://ezproxy.library.und.edu/login?url=https://search.proquest.com/docview/1731939445?accountid=28267>.
- [119] J. Beránek, D.A. Muggli, A. Kubátová, Detection limits of electron and electron capture negative ionization-mass spectrometry for aldehydes derivatized with o-(2,3,4,5,6-pentafluorobenzyl)-hydroxylamine hydrochloride, *J. Am. Soc. Mass Spectrom.* 21 (2010) 592–602. doi:10.1016/j.jasms.2009.12.009.
- [120] N. Li, C. Deng, N. Yao, X. Shen, X. Zhang, Determination of acetone, hexanal and heptanal in blood samples by derivatization with pentafluorobenzyl hydroxylamine followed by headspace single-drop microextraction and gas chromatography-mass spectrometry, *Anal. Chim. Acta.* 540 (2005) 317–323. doi:10.1016/j.aca.2005.03.047.
- [121] H.G. Schmarr, T. Potouridis, S. Ganß, W. Sang, B. Köpp, U. Bokuz, U. Fischer, Analysis of carbonyl compounds via headspace solid-phase microextraction with on-fiber derivatization and gas chromatographic-ion trap tandem mass spectrometric determination of their O-(2,3,4,5,6-pentafluorobenzyl)oxime derivatives, *Anal. Chim. Acta.* 617 (2008) 119–131. doi:10.1016/j.aca.2008.02.002.
- [122] J. Beránek, A. Kubátová, Evaluation of solid-phase microextraction methods for determination of trace concentration aldehydes in aqueous solution, *J. Chromatogr. A.* 1209 (2008) 44–54. doi:10.1016/j.chroma.2008.09.013.

- [123] D. Bourdin, V. Desauziers, Development of SPME on-fiber derivatization for the sampling of formaldehyde and other carbonyl compounds in indoor air, *Anal. Bioanal. Chem.* 406 (2014) 317–328. doi:10.1007/s00216-013-7460-6.
- [124] A.N. Alekseenko, O.M. Zhurba, N. V Efimova, V.S. Rukavishnikov, Headspace gas-chromatographic determination of formaldehyde in urine, *J. Anal. Chem.* 72 (2017) 83–86. doi:10.1134/S1061934816110022.
- [125] M. Ahmed, X. Guo, X.-M. Zhao, Application of simple ultrasonic assisted extraction coupled with HPLC and GC/MS for the determination of surface active compounds in atmospheric particulate matter, *Microchem. J.* 130 (2017) 400–411. doi:http://dx.doi.org/10.1016/j.microc.2016.10.023.
- [126] A. Kubátová, T.J. Lahren, J. Beránek, I.P. Smoliakova, A. Braun, F.E. Huggins, Extractable Organic Carbon and its Differentiation by Polarity in Diesel Exhaust, Wood Smoke, and Urban Particulate Matter, *Aerosol Sci. Technol.* 43 (2009) 714–729. doi:10.1080/02786820902889853.
- [127] A. Kubátová, R. Vermeylen, M. Claeys, J. Cafmeyer, W. Maenhaut, Organic compounds in urban aerosols from Gent, Belgium: Characterization, sources, and seasonal differences, *J. Geophys. Res. Atmos.* 107 (2002) ICC 5-1--ICC 5-12. doi:10.1029/2001JD000556.
- [128] J. Jung, B. Tsatsral, Y.J. Kim, K. Kawamura, Organic and inorganic aerosol compositions in Ulaanbaatar, Mongolia, during the cold winter of 2007 to 2008: Dicarboxylic acids, ketocarboxylic acids, and  $\alpha$ -dicarbonyls, *J. Geophys. Res. Atmos.* 115 (2010) n/a--n/a. doi:10.1029/2010JD014339.
- [129] K. Kawamura, S. Steinberg, I.R. Kaplan, Concentrations of monocarboxylic and dicarboxylic

acids and aldehydes in Southern California wet precipitations: Comparison of urban and nonurban samples and compositional changes during scavenging, *Atmos. Environ.* 30 (1996) 1035–1052. doi:10.1016/1352-2310(95)00404-1.

[130] J.-J. Meng, Z.-F. Hou, X.-D. Liu, J.-Z. Xing, Compositions and sources of summertime dicarboxylic acids and related SOA in PM<sub>2.5</sub> from Mt. Taishan, *Huanjing Kexue/Environmental Sci.* 38 (2017) 445–452. doi:10.13227/j.hjkx.201607199.